



Universiteit  
Leiden  
The Netherlands

## Personalized treatment for von Willebrand disease by RNA-targeted therapies

Jong, A. de

### Citation

Jong, A. de. (2020, April 7). *Personalized treatment for von Willebrand disease by RNA-targeted therapies*. Retrieved from <https://hdl.handle.net/1887/136853>

Version: Publisher's Version

License: [Licence agreement concerning inclusion of doctoral thesis in the Institutional Repository of the University of Leiden](#)

Downloaded from: <https://hdl.handle.net/1887/136853>

**Note:** To cite this publication please use the final published version (if applicable).

Cover Page



Universiteit Leiden

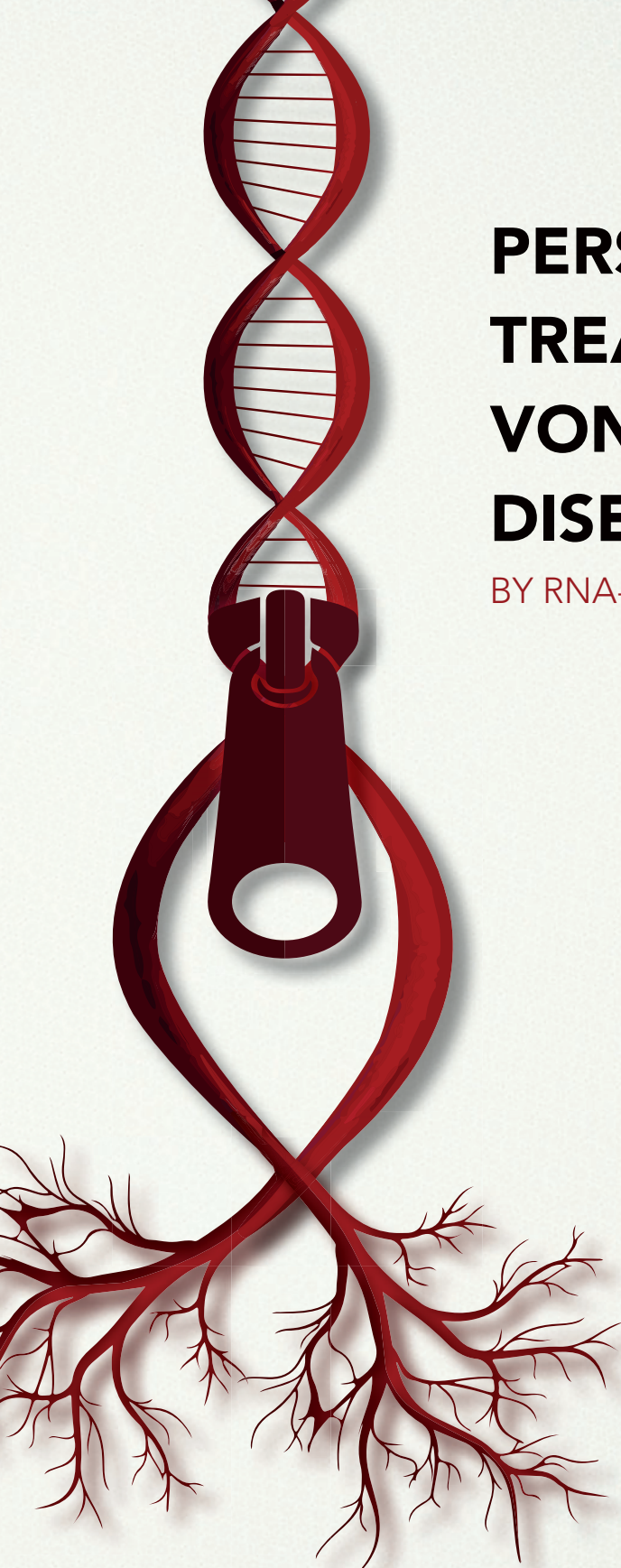


The handle <http://hdl.handle.net/1887/136853> holds various files of this Leiden University dissertation.

**Author:** Jong, A. de

**Title:** Personalized treatment for von Willebrand disease by RNA-targeted therapies

**Issue date:** 2020-04-07



# **PERSONALIZED TREATMENT FOR VON WILLEBRAND DISEASE**

BY RNA-TARGETED THERAPIES

ANNIKA DE JONG



# **Personalized treatment for von Willebrand disease**

by RNA-targeted therapies

Annika de Jong

**Personalized treatment for von Willebrand disease by RNA-targeted therapies**

ISBN: 978-94-6375-766-9

Cover design: Marilou Maes ([persoonlijkproefschrift.nl](http://persoonlijkproefschrift.nl))

Printing: Ridderprint BV

Copyright © Annika de Jong, Leiden 2020

All rights are reserved. No parts of this publication may be reproduced, stored in a retrieval system or transmitted in any form or by any means, without permission of the copyright owners

# **Personalized treatment for von Willebrand disease**

by RNA-targeted therapies

Proefschrift

ter verkrijging van  
de graad van Doctor aan de Universiteit Leiden  
op gezag van de Rector Magnificus Prof. mr. C.J.J.M. Stolker  
volgens besluit van het College voor Promoties  
te verdedigen op dinsdag 7 april 2020  
klokke 16.15 uur

door

Annika de Jong

Geboren te Spijkenisse in 1988

**Promotor**

Prof. dr. H.C.J. Eikenboom

**Copromotor**

Dr. B.J.M. van Vlijmen

**Leden promotiecommissie**

Prof. dr. H.H. Versteeg

Prof. dr. F.W.G. Leebeek

Prof. dr. J.J. Voorberg

Dr. C.V. Denis

Erasmus Universiteit Rotterdam

Universiteit van Amsterdam

Inserm U1176, Parijs, Frankrijk

The research described in this thesis was funded by a grant of The Landsteiner Foundation for Blood Transfusion Research (LSBR 1504) and by a research grant from CSL Behring.

Financial support by the Dutch Heart Foundation for the publication of this thesis is gratefully acknowledged.







## Table of contents

<b>Chapter 1:</b>	General introduction and outline of the thesis	9
<b>Chapter 2:</b>	Developments in the diagnostic procedures for von Willebrand disease	23
<b>Chapter 3:</b>	Von Willebrand disease mutation spectrum and associated mutation mechanisms	47
<b>Chapter 4:</b>	Correction of a dominant-negative von Willebrand factor multimerization defect by small interfering RNA-mediated allele-specific inhibition of mutant von Willebrand factor	73
<b>Chapter 5:</b>	Variability of von Willebrand factor-related parameters in endothelial colony forming cells	99
<b>Chapter 6:</b>	Defective von Willebrand factor multimerization in endothelial colony forming cells with low von Willebrand factor production	127
<b>Chapter 7:</b>	<i>Ex vivo</i> improvement of a von Willebrand disease type 2A phenotype using an allele-specific small interfering RNA	141
<b>Chapter 8:</b>	Amelioration of the murine von Willebrand disease type 2B phenotype using an allele-specific small interfering RNA	161
<b>Chapter 9:</b>	General discussion and perspectives	179
<b>Chapter 10:</b>	English summary	207
	Nederlandse samenvatting	212
<b>Appendix:</b>	Dankwoord	220
	Curriculum Vitae	221
	Publication list	222
	PhD portfolio	223



# 1

## General introduction and outline of the thesis



In 1998, Andrew Fire and Craig Mello discovered that double-stranded RNA molecules corresponding to the coding region of specific genes, can interfere with the production of proteins.<sup>1</sup> Fire and Mello named this phenomenon RNA interference (RNAi) and the invention of it has had many implications in fundamental as well as translational medical sciences.<sup>2</sup> It is therefore not without merit that both inventors received the Nobel Prize in physiology or medicine for this discovery in 2006. The discovery of RNAi was quickly followed by studies that shed light on the mechanism of RNAi.<sup>3-6</sup> Most importantly, it was established that small double-stranded RNA molecules of about 20-25 nucleotides are responsible for the interference process.<sup>3-5</sup> These short double-stranded RNA molecules are called small interfering RNAs (siRNAs) and can be generated intracellularly as a cleavage product of long double-stranded RNA molecules or can chemically be synthesized and experimentally introduced into cells.<sup>7,8</sup> For fundamental scientific purposes, siRNAs are used as a tool to inhibit the production of proteins and follow the consequences of this inhibition to better understand functional aspects and cellular mechanisms of proteins.<sup>9</sup> In translational science, synthetic siRNAs are used to minimize production of mutant or deleterious proteins and correct for disease phenotypes.<sup>10,11</sup> The use of synthetic siRNAs are also central to this thesis. Here, siRNAs are applied to correct phenotypes of the bleeding disorder von Willebrand disease (VWD).

### ***Von Willebrand disease and von Willebrand factor***

VWD is the most common inherited bleeding disorder, named after Erik von Willebrand who first described the disease in 1926.<sup>12</sup> VWD is mainly associated with easy bruising, post-surgical or traumatic bleeding, and mucocutaneous bleeding (e.g. nose or menstrual bleeding).<sup>13</sup> The bleeding phenotype of patients varies from mild, with only bruises and sparse nose bleeding, to severe, with bleeding from the gastrointestinal tract or joints.<sup>13,14</sup> In the past, many patients with mild bleeding symptoms have gone unnoticed since bleeding also occurs in the normal population. However, better awareness of the disease among clinicians and developments in the diagnostic procedures for VWD have resulted in better recognition of the disease.<sup>15</sup> This is especially essential when a patient undergoes surgical or dental procedures.

VWD is caused by defects in the multimeric protein von Willebrand factor (VWF), a highly glycosylated protein produced by endothelial cells and megakaryocytes.<sup>16</sup> Upon expression in the endothelial cells, VWF undergoes several modifications before it is constitutively secreted or stored as multimers in the endothelial storage organelles, the Weibel-Palade bodies (WPBs).<sup>17-20</sup> Endothelial activation by vascular damage or inflammation leads to the release of VWF from the WPBs.<sup>21</sup> The released VWF multimers will unroll into ultra-large VWF strings, a process that is mediated by shear stress induced by vascular flow.<sup>22,23</sup> These ultra-large VWF strings expose their A1 domain, allowing platelet binding through the platelet glycoprotein Iba (GPIba) receptor followed by platelet activation and aggregation.<sup>24</sup> The elongated form of VWF also opens up the cleavage site for the metalloprotease ADAMTS13

(a disintegrin and metalloprotease with thrombospondin type motifs 13) in the A2 domain. Cleavage of VWF by ADAMTS13 degrades the ultra-large VWF multimers in smaller sized multimers that are present in a globular form in the circulation.<sup>25,26</sup> In the circulation, VWF is the binding partner of coagulation factor VIII (FVIII), thereby increasing the FVIII half-life.<sup>27</sup>

Three types of VWD can be distinguished, VWD types 1, 2 and 3 (an overview of the VWD types is summarized in Table 1).<sup>28</sup> VWD type 1 is associated with decreased VWF plasma levels (<30 IU/dL) and is mainly caused by dominant negative mutations in VWF.<sup>28-30</sup> These mutations are distributed throughout the whole protein and may lead to decreased secretion of VWF from the endothelial cells, or increased clearance of VWF from the circulation.<sup>20</sup> VWD type 2 is associated with qualitative defects in VWF and patients are categorized among VWD types 2A, 2B, 2M and 2N, depending on the specific defect.<sup>28</sup> VWD type 2A patients have abnormal plasma multimers which is the result of either defective intracellular multimerization or increased cleavage of VWF by ADAMTS13.<sup>20</sup> VWD type 2B patients have gain-of-function mutations in the GPIIb $\alpha$  binding site in VWF and therefore platelets bind VWF even when VWF is in its inactive and globular form.<sup>20</sup> This VWF-platelet complex is cleared fast from the circulation which results in low platelet counts. In VWD type 2M, loss-of-function mutations in the GPIIb $\alpha$  binding site in VWF results in decreased affinity of VWF to platelets. Also, patients with a collagen binding defect are categorized among VWD type 2M.<sup>20,28,31</sup> VWD types 2A, 2B and 2M are all caused by dominant negative mutations in specific domains of VWF. VWD type 2N patients have a decreased binding to coagulation FVIII caused by homozygous or compound heterozygous mutations in the FVIII binding site.<sup>20,32</sup> Lastly, VWD type 3 patients have a complete absence of plasma VWF, which is generally caused by homozygous or compound heterozygous null mutations.<sup>20,28</sup>

### ***Treatment of von Willebrand disease***

The choice of VWD treatment depends on the type and severity of VWD. Mild cases of VWD are generally treated on demand using desmopressin (DDAVP).<sup>33</sup> DDAVP mediates the release of VWF from the endothelial cells through the Vasopressin receptor 2.<sup>34</sup> This leads to a short-term increase of endogenously produced circulating VWF, which is usually sufficient to stop bleeding after trauma or prevent bleeding during a planned intervention. DDAVP is, however, not effective in VWD type 3 patients since they do not synthesize VWF at all. Furthermore, DDAVP is contra-indicated in VWD type 2B patients, because increased release of endogenous mutant VWF will capture circulating platelets and therefore induce thrombocytopenia.<sup>35</sup> In cases where DDAVP is not effective or contra-indicated, a second treatment option is the administration of VWF-containing concentrates.<sup>36,37</sup> VWF-containing concentrate is an exogenous source of VWF and is either plasma-derived or recombinant. Recombinant VWF is only recently approved by the FDA and superiority of recombinant VWF over plasma-derived VWF has yet to be proven.<sup>38-41</sup>

**Table 1.** Overview of the VWD types, detailing the phenotype, pathophysiological mechanism, main VWF defect, affected domains and main inheritance

VWD type:	Phenotype	Pathophysiological mechanism:	Main VWF defect:	Affected domains:	Main inheritance pattern:
1	Decreased VWF plasma levels	<ul style="list-style-type: none"><li>Decreased synthesis of VWF</li><li>Decreased secretion of VWF from endothelial cells</li><li>Increased clearance of VWF from circulation</li></ul>	<ul style="list-style-type: none"><li>Null alleles</li><li>Missense mutations</li><li>Missense mutations</li></ul>	<ul style="list-style-type: none"><li>Any domain</li><li>Any domain</li><li>D3, A1, A3</li></ul>	Autosomal dominant
2A	Decreased high molecular weight VWF multimers	<ul style="list-style-type: none"><li>Affected intracellular VWF dimerization/multimerization</li><li>Increased cleavage of VWF by ADAMTS13</li></ul>	<ul style="list-style-type: none"><li>Missense mutations</li><li>Missense mutations</li></ul>	<ul style="list-style-type: none"><li>Propeptide, D3, A1, A2, CK</li><li>A2</li></ul>	Autosomal dominant
2B	Increased VWF-platelet binding	<ul style="list-style-type: none"><li>Mutant GPIIb<math>\alpha</math> binding site</li></ul>	<ul style="list-style-type: none"><li>Missense mutations</li></ul>	<ul style="list-style-type: none"><li>A1</li></ul>	Autosomal dominant
2M	Decreased VWF-platelet binding Decreased VWF collagen binding	<ul style="list-style-type: none"><li>Mutant GPIIb<math>\alpha</math> binding site</li><li>Mutant collagen binding site</li></ul>	<ul style="list-style-type: none"><li>Missense mutations</li><li>Missense mutations</li></ul>	<ul style="list-style-type: none"><li>A1</li><li>A1, A3</li></ul>	Autosomal dominant
2N	Decreased VWF-FVIII binding	<ul style="list-style-type: none"><li>Mutant factor VIII binding site</li></ul>	<ul style="list-style-type: none"><li>Missense mutations</li></ul>	<ul style="list-style-type: none"><li>D', D3</li></ul>	Autosomal recessive
3	Absence of VWF plasma levels	<ul style="list-style-type: none"><li>No VWF synthesis</li></ul>	<ul style="list-style-type: none"><li>Null alleles</li></ul>	<ul style="list-style-type: none"><li>Any domain</li></ul>	Autosomal recessive

Although both treatment modalities are generally sufficient to stop bleeding, multiple limitations can be described. Firstly, repeated dosing of DDAVP has been associated with tachyphylaxis, and side-effects like flushing of the face, nausea and headaches.<sup>42</sup> Incidentally, also deep-vein thrombosis has been reported as adverse event to administration of VWF-containing concentrates.<sup>43</sup> Secondly, the effects of both treatments are short-term and, unless being on long-term prophylaxis of VWF-containing concentrates, patients are not protected for sudden bleeding which decreases the quality of life.<sup>44,45</sup> Then, mutant VWF remains to be produced and secreted into the circulation. This may lead to dangerously deep thrombocytopenia in VWD type 2B patients during stress-induced VWF release of mutant VWF.<sup>46-48</sup> Lastly, both DDAVP and VWF-containing concentrates cannot correct for phenotypes developed by long-term exposure to mutant VWF. An important example is the development of intestinal angiodysplasia, resulting in severe intestinal bleeding. A trait that is more common among VWD patients compared to the normal population.<sup>49,50</sup> Recent evidence showed that angiodysplasia is the result of defective VWF and cannot be corrected by DDAVP or VWF-containing concentrates.<sup>9,51-54</sup>



Since presence of mutant VWF is detrimental in several situations, we hypothesized that inhibition of mutant VWF in dominant negative VWD improves the function of VWF and ameliorate VWD phenotypes. In this thesis, we propose the use of allele-specific siRNAs to target mutant *VWF* alleles.

### ***Small interfering RNAs***

siRNAs are small double-stranded RNA molecules, containing a passenger (sense) strand and a guide (antisense) strand. siRNAs can intracellularly be generated by cleavage of long double-stranded RNA molecules by the endo-ribonuclease dicer, or can chemically be synthesized and experimentally introduced into cells.<sup>8</sup> In this thesis, we make use of synthetic siRNAs. Synthetic siRNAs generally have a length of 21 nucleotides and are asymmetric because of a two nucleotide overhang at the 3' end of both strands. When an siRNA enters a human cell, it associates with proteins from the RNA-induced silencing complex (RISC; Fig. 1).<sup>55</sup> Although siRNAs were discovered already 30 years ago, the precise mechanism of siRNA loading into RISC is not yet fully elucidated. In humans, it is known that RISC consists of at least Dicer, a double-stranded RNA binding protein, the endonuclease Argonaute 2 (Ago2) and the chaperone heat shock protein 90 (HSP90).<sup>56</sup> Dicer and the trans-activation responsive RNA binding protein (TRBP) bind the asymmetric siRNA and attract Ago2 and HSP90.<sup>57</sup> HSP90 facilitates direct binding of Ago2 to the siRNA, which is followed by unwinding of the duplex and passenger strand removal.<sup>58</sup> Ago2 then directs the guide strand to the targeted mRNA. The guide strand of the siRNA binds the target mRNA through Watson-Crick base pairing.<sup>59</sup> Ago2 then cleaves the mRNA, preventing translation of the mRNA into protein.<sup>60</sup>

siRNAs are able to downregulate genes when the siRNA sequence is in full complementarity with the mRNA sequence. Mismatches between the siRNA and the mRNA might prevent the cleavage ability.<sup>59</sup> This feature enables the use of siRNAs for allele-specific inhibition of mutant alleles in diseases caused by dominant negative mutations. This approach already proved successful *in vitro* as well as *in vivo* for several dominant negative diseases.<sup>61-65</sup> Two approaches of allele-specific inhibition based on single nucleotide mismatches might be applied. You could target the dominant negative mutation itself, because a patient is always heterozygous for that mutation.<sup>61,63,64</sup> Or you could target a single-nucleotide polymorphism (SNP) for which a patient is heterozygous.<sup>63,65</sup> In the latter, linkage analysis should be performed to identify which of the SNP-alleles is located on the diseased allele. Both approaches have been described in this thesis to target dominant negative VWD.

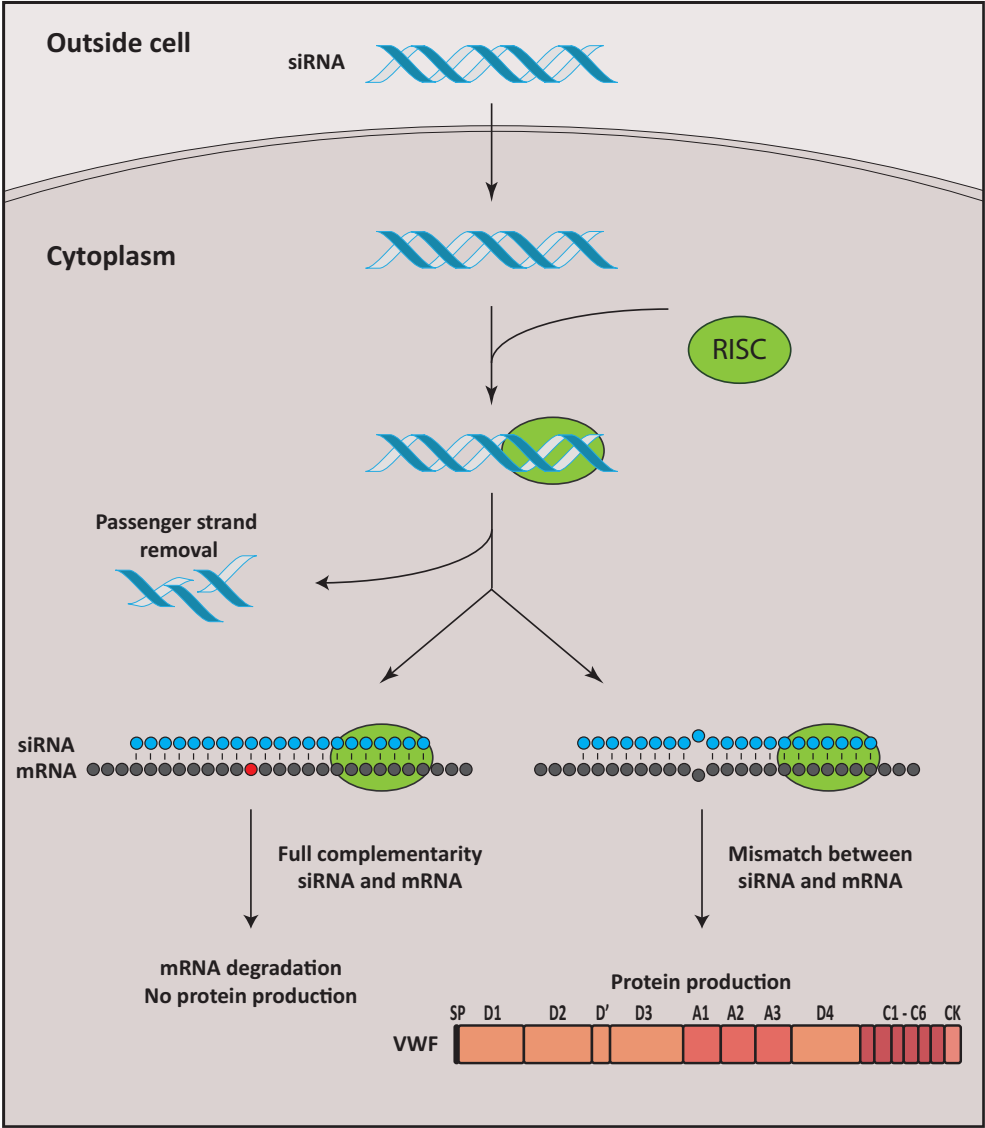


**Figure 1. Allele-specific siRNA mechanism.** After experimental introduction of a synthetic siRNA into the cell, it associates with the RNA-induced silencing complex (RISC). In humans, RISC consists of at least Dicer, Argonaute 2, the trans-activation responsive RNA binding protein (TRBP) and heat shock protein 90 (HSP90). RISC binding induces unwinding of the siRNA and passenger strand removal. The guide strand is then transported by RISC to the targeted mRNA. Full complementarity of the guide strand to the mRNA leads to mRNA degradation. A nucleotide mismatch between the siRNA and the mRNA might prevent cleavage of the mRNA, which results in normal translation of the mRNA into protein. This feature allows the use of siRNAs to inhibit single (mutant) alleles when a heterozygous variation within a gene is targeted. mRNA, messenger RNA; siRNA, small interfering RNA; VWF, von Willebrand factor

## Outline of the thesis

This thesis brings together the fields of the hemorrhagic disorder VWD and RNA therapeutics. First, in **Chapter 2**, the developments in the diagnostic procedures for VWD are reviewed. This chapter explains the diagnostic tests that are required for correct diagnosis of VWD patients. Diagnosis of VWD can especially be challenging because of the heterogeneity of the disease.

The heterogeneity of VWD and the disease-causing protein VWF clearly emerges from **Chapter 3**. In this chapter, all VWF mutations that have been described in literature until early 2017 are reviewed and assessed with respect to pathogenic mechanisms. The disease-causing mechanisms of the mutations are explained throughout this chapter per VWD type. Also, an elaborative description of the VWF synthesis is included.

Most mutations that cause VWD are dominant negative mutations, meaning that only one of the two alleles is affected. This allows the hypothesis that allele-specific inhibition of the mutant *VWF* allele would improve VWF function and ameliorate VWD phenotypes. This hypothesis is tested in several cellular and animal models.

**Chapter 4** describes the first *in vitro* proof of principle studies of allele-specific *VWF* inhibition in Human Embryonic Kidney 293 (HEK293) cells. In this study, we show that allele-specific siRNAs that target frequent SNPs in *VWF* can discriminate between two *VWF* alleles in *VWF* overexpressing HEK293 cells. When we targeted a SNP located on the same allele as a known *VWF* mutation causing a VWD type 2A phenotype, we were able to correct for the VWD type 2A multimerization defect.

HEK293 cells are a good model to prove the principle of allele-specific inhibition and to select a set of effective siRNAs. They, however, have no endogenous VWF expression. An endothelial VWD cell model is therefore necessary to extend the proof of principle to a more physiological relevant environment. Endothelial colony forming cells (ECFCs) are cultured endothelial cells that can be isolated from peripheral blood. These cells can be isolated from VWD patients and are therefore an ideal model to test the approach of allele-specific inhibition to correct for a patient's phenotype.

**Chapter 5** describes the validation of the ECFCs as *ex vivo* model for VWD. In this study we standardized the experimental procedures of ECFCs. With this standardized experimental set-up, we show clear variations in cell morphologies and VWF expression. These variations are important to keep in mind when performing experiments with (patient-derived) ECFCs.

The effects of siRNA-mediated inhibition of *VWF* on healthy control ECFCs are described in **Chapter 6**. Interestingly, we observed that downregulation of the production of VWF in

healthy control ECFCs does affect the processing of VWF. In VWF downregulated ECFCs, a larger proportion of the produced VWF is secreted from the cells and this VWF has decreased high molecular weight VWF multimers.

**Chapter 7** describes allele-specific inhibition of *VWF* in healthy control and patient-derived ECFCs. We show that the allele-specific siRNAs that were selected in Chapter 4, are also effective in ECFCs. Furthermore, we show the characterization and correction of ECFCs that have been isolated from a VWD type 2A patient.

In **Chapter 8**, we extend the proof of principle of allele-specific *VWF* inhibition to a heterozygous VWD type 2B mouse model. We use a mouse model based on hydrodynamic injection of *Vwf* cDNA in a VWF deficient mouse resulting in hepatic VWF expression, and show that an siRNA against mouse *Vwf* p.Val1316Met is able to improve the VWD type 2B platelet phenotype.

## References

1. Fire A, Xu S, Montgomery MK, Kostas SA, Driver SE, Mello CC. Potent and specific genetic interference by double-stranded RNA in *Caenorhabditis elegans*. *Nature*. 1998;**391**(6669):806-811.
2. Cejka D, Losert D, Wacheck V. Short interfering RNA (siRNA): tool or therapeutic? *Clin Sci*. 2006;**110**(1):47-58.
3. Zamore PD, Tuschl T, Sharp PA, Bartel DP. RNAi: Double-stranded RNA directs the ATP-dependent cleavage of mRNA at 21 to 23 nucleotide intervals. *Cell*. 2000;**101**(1):25-33.
4. Hammond SM, Bernstein E, Beach D, Hannon GJ. An RNA-directed nuclease mediates post-transcriptional gene silencing in *Drosophila* cells. *Nature*. 2000;**404**(6775):293-296.
5. Elbashir SM, Lendeckel W, Tuschl T. RNA interference is mediated by 21- and 22-nucleotide RNAs. *Genes Dev*. 2001;**15**(2):188-200.
6. Bernstein E, Caudy AA, Hammond SM, Hannon GJ. Role for a bidentate ribonuclease in the initiation step of RNA interference. *Nature*. 2001;**409**(6818):363-366.
7. Caplen NJ, Parrish S, Imani F, Fire A, Morgan RA. Specific inhibition of gene expression by small double-stranded RNAs in invertebrate and vertebrate systems. *Proc Natl Acad Sci U S A*. 2001;**98**(17):9742-9747.
8. Snead NM, Wu X, Li A, et al. Molecular basis for improved gene silencing by Dicer substrate interfering RNA compared with other siRNA variants. *Nucleic Acids Res*. 2013;**41**(12):6209-6221.
9. Starke RD, Ferraro F, Paschalaki KE, et al. Endothelial von Willebrand factor regulates angiogenesis. *Blood*. 2011;**117**(3):1071-1080.
10. Adams D, Gonzalez-Duarte A, O'Riordan WD, et al. Patisiran, an RNAi Therapeutic, for Hereditary Transthyretin Amyloidosis. *N Engl J Med*. 2018;**379**(1):11-21.
11. Setten RL, Rossi JJ, Han SP. The current state and future directions of RNAi-based therapeutics. *Nat Rev Drug Discov*. 2019;**18**(6):421-446.
12. Von Willebrand EA. Hereditär pseudohemofili. *Finska Läkaresällskapets Handlingar*. 1926;**69**:87-112.
13. Tosetto A, Rodeghiero F, Castaman G, et al. A quantitative analysis of bleeding symptoms in type 1 von Willebrand disease: results from a multicenter European study (MCMDM-1 VWD). *J Thromb Haemost*. 2006;**4**(4):766-773.
14. deWee EM, Sanders YV, Mauser-Bunschoten EP, et al. Determinants of bleeding phenotype in adult patients with moderate or severe von Willebrand disease. *Thromb Haemost*. 2012;**108**(4):683-692.
15. de Jong A, Eikenboom J. Developments in the diagnostic procedures for von Willebrand disease. *J Thromb Haemost*. 2016;**14**(3):449-460.
16. Leebeek FW, Eikenboom JC. Von Willebrand's Disease. *N Engl J Med*. 2016;**375**(21):2067-2080.
17. Lopes da Silva M, Cutler DF. von Willebrand factor multimerization and the polarity of secretory pathways in endothelial cells. *Blood*. 2016;**128**(2):277-285.
18. Mourik MJ, Faas FG, Zimmermann H, Voorberg J, Koster AJ, Eikenboom J. Content delivery

- to newly forming Weibel-Palade bodies is facilitated by multiple connections with the Golgi apparatus. *Blood*. 2015;**125**(22):3509-3516.
19. Valentijn KM, Eikenboom J. Weibel-Palade bodies: a window to von Willebrand disease. *J Thromb Haemost*. 2013;**11**(4):581-592.
  20. de Jong A, Eikenboom J. Von Willebrand disease mutation spectrum and associated mutation mechanisms. *Thromb Res*. 2017;**159**:65-75.
  21. Rondaij MG, Bierings R, Kragt A, van Mourik JA, Voorberg J. Dynamics and plasticity of Weibel-Palade bodies in endothelial cells. *Arterioscler Thromb Vasc Biol*. 2006;**26**(5):1002-1007.
  22. Dong JF, Moake JL, Nolasco L, et al. ADAMTS-13 rapidly cleaves newly secreted ultralarge von Willebrand factor multimers on the endothelial surface under flowing conditions. *Blood*. 2002;**100**(12):4033-4039.
  23. De Ceunynck K, De Meyer SF, Vanhoorelbeke K. Unwinding the von Willebrand factor strings puzzle. *Blood*. 2013;**121**(2):270-277.
  24. Savage B, Saldivar E, Ruggeri ZM. Initiation of platelet adhesion by arrest onto fibrinogen or translocation on von Willebrand factor. *Cell*. 1996;**84**(2):289-297.
  25. Crawley JT, de Groot R, Xiang Y, Luken BM, Lane DA. Unraveling the scissile bond: how ADAMTS13 recognizes and cleaves von Willebrand factor. *Blood*. 2011;**118**(12):3212-3221.
  26. Lippok S, Radtke M, Obser T, et al. Shear-Induced Unfolding and Enzymatic Cleavage of Full-Length VWF Multimers. *Biophys J*. 2016;**110**(3):545-554.
  27. Weiss HJ, Sussman II, Hoyer LW. Stabilization of factor VIII in plasma by the von Willebrand factor. Studies on posttransfusion and dissociated factor VIII and in patients with von Willebrand's disease. *J Clin Invest*. 1977;**60**(2):390-404.
  28. Sadler JE, Budde U, Eikenboom JC, et al. Update on the pathophysiology and classification of von Willebrand disease: a report of the Subcommittee on von Willebrand Factor. *J Thromb Haemost*. 2006;**4**(10):2103-2114.
  29. Goodeve A, Eikenboom J, Castaman G, et al. Phenotype and genotype of a cohort of families historically diagnosed with type 1 von Willebrand disease in the European study, Molecular and Clinical Markers for the Diagnosis and Management of Type 1 von Willebrand Disease (MCMDM-1VWD). *Blood*. 2007;**109**(1):112-121.
  30. Flood VH, Christopherson PA, Gill JC, et al. Clinical and laboratory variability in a cohort of patients diagnosed with type 1 VWD in the United States. *Blood*. 2016;**127**(20):2481-2488.
  31. Flood VH, Gill JC, Christopherson PA, et al. Critical von Willebrand factor A1 domain residues influence type VI collagen binding. *J Thromb Haemost*. 2012;**10**(7):1417-1424.
  32. Casonato A, Galletta E, Sarolo L, Daidone V. Type 2N von Willebrand disease: Characterization and diagnostic difficulties. *Haemophilia*. 2018;**24**(1):134-140.
  33. Sharma R, Flood VH. Advances in the diagnosis and treatment of Von Willebrand disease. *Blood*. 2017;**130**(22):2386-2391.
  34. Mannucci PM, Ruggeri ZM, Pareti FI, Capitanio A. 1-Deamino-8-d-arginine vasopressin: a new pharmacological approach to the management of haemophilia and von Willebrands' diseases.

- Lancet*. 1977;**1**(8017):869-872.
35. Kruse-Jarres R, Johnsen JM. How I treat type 2B von Willebrand disease. *Blood*. 2018;**131**(12):1292-1300.
  36. Srivastava A, Serban M, Werner S, Schwartz BA, Kessler CM, Investigators WS. Efficacy and safety of a VWF/FVIII concentrate (wilate (R)) in inherited von Willebrand disease patients undergoing surgical procedures. *Haemophilia*. 2017;**23**(2):264-272.
  37. Miesbach W, Krekeler S, Wolf Z, Seifried E. Clinical use of Haemate (R) P in von Willebrand disease: A 25-year retrospective observational study. *Thrombosis Research*. 2015;**135**(3):479-484.
  38. Peyvandi F, Kouides P, Turecek PL, Dow E, Berntorp E. Evolution of replacement therapy for von Willebrand disease: From plasma fraction to recombinant von Willebrand factor. *Blood Rev*. 2019;**38**:100572.
  39. Peyvandi F, Mamaev A, Wang JD, et al. Phase 3 study of recombinant von Willebrand factor in patients with severe von Willebrand disease who are undergoing elective surgery. *J Thromb Haemost*. 2019;**17**(1):52-62.
  40. Franchini M, Mannucci PM. Von Willebrand factor (Vonvendi(R)): the first recombinant product licensed for the treatment of von Willebrand disease. *Expert Rev Hematol*. 2016;**9**(9):825-830.
  41. Rajpurkar M, Frey MJ, Sabo C, Hollon W. Recombinant Von Willebrand factor concentrate in 2A Von Willebrand disease: comparison to plasma-derived Von Willebrand factor concentrate therapy. *Blood Coagul Fibrinolysis*. 2019;**30**(4):168-170.
  42. Stoof SC, Cnossen MH, de Maat MP, Leebeek FW, Kruip MJ. Side effects of desmopressin in patients with bleeding disorders. *Haemophilia*. 2016;**22**(1):39-45.
  43. Gill JC, Mannucci PM. Thromboembolic incidence with transiently elevated levels of coagulation factors in patients with von Willebrand disease treated with VWF:FVIII concentrate during surgery. *Haemophilia*. 2014;**20**(6):E404-E406.
  44. de Wee EM, Fijnvandraat K, de Goede-Bolder A, et al. Impact of von Willebrand disease on health-related quality of life in a pediatric population. *J Thromb Haemost*. 2011;**9**(3):502-509.
  45. Berntorp E, Petrini P. Long-term prophylaxis in von Willebrand disease. *Blood Coagul Fibrinolysis*. 2005;**16 Suppl 1**:S23-26.
  46. Casonato A, Sartori MT, Bertomoro A, Fede T, Vasoin F, Girolami A. Pregnancy-induced worsening of thrombocytopenia in a patient with type IIB von Willebrand's disease. *Blood Coagul Fibrinolysis*. 1991;**2**(1):33-40.
  47. Rick ME, Williams SB, Sacher RA, McKeown LP. Thrombocytopenia associated with pregnancy in a patient with type IIB von Willebrand's disease. *Blood*. 1987;**69**(3):786-789.
  48. Hultin MB, Sussman II. Postoperative thrombocytopenia in type IIB von Willebrand disease. *Am J Hematol*. 1990;**33**(1):64-68.
  49. Selvam S, James P. Angiodysplasia in von Willebrand Disease: Understanding the Clinical and Basic Science. *Semin Thromb Hemost*. 2017;**43**(6):572-580.
  50. Castaman G, Federici AB, Tassetto A, et al. Different bleeding risk in type 2A and 2M von Willebrand disease: a 2-year prospective study in 107 patients. *J Thromb Haemost*. 2012;**10**(4):632-638.

51. Starke RD, Paschalaki KE, Dyer CE, et al. Cellular and molecular basis of von Willebrand disease: studies on blood outgrowth endothelial cells. *Blood*. 2013;**121**(14):2773-2784.
52. Groeneveld DJ, van Bakkum T, Dirven RJ, et al. Angiogenic characteristics of blood outgrowth endothelial cells from patients with von Willebrand disease. *J Thromb Haemost*. 2015;**13**(10):1854-1866.
53. Ishihara J, Ishihara A, Starke RD, et al. The heparin binding domain of von Willebrand factor binds to growth factors and promotes angiogenesis in wound healing. *Blood*. 2019;**133**(24):2559-2569.
54. Cossutta M, Darche M, Carpentier G, et al. Weibel-Palade Bodies Orchestrate Pericytes During Angiogenesis. *Arterioscler Thromb Vasc Biol*. 2019;**39**(9):1843-1858.
55. Pratt AJ, MacRae IJ. The RNA-induced silencing complex: a versatile gene-silencing machine. *J Biol Chem*. 2009;**284**(27):17897-17901.
56. Meister G. Argonaute proteins: functional insights and emerging roles. *Nat Rev Genet*. 2013;**14**(7):447-459.
57. Chendrimada TP, Gregory RI, Kumaraswamy E, et al. TRBP recruits the Dicer complex to Ago2 for microRNA processing and gene silencing. *Nature*. 2005;**436**(7051):740-744.
58. Iwasaki S, Kobayashi M, Yoda M, et al. Hsc70/Hsp90 Chaperone Machinery Mediates ATP-Dependent RISC Loading of Small RNA Duplexes. *Molecular Cell*. 2010;**39**(2):292-299.
59. Kunne T, Swarts DC, Brouns SJ. Planting the seed: target recognition of short guide RNAs. *Trends Microbiol*. 2014;**22**(2):74-83.
60. Liu J, Carmell MA, Rivas FV, et al. Argonaute2 is the catalytic engine of mammalian RNAi. *Science*. 2004;**305**(5689):1437-1441.
61. Noguchi S, Ogawa M, Kawahara G, Malicdan MC, Nishino I. Allele-specific Gene Silencing of Mutant mRNA Restores Cellular Function in Ullrich Congenital Muscular Dystrophy Fibroblasts. *Mol Ther Nucleic Acids*. 2014;**3**:e171.
62. Zaleta-Rivera K, Dainis A, Ribeiro AJS, et al. Allele-Specific Silencing Ameliorates Restrictive Cardiomyopathy Attributable to a Human Myosin Regulatory Light Chain Mutation. *Circulation*. 2019;**140**(9):765-778.
63. Miller VM, Xia H, Marrs GL, et al. Allele-specific silencing of dominant disease genes. *Proc Natl Acad Sci U S A*. 2003;**100**(12):7195-7200.
64. Novelli F, Lena AM, Panatta E, et al. Allele-specific silencing of EEC p63 mutant R304W restores p63 transcriptional activity. *Cell Death Dis*. 2016;**7**:e2227.
65. Pfister EL, Kennington L, Straubhaar J, et al. Five siRNAs targeting three SNPs may provide therapy for three-quarters of Huntington's disease patients. *Curr Biol*. 2009;**19**(9):774-778.









# 2

## Developments in the diagnostic procedures for von Willebrand disease

Annika de Jong  
Jeroen Eikenboom

*Journal of Thrombosis and Haemostasis* (2015) 14 (3):449-460

## Abstract

Von Willebrand disease (VWD) is the most common inherited bleeding disorder but its diagnosis can be challenging due to the heterogeneity of the disease. VWD is mainly associated with mild mucocutaneous bleeding, although there are more severe phenotypes with bleeding from the gastrointestinal tract or even the joints. Also, surgical interventions and trauma may lead to critical bleeding events. These bleeding episodes are all related to quantitative or qualitative defects of von Willebrand factor (VWF), a multimeric glycoprotein produced by endothelial cells and megakaryocytes, which mediates platelet adhesion and aggregation and binds factor VIII (FVIII) in the circulation. This review describes the diagnostic procedures required for correct diagnosis. Accurate diagnosis and classification is required for proper treatment and counseling. Assessment of bleeding starts with the medical history. After a positive bleeding or family history, subsequent laboratory investigations will start with a panel of standard screening tests for hemostatic defects. Patients suspected of having VWD will be tested for plasma VWF antigen levels, the ability of VWF to bind platelets and FVIII activity. When VWD is confirmed, a set of subtyping tests can classify the patients as VWD types 1, 2 (A, B, M or N) or 3. The performance of some additional assays and analyses, such as VWF propeptide measurement or genetic analysis, may help in identifying the pathological mechanism behind certain defects or can guide in the choice of treatment.

## Introduction

von Willebrand disease (VWD) is the most common inherited bleeding disorder and is mainly associated with mucocutaneous and postoperative bleeding. The underlying cause of these symptoms is a qualitative or quantitative defect of the von Willebrand factor (VWF) protein. According to population studies, about 1% of the population shows defects of VWF fitting the diagnostic criteria; however, only about 0.01% of the population is reported to develop clinically significant bleeding.<sup>1-5</sup> The actual prevalence probably lies somewhere in the middle, with many people having undiagnosed VWD-related bleeding.

VWF is a large multimeric glycoprotein produced in endothelial cells and megakaryocytes. Endothelial cells are the main source of circulating VWF and store VWF multimers in cigar-shaped vesicles called Weibel-Palade bodies (WPBs).<sup>6</sup> Signals released after vascular injury stimulate the secretion of the contents of WPBs, including VWF, into the circulation. There, VWF unfolds under flow into ultra-long VWF (UL-VWF) strings that attract platelets by binding the platelet glycoprotein Ib (GPIb) receptor to the A1-domain of VWF. The multimeric size, and therefore the platelet binding activity of VWF, is regulated by cleavage of the UL-VWF strings by ADAMTS13 (a disintegrin and metalloproteinase with a thrombospondin type 1 motif, member 13).<sup>7</sup> In the circulation, VWF has a half-life of about 12 hours and functions, apart from its platelet binding activity, as a binding protein and stabilizer of coagulation factor VIII (FVIII).<sup>8,9</sup>

Defects in VWF synthesis, storage, secretion or clearance, or a combination thereof, can lead to a deficiency of plasma VWF.<sup>10-15</sup> This can be either a partial deficiency leading to VWD type 1 or a (virtually) complete deficiency causing VWD type 3. Qualitative defects of plasma VWF cause VWD type 2, which can be subcategorized into types 2A, 2B, 2M and 2N.<sup>16</sup> VWD type 2A is characterized by a decreased ability of VWF to bind platelet GPIb due to a decreased level of high-molecular-weight (HMW) VWF multimers. In VWD type 2B, a gain-of-function mutation in the GPIb binding site of VWF leads to the spontaneous binding of VWF to platelets without prior activation of VWF. The spontaneously formed VWF-platelet aggregates are quickly cleared, resulting in a variable degree of thrombocytopenia and consumption of HMW VWF multimers. In VWD type 2M, usually a loss-of-function mutation in the region of GPIb binding leads to a decreased binding affinity for platelets. However, other defects, such as an isolated defect in collagen binding, are also classified among VWD type 2M. Binding of FVIII to VWF is decreased in VWD type 2N, as a result of mutations in the FVIII binding site on VWF. Most VWD types 1 and 2 are inherited as an autosomal dominant trait with mainly dominant negative missense mutations in *VWF* as the causative factor.<sup>17</sup> VWD type 2N and type 3 are inherited as an autosomal recessive trait mainly caused by homozygous or compound heterozygous *VWF* mutations, although co-dominant *VWF* mutations are also observed (Table 1).<sup>18</sup>

**Table 1.** Classification and etiology of VWD

Type	Disease mechanism	Inheritance	Genetic defects*
1	Partial quantitative deficiency of VWF	Autosomal dominant	Missense mutations (85-90%), null alleles (10-15%), variable penetrance
2A	Decreased VWF-dependent platelet adhesion due to a selective deficiency of HMW VWF multimers	Autosomal dominant Autosomal recessive	Missense mutations, mainly in D3, A2, and CK domains Missense mutations in propeptide
2B	Increased affinity of VWF for platelet GPIb	Autosomal dominant	Missense mutations in A1 domain
2M	Decreased VWF-dependent platelet adhesion without a selective deficiency of HMW VWF multimers	Autosomal dominant	Missense mutations in A1 domain
2N	Decreased binding affinity of VWF for factor VIII	Autosomal recessive	Missense mutations in D' and D3 domains
3	Virtually complete deficiency of VWF	Autosomal recessive	Mainly null alleles, often consanguinity

\* The majority of the genetic defects are found in the indicated domains, however there are exceptions. VWF, von Willebrand factor; HMW, high molecular weight; GPIb, glycoprotein Ib.

Accurate diagnosis and classification of VWD patients is of importance in the choice of treatment and in counseling regarding inheritance. However, a good diagnosis of VWD is difficult due to the heterogeneity of the disease and several different diagnostic tests are required. An overview of the diagnostic tests required can be found in Fig. 1. In this review we will describe and discuss the diagnostic approach from a first suspicion of a patient having a bleeding disorder to the specific sub-classification of VWD. Finally, additional tools will be described that can help to identify the pathophysiologic mechanisms behind VWF defects.

**Assessment of bleeding history**

The assessment of bleeding history is the first and possibly the most important test in the analysis of a suspected bleeding tendency, as laboratory evaluation will only be initiated after the suspicion has arisen. In general, hemostatic defects are more likely when someone has multiple bleeding symptoms or bleeding at different sites. The severity of the bleeding disorder can be judged from the frequency of bleeding and the age at which the bleeding problems started. The nature of the bleeding symptoms is also important and may already be suggestive of specific defects of hemostasis. In VWD, mucocutaneous bleeding is particularly present: bruises, bleeding from minor wounds, gum bleeding, epistaxis, menorrhagia, and bleeding from the gastrointestinal tract. Apart from spontaneous bleeding, patients with VWD also experience bleeding after procedures such as surgery or tooth extraction and at hemostatic challenges such as childbirth or trauma. The severity of VWD ranges from very mild with bleeding after major procedures only, up to spontaneous bleeding, including muscle and joint bleeding, in the most severe cases.

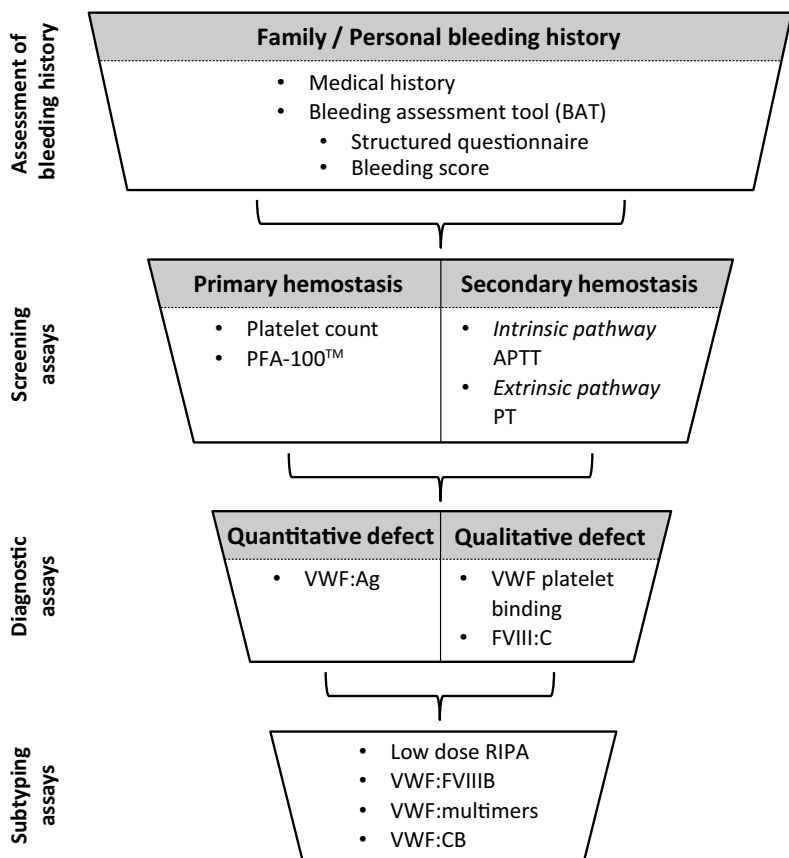


**Figure 1. Overview of the phases in diagnosis of von Willebrand disease (VWD).** Each phase describes the diagnostic tests required for diagnosing VWD. In the assessment of the bleeding history, hemostatic defects can be identified by the medical history, which can be guided by the bleeding assessment tool. Screening assays are performed to exclude other hemostatic disorders. Suggested VWD is confirmed by a set of standard diagnostic tests and the subtyping assays can categorize VWD into VWD types 1, 2 (A, B, M and N) and 3. PFA, platelet function analyzer; APTT, activated partial thromboplastin time; PT, prothrombin time; VWF:Ag, VWF antigen; FVIII:C, FVIII activity; RIPA, ristocetin-induced platelet aggregation; VWF:FVIII B, VWF-FVIII binding assay; VWF:CB, VWF collagen binding.

To improve bleeding history as a diagnostic tool, structured questionnaires and quantitative scoring systems have been developed.<sup>19-21</sup> The bleeding score most often used, and frequently referred to as the ‘Tosetto’ bleeding score, was validated in a European population of 417 patients with a mild form of VWD, 295 unaffected family members of those patients and 195 healthy controls.<sup>21</sup> The scoring system evaluates 12 different bleeding symptoms and the symptoms are scored from -1 (e.g. no bleeding after multiple tooth extractions) to +4 (e.g. requirement of blood transfusion after tooth extraction) depending on the presence and severity of the symptom. This leads to a cumulative score reflecting the severity of the bleeding history. Recently, more condensed, pediatric and self-administered versions

of the bleeding score have been developed.<sup>22-24</sup> Also, a web-based version of the bleeding assessment tool, endorsed by the International Society on Thrombosis and Haemostasis, has been published (ISTH-BAT; <https://bh.rockefeller.edu/ISTHBATR/>). These bleeding scores are evidently valuable in research and allow quantitative comparison between different types of VWD patients and between cohorts of patients. However, the individual diagnostic value of the scores is limited: the scores are age dependent (increasing with age); the scores record the severest bleeding event only (lacking information on frequency); the symptoms are not diagnosis specific; and the questionnaires are time consuming. The main clinical value of the bleeding assessment tools may be in excluding a bleeding disorder. We found in a prospective study using a simplified version of the tool that a normal bleeding score ( $\leq 3$ ) had a negative predictive value of 99.2%. The positive predictive value was limited when assuming a low prevalence of the bleeding disorder in the general population. However, the positive predictive value was reasonable (about 70%) among patients referred for evaluation of an abnormal clotting test or family investigation.<sup>23</sup>

## Screening assays for bleeding disorders

When the bleeding or family history of a patient suggests the possible presence of a bleeding disorder, a series of standard hemostatic screening assays will usually be performed. In the context of this review on the diagnosis of VWD it should be remembered that those assays are not intended for the diagnosis of VWD per se, but are performed to exclude alternative diagnoses.

Screening tests for defects in primary hemostasis include platelet count and functional tests such as bleeding time (BT) or platelet function analyzer (PFA-100™), which has replaced BT measurements in most laboratories.<sup>25-27</sup> Decreased platelet count may be indicative of the thrombocytopenia that can be present in VWD type 2B. An increased PFA-100™ closure time indicates a defect in primary hemostasis. More severe platelet function disorders, such as Glanzmann thrombasthenia, Bernard–Soulier syndrome and severe forms of VWD, can be excluded using this test.<sup>28</sup> However, the test is not sensitive enough to detect all forms of VWD.<sup>26,29,30</sup> Therefore, more specific diagnostic tests for VWD are required.

Screening tests for defects in secondary hemostasis include the activated partial thromboplastin time (APTT) and the prothrombin time (PT). Prolonged APTT indicates a defect in the intrinsic pathway of coagulation, whereas prolonged PT identifies defects in the extrinsic pathway of coagulation. Prolongation of the APTT can be indicative of the diagnosis of VWD as it may reflect the concurrent decrease of FVIII in VWD, especially in VWD types 3 and 2N. The results of the above-mentioned screening tests can guide in the selection of further



specific VWD testing. A prolonged BT or PFA-100™ in combination with prolonged APTT may suggest VWD, but milder cases of VWD may show normal results for all these screening tests.

## Diagnostic assays for VWD

To confirm or exclude VWD, a set of diagnostic tests needs to be performed. These tests include determination of the quantity of circulating VWF, VWF-platelet binding activity and FVIII activity. Based on these results, VWD can either be excluded or the patients can roughly be categorized as type 1, 2 or 3 VWD. Only when these tests indicate VWD, are additional subtyping assays required.

### VWF antigen levels

The quantity of VWF antigen (VWF:Ag) in plasma can be determined by enzyme-linked immunosorbent assay (ELISA) or automated latex immunoassay (LIA).<sup>31,32</sup> LIA has the advantage that it is an automated assay and that it is very reproducible, but has limitations when measuring VWF plasma levels lower than 10 IU/dL or higher than 125 IU/dL.<sup>33</sup> Therefore it may not be possible to distinguish severe VWD type 1 and VWD type 3. The lower limit of detection of the VWF:Ag ELISA in the study by Castaman *et al.*<sup>33</sup> was 5 IU/dL, but with adaptation of the ELISA lower limits are possible. The VWF:Ag ELISA is, however, somewhat less reproducible than the LIA.

Plasma VWF:Ag levels of a healthy population are very variable and depend on many factors. Most studies have been performed on subjects from European descent and do not reflect all subjects worldwide. In a large European study among 1049 healthy individuals, the mean VWF:Ag level was determined to be 100.1 IU/dL, with a standard deviation (SD) of 31.9 IU/dL.<sup>33</sup> This results in a normal reference range for the Caucasian population, defined as mean  $\pm$  2 SD of 36.3-163.9 IU/dL. Higher levels of VWF:Ag are, however, found in subjects with African and Korean ancestry.<sup>34-36</sup> Blood group and age are other important determinants: blood group O is associated with 25% lower VWF:Ag levels<sup>37,38</sup> and VWF:Ag levels increase with age.<sup>37,39,40</sup> Other factors leading to fluctuating VWF:Ag levels are the menstrual cycle, stress, pregnancy and immune responses.<sup>41-44</sup>

Diagnosis of VWD by VWF:Ag measurements can only be conclusive in VWD type 3, where there is a virtually complete deficiency of VWF:Ag, or VWF:Ag is  $< 5$  IU/dL.<sup>16</sup> In VWD type 1, VWF:Ag is by definition decreased. It is, however, very difficult to define a clear cut-off point. Usually, levels below 30 IU/dL are considered diagnostic; however, levels between 30 and 50 IU/dL should be interpreted in the context of the clinical bleeding phenotype. In VWD type 2, plasma

VWF:Ag may vary from normal to mildly reduced.<sup>16</sup> Due to the variable VWF:Ag levels, the interpretation of borderline levels may be ambiguous and repeated measurements are often required. It is important not to over-diagnose patients, which leads to unnecessary use of costly medication and unjustified labelling of patients. Depending on the clinical phenotype, borderline levels of VWF may be considered as a risk factor for bleeding rather than a disease.<sup>45</sup>

**VWF-platelet binding activity**

The major function of VWF is VWF-dependent platelet adhesion. VWF-platelet binding activity can be determined by several different assays. The VWF ristocetin cofactor activity (VWF:RCo) assay has been the gold standard for many years.<sup>46</sup> However, several new assays have been developed to overcome imprecision and insensitivity of the classical VWF:RCo assay. Recently, a new nomenclature for platelet-dependent VWF activity has been adopted and published by the VWF subcommittee of the Scientific and Standardization Committee (SSC) of the ISTH to recognize differences between the tests (Table 2).<sup>47</sup>

**Table 2.** Nomenclature of platelet-dependent VWF activity

Assay	Activator	Description of activity
VWF:RCo	Ristocetin	Ristocetin-induced VWF binding to GPIb on platelets
VWF:GPIbR	Ristocetin	Ristocetin-induced VWF binding to recombinant wild type GPIb fragment
VWF:GPIbM	-	Spontaneous VWF binding to recombinant gain-of-function mutant GPIb fragment
VWF:Ab	-	Binding of monoclonal antibody to the GPIb binding site in VWF (A1 domain epitope)

Adapted from Bodó *et al.*<sup>47</sup> VWF, von Willebrand factor; GPIb, glycoprotein Ib.

The VWF:RCo assay uses the antibiotic ristocetin with platelet-poor plasma to agglutinate an external source of formalin-fixed platelets. Low VWF:RCo indicates a defect in VWF-platelet binding. A drawback of the assay is the low sensitivity and precision; however, newer fully automated assays have been developed and show better sensitivity and precision.<sup>48</sup> The binding site of ristocetin in VWF is found to be inside the A1 domain and some mutations in this region affect ristocetin-mediated activation of VWF, leading to a false-positive VWD diagnosis. Mutations or variations known to interfere with VWF-ristocetin binding are p.Asp1472His and p.Pro1476Ser, with p.Asp1472His being a common variant found in the Afro-American population.<sup>49,50</sup>

An improved limit of detection and coefficient of variation (CV) compared with the standard VWF:RCo assays is obtained by ristocetin-triggered GPIb binding (VWF:GPIbR) assays.<sup>47</sup> In these assays, the external source of platelets has been replaced by a recombinant GPIb fragment bound to a monoclonal antibody<sup>51,52</sup> or latex or magnetic particles.<sup>53</sup> As the VWF:GPIbR assay

uses ristocetin to induce platelet agglutination, this assay has the same drawbacks as the VWF:RCo assay with respect to the variations in the ristocetin binding site. Another drawback is the use of different monoclonal antibodies and GPIb sources in all the assays, rendering substitution of reagents impossible.

The drawback of misclassification of certain subjects by the use of ristocetin can be bypassed by platelet-dependent VWF assays using recombinant mutant gain-of-function GPIb fragments (GPIbM assay). These GPIb fragments contain gain-of-function mutations that spontaneously bind VWF without the need for VWF activation by ristocetin. Several assays have been developed, including ELISA-based assays<sup>54</sup> and automated systems.<sup>55</sup>

In addition to the above-mentioned VWF-platelet binding activity assays, an alternative assay has been developed in which the platelets have been replaced by a monoclonal antibody detecting an epitope in the GPIb binding site (A1 domain) of VWF (indicated as VWF:Ab).<sup>56,57</sup> Although the results of this assay are closely correlated with the VWF:RCo assay, it is not an activity assay in the strict sense.

The VWF:RCo, VWF:GPIbR and GPIbM assays can be used to identify qualitative defects of VWF in the platelet binding. In VWD type 3 there is no platelet binding activity due to the absence of VWF:Ag and in VWD type 1 the platelet binding activity correspondingly decreases with the VWF:Ag level. Significantly decreased levels of platelet binding activity in comparison with VWF:Ag levels are found in VWD types 2A and 2M. This reduction, although less pronounced, is also observed in VWD type 2B. In VWD type 2N, there is no defect in platelet binding and hence no decrease in platelet binding activity in comparison with VWF:Ag levels (Table 3).

**Table 3.** Interpretation of laboratory assays in VWD

Assay	Type 1	Type 2A	Type 2B	Type 2M	Type 2N	Type 3	PT-VWD
Bleeding time or PFA-100™	n/↑	↑	↑	↑	n	↑↑	↑
VWF:Ag	↓	n/↓	n/↓	n/↓	n	↓↓↓	n/↓
VWF:RCo*	↓	↓↓	↓↓	↓↓	n	↓↓↓	↓
FVIII:C	n/↓	n/↓	n/↓	n/↓	↓	↓	n/↓
VWF:RCo*/VWF:Ag	> 0.6	< 0.6	< 0.6	< 0.6	> 0.6	NA	< 0.6
RIPA	n/↓	↓↓	↑	↓↓	n	absent	↑
Multimers	n	loss HMW	loss HMW	n	n	absent	loss HMW
VWF:FVIIIIB	n	n	n	n	↓	NA	n
VWF:CB	↓	↓↓	↓↓	n/↓	n	↓↓↓	↓

PFA-100™, platelet function analyzer; VWF, von Willebrand factor; VWF:Ag, VWF antigen; VWF:RCo, VWF ristocetin cofactor activity; FVIII:C, FVIII coagulant activity; RIPA, ristocetin-induced platelet aggregation; VWF:FVIIIIB, VWF-FVIII binding; HMW, high molecular weight; PT-VWD, platelet-type VWD; VWF:CB, VWF collagen binding; n, normal; ↑, increased (or prolonged for bleeding time or PFA-100™); ↓, decreased; NA, not applicable. \*Or other assays measuring platelet binding activity (see Table 2).

### ***VWF-platelet binding activity/VWF:Ag ratio***

The ratio between VWF-platelet binding activity (VWF:RCo, VWF:GPIbR or VWF:GPIbM) and VWF:Ag level is used to roughly distinguish qualitative VWD from quantitative VWD.<sup>16,58</sup> Qualitative defects of VWF (except for VWD type 2N) are associated with decreased VWF-platelet binding and therefore a decreased VWF-platelet binding activity/VWF:Ag ratio. Most studies that analyzed ratios reported the VWF:RCo/VWF:Ag ratio; however, the results are likely to be equally true for the other platelet binding activity assays.<sup>58</sup> Generally, a VWF:RCo/VWF:Ag ratio below 0.6 is used for diagnosis of VWD type 2A, 2B and 2M. VWD type 2N patients do not have a defect in platelet binding and therefore no decreased VWF:RCo/VWF:Ag. When using VWF:RCo, repeated measurements are needed for correct diagnosis, due to a high CV of the VWF:RCo assay. In some cases with very low levels of VWF:Ag and/or VWF:RCo, the ratio may not be reliably calculated and the distinction between quantitative and qualitative defects may be difficult. However, after administration of desmopressin (DDAVP), VWF levels and potentially the VWF-platelet binding activity will rise above the detection limit. It will then be possible to calculate the VWF-platelet binding activity/VWF:Ag ratio. This may help in subtyping newly diagnosed VWD patients.

### ***Factor VIII activity***

VWF binds coagulation FVIII in the circulation, increasing the FVIII half-life.<sup>9</sup> Reduction of the FVIII activity (FVIII:C) can be due to either a decreased VWF:Ag level or a reduced binding affinity of VWF for FVIII. In VWD type 3, FVIII:C is severely decreased due to the absence of VWF:Ag. The remaining level of FVIII:C in VWD type 3 is an important determinant of the bleeding risk.<sup>59</sup> Due to very low FVIII:C levels, type 3 patients also experience hemophilia-like bleeding as joint and muscle bleeding.<sup>59</sup> In VWD types 1 and 2 (except for 2N), FVIII:C may be variable, sometimes reduced in line with the VWF:Ag level, sometimes within the normal range. Finally, decreased levels of FVIII:C may be the only detectable defect in VWD type 2N, which may thus be missed when relying on VWF:Ag and VWF:RCo levels as diagnostic tests only.

## **Subtyping assays**

Diagnosis of VWD can be confirmed or excluded by the diagnostic assays described in the previous section. However, for conclusive diagnosis of the respective types of VWD, specific subtyping assays are required.

### ***Ristocetin-induced platelet aggregation***

VWF mutations found in VWD type 2B patients force a conformational change in the GPIb binding site leading to spontaneous binding of VWF to GPIb. Due to this increased affinity of VWF to GPIb, lower *in vitro* concentrations of ristocetin are already sufficient to induce binding of VWF to GPIb.<sup>60</sup> Using this feature, a distinction between VWD type 2B and VWD types 2A and 2M can be made by the ristocetin-induced platelet aggregation (RIPA) assay using low concentrations of ristocetin. However, an increased binding of VWF to GPIb can also be caused by a gain-of-function mutation in the GPIb receptor itself. Patients having such mutations are classified as platelet-type VWD (PT-VWD) and will also test positive in the low-dose RIPA assay.<sup>61</sup> To distinguish VWD type 2B from PT-VWD, one can vary the source of plasma and platelets in the low-dose RIPA assay.<sup>62</sup> It is, however, difficult to distinguish with certainty, so nowadays mutation analysis is usually performed to confirm either diagnosis.

### ***VWF multimer analysis***

A decreased VWF-dependent platelet adhesion may be due to a selective deficiency of HMW VWF multimers as seen in types 2A, 2B and PT-VWD or due to an intrinsic decreased GPIb binding affinity of VWF as seen in type 2M. To make this distinction, VWF multimers should be analyzed. Defects in the multimerization of VWF can be identified by VWF multimer analysis in which non-reduced plasma samples are run through medium (1.4–2%) and low (0.7–1.2%) resolution agarose gels. Subsequently, the VWF multimers can be visualized by Western blot.<sup>63</sup> The VWF multimer analysis is a complex and laborious assay, which is generally performed by specialized laboratories only. Even in those laboratories there is a high error rate, with inconsistent interpretation of multimer profiles and false classification.<sup>64</sup> The multimer pattern, when performed with high quality in specialized laboratories, may, however, be indicative of specific genetic defects in VWF.<sup>65</sup>

Normal plasma VWF shows an equal distribution of low, intermediate and HMW VWF multimers. In a high resolution gel, each multimeric band is reproduced as a triplet structure, with the outer bands reflecting the proteolytic cleavage of VWF by ADAMTS13. Decreased levels of HMW VWF multimers are found in VWD type 2A as a consequence of defects in dimerization and multimerization, or due to enhanced susceptibility to proteolysis by ADAMTS13. The decrease of HMW multimers in type 2B and PT-VWD is the consequence of enhanced *in vivo* binding of VWF to platelets, which leads to increased VWF proteolysis and clearance of the HMW multimers from the circulation. In VWD type 2M there is no decrease in HMW multimers as the decrease in VWF-dependent platelet adhesion is mainly due to loss-of-function mutations in the GPIb binding site of VWF (A1 domain). Although VWD type 1 is defined as a quantitative defect of VWF, a subtle decrease in HMW VWF multimers is occasionally observed. According to the recommendation of the SSC of the ISTH, this subtle decrease in HMW VWF multimers

(if VWF:RCo/VWF: Ag > 0.6) is classified as VWD type 1.<sup>16</sup> As these patients do show a minimal, qualitative defect in the multimerization of VWF, there is still an ongoing debate over whether they should be diagnosed as VWD type 1 or 2A. Nevertheless, this will not influence the management of treatment.

### ***VWF-FVIII binding***

Decreased FVIII:C can be found in all VWD types as a consequence of reduced VWF:Ag levels. However, in VWD type 2N there is a more obvious decrease in FVIII:C due to a mutation in the FVIII binding site of VWF disrupting the affinity for FVIII. Defects in the capacity of VWF to bind to FVIII, as found in VWD type 2N, can be identified by the VWF-FVIII binding assay (VWF:FVIII:B).<sup>66</sup> Decreased binding affinity of a patient's plasma VWF to recombinant FVIII in this ELISA-based assay indicates a binding defect. The assay is especially important for distinguishing VWD type 2N and mild hemophilia A, characterized, respectively, by reduced and normal VWF:FVIII:B. VWF:FVIII:B cannot be measured in type 3 due to absence of VWF:Ag. In all other VWD types, the VWF:FVIII:B is within the normal range.

### ***VWF collagen binding***

UL-VWF strings bind collagen types I and III in the VWF A3 domain and collagen types IV and VI in the A1 domain after vascular damage.<sup>67-70</sup> Reduced collagen binding may be a consequence of a decrease in VWF:Ag as in types 1 and 3, a specific lack of HMW VWF multimers as in types 2A and 2B, or specific collagen binding defects, categorized among type 2M.

The ability of VWF to bind collagen can be measured by the VWF collagen binding assay (VWF:CB). Many commercial VWF:CB assays are available, mainly using collagen I or III, or a combination of both. Drawbacks of these tests are the different sources of collagen and reference plasmas used, which makes the optimization and standardization of the VWF:CB assay difficult.<sup>71</sup> Furthermore, patients with defects in binding to collagen IV and VI will be missed using any of these assays.<sup>68,69</sup> However, defects in collagen IV and VI binding are found in affected patients as well as in healthy controls and are therefore considered to only increase the risk of bleeding rather than being a causative factor for VWD.<sup>68,69</sup>

Currently, the VWF:CB is not generally included among the standard diagnostic tests for VWD. However, there is reason to reconsider this. First of all, VWF:CB is able to identify patients with an isolated collagen binding defect that will go unnoticed with any of the other diagnostic assays.<sup>68</sup> This would, however, force to test all the collagen types separately. Secondly, the VWF:CB assay has been shown to be as effective in distinguishing VWD type 1 from type 2 as the VWF:RCo assay.<sup>71,72</sup> The best distinction between VWD types 1 and 2 has been observed

when a mixture of collagen I and III is used. As a subtyping test, the VWF:CB assay may even be a substitute for the complicated VWF multimer assay in the identification of patients with reduced HMW VWF multimers.<sup>73</sup> Although there are many reasons to include the VWF:CB assay in standard diagnosis, it is difficult to pinpoint which test is best. At this time, a mixture of collagen types I and III seems most appropriate. However, more optimization of the commercial tests is necessary.

The interpretation of the diagnostic and subtyping tests and the corresponding classification of VWD is summarized in Table 3 and a diagnostic algorithm is shown in Fig. 2.

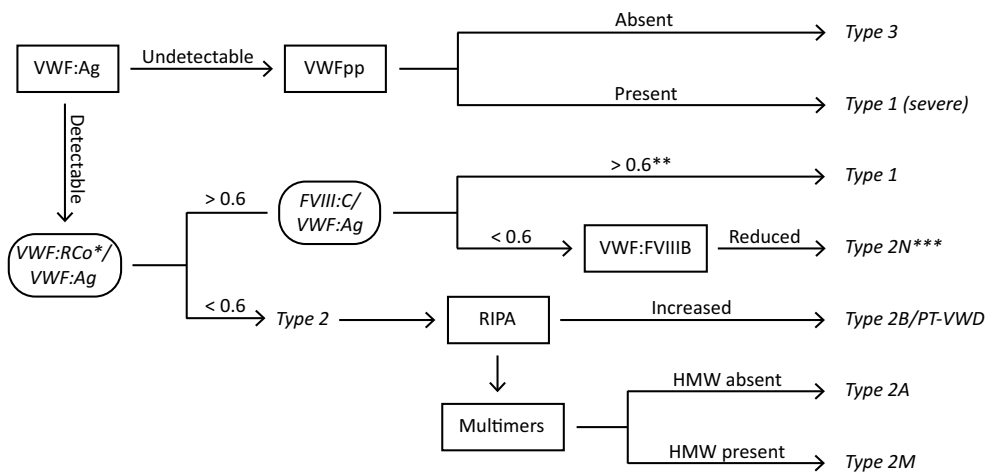


**Figure 2. Diagnostic algorithm for von Willebrand disease (VWD) classification.** Diagnosis of VWD is based on abnormal levels found in one or more of the standard diagnostic tests: VWF:Ag, VWF:RCo and FVIII:C. Specific VWD subtypes can be identified by performing the RIPA assay using low-dose ristocetin, VWF multimer analysis and the VWF:FVIIIIB assay. VWFpp can be used to distinguish between true VWD type 3 and severe VWD type 1, and can help in the identification of the pathophysiological mechanism behind VWD. \*VWF:RCo or other assays measuring VWF-platelet binding activity (see Table 2). \*\*VWD is excluded when FVIII:C/VWF:Ag is  $> 0.6$  and VWF:Ag and VWF:RCo are within the normal range. \*\*\*Normal VWF:FVIIIIB but FVIII:C/VWF:Ag  $< 0.6$  suggests hemophilia A. VWF, von Willebrand factor; VWF:Ag, VWF antigen; VWF:RCo, VWF ristocetin cofactor activity; FVIII:C, FVIII activity; RIPA, ristocetin-induced platelet aggregation; VWF:FVIIIIB, VWF-FVIII binding; VWFpp, VWF propeptide; PT-VWD, platelet-type VWD.

## The value of VWF ratios and VWF mutation analysis

The tests outlined above are sufficient to diagnose and classify most VWD. Additional assays and analyses can be performed to confirm certain subtypes or identify the underlying pathophysiological mechanisms. The pathophysiological mechanisms are of scientific interest, but may also guide the choice of treatment.

### ***VWF propeptide and its ratio to VWF:Ag***

VWF is synthesized as pre-proVWF. The signal peptide is cleaved off right after synthesis. The propeptide is cleaved off in the endoplasmic reticulum (ER) and functions as a chaperone for the formation of VWF multimers.<sup>74</sup> VWF and its propeptide (VWFpp) are synthesized and secreted into the circulation in a 1:1 ratio.<sup>75</sup> However, in the circulation both molecules are cleared at different rates, with a circulating half-life of about 12 hours for VWF and about 2-3 hours for VWFpp.<sup>8,76</sup>

VWFpp levels in plasma can be determined by an ELISA-based assay and may be indicative of synthesis, secretion or clearance defects of VWF. Decreased VWFpp levels indicate reduced synthesis of VWF or impaired secretion of VWF from the WPBs, and may be found in VWD type 1 patients having a null allele or ER retention.<sup>14,15</sup> In VWD type 2, the qualitative defect of VWF is generally not caused by impaired synthesis or secretion and normal VWFpp plasma levels are expected.<sup>14</sup> Although VWD type 3 is associated with undetectable VWF:Ag levels, a subset of patients does show circulating VWFpp.<sup>14</sup> We found that patients historically diagnosed as VWD type 3 with undetectable VWFpp were homozygous or compound heterozygous for null alleles, whereas the majority of patients with detectable VWFpp were heterozygous for a missense mutation associated with increased VWF clearance.<sup>14</sup> The patients with detectable VWFpp also had a lower bleeding score. We therefore suggest that these patients should be reclassified as severe type 1 VWD instead of type 3. Altogether, VWFpp can discriminate between VWD type 3 with a complete absence of VWF:Ag and VWFpp and severe type 1 VWD with extremely low VWF:Ag levels.

The ratio of VWFpp to VWF:Ag gives a measure of the clearance rate of mature VWF, assuming a constant clearance rate for VWFpp.<sup>14,15,77,78</sup> Clearance defects can be found in all types of VWD and can be due to a mutation in VWF itself, such as the Vicenza mutation p.Arg1205His, or due to variations in proteins involved in the clearance of VWF.<sup>13,79,80</sup> In VWD type 2B, almost all patients show increased clearance rates. This is suggested to be caused by increased uptake of the VWF-platelet complex by macrophages, mediated by increased lipoprotein receptor 1 binding.<sup>81</sup>

Information about clearance defects may have therapeutic implications. DDAVP is for example the treatment of choice in VWD type 1 patients, but increasing the endogenous VWF levels may not be sufficient in patients with a major VWF clearance defect.

### ***FVIII:C/VWF:Ag ratio***

Binding of coagulation FVIII to VWF occurs at a 1:50 molar ratio. However, coagulation factors are determined in arbitrary units per milliliter and therefore the ratio of FVIII:C to VWF:Ag in



healthy controls is by definition approximately one.<sup>82</sup> Due to the excess of FVIII binding sites on VWF, a reduction in VWF synthesis will not lead to a concomitant decrease of FVIII levels. However, when VWF is reduced due to increased clearance of the protein, then the FVIII levels drop accordingly as VWF-FVIII is cleared as a complex. The ratio of FVIII:C to VWF:Ag could therefore identify defects in the synthesis or secretion of VWF.<sup>14,83</sup> Heterozygous VWF null mutations, mainly found in carriers of VWD type 3 and some carriers of VWD type 1, have been shown to be associated with a FVIII:C/VWF:Ag ratio of  $> 2$ .<sup>15,83</sup> As VWF and FVIII are cleared as a complex, FVIII:C/VWF:Ag is not altered in patients showing a pure clearance defect of VWF. However, a combined effect of decreased synthesis and increased clearance is possible and could be identified by plotting VWFpp/VWF:Ag to FVIII:C/VWF:Ag.<sup>14</sup> Finally, the FVIII:C/VWF:Ag ratio when reduced ( $< 0.6$ ) suggests VWD type 2N or hemophilia A.

## Mutation analysis

In most cases of VWD, a proper diagnosis and classification can be made based on the phenotypic assays and thus mutation analysis is not required. Also, because of the large size of *VWF*, it is suggested that mutation analysis should only be performed when phenotypic assays fall short and when additional mutation analysis is relevant for management or counseling of the patient. However, new developments, such as next generation sequencing, resulted in the implementation of routine gene analysis of *VWF* in some laboratories.<sup>84</sup> Deletions or duplication of exons can furthermore be identified by multiplex ligation-dependent probe amplification dosage analysis.<sup>85</sup> When it is decided to use sequencing for diagnosis, special care should be taken with regard to the *VWF* pseudogene located on chromosome 22.<sup>86</sup> The pseudogene corresponds to exons 23-34 of the *VWF* gene with a 97% similarity.

Quantitative defects of VWF found in VWD type 1 are mainly caused by missense mutations spread throughout the whole gene, and mutations have been identified only for ~ 70% of the sequenced patients.<sup>17,87-89</sup> Sequencing these patients would be labor intensive and costly, and would in most cases not benefit the patient. Especially in VWD type 1 with its variable penetrance, identification of a mutation is no proof of disease and not identifying a mutation does not reject the bleeding phenotype.

Qualitative defects, found in VWD type 2, are usually restricted to specific VWF domains and mutations have been identified in almost all sequenced patients.<sup>17</sup> When a qualitative defect of VWF is expected, sequencing the restricted domain would be sufficient and is usually performed to distinguish VWD from VWF-related diseases. An example is the distinction between VWD type 2N and mild hemophilia A, which has major implications for genetic counseling as well as the choice of treatment. Another example is the differentiation between

VWD type 2B and PT-VWD, which is also relevant for treatment.

The quantitative defect in VWD type 3 is largely explained by *VWF* null alleles.<sup>17</sup> Important reasons for sequencing these patients are genetic counseling and prenatal diagnosis. Furthermore, homozygous gene deletions that may predict the formation of VWF inhibitors after replacement therapy can be identified.<sup>90</sup>

## Conclusion

The heterogeneity of VWD necessitates undertaking multiple diagnostic tests, which may have to be repeated several times before a proper diagnosis can be made. Adequate diagnosis and classification is important for the choice of treatment and for counseling with regard to inheritance. The broad diagnostic armamentarium for VWD is still insufficient as it does not take some very important aspects of VWF into account. All current tests are performed in static conditions, although flow plays a major role in the structural and functional properties of VWF. Also, the contribution of the vascular wall and the VWF string formation on the endothelial surface are not considered in the diagnosis. Recently, patient-derived blood outgrowth endothelial cells (BOECs) have been described as a model to study VWF in its native environment.<sup>10,11</sup> Although BOECs are not feasible for diagnostic purposes at this time, new innovative diagnostic tests could be focusing on combining patient-derived BOECs with aspects of flow for a more physiological evaluation of VWF function.

## References

1. Rodeghiero F, Castaman G, Dini E. Epidemiological investigation of the prevalence of von Willebrand's disease. *Blood*. 1987;**69**(2):454-459.
2. Bowman M, Hopman WM, Rapson D, Lillicrap D, Silva M, James P. A prospective evaluation of the prevalence of symptomatic von Willebrand disease (VWD) in a pediatric primary care population. *Pediatr Blood Cancer*. 2010;**55**(1):171-173.
3. Werner EJ, Broxson EH, Tucker EL, Giroux DS, Shults J, Abshire TC. Prevalence of von Willebrand disease in children: a multiethnic study. *J Pediatr*. 1993;**123**(6):893-898.
4. Flood VH, Gill JC, Friedman KD, Bellissimo DB, Haberichter SL, Montgomery RR. Von Willebrand disease in the United States: a perspective from Wisconsin. *Semin Thromb Hemost*. 2011;**37**(5):528-534.
5. de Wee EM, Leebeek FW, Eikenboom JC. Diagnosis and management of von Willebrand disease in The Netherlands. *Semin Thromb Hemost*. 2011;**37**(5):480-487.
6. Valentijn KM, Eikenboom J. Weibel-Palade bodies: a window to von Willebrand disease. *J Thromb Haemost*. 2013;**11**(4):581-592.
7. De Ceunynck K, De Meyer SF, Vanhoorelbeke K. Unwinding the von Willebrand factor strings puzzle. *Blood*. 2013;**121**(2):270-277.
8. Borchellini A, Fijnvandraat K, ten Cate JW, et al. Quantitative analysis of von Willebrand factor propeptide release in vivo: effect of experimental endotoxemia and administration of 1-deamino-8-D-arginine vasopressin in humans. *Blood*. 1996;**88**(8):2951-2958.
9. Weiss HJ, Sussman II, Hoyer LW. Stabilization of factor VIII in plasma by the von Willebrand factor. Studies on posttransfusion and dissociated factor VIII and in patients with von Willebrand's disease. *J Clin Invest*. 1977;**60**(2):390-404.
10. Starke RD, Paschalaki KE, Dyer CE, et al. Cellular and molecular basis of von Willebrand disease: studies on blood outgrowth endothelial cells. *Blood*. 2013;**121**(14):2773-2784.
11. Wang JW, Bouwens EA, Pintao MC, et al. Analysis of the storage and secretion of von Willebrand factor in blood outgrowth endothelial cells derived from patients with von Willebrand disease. *Blood*. 2013;**121**(14):2762-2772.
12. Groeneveld DJ, Wang JW, Mourik MJ, et al. Storage and secretion of naturally occurring von Willebrand factor A domain variants. *Br J Haematol*. 2014;**167**(4):529-540.
13. Rydz N, Swystun LL, Notley C, et al. The C-type lectin receptor CLEC4M binds, internalizes, and clears von Willebrand factor and contributes to the variation in plasma von Willebrand factor levels. *Blood*. 2013;**121**(26):5228-5237.
14. Sanders YV, Groeneveld D, Meijer K, et al. von Willebrand factor propeptide and the phenotypic classification of von Willebrand disease. *Blood*. 2015;**125**(19):3006-3013.
15. Eikenboom J, Federici AB, Dirven RJ, et al. VWF propeptide and ratios between VWF, VWF propeptide, and FVIII in the characterization of type 1 von Willebrand disease. *Blood*. 2013;**121**(12):2336-2339.
16. Sadler JE, Budde U, Eikenboom JC, et al. Update on the pathophysiology and classification

- of von Willebrand disease: a report of the Subcommittee on von Willebrand Factor. *J Thromb Haemost.* 2006;**4**(10):2103-2114.
17. Goodeve AC. The genetic basis of von Willebrand disease. *Blood Rev.* 2010;**24**(3):123-134.
  18. Bowman M, Tuttle A, Notley C, et al. The genetics of Canadian type 3 von Willebrand disease: further evidence for co-dominant inheritance of mutant alleles. *J Thromb Haemost.* 2013;**11**(3):512-520.
  19. Srámek A, Eikenboom JC, Briët E, Vandenbroucke JP, Rosendaal FR. Usefulness of patient interview in bleeding disorders. *Arch Intern Med.* 1995;**155**(13):1409-1415.
  20. Rodeghiero F, Castaman G, Tosetto A, et al. The discriminant power of bleeding history for the diagnosis of type 1 von Willebrand disease: an international, multicenter study. *J Thromb Haemost.* 2005;**3**(12):2619-2626.
  21. Tosetto A, Rodeghiero F, Castaman G, et al. A quantitative analysis of bleeding symptoms in type 1 von Willebrand disease: results from a multicenter European study (MCMDM-1 VWD). *J Thromb Haemost.* 2006;**4**(4):766-773.
  22. Bowman M, Riddel J, Rand ML, Tosetto A, Silva M, James PD. Evaluation of the diagnostic utility for von Willebrand disease of a pediatric bleeding questionnaire. *J Thromb Haemost.* 2009;**7**(8):1418-1421.
  23. Tosetto A, Castaman G, Plug I, Rodeghiero F, Eikenboom J. Prospective evaluation of the clinical utility of quantitative bleeding severity assessment in patients referred for hemostatic evaluation. *J Thromb Haemost.* 2011;**9**(6):1143-1148.
  24. Deforest M, Grabell J, Albert S, et al. Generation and optimization of the self-administered bleeding assessment tool and its validation as a screening test for von Willebrand disease. *Haemophilia.* 2015;**21**(5):e384-388.
  25. Burns ER, Lawrence C. Bleeding time. A guide to its diagnostic and clinical utility. *Arch Pathol Lab Med.* 1989;**113**(11):1219-1224.
  26. Castaman G, Tosetto A, Goodeve A, et al. The impact of bleeding history, von Willebrand factor and PFA-100((R)) on the diagnosis of type 1 von Willebrand disease: results from the European study MCMDM-1VWD. *Br J Haematol.* 2010;**151**(3):245-251.
  27. Kundu SK, Heilmann EJ, Sio R, Garcia C, Davidson RM, Ostgaard RA. Description of an in vitro platelet function analyzer--PFA-100. *Semin Thromb Hemost.* 1995;**21 Suppl 2**:106-112.
  28. Hayward CP, Harrison P, Cattaneo M, Ortel TL, Rao AK. Platelet function analyzer (PFA)-100 closure time in the evaluation of platelet disorders and platelet function. *J Thromb Haemost.* 2006;**4**(2):312-319.
  29. Quiroga T, Goycoolea M, Muñoz B, et al. Template bleeding time and PFA-100 have low sensitivity to screen patients with hereditary mucocutaneous hemorrhages: comparative study in 148 patients. *J Thromb Haemost.* 2004;**2**(6):892-898.
  30. Dean JA, Blanchette VS, Carcao MD, et al. von Willebrand disease in a pediatric-based population--comparison of type 1 diagnostic criteria and use of the PFA-100 and a von Willebrand factor/collagen-binding assay. *Thromb Haemost.* 2000;**84**(3):401-409.

31. Cejka J. Enzyme immunoassay for factor VIII-related antigen. *Clin Chem*. 1982;**28**(6):1356-1358.
32. Veyradier A, Fressinaud E, Sigaud M, Wolf M, Meyer D. A new automated method for von Willebrand factor antigen measurement using latex particles. *Thromb Haemost*. 1999;**81**(2):320-321.
33. Castaman G, Tositto A, Cappelletti A, et al. Validation of a rapid test (VWF-LIA) for the quantitative determination of von Willebrand factor antigen in type 1 von Willebrand disease diagnosis within the European multicenter study MCMDM-1VWD. *Thromb Res*. 2010;**126**(3):227-231.
34. Zhou Z, Yu F, Buchanan A, et al. Possible race and gender divergence in association of genetic variations with plasma von Willebrand factor: a study of ARIC and 1000 genome cohorts. *PLoS One*. 2014;**9**(1):e84810.
35. Jang JH, Seo JY, Bang SH, Park IA, Kim HJ, Kim SH. Establishment of reference intervals for von Willebrand factor antigen and eight coagulation factors in a Korean population following the Clinical and Laboratory Standards Institute guidelines. *Blood Coagul Fibrinolysis*. 2010;**21**(3):251-255.
36. Bellissimo DB, Christopherson PA, Flood VH, et al. VWF mutations and new sequence variations identified in healthy controls are more frequent in the African-American population. *Blood*. 2012;**119**(9):2135-2140.
37. Gill JC, Endres-Brooks J, Bauer PJ, Marks WJ, Jr., Montgomery RR. The effect of ABO blood group on the diagnosis of von Willebrand disease. *Blood*. 1987;**69**(6):1691-1695.
38. Gallinaro L, Cattini MG, Sztukowska M, et al. A shorter von Willebrand factor survival in O blood group subjects explains how ABO determinants influence plasma von Willebrand factor. *Blood*. 2008;**111**(7):3540-3545.
39. Sanders YV, Giezenaar MA, Laros-van Gorkom BA, et al. von Willebrand disease and aging: an evolving phenotype. *J Thromb Haemost*. 2014;**12**(7):1066-1075.
40. Rydz N, Grabell J, Lillicrap D, James PD. Changes in von Willebrand factor level and von Willebrand activity with age in type 1 von Willebrand disease. *Haemophilia*. 2015;**21**(5):636-641.
41. Knol HM, Kemperman RF, Kluin-Nelemans HC, Mulder AB, Meijer K. Haemostatic variables during normal menstrual cycle. A systematic review. *Thromb Haemost*. 2012;**107**(1):22-29.
42. van Loon JE, Sonneveld MA, Praet SF, de Maat MP, Leebeek FW. Performance related factors are the main determinants of the von Willebrand factor response to exhaustive physical exercise. *PLoS One*. 2014;**9**(3):e91687.
43. Castaman G. Changes of von Willebrand Factor during Pregnancy in Women with and without von Willebrand Disease. *Mediterr J Hematol Infect Dis*. 2013;**5**(1):e2013052.
44. Pottinger BE, Read RC, Paleolog EM, Higgins PG, Pearson JD. von Willebrand factor is an acute phase reactant in man. *Thromb Res*. 1989;**53**(4):387-394.
45. Sadler JE. Von Willebrand disease type 1: a diagnosis in search of a disease. *Blood*. 2003;**101**(6):2089-2093.
46. Weiss HJ, Hoyer LW, Rickles FR, Varma A, Rogers J. Quantitative assay of a plasma factor deficient

- in von Willebrand's disease that is necessary for platelet aggregation. Relationship to factor VIII procoagulant activity and antigen content. *J Clin Invest*. 1973;**52**(11):2708-2716.
47. Bodó I, Eikenboom J, Montgomery R, Patzke J, Schneppenheim R, Di Paola J. Platelet-dependent von Willebrand factor activity. Nomenclature and methodology: communication from the SSC of the ISTH. *J Thromb Haemost*. 2015;**13**(7):1345-1350.
  48. Hillarp A, Stadler M, Haderer C, Weinberger J, Kessler CM, Romisch J. Improved performance characteristics of the von Willebrand factor ristocetin cofactor activity assay using a novel automated assay protocol. *J Thromb Haemost*. 2010;**8**(10):2216-2223.
  49. Flood VH, Friedman KD, Gill JC, et al. Limitations of the ristocetin cofactor assay in measurement of von Willebrand factor function. *J Thromb Haemost*. 2009;**7**(11):1832-1839.
  50. Flood VH, Gill JC, Morateck PA, et al. Common VWF exon 28 polymorphisms in African Americans affecting the VWF activity assay by ristocetin cofactor. *Blood*. 2010;**116**(2):280-286.
  51. Vanhoorelbeke K, Cauwenberghs N, Vauterin S, Schlammadinger A, Mazurier C, Deckmyn H. A reliable and reproducible ELISA method to measure ristocetin cofactor activity of von Willebrand factor. *Thromb Haemost*. 2000;**83**(1):107-113.
  52. Federici AB, Canciani MT, Forza I, et al. A sensitive ristocetin co-factor activity assay with recombinant glycoprotein Ibalpha for the diagnosis of patients with low von Willebrand factor levels. *Haematologica*. 2004;**89**(1):77-85.
  53. Stufano F, Lawrie AS, La Marca S, Berbenni C, Baronciani L, Peyvandi F. A two-centre comparative evaluation of new automated assays for von Willebrand factor ristocetin cofactor activity and antigen. *Haemophilia*. 2014;**20**(1):147-153.
  54. Flood VH, Gill JC, Morateck PA, et al. Gain-of-function GPIb ELISA assay for VWF activity in the Zimmerman Program for the Molecular and Clinical Biology of VWD. *Blood*. 2011;**117**(6):e67-74.
  55. Patzke J, Budde U, Huber A, et al. Performance evaluation and multicentre study of a von Willebrand factor activity assay based on GPIb binding in the absence of ristocetin. *Blood Coagul Fibrinolysis*. 2014;**25**(8):860-870.
  56. Murdock PJ, Woodhams BJ, Matthews KB, Pasi KJ, Goodall AH. von Willebrand factor activity detected in a monoclonal antibody-based ELISA: an alternative to the ristocetin cofactor platelet agglutination assay for diagnostic use. *Thromb Haemost*. 1997;**78**(4):1272-1277.
  57. Favaloro EJ, Henniker A, Facey D, Hertzberg M. Discrimination of von Willebrand's disease (VWD) subtypes: direct comparison of von Willebrand factor:collagen binding assay (VWF:CBA) with monoclonal antibody (MAB) based VWF-capture systems. *Thromb Haemost*. 2000;**84**(4):541-547.
  58. Geisen U, Zieger B, Nakamura L, et al. Comparison of Von Willebrand factor (VWF) activity VWF:Ac with VWF ristocetin cofactor activity VWF:RCo. *Thromb Res*. 2014;**134**(2):246-250.
  59. Sood SL, Cuker A, Wang C, et al. Similarity in joint function limitation in Type 3 von Willebrand's disease and moderate haemophilia A. *Haemophilia*. 2013;**19**(4):595-601.
  60. Ruggeri ZM, Pareti FI, Mannucci PM, Ciavarella N, Zimmerman TS. Heightened interaction between platelets and factor VIII/von Willebrand factor in a new subtype of von Willebrand's disease. *N Engl J Med*. 1980;**302**(19):1047-1051.

61. Frontroth JP, Hepner M, Sciuccati G, Feliú Torres A, Pieroni G, Bonduel M. Prospective study of low-dose ristocetin-induced platelet aggregation to identify type 2B von Willebrand disease (VWD) and platelet-type VWD in children. *Thromb Haemost.* 2010;**104**(6):1158-1165.
62. Favalaro EJ, Patterson D, Denholm A, et al. Differential identification of a rare form of platelet-type (pseudo-) von Willebrand disease (VWD) from Type 2B VWD using a simplified ristocetin-induced-platelet-agglutination mixing assay and confirmed by genetic analysis. *Br J Haematol.* 2007;**139**(4):623-626.
63. Budde U, Pieconka A, Will K, Schneppenheim R. Laboratory testing for von Willebrand disease: contribution of multimer analysis to diagnosis and classification. *Semin Thromb Hemost.* 2006;**32**(5):514-521.
64. Meijer P, Haverkate F. An external quality assessment program for von Willebrand factor laboratory analysis: an overview from the European concerted action on thrombosis and disabilities foundation. *Semin Thromb Hemost.* 2006;**32**(5):485-491.
65. Budde U, Schneppenheim R, Eikenboom J, et al. Detailed von Willebrand factor multimer analysis in patients with von Willebrand disease in the European study, molecular and clinical markers for the diagnosis and management of type 1 von Willebrand disease (MCMDM-1VWD). *J Thromb Haemost.* 2008;**6**(5):762-771.
66. Caron C, Mazurier C, Goudemand J. Large experience with a factor VIII binding assay of plasma von Willebrand factor using commercial reagents. *Br J Haematol.* 2002;**117**(3):716-718.
67. Pareti FI, Niiya K, McPherson JM, Ruggeri ZM. Isolation and characterization of two domains of human von Willebrand factor that interact with fibrillar collagen types I and III. *J Biol Chem.* 1987;**262**(28):13835-13841.
68. Flood VH, Schlauderer AC, Haberichter SL, et al. Crucial role for the VWF A1 domain in binding to type IV collagen. *Blood.* 2015;**125**(14):2297-2304.
69. Flood VH, Gill JC, Christopherson PA, et al. Critical von Willebrand factor A1 domain residues influence type VI collagen binding. *J Thromb Haemost.* 2012;**10**(7):1417-1424.
70. Hoylaerts MF, Yamamoto H, Nuyts K, Vreys I, Deckmyn H, Vermeylen J. von Willebrand factor binds to native collagen VI primarily via its A1 domain. *Biochem J.* 1997;**324** ( Pt 1):185-191.
71. Favalaro EJ. Evaluation of commercial von Willebrand factor collagen binding assays to assist the discrimination of types 1 and 2 von Willebrand disease. *Thromb Haemost.* 2010;**104**(5):1009-1021.
72. Ni Y, Nesrallah J, Agnew M, Geske FJ, Favalaro EJ. Establishment and characterization of a new and stable collagen-binding assay for the assessment of von Willebrand factor activity. *Int J Lab Hematol.* 2013;**35**(2):170-176.
73. Flood VH, Gill JC, Friedman KD, et al. Collagen Binding Provides a Sensitive Screen for Variant von Willebrand Disease. *Clinical Chemistry.* 2013;**59**(4):684-691.
74. Mayadas TN, Wagner DD. In vitro multimerization of von Willebrand factor is triggered by low pH. Importance of the propolypeptide and free sulfhydryls. *J Biol Chem.* 1989;**264**(23):13497-13503.
75. Wagner DD, Fay PJ, Sporn LA, Sinha S, Lawrence SO, Marder VJ. Divergent fates of von Willebrand

- factor and its propolypeptide (von Willebrand antigen II) after secretion from endothelial cells. *Proc Natl Acad Sci U S A*. 1987;**84**(7):1955-1959.
76. van Mourik JA, Boertjes R, Huisveld IA, et al. von Willebrand factor propeptide in vascular disorders: A tool to distinguish between acute and chronic endothelial cell perturbation. *Blood*. 1999;**94**(1):179-185.
  77. Haberichter SL, Balistreri M, Christopherson P, et al. Assay of the von Willebrand factor (VWF) propeptide to identify patients with type 1 von Willebrand disease with decreased VWF survival. *Blood*. 2006;**108**(10):3344-3351.
  78. Haberichter SL, Castaman G, Budde U, et al. Identification of type 1 von Willebrand disease patients with reduced von Willebrand factor survival by assay of the VWF propeptide in the European study: molecular and clinical markers for the diagnosis and management of type 1 VWD (MCMDM-1VWD). *Blood*. 2008;**111**(10):4979-4985.
  79. Sztukowska M, Gallinaro L, Cattini MG, et al. Von Willebrand factor propeptide makes it easy to identify the shorter Von Willebrand factor survival in patients with type 1 and type Vicenza von Willebrand disease. *Br J Haematol*. 2008;**143**(1):107-114.
  80. Sanders YV, van der Bom JG, Isaacs A, et al. CLEC4M and STXBP5 gene variations contribute to von Willebrand factor level variation in von Willebrand disease. *J Thromb Haemost*. 2015;**13**(6):956-966.
  81. Wohner N, Legendre P, Casari C, Christophe OD, Lenting PJ, Denis CV. Shear stress-independent binding of von Willebrand factor-type 2B mutants p.R1306Q & p.V1316M to LRP1 explains their increased clearance. *J Thromb Haemost*. 2015;**13**(5):815-820.
  82. Vlot AJ, Koppelman SJ, van den Berg MH, Bouma BN, Sixma JJ. The affinity and stoichiometry of binding of human factor VIII to von Willebrand factor. *Blood*. 1995;**85**(11):3150-3157.
  83. Eikenboom JC, Castaman G, Kamphuisen PW, Rosendaal FR, Bertina RM. The factor VIII/von Willebrand factor ratio discriminates between reduced synthesis and increased clearance of von Willebrand factor. *Thromb Haemost*. 2002;**87**(2):252-257.
  84. Batlle J, Pérez-Rodríguez A, Corrales I, et al. Molecular and clinical profile of von Willebrand disease in Spain (PCM-EVW-ES): Proposal for a new diagnostic paradigm. *Thromb Haemost*. 2016;**115**(1):40-50.
  85. Acquila M, Bottini F, Di Duca M, Vijzelaar R, Molinari AC, Bicocchi MP. Multiplex ligation-dependent probe amplification to detect a large deletion within the von Willebrand gene. *Haemophilia*. 2009;**15**(6):1346-1348.
  86. Mancuso DJ, Tuley EA, Westfield LA, et al. Human von Willebrand factor gene and pseudogene: structural analysis and differentiation by polymerase chain reaction. *Biochemistry*. 1991;**30**(1):253-269.
  87. Goodeve A, Eikenboom J, Castaman G, et al. Phenotype and genotype of a cohort of families historically diagnosed with type 1 von Willebrand disease in the European study, Molecular and Clinical Markers for the Diagnosis and Management of Type 1 von Willebrand Disease (MCMDM-1VWD). *Blood*. 2007;**109**(1):112-121.



88. James PD, Notley C, Hegadorn C, et al. The mutational spectrum of type 1 von Willebrand disease: Results from a Canadian cohort study. *Blood*. 2007;**109**(1):145-154.
89. Cumming A, Grundy P, Keeney S, et al. An investigation of the von Willebrand factor genotype in UK patients diagnosed to have type 1 von Willebrand disease. *Thromb Haemost*. 2006;**96**(5):630-641.
90. James PD, Lillicrap D, Mannucci PM. Alloantibodies in von Willebrand disease. *Blood*. 2013;**122**(5):636-640.



Online supplemental data



# 3

## **Von Willebrand disease mutation spectrum and associated mutation mechanisms**

Annika de Jong  
Jeroen Eikenboom

*Thrombosis research (2017) 159:65-75*



## Abstract

Von Willebrand disease (VWD) is a bleeding disorder that is mainly caused by mutations in the multimeric protein von Willebrand factor (VWF). These mutations may lead to deficiencies in plasma VWF or dysfunctional VWF. VWF is a heterogeneous protein and over the past three decades, hundreds of VWF mutations have been identified. In this review we have organized all reported mutations, spanning a timeline from the late eighties until early 2017. This resulted in an overview of 750 unique mutations that are divided over the VWD types 1, 2A, 2B, 2M, 2N and 3. For many of these mutations the disease-causing effects have been characterized *in vitro* through expression studies, *ex vivo* by analysis of patient-derived endothelial cells, as well as in animal or (bio)physical models. Here we describe the mechanisms associated with the VWF mutations per VWD type.

## Introduction

Von Willebrand factor (VWF) is a multimeric hemostatic protein produced solely by endothelial cells and megakaryocytes.<sup>1,2</sup> VWF is transcribed from the small arm of chromosome 12 (12p13.31) and translates into a 2813 amino acid protein. Newly synthesized VWF consists of 16 domains: a 22 amino acid signal peptide at the N-terminal end of the protein, a propeptide comprising the D1 and D2 domains, and mature VWF comprising the D<sup>1</sup>-D3-A1-A2-A3-D4-C1-C2-C3-C4-C5-C6-CK domains (Fig. 1A).<sup>3</sup> The signal peptide is cleaved off after synthesis in the endoplasmic reticulum (ER). Then, proVWF undergoes several post-translational modifications, like glycosylation and C-terminal dimerization.<sup>4,5</sup> In the trans-Golgi network (TGN), the propeptide is cleaved by furin, but remains non-covalently linked to mature VWF and helps to chaperone mature VWF in the multimerization process.<sup>6</sup> VWF multimers can contain up to 80 subunits, which are translocated from the TGN to the alpha granules in megakaryocytes and to the cigar-shaped vesicles called Weibel-Palade bodies in endothelium.<sup>7,8</sup> Upon vascular damage, VWF multimers are released from the endothelial cells and through the aid of vascular flow form ultra-large VWF strings attached to the exposed collagen.<sup>9</sup> The unwinding of VWF into large strings exposes the binding site for platelet glycoprotein Ib (GPIb) in the A1 domain, thereby attracting platelets to sites of vascular damage and starting primary hemostasis.<sup>10</sup> Opening up the A2 domain exposes the cleavage site of the metalloprotease ADAMTS13 (A Disintegrin And Metalloprotease with ThromboSpondin motif repeats 13), which cleaves VWF between amino acid positions 1605 and 1606.<sup>9</sup> This leads to the release of smaller and larger VWF multimers into the circulation. In the circulation factor VIII (FVIII) is bound to VWF, which extends the half-life of FVIII.<sup>11</sup> VWF has a half-life of 8-12 hours and remains in the circulation until it is cleared from the system by macrophages in the liver and spleen.<sup>12,13</sup>

Malfunction in one of the processes described above may lead to von Willebrand disease (VWD), the most common inherited bleeding disorder that is mainly associated with mucocutaneous and surgical bleeding.<sup>14</sup> Based on the plasma phenotype, VWD patients are categorized into one of the VWD types: 1, 2A, 2B, 2M, 2N and 3.<sup>15</sup> VWD type 1 and 3 patients are typified by a partial or complete deficiency in plasma VWF respectively. These deficiencies are caused by loss of production, reduced secretion from endothelial cells and platelets, or increased clearance of VWF from the circulation. Four different qualitative defects lead to VWD type 2, and include a defect in plasma multimers in type 2A, increased binding to GPIb in type 2B, decreased binding to GPIb or collagen in type 2M and defective binding to coagulation FVIII in type 2N.

In 1985 four independent groups succeeded to clone and sequence the *VWF* gene.<sup>16-19</sup> From this moment on many groups sequenced *VWF* of VWD patients and this led to the identification of hundreds of variations in *VWF*. To prove that the identified variations are indeed disease-causing, VWF constructs containing many of these variants have been overexpressed in

heterologous cell systems. For VWF, studies have been performed in stable furin producing BHK, COS-7, AtT-20, HEK293, HEK293T and HEK293 EBNA cells, with only HEK293 and AtT-20 cells being able to store VWF in pseudo-Weibel-Palade bodies.<sup>20</sup> Expression studies led to the identification of secretion and multimerization defects and binding defects to FVIII and GPIb. Recent advances also allow for the culture of endothelial cells from VWD patients directly and have been helpful in unraveling mutation mechanisms in a patient-specific environment.<sup>21,22</sup> Although the *in vitro* systems have been useful, the effects of flow on VWF and clearance of the protein are difficult to determine. However, by the use of several plasma parameters and VWD mouse models, clearance defects and the *in vivo* effect of ADAMTS13 on VWF have also been investigated.<sup>23-26</sup>

In this review we endeavored to organize all published VWF mutations and their disease causing mechanism based on an extensive literature search (search term in supplemental information). Throughout this review the mutations and mechanisms will be explained per VWD type. Some mutations have been assigned in literature to different VWD types, which could be explained in various ways: a patient could have been misdiagnosed, the mutation may truly result in different phenotypes or a mutation may have combined phenotypic characteristics of multiple VWD types. We have depicted mutations in this review as they were assigned in literature. Furthermore, it is important to note that if more than one mutation was reported for a single patient and the disease-causing mutation was not certain, the mutations were not included in this review. Also for many candidate mutations the disease causing effect has not been proven yet, however for simplicity we call them mutations throughout this review.

## VWD type 1

VWD type 1 is the most common type comprising about 60-70% of the patient population.<sup>27</sup> Type 1 patients show a partial deficiency in VWF with a comparable decrease of VWF antigen (VWF:Ag) and VWF activity (VWF ristocetin cofactor activity, VWF:RCo). A VWF:Ag below a cut-off of 30 IU/dL in combination with a VWF:RCo/VWF:Ag ratio > 0.6 and a normal VWF collagen binding is diagnostic for type 1 VWD, thereby accepting minor abnormalities in VWF multimers.<sup>14,15,28</sup> VWF:Ag levels between 30 and 50 IU/dL may be considered as VWD depending on the bleeding phenotype. Although VWD type 1 is the most frequent type of VWD, extensive investigations to the mutation mechanisms of VWD type 1 started only between 2000 and 2010 with three large studies conducted in the United Kingdom, Europe and Canada.<sup>29-31</sup> In these studies mutations were identified in 53-70% of the patients. Later studies in Sweden and Canada confirmed these numbers.<sup>32,33</sup> Importantly, some type 1 patients included in the European MCMDM-1VWD study showed minor multimer abnormalities and were later reassessed to other VWD types. Those cases with minor multimer abnormalities

showed a higher proportion of mutations, whereas in individuals with completely normal VWF multimers mutations were identified in approximately 50% of the individuals.<sup>34</sup> More recently, large VWD population studies increased the number of identified type 1 mutations, with the most recent studies reporting identification of mutations in about 90% of the patients.<sup>27,35,36</sup> These studies, however, had strict inclusion criteria increasing the chance to identify mutations. Overall, a little more than 250 unique mutations have been assigned to VWD type 1 patients (Table S1A-D; in supplemental data online). However, the disease-causing effect was only proven by *in vitro* investigations for about one quarter of these mutations.

Mutations associated with VWD type 1 are dispersed throughout the whole VWF protein (Fig. 1A-C). Most mutations identified are heterozygous missense mutations, however also (small) deletions/insertions, splice site and nonsense mutations have been reported. The mutation mechanisms can roughly be divided in three groups: decreased VWF production, decreased secretion and increased clearance.

### **Decreased VWF production**

A lower VWF production has mostly been reported for patients heterozygous for a null allele. These heterozygous null alleles can be the result of nonsense mutations, frameshift mutations caused by (small) deletions or insertions and by splice site mutations. Heterozygosity for a null allele leads to production of protein from the non-mutated allele only, resulting in an expected production of only 50% of the normal VWF production. Since normal levels of VWF in plasma range between ~50 and 200 IU/dL, heterozygosity for a null allele will lead to VWF levels ranging between ~25 and 100 IU/dL.<sup>37</sup> Therefore, some people at the lower end of this distribution will be diagnosed as VWD type 1 and some people will be considered unaffected and are probably asymptomatic.

Small deletions and insertions often lead to a frameshift, which generates a premature stop codon usually within a few amino acids (indicated as for example p.Pro812Arg fs\*31). Premature stop codons caused by frameshift or nonsense mutations lead to an mRNA product which is mostly degraded by nonsense-mediated decay. Splice site mutations are also found in VWD type 1 patients and may lead to exon skipping or intron retention. Depending on the reading frame of an exon, this could lead either to the production of a truncated protein or to a premature stop codon. Whether exon skipping forms a truncated or nonsense allele is partly predicted by the reading frame (Fig. 1B), however this can only be proven by investigating RNA products in platelets or patient-derived endothelial cells.<sup>38-41</sup> For example, in the case of c.1534-3C>A and for c.5842+1G>C, this results in three different mRNA products.<sup>39,41</sup> Although not frequently reported, some mutations have been identified in the promoter region of *VWF* as well.<sup>29-31,42</sup> These may lead to altered binding of transcription factors to the *VWF* promoter region.<sup>42</sup>

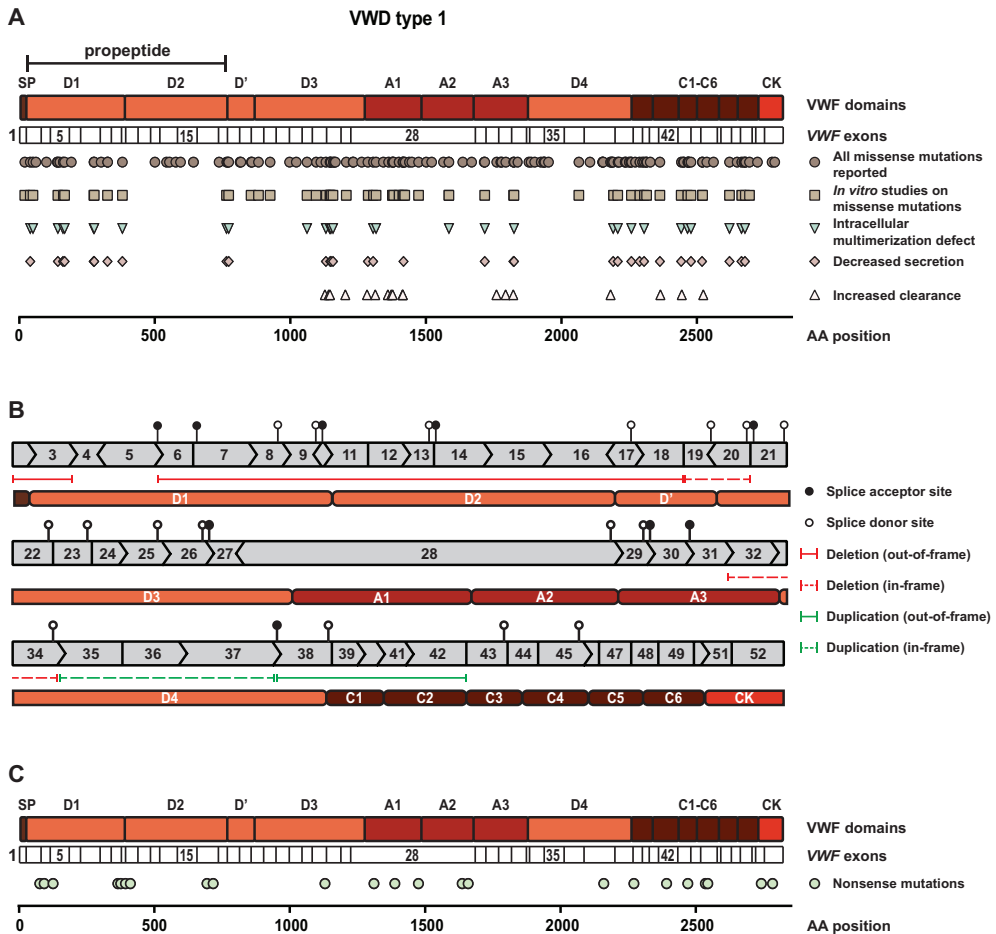
### **Decreased secretion**

Some patients have normal VWF production, but a decreased secretion of VWF from the endothelial cells. Existence of secretion defects from platelets is likely but has so far not been studied. Secretion defects encompass retention of VWF in the ER or Golgi, decreased Weibel-Palade body exocytosis and possibly degradation of mutant VWF by the proteasome. Secretion defects have been studied on a cellular level by *in vitro* overexpression of mutant VWF constructs in heterologous cell systems, or by studies on patient-derived endothelial cells. Decreased secretion from mutant VWF producing cells compared to normal VWF producing cells has been identified for many of the VWD type 1 mutations tested *in vitro* and decreased secretion is often seen in combination with an *in vitro* multimerization defect (Fig. 1A, Table S1A-D; in supplemental data online). Whether decreased secretion of VWF is caused by retention of VWF in the ER or Golgi can easily be studied by co-staining of VWF with an ER or Golgi marker and this defect has been identified for among others: p.Arg782Gln, p.Cys1130Phe, p.Cys1149Arg, p.Ser1285Pro, p.Val1822Gly and p.Cys2693Tyr.<sup>22,43-47</sup> For many mutations decreased VWF:Ag levels were found in conditioned medium, while normal VWF:Ag levels were found in the cell lysates. A suggested mechanism for the loss of VWF within the cell is the degradation of mutant VWF by the proteasome, which has been studied by Bodó *et al.* for VWF p.Cys1149Arg.<sup>48,49</sup> Besides *in vitro* investigations, the response of a patient to DDAVP could also be indicative for a secretion defect. However, DDAVP unresponsiveness can also relate to production defects, and therefore only *in vitro* studies can be conclusive in the identification of secretion defects.

### **Increased clearance**

VWF has a half-life in the circulation of about 8-12 hours. Increased clearance rates result in lower steady state plasma VWF:Ag levels and are associated with VWD type 1 and type 2B. Clearance defects of VWF are identified by an increased VWF propeptide to VWF:Ag ratio (VWFpp/VWF:Ag) and by shortened survival of plasma VWF:Ag levels after a DDAVP infusion.<sup>26,50,51</sup> Also, mouse experiments in which mutant VWF constructs are intravenously administered, or expressed in the hepatocytes after a hydrodynamic tail vein injection, proved clearance defects for a few mutations.<sup>26,52-54</sup> For VWD type 1, some mutations have been described that cause a clearance defect. Most mutations described are located in the D3 domain and include mutations at positions p.Cys1130, p.Trp1144, p.Cys1149 and p.Arg1205. The most common described variant is the VWD Vicenza mutation, p.Arg1205His, for which a macrophage-dependent increased clearance has been described.<sup>54,55</sup> Besides mutations in the D3 domain, also mutations in the A1, A3 and D4 domains have been associated with increased clearance in VWD type 1.<sup>30,34-36,51,56,57</sup>





VWD type 2A

VWD type 2A is associated with defective plasma multimers as a result of an intracellular multimerization defect or an increased susceptibility of VWF for cleavage by ADAMTS13. Diagnosis is based on a decreased VWF activity (VWF:RCo/VWF:Ag < 0.6), absent ristocetin induced platelet aggregation (RIPA) using low-dose ristocetin and lack of high molecular weight (HMW) multimers visualized by the VWF multimer analysis.<sup>28</sup> In total, a little more than 170 different type 2A mutations have been described in literature and for about half of these mutations, the disease-causing mechanism has been proven by *in vitro* studies (Fig. 2A, Table S2A-C; in supplemental data online). Type 2A mutations can be found in many VWF domains, although there is a cluster in the region D3-A2. Several different mutation mechanisms can be distinguished based on the location within the protein (Fig. 2A).

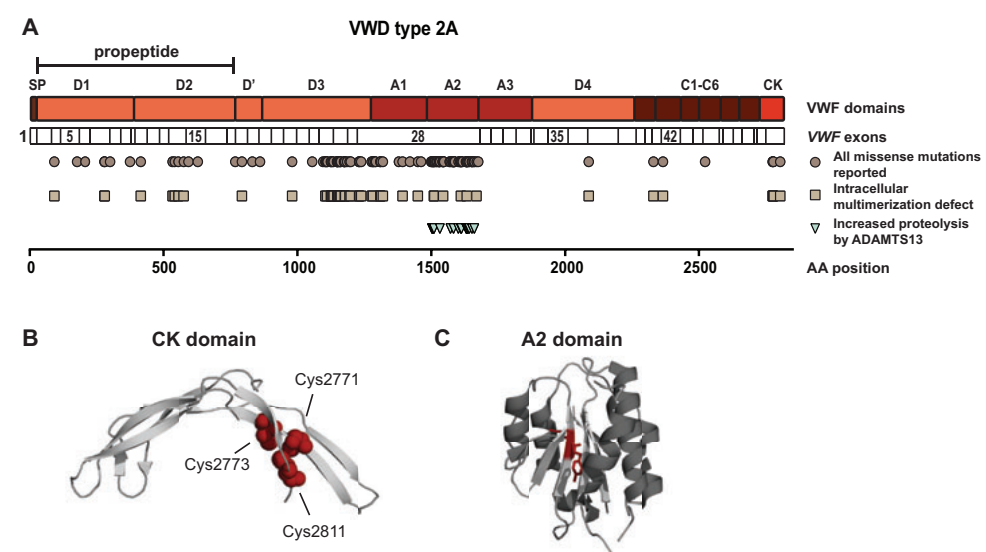


**Figure 2. Overview of VWD type 2A mutations.** (A) Representation of VWD type 2A mutations. The distribution of all VWD type 2A missense mutations reported so far is indicated in the upper line below the VWF domain structure and the VWF exon numbering. In the second line all missense mutations are displayed that have been associated with an intracellular multimerization defect proven by *in vitro* studies. In the lower line all missense mutations are displayed that result in increased proteolysis by ADAMTS13. (B) Crystal structure of the CK domain of VWF that is involved in the C-terminal dimerization process of VWF (PDB: 4NT5). The three amino acids, p.Cys2771, p.Cys2773 and p.Cys2811, involved in intermolecular disulfide bonding are indicated in red. Mutations p.Cys2771Arg/Ser/Tyr and p.Cys2773Ser/Arg are associated with VWD subtype 2A (IID). (C) Crystal structure of the VWD A2 domain (PDB: 3ZQK), which contains the cleavage site for ADAMTS13. ADAMTS13 cleaves VWF between Tyr 1605 and Met1606. Both amino acids are buried in the A2 domain and are indicated as ribbon structure in red.

Intracellular multimerization defects

VWF dimerization and multimerization takes place in the ER and TGN of endothelial cells and megakaryocytes. First, VWF dimers are formed by C-terminal dimerization

of the cysteine knot (CK) (Fig. 2B).<sup>58</sup> This process involves the formation of three intermolecular disulfide bonds Cys2771-2773', Cys2771'-2773 and Cys2811-2811' which was recently shown to be catalyzed by protein disulfide isomerase (PDI) (Fig. 2B).<sup>58</sup> Mutations described at positions Cys2771 and Cys2773 are associated with an intracellular dimerization defect, showing loss of HMW VWF and the presence of uneven bands.<sup>59-61</sup> These mutations have historically been subcategorized as subtype 2A (IID). Also a few other mutations in the CK domain have been assigned to subtype 2A (IID), including homozygous p.Ala2801Asp and heterozygous p.Ser2775Cys.<sup>62,63</sup> Interestingly, homozygous cysteine mutations in the CK domain causing disruption of intramolecular disulfide bonds are associated with VWD type 3.<sup>64</sup>

After dimerization of VWF, two VWF monomers will align to form a so-called dimeric bouquet.<sup>65</sup> The low pH and high Ca<sup>2+</sup> concentration present in the TGN facilitate dimerization of two D1-D2 domains and allow intermolecular disulfide bond formation between two cysteine residues (p.Cys1099-p.Cys1099' and p.Cys1142-p.Cys1142') of the D3 domain.<sup>66,67</sup> Defects in N-terminal dimerization can be caused by two different mechanisms. First, homozygous mutations in the propeptide (D1 and D2 domains) of VWF, or patients being compound heterozygous for a propeptide mutation and a null allele, are associated with severely affected multimerization and intracellular retention and are described as both subtype 2A (IIC) and type 3 VWD.<sup>63,68-72</sup> Co-expression of normal and mutant VWF constructs in heterologous cell systems show a normal multimers profile and heterozygous carriers of propeptide mutations are unaffected or diagnosed with VWD type 1.<sup>72</sup> Secondly, several type 2A mutations have been described in the D3 domain as well, and are mostly inherited in a heterozygous fashion. These mutations are assigned as subtype 2A (IIE) and generally show some loss of HMW VWF and a decrease of proteolytic bands in the multimeric pattern in plasma. The exact mechanism behind the reduced proteolytic bands has not been elucidated yet, but could potentially be the result of increased clearance seen for these mutants, or lower sensitivity for the proteolytic effects of ADAMTS13. Mutations in the D3 domain cause a loss of HMW VWF in *in vitro* studies too, indicating an intracellular multimerization defect as well. Most mutations involve cysteine residues affecting intramolecular disulfide bonds.<sup>67</sup>

Several VWD type 2A mutations have been described in the A1 domain of VWF with no clear common mechanism. Many of these type 2A mutations have been assigned to VWD type 2B or 2M patients as well, and might have a combined mechanism of defective multimerization and defective GPIb binding. Overexpression of most of the A1 mutations in heterologous cell systems result in an intracellular multimerization defect, but also increased clearance rates are detected for some mutations (Table S2A-C; in supplemental data online).

### ***Increased proteolysis by ADAMTS13***

After secretion of VWF from the endothelial cells, VWF unwinds into ultra-large VWF strings making the A2 domain accessible for proteolysis by ADAMTS13.<sup>73</sup> This results in the release of all sizes of VWF multimers in the circulation. Normal proteolysis by ADAMTS13 in plasma can be visualized on a multimer blot by the presence of small satellite bands above and below the thick multimeric band. ADAMTS13 cleaves VWF between p.Tyr1605 and p.Met1606, two amino acids buried deep inside the A2 domain (Fig. 2C). Several mutations in the A2 domain increase the sensitivity to proteolysis by ADAMTS13, which results in a decrease in HMW VWF and the presence of broad proteolytic (satellite) bands in plasma. Intracellular multimerization is not affected for these mutations and therefore a normal multimer pattern will be generated *in vitro*. The disease-causing mechanism can therefore only be identified by multimer analysis on plasma samples or by the addition of ADAMTS13 to *in vitro* expression systems.<sup>74-77</sup>

### **VWD type 2B**

The VWF A1 domain binds platelets through GPIb; this only occurs when the A1 domain is in its elongated form as induced by high shear of the microvasculature.<sup>78</sup> Without the presence of flow or activation of VWF by ristocetin, the VWF A1 domain is not able to interact with GPIb. However, gain-of-function mutations in the A1 domain can make VWF more active and therefore VWF can bind GPIb without activation of VWF by shear *in vivo* or by ristocetin *in vitro*. These mutations are associated with VWD type 2B. Type 2B diagnosis is based on a low VWF activity *versus* VWF:Ag level (VWF:RCO/VWF:Ag < 0.6) and increased RIPA in the presence of low concentrations ristocetin.<sup>28</sup> These diagnostic tools will not distinguish VWD type 2B from platelet-type VWD. As platelet-type VWD does not reflect a VWF mutation platelet-type VWD is not further considered in the review. Many type 2B patients also show increased clearance of the VWF-platelet complex and this may result in variable degrees of secondary thrombocytopenia and a loss of HMW VWF.<sup>79,80</sup> It was recently identified that the increased clearance is the result of a higher affinity of macrophages' LRP1 to the A1 domain for certain type 2B mutations.<sup>12</sup> Furthermore, blood smears of type 2B patients often show giant platelets and platelet aggregates.<sup>81</sup>

In total, 43 type 2B mutations have been reported and for about half of them the disease-causing mechanism was proven by *in vitro*, *in vivo* or *in silico* studies (Fig. 3A, Table S3; in supplemental data online). Although *in vitro* studies help to determine the severity of the mutation, they are not necessary for identification of the mechanism of type 2B mutations. Most mutations are located in the A1 domain, with the exception of a few mutations that have been reported at the C-terminal end of the D3 domain (Fig. 3A). Crystal structures of the VWF A1 domain and platelet GPIb have revealed two interactions between VWF A1 and GPIb (Fig.

3B).<sup>82-84</sup> The primary interaction is located between the  $\beta$ -sheet of the  $\beta$ -switch region of GPIb and the  $\beta$ -sheet of VWF, generating an extended  $\beta$ -sheet between the two molecules (Fig. 3B).<sup>82-84</sup> The second interaction is located between the N-cap of GPIb and the A1 domain of VWF, and in proximity of this interaction in the A1 domain, most VWD type 2B mutations are identified (Fig. 3C, light blue). The A1 domain at this site is stabilized by several hydrogen bonds and a disulfide bond between p.Cys1272 and p.Cys1458.<sup>82-84</sup> Mutations in this region can destabilize the domain, thereby inducing increased affinity to GPIb.

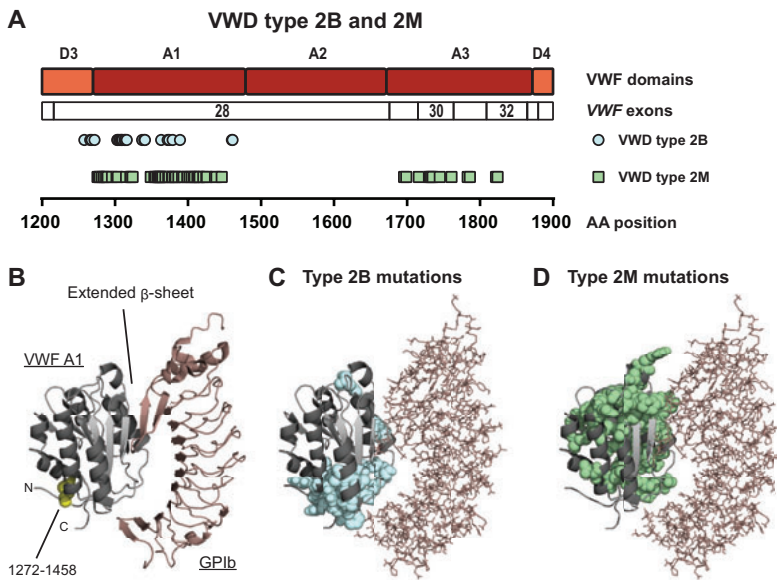


**Figure 3. Overview of VWD type 2B and type 2M mutations.** (A) Representation of VWD type 2B and type 2M mutations. The distribution of all VWD type 2B mutations reported so far is indicated in the upper line below the VWF domain structure and the VWF exon numbering. All these mutations are located in the A1 domain or at the C-terminal end of the D3 domain. In the lower line all positions of mutations are displayed that have been reported for VWD type 2M. Mutations that are associated with decreased binding to GPIb are located in the A1 domain. Mutations with an isolated collagen binding defect are located in the A3 domain. (B) Crystal structure of the VWF A1 domain (grey) together with GPIb (pink) (PDB: 1SQ0). The A1 domain interacts with GPIb through the extended  $\beta$ -sheet and by the N-cap of GPIb located in the bottom of this figure. The intermolecular disulfide bond in the A1 domain is indicated in yellow and is important in the structure of the domain. (C) Crystal structure of the A1 domain and GPIb in which the location of the VWD type 2B mutations are indicated in light blue. Most mutations are located in close proximity of the intermolecular disulfide bond and the interaction with the N-cap of GPIb. (D) Crystal structure of the A1 domain and GPIb in which the location of the VWD type 2M mutations are indicated in green. Mutations are spread throughout the whole domain.

Although all type 2B mutations lead to an increased binding to GPIb, clear differences have been observed between the phenotypes of certain mutations. These differences include platelet count and the ability of mutant VWF to bind platelets or immobilized GPIb in the absence or the presence of low concentrations ristocetin. A very severe phenotype can be

found in patients with for example p.Val1316Met with thrombocytopenia in resting state and a very strong binding to GPIb in the absence of ristocetin. In most patients with this mutation, also giant platelets and platelet aggregates are observed on blood smears.<sup>85</sup> Intermediate phenotypes are associated with thrombocytopenia only during stress situations, like surgery or pregnancy. In milder affected patients, no thrombocytopenia is observed and a low concentration of ristocetin is needed to agglutinate VWF.

## VWD type 2M

VWD type 2M is usually associated with low VWF activity (VWF:RCo/VWF:Ag < 0.6), a more or less normal multimer pattern and no RIPA in the presence of low concentrations ristocetin.<sup>28</sup> However, patients with an isolated collagen binding defect, but normal VWF:RCo, are also assigned to VWD type 2M. In total, somewhat over 80 mutations have been assigned to VWD type 2M, of which most are located in the A1 domain (Fig. 3A, Table S4A-B; in supplemental data online).

### *GPIb binding defect*

Most mutations associated with a decreased binding to GPIb are heterozygous mutations located in the A1 domain of VWF (Fig. 3A). These mutations can either affect the direct binding of VWF to GPIb or enhance the stability of the A1 domain, thereby reducing the rate of unfolding of the A1 domain under flow.<sup>86,87</sup> A lower rate of unfolding has for example been observed in VWF p.Gly1324Ala and p.Gly1324Ser.<sup>87</sup> A direct binding effect is usually associated with a destabilized protein, also described as molten globule, and has been seen in for example p.Ser1285Phe.<sup>88</sup> Whether a type 2M mutation is associated with decreased or increased stability of the A1 domain can be identified by the binding of monoclonal antibodies to specific A1 domains, or biophysical studies on for example the crystal structure of mutants or the thermodynamic stability of the protein.<sup>86,87</sup> Type 2M mutations that affect platelet binding are identified throughout the whole VWF A1 domain (Fig. 3A and D).

### *Collagen binding defect*

VWF binds collagen types I and III via its A1 and A3 domains and collagen types IV and VI via its A1 domain.<sup>89-91</sup> Defects in collagen binding might lead to VWD or an increased risk of bleeding. Collagen binding defects could be identified by the VWF-collagen binding assay, however this assay is usually not included in diagnostic procedures.<sup>28</sup> And if the assay is performed, it usually only includes types I and/or III collagen.<sup>92</sup> Therefore, many mutations associated with collagen binding defects might remain unidentified.

Most collagen binding defects identified are restricted to binding of collagen I and III, since commercial assays are only developed for these two types of collagen.<sup>92</sup> Identified mutations associated with defective collagen binding are mainly heterozygous mutations located in the A3 domain of VWF (Fig. 3A).<sup>93-98</sup>

Collagen IV and VI binding assays are not included in regular diagnostic procedures and mutations affecting binding to these collagens have only occasionally been reported.<sup>90,91</sup> A combined collagen IV and VI binding defect has been reported for the A1 mutations p.Arg1399His, p.Gln1402Pro and p.Arg1392\_Gln1402 del. Furthermore, a collagen IV binding defect was reported for p.Arg1315Cys (also reported as type 1 and 2A mutation) and p.Ser1358Asn, and a collagen VI binding defect for p.Ser1387Ile. It is however important to state that Arg1399His has also been identified among healthy controls, and therefore it cannot be seen as a definite VWD causing mutation, however it may be associated with an increased risk for bleeding.<sup>90</sup>

## VWD type 2N

VWD type 2N is characterized by a loss of binding to coagulation FVIII resulting in decreased FVIII plasma levels and activity. Diagnosis is based on a normal VWF:RCo/VWF:Ag ratio ( $> 0.6$ ), but a decrease in FVIII activity *versus* VWF:Ag level (FVIII:C/VWF:Ag  $< 0.6$ ) and decreased VWF-FVIII binding (VWF:FVIIIIB).<sup>28</sup> Since the stoichiometry of FVIII and VWF is 1:50 (one FVIII molecule for every 50 VWF monomers) there is an excess of FVIII binding sites in a VWF multimer and thus the type 2N phenotype will only be expressed in case of a homozygous FVIII binding defect or in case of compound heterozygosity for a FVIII binding defect and a VWF null allele.<sup>99</sup> In total, 31 different mutations in the VWF D2, D' and D3 domains have been described that affect FVIII binding (Table S5; in supplemental data online).

The major FVIII binding site in VWF is located in the D' domain of VWF.<sup>100</sup> The D' domain of VWF contains 2 modules, the trypsin-inhibitor-like (TIL') and E' modules.<sup>3,100</sup> Most type 2N mutations are located in, or in close vicinity of the TIL' module, which is a very flexible region within VWF (Fig. 4A-C).<sup>65,100</sup> Since the D' domain contains several disulfide bonds important in N-terminal multimerization of VWF, several type 2N mutations are associated with defective multimerization as well.<sup>101-103</sup> One of the most common type 2N mutation is the p.Arg854Gln mutation that, because of the high frequency, has a high prevalence of co-inheritance with other types of VWD.<sup>104</sup>

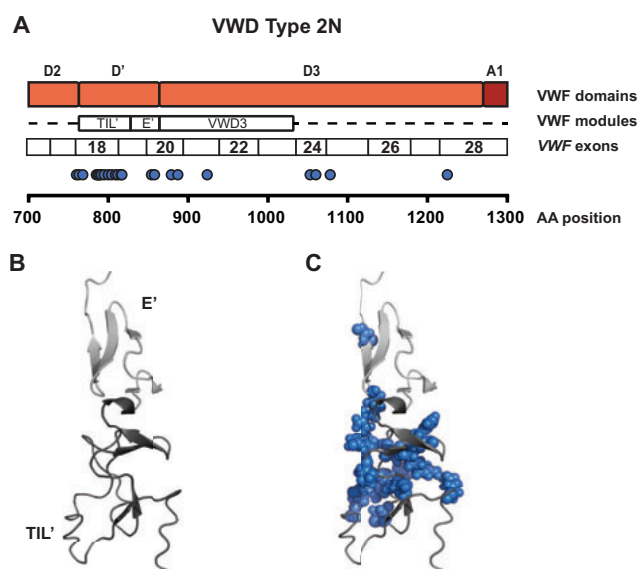


**Figure 4. Overview of VWD type 2N mutations.** (A) Representation of VWD type 2N mutations. The distribution of all VWD type 2N mutations reported so far is indicated below the VWF domain structure and the *VWF* exon numbering. Mutations are located in the D2, D' and D3 domain of VWF. (B) Solution structure of the D' domain of VWF, the major FVIII binding region (PDB: 2MHP). The D' domain consists of two modules, the E' and TIL' modules. The TIL' module is very flexible and is indicated in dark grey. The E' module (light grey) contains a  $\beta$ -sheet and is less flexible. (C) Solution structure of the D' domain of VWF with the VWD type 2N mutations indicated in blue. Most mutations are located in the flexible TIL' module.

### VWD type 3

VWD type 3 patients have undetectable VWF:Ag levels in their plasma and show a severe bleeding phenotype.<sup>28</sup> Most patients do not produce VWF at all, as is the consequence of homozygous or compound heterozygous null alleles. Some patients, however, are homozygous or compound heterozygous for missense mutations. These patients normally produce VWF, but the mutant VWF is not secreted from the endothelial cells, or undergoes a very rapid clearance. In total, more than 280 unique mutations have been identified with VWD type 3 (Table S6A-E; in supplemental data online).

#### Null alleles

Most VWD type 3 patients develop the phenotype by the presence of two null alleles caused by homozygous or compound heterozygous nonsense, frameshift or splice site mutations. Since no or very low VWF:Ag levels are detected in VWD type 3 patients, there is a high probability that the splice site mutations identified in type 3 patients also result in a frameshift and nonsense-mediated decay. Mutations associated with null alleles are located throughout the whole *VWF* gene (Fig. 5A and B). Although not frequently reported, some patients were identified having a whole *VWF* gene deletion.<sup>35,105-107</sup>



Null alleles could also result from a gene conversion with the pseudogene of *VWF*. This pseudogene is located on chromosome 22 and has a high sequence similarity with exons 23 until 34.<sup>108</sup> Depending on the length of the conversion, the conversion may be associated with mutations: p.Val1229Gly, p.Asn1231Thr, p.Ser1263Pro, p.Pro1266Leu, p.Val1279Ile, p.Leu1288Val, p.Gln1311\*, p.Ile1343Val, p.Val1360Ala, and p.Phe1369Ile.<sup>109-111</sup> Homozygous or compound heterozygous gene conversions including p.Gln1311\* will lead to VWD type 3.<sup>111</sup> Heterozygous gene conversions may lead to VWD type 1, depending on the variation in VWF:Ag levels as described under VWD type 1.

### ***Homozygous/compound heterozygous missense mutations***

Although most VWD type 3 is associated with null alleles, some patients have very low VWF:Ag plasma levels because of missense mutations, which are mostly inherited in a homozygous or compound heterozygous fashion (Fig. 5A; Table S6A; in supplemental data online). The effect of several missense mutations was studied in heterologous cell systems, and for all mutations tested a severe secretion defect was found confirming the plasma phenotype of very low or undetectable VWF:Ag levels (Fig. 5A).<sup>64</sup> Most of these mutations replace a cysteine and/or are located at the C- or N-terminal ends of VWF and are important in the multimerization process.<sup>64,112-116</sup>

Clearance defects cannot be detected in *in vitro* systems, however several mutations known to be associated with rapid clearance were identified in type 3 patients.<sup>117</sup> These patients showed increased VWFpp/VWF:Ag ratios and had a lower bleeding score compared to type 3 caused by null alleles.<sup>117</sup>

## **Conclusions**

Advances in sequencing technology along with lower associated costs have resulted in an ever increasing number of patients sequenced for the *VWF* gene. This has resulted in the identification of more than 750 unique mutations in *VWF*. The disease causing mechanism behind these mutations has been proven either through *in vitro* or *in vivo* studies for approximately 220 mutations, and for several others, the mechanism became evident based on the type or location of the mutation and the patients' phenotype. However, many of the identified mutations remain candidate mutations, as the disease causing effects are yet to be elucidated.

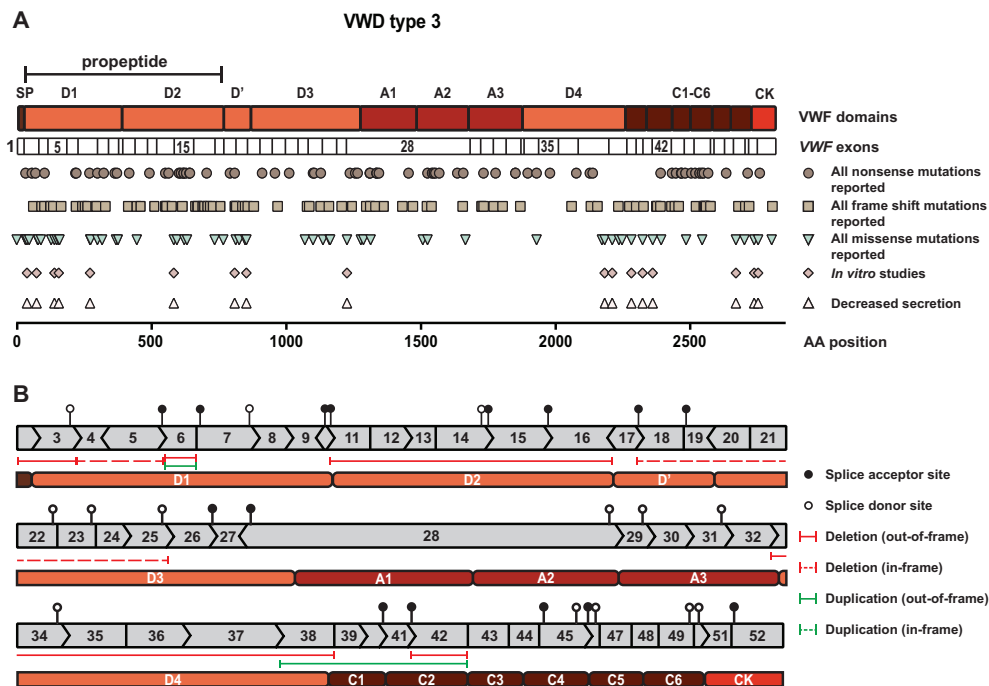


**Figure 5. Overview of VWD type 3 mutations.** (A) Representation of VWD type 3 mutations. The distribution of all VWD type 3 nonsense mutations reported so far is indicated below the VWF domain structure and the VWF exon numbering. In the second line all frameshift mutations and in the third line all missense mutations are indicated. All mutations that have been studied by *in vitro* experiments are displayed in the fourth line, and all those mutations associated with a clear secretion defect are in the lower line. (B) Representation of the open reading frame of the VWF exons including most of the VWD type 3 deletions and duplications described and mutations described in splice acceptor (solid circles) and splice donor sites (open circles). All exons are depicted to scale. For explanation of the open reading frame see the legend of Fig. 1.

## Acknowledgements

This review was financially supported by a research grant from the Landsteiner Foundation for Blood Transfusion Research (grant 1504). We would like to thank dhr. J.W. Schoones of the Walaeus library of the Leiden University Medical Center for composition of the advanced literature search strategy.

## References

1. Jaffe EA, Nachman RL, Becker CG, Minick CR. Culture of human endothelial cells derived from umbilical veins. Identification by morphologic and immunologic criteria. *J Clin Invest.* 1973;**52**(11):2745-2756.
2. Sporn LA, Chavin SI, Marder VJ, Wagner DD. Biosynthesis of von Willebrand protein by human megakaryocytes. *J Clin Invest.* 1985;**76**(3):1102-1106.
3. Zhou YF, Eng ET, Zhu J, Lu C, Walz T, Springer TA. Sequence and structure relationships within von Willebrand factor. *Blood.* 2012;**120**(2):449-458.
4. Zhou YF, Springer TA. Highly reinforced structure of a C-terminal dimerization domain in von Willebrand factor. *Blood.* 2014;**123**(12):1785-1793.
5. Vischer UM, Wagner DD. von Willebrand factor proteolytic processing and multimerization precede the formation of Weibel-Palade bodies. *Blood.* 1994;**83**(12):3536-3544.
6. Mayadas TN, Wagner DD. In vitro multimerization of von Willebrand factor is triggered by low pH. Importance of the propolypeptide and free sulfhydryls. *J Biol Chem.* 1989;**264**(23):13497-13503.
7. Mourik MJ, Faas FG, Zimmermann H, Voorberg J, Koster AJ, Eikenboom J. Content delivery to newly forming Weibel-Palade bodies is facilitated by multiple connections with the Golgi apparatus. *Blood.* 2015;**125**(22):3509-3516.
8. McGrath RT, McRae E, Smith OP, O'Donnell JS. Platelet von Willebrand factor--structure, function and biological importance. *Br J Haematol.* 2010;**148**(6):834-843.
9. De Ceunynck K, De Meyer SF, Vanhoorelbeke K. Unwinding the von Willebrand factor strings puzzle. *Blood.* 2013;**121**(2):270-277.
10. Andre P, Denis CV, Ware J, et al. Platelets adhere to and translocate on von Willebrand factor presented by endothelium in stimulated veins. *Blood.* 2000;**96**(10):3322-3328.
11. Weiss HJ, Sussman II, Hoyer LW. Stabilization of factor VIII in plasma by the von Willebrand factor. Studies on posttransfusion and dissociated factor VIII and in patients with von Willebrand's disease. *J Clin Invest.* 1977;**60**(2):390-404.
12. Wohner N, Legendre P, Casari C, Christophe OD, Lenting PJ, Denis CV. Shear stress-independent binding of von Willebrand factor-type 2B mutants p.R1306Q & p.V1316M to LRP1 explains their increased clearance. *J Thromb Haemost.* 2015;**13**(5):815-820.
13. Casari C, Lenting PJ, Wohner N, Christophe OD, Denis CV. Clearance of von Willebrand factor. *J Thromb Haemost.* 2013;**11 Suppl 1**:202-211.
14. Leebeek FWG, Eikenboom JCJ. Von Willebrand's Disease. *N Engl J Med.* 2016;**375**(21):2067-2080.
15. Sadler JE, Budde U, Eikenboom JC, et al. Update on the pathophysiology and classification of von Willebrand disease: a report of the Subcommittee on von Willebrand Factor. *J Thromb Haemost.* 2006;**4**(10):2103-2114.
16. Ginsburg D, Handin RI, Bonthron DT, et al. Human von Willebrand factor (vWF): isolation of complementary DNA (cDNA) clones and chromosomal localization. *Science.* 1985;**228**(4706):1401-1406.
17. Lynch DC, Zimmerman TS, Collins CJ, et al. Molecular cloning of cDNA for human von Willebrand

- factor: authentication by a new method. *Cell*. 1985;**41**(1):49-56.
18. Sadler JE, Shelton-Inloes BB, Sorace JM, Harlan JM, Titani K, Davie EW. Cloning and characterization of two cDNAs coding for human von Willebrand factor. *Proc Natl Acad Sci U S A*. 1985;**82**(19):6394-6398.
  19. Verweij CL, de Vries CJ, Distel B, et al. Construction of cDNA coding for human von Willebrand factor using antibody probes for colony-screening and mapping of the chromosomal gene. *Nucleic Acids Res*. 1985;**13**(13):4699-4717.
  20. Michaux G, Hewlett LJ, Messenger SL, et al. Analysis of intracellular storage and regulated secretion of 3 von Willebrand disease-causing variants of von Willebrand factor. *Blood*. 2003;**102**(7):2452-2458.
  21. Starke RD, Paschalaki KE, Dyer CE, et al. Cellular and molecular basis of von Willebrand disease: studies on blood outgrowth endothelial cells. *Blood*. 2013;**121**(14):2773-2784.
  22. Wang JW, Bouwens EA, Pintao MC, et al. Analysis of the storage and secretion of von Willebrand factor in blood outgrowth endothelial cells derived from patients with von Willebrand disease. *Blood*. 2013;**121**(14):2762-2772.
  23. Denis C, Methia N, Frenette PS, et al. A mouse model of severe von Willebrand disease: defects in hemostasis and thrombosis. *Proc Natl Acad Sci U S A*. 1998;**95**(16):9524-9529.
  24. Adam F, Casari C, Prevost N, et al. A genetically-engineered von Willebrand disease type 2B mouse model displays defects in hemostasis and inflammation. *Sci Rep*. 2016;**6**:26306.
  25. Pruss CM, Golder M, Bryant A, et al. Pathologic mechanisms of type 1 VWD mutations R1205H and Y1584C through in vitro and in vivo mouse models. *Blood*. 2011;**117**(16):4358-4366.
  26. Haberichter SL, Castaman G, Budde U, et al. Identification of type 1 von Willebrand disease patients with reduced von Willebrand factor survival by assay of the VWF propeptide in the European study: molecular and clinical markers for the diagnosis and management of type 1 VWD (MCMDM-1VWD). *Blood*. 2008;**111**(10):4979-4985.
  27. Federici AB, Bucciarelli P, Castaman G, et al. Management of inherited von Willebrand disease in Italy: results from the retrospective study on 1234 patients. *Semin Thromb Hemost*. 2011;**37**(5):511-521.
  28. de Jong A, Eikenboom J. Developments in the diagnostic procedures for von Willebrand disease. *J Thromb Haemost*. 2016;**14**(3):449-460.
  29. Cumming A, Grundy P, Keeney S, et al. An investigation of the von Willebrand factor genotype in UK patients diagnosed to have type 1 von Willebrand disease. *Thromb Haemost*. 2006;**96**(5):630-641.
  30. Goodeve A, Eikenboom J, Castaman G, et al. Phenotype and genotype of a cohort of families historically diagnosed with type 1 von Willebrand disease in the European study, Molecular and Clinical Markers for the Diagnosis and Management of Type 1 von Willebrand Disease (MCMDM-1VWD). *Blood*. 2007;**109**(1):112-121.
  31. James PD, Notley C, Hegadorn C, et al. The mutational spectrum of type 1 von Willebrand disease: Results from a Canadian cohort study. *Blood*. 2007;**109**(1):145-154.

32. Johansson AM, Hallden C, Sall T, Lethagen S. Variation in the VWF gene in Swedish patients with type 1 von Willebrand Disease. *Ann Hum Genet.* 2011;**75**(4):447-455.
33. Robertson JD, Yenson PR, Rand ML, et al. Expanded phenotype-genotype correlations in a pediatric population with type 1 von Willebrand disease. *J Thromb Haemost.* 2011;**9**(9):1752-1760.
34. Budde U, Schneppenheim R, Eikenboom J, et al. Detailed von Willebrand factor multimer analysis in patients with von Willebrand disease in the European study, molecular and clinical markers for the diagnosis and management of type 1 von Willebrand disease (MCMDM-1VWD). *J Thromb Haemost.* 2008;**6**(5):762-771.
35. Veyradier A, Boisseau P, Fressinaud E, et al. A Laboratory Phenotype/Genotype Correlation of 1167 French Patients From 670 Families With von Willebrand Disease: A New Epidemiologic Picture. *Medicine.* 2016;**95**(11):e3038.
36. Batlle J, Pérez-Rodríguez A, Corrales I, et al. Molecular and clinical profile of von Willebrand disease in Spain (PCM-EVW-ES): Proposal for a new diagnostic paradigm. *Thromb Haemost.* 2016;**115**(1):40-50.
37. Castaman G, Tosetto A, Cappelletti A, et al. Validation of a rapid test (VWF-LIA) for the quantitative determination of von Willebrand factor antigen in type 1 von Willebrand disease diagnosis within the European multicenter study MCMDM-1VWD. *Thromb Res.* 2010;**126**(3):227-231.
38. Castaman G, Plate M, Giacomelli SH, Rodeghiero F, Duga S. Alterations of mRNA processing and stability as a pathogenic mechanism in von Willebrand factor quantitative deficiencies. *J Thromb Haemost.* 2010;**8**(12):2736-2742.
39. Hawke L, Bowman ML, Poon MC, Scully MF, Rivard GE, James PD. Characterization of aberrant splicing of von Willebrand factor in von Willebrand disease: an underrecognized mechanism. *Blood.* 2016;**128**(4):584-593.
40. Yadegari H, Biswas A, Akhter MS, et al. Intron retention resulting from a silent mutation in the VWF gene that structurally influences the 5' splice site. *Blood.* 2016;**128**(17):2144-2152.
41. Gallinaro L, Sartorello F, Pontara E, et al. Combined partial exon skipping and cryptic splice site activation as a new molecular mechanism for recessive type 1 von Willebrand disease. *Thromb Haemost.* 2006;**96**(6):711-716.
42. Othman M, Chirinian Y, Brown C, et al. Functional characterization of a 13-bp deletion (c.-1522\_-1510del13) in the promoter of the von Willebrand factor gene in type 1 von Willebrand disease. *Blood.* 2010;**116**(18):3645-3652.
43. Wang JW, Groeneveld DJ, Cosemans G, et al. Biogenesis of Weibel-Palade bodies in von Willebrand's disease variants with impaired von Willebrand factor intrachain or interchain disulfide bond formation. *Haematologica.* 2012;**97**(6):859-866.
44. White-Adams TC, Ng CJ, Jacobi PM, Haberichter SL, Di Paola JA. Mutations in the D'D3 region of VWF traditionally associated with type 1 VWD lead to quantitative and qualitative deficiencies of VWF. *Thromb Res.* 2016;**145**:112-118.

45. Wang JW, Valentijn KM, de Boer HC, et al. Intracellular storage and regulated secretion of von Willebrand factor in quantitative von Willebrand disease. *J Biol Chem*. 2011;**286**(27):24180-24188.
46. Eikenboom JC, Matsushita T, Reitsma PH, et al. Dominant type 1 von Willebrand disease caused by mutated cysteine residues in the D3 domain of von Willebrand factor. *Blood*. 1996;**88**(7):2433-2441.
47. Groeneveld DJ, Wang JW, Mourik MJ, et al. Storage and secretion of naturally occurring von Willebrand factor A domain variants. *Br J Haematol*. 2014;**167**(4):529-540.
48. Bodó I, Katsumi A, Tuley EA, Eikenboom JC, Dong Z, Sadler JE. Type 1 von Willebrand disease mutation Cys1149Arg causes intracellular retention and degradation of heterodimers: a possible general mechanism for dominant mutations of oligomeric proteins. *Blood*. 2001;**98**(10):2973-2979.
49. Lyons SE, Bruck ME, Bowie EJ, Ginsburg D. Impaired intracellular transport produced by a subset of type IIA von Willebrand disease mutations. *J Biol Chem*. 1992;**267**(7):4424-4430.
50. Borchiellini A, Fijnvandraat K, ten Cate JW, et al. Quantitative analysis of von Willebrand factor propeptide release in vivo: effect of experimental endotoxemia and administration of 1-deamino-8-D-arginine vasopressin in humans. *Blood*. 1996;**88**(8):2951-2958.
51. Eikenboom J, Federici AB, Dirven RJ, et al. VWF propeptide and ratios between VWF, VWF propeptide, and FVIII in the characterization of type 1 von Willebrand disease. *Blood*. 2013;**121**(12):2336-2339.
52. Schooten CJ, Tjernberg P, Westein E, et al. Cysteine-mutations in von Willebrand factor associated with increased clearance. *J Thromb Haemost*. 2005;**3**(10):2228-2237.
53. Lenting PJ, Westein E, Terraube V, et al. An experimental model to study the in vivo survival of von Willebrand factor. Basic aspects and application to the R1205H mutation. *J Biol Chem*. 2004;**279**(13):12102-12109.
54. Rawley O, O'Sullivan JM, Chion A, et al. von Willebrand factor arginine 1205 substitution results in accelerated macrophage-dependent clearance in vivo. *J Thromb Haemost*. 2015;**13**(5):821-826.
55. Casonato A, Pontara E, Sartorello F, et al. Reduced von Willebrand factor survival in type Vicenza von Willebrand disease. *Blood*. 2002;**99**(1):180-184.
56. Castaman G, Lethagen S, Federici AB, et al. Response to desmopressin is influenced by the genotype and phenotype in type 1 von Willebrand disease (VWD): results from the European Study MCMDM-1VWD. *Blood*. 2008;**111**(7):3531-3539.
57. Millar CM, Riddell AF, Brown SA, et al. Survival of von Willebrand factor released following DDAVP in a type 1 von Willebrand disease cohort: influence of glycosylation, proteolysis and gene mutations. *Thromb Haemost*. 2008;**99**(5):916-924.
58. Lippok S, Kolsek K, Lof A, et al. von Willebrand factor is dimerized by protein disulfide isomerase. *Blood*. 2016;**127**(9):1183-1191.
59. Tjernberg P, Vos HL, Spaargaren-van Riel CC, et al. Differential effects of the loss of intrachain-

- versus interchain-disulfide bonds in the cystine-knot domain of von Willebrand factor on the clinical phenotype of von Willebrand disease. *Thromb Haemost.* 2006;**96**(6):717-724.
60. Enayat MS, Guilliatt AM, Surdhar GK, et al. Aberrant dimerization of von Willebrand factor as the result of mutations in the carboxy-terminal region: identification of 3 mutations in members of 3 different families with type 2A (phenotype IID) von Willebrand disease. *Blood.* 2001;**98**(3):674-680.
  61. Schneppenheim R, Budde U, Obser T, et al. Expression and characterization of von Willebrand factor dimerization defects in different types of von Willebrand disease. *Blood.* 2001;**97**(7):2059-2066.
  62. Hommais A, Stépanian A, Fressinaud E, et al. Impaired dimerization of von Willebrand factor subunit due to mutation A2801D in the CK domain results in a recessive type 2A subtype IID von Willebrand disease. *Thromb Haemost.* 2006;**95**(5):776-781.
  63. Brehm MA, Huck V, Aponte-Santamaria C, et al. von Willebrand disease type 2A phenotypes IIC, IID and IIE: A day in the life of shear-stressed mutant von Willebrand factor. *Thromb Haemost.* 2014;**112**(1):96-108.
  64. Tjernberg P, Vos HL, Castaman G, Bertina RM, Eikenboom JC. Dimerization and multimerization defects of von Willebrand factor due to mutated cysteine residues. *J Thromb Haemost.* 2004;**2**(2):257-265.
  65. Zhou YF, Eng ET, Nishida N, Lu C, Walz T, Springer TA. A pH-regulated dimeric bouquet in the structure of von Willebrand factor. *EMBO J.* 2011;**30**(19):4098-4111.
  66. Huang RH, Wang Y, Roth R, et al. Assembly of Weibel-Palade body-like tubules from N-terminal domains of von Willebrand factor. *Proc Natl Acad Sci U S A.* 2008;**105**(2):482-487.
  67. Purvis AR, Gross J, Dang LT, et al. Two Cys residues essential for von Willebrand factor multimer assembly in the Golgi. *Proc Natl Acad Sci U S A.* 2007;**104**(40):15647-15652.
  68. Holmberg L, Karpman D, Isaksson C, Kristoffersson AC, Lethagen S, Schneppenheim R. Ins405AsnPro mutation in the von Willebrand factor propeptide in recessive type 2A (IIC) von Willebrand's disease. *Thromb Haemost.* 1998;**79**(4):718-722.
  69. Lanke E, Kristoffersson AC, Philips M, Holmberg L, Lethagen S. Characterization of a novel mutation in the von Willebrand factor propeptide in a distinct subtype of recessive von Willebrand disease. *Thromb Haemost.* 2008;**100**(2):211-216.
  70. Obser T, Ledford-Kraemer M, Oyen F, et al. Identification and characterization of the elusive mutation causing the historical von Willebrand Disease type IIC Miami. *J Thromb Haemost.* 2016;**14**(9):1725-1735.
  71. Enayat MS, Ravanbod S, Rassoulzadegan M, et al. Identification of a homozygous Cys410Ser mutation in the von Willebrand factor D2 domain causing type 2A(IIC) von Willebrand disease phenotype in an Iranian patient. *Haemophilia.* 2013;**19**(4):e261-264.
  72. Habrichter SL, Budde U, Obser T, Schneppenheim S, Wermes C, Schneppenheim R. The mutation N528S in the von Willebrand factor (VWF) propeptide causes defective multimerization and storage of VWF. *Blood.* 2010;**115**(22):4580-4587.

73. Fujikawa K, Suzuki H, McMullen B, Chung D. Purification of human von Willebrand factor-cleaving protease and its identification as a new member of the metalloproteinase family. *Blood*. 2001;**98**(6):1662-1666.
74. van den Heuvel E, de Laat B, Eckmann CM, et al. A novel type 2A von Willebrand factor mutation (V1499E) associated with variable clinical expression. *J Pediatr Hematol Oncol*. 2009;**31**(4):277-280.
75. O'Brien LA, Sutherland JJ, Hegadorn C, et al. A novel type 2A (Group II) von Willebrand disease mutation (L1503Q) associated with loss of the highest molecular weight von Willebrand factor multimers. *J Thromb Haemost*. 2004;**2**(7):1135-1142.
76. Hassenpflug WA, Budde U, Obser T, et al. Impact of mutations in the von Willebrand factor A2 domain on ADAMTS13-dependent proteolysis. *Blood*. 2006;**107**(6):2339-2345.
77. Jacobi PM, Gill JC, Flood VH, Jakab DA, Friedman KD, Haberichter SL. Intersection of mechanisms of type 2A VWD through defects in VWF multimerization, secretion, ADAMTS-13 susceptibility, and regulated storage. *Blood*. 2012;**119**(19):4543-4553.
78. Schneider SW, Nuschele S, Wixforth A, et al. Shear-induced unfolding triggers adhesion of von Willebrand factor fibers. *Proc Natl Acad Sci U S A*. 2007;**104**(19):7899-7903.
79. Casari C, Du V, Wu YP, et al. Accelerated uptake of VWF/platelet complexes in macrophages contributes to VWD type 2B-associated thrombocytopenia. *Blood*. 2013;**122**(16):2893-2902.
80. Casonato A, Gallinaro L, Cattini MG, et al. Reduced survival of type 2B von Willebrand factor, irrespective of large multimer representation or thrombocytopenia. *Haematologica*. 2010;**95**(8):1366-1372.
81. Nurden P, Gobbi G, Nurden A, et al. Abnormal VWF modifies megakaryocytopoiesis: studies of platelets and megakaryocyte cultures from patients with von Willebrand disease type 2B. *Blood*. 2010;**115**(13):2649-2656.
82. Blenner MA, Dong X, Springer TA. Structural basis of regulation of von Willebrand factor binding to glycoprotein Ib. *J Biol Chem*. 2014;**289**(9):5565-5579.
83. Dumas JJ, Kumar R, McDonagh T, et al. Crystal structure of the wild-type von Willebrand factor A1-glycoprotein Ibalpha complex reveals conformation differences with a complex bearing von Willebrand disease mutations. *J Biol Chem*. 2004;**279**(22):23327-23334.
84. Huizinga EG, Tsuji S, Romijn RA, et al. Structures of glycoprotein Ibalpha and its complex with von Willebrand factor A1 domain. *Science*. 2002;**297**(5584):1176-1179.
85. Jackson SC, Sinclair GD, Cloutier S, Duan Z, Rand ML, Poon MC. The Montreal platelet syndrome kindred has type 2B von Willebrand disease with the VWF V1316M mutation. *Blood*. 2009;**113**(14):3348-3351.
86. Tischer A, Madde P, Moon-Tasson L, Auton M. Misfolding of vWF to pathologically disordered conformations impacts the severity of von Willebrand disease. *Biophys J*. 2014;**107**(5):1185-1195.
87. Tischer A, Campbell JC, Machha VR, et al. Mutational Constraints on Local Unfolding Inhibit the Rheological Adaptation of von Willebrand Factor. *J Biol Chem*. 2016;**291**(8):3848-3859.
88. Stepanian A, Ribba AS, Lavergne JM, et al. A new mutation, S1285F, within the A1 loop of von



- Willebrand factor induces a conformational change in A1 loop with abnormal binding to platelet GPIb and botrocetin causing type 2M von Willebrand disease. *Br J Haematol.* 2003;**120**(4):643-651.
89. Lankhof H, van Hoeij M, Schiphorst ME, et al. A3 domain is essential for interaction of von Willebrand factor with collagen type III. *Thromb Haemost.* 1996;**75**(6):950-958.
  90. Flood VH, Gill JC, Christopherson PA, et al. Critical von Willebrand factor A1 domain residues influence type VI collagen binding. *J Thromb Haemost.* 2012;**10**(7):1417-1424.
  91. Flood VH, Schlauderaff AC, Haberichter SL, et al. Crucial role for the VWF A1 domain in binding to type IV collagen. *Blood.* 2015;**125**(14):2297-2304.
  92. Favaloro EJ. Evaluation of commercial von Willebrand factor collagen binding assays to assist the discrimination of types 1 and 2 von Willebrand disease. *Thromb Haemost.* 2010;**104**(5):1009-1021.
  93. Riddell AF, Gomez K, Millar CM, et al. Characterization of W1745C and S1783A: 2 novel mutations causing defective collagen binding in the A3 domain of von Willebrand factor. *Blood.* 2009;**114**(16):3489-3496.
  94. Flood VH, Lederman CA, Wren JS, et al. Absent collagen binding in a VWF A3 domain mutant: utility of the VWF:CB in diagnosis of VWD. *J Thromb Haemost.* 2010;**8**(6):1431-1433.
  95. Keeling D, Beavis J, Marr R, Sukhu K, Bignell P. A family with type 2M VWD with normal VWF:RCO but reduced VWF:CB and a M1761K mutation in the A3 domain. *Haemophilia.* 2012;**18**(1):e33.
  96. Ong DM, Aumann H, Andrews RK, Gardiner EE, Rodgers SE, Davis AK. M1761K mutation in the von Willebrand factor A3 domain associated with impaired collagen binding and without platelet dysfunction. *Haemophilia.* 2016;**22**(4):e345-346.
  97. Legendre P, Navarrete AM, Rayes J, et al. Mutations in the A3 domain of von Willebrand factor inducing combined qualitative and quantitative defects in the protein. *Blood.* 2013;**121**(11):2135-2143.
  98. Ribba AS, Loisel I, Lavergne JM, et al. Ser968Thr mutation within the A3 domain of von Willebrand Factor (VWF) in two related patients leads to a defective binding of VWF to collagen. *Thromb Haemost.* 2001;**86**(3):848-854.
  99. Vlot AJ, Koppelman SJ, van den Berg MH, Bouma BN, Sixma JJ. The affinity and stoichiometry of binding of human factor VIII to von Willebrand factor. *Blood.* 1995;**85**(11):3150-3157.
  100. Shiltagh N, Kirkpatrick J, Cabrita LD, et al. Solution structure of the major factor VIII binding region on von Willebrand factor. *Blood.* 2014;**123**(26):4143-4151.
  101. Schneppenheim R, Lenk H, Obser T, et al. Recombinant expression of mutations causing von Willebrand disease type Normandy: characterization of a combined defect of factor VIII binding and multimerization. *Thromb Haemost.* 2004;**92**(1):36-41.
  102. Hilbert L, Jorieux S, Fontenay-Roupie M, et al. Expression of two type 2N von Willebrand disease mutations identified in exon 18 of von Willebrand factor gene. *Br J Haematol.* 2004;**127**(2):184-189.
  103. Allen S, Abuzenadah AM, Blagg JL, et al. Two novel type 2N von Willebrand disease-causing

- mutations that result in defective factor VIII binding, multimerization, and secretion of von Willebrand factor. *Blood*. 2000;**95**(6):2000-2007.
104. Eikenboom JC, Reitsma PH, Peerlinck KM, Briët E. Recessive inheritance of von Willebrand's disease type I. *Lancet*. 1993;**341**(8851):982-986.
  105. Schneppenheim R, Castaman G, Federici AB, et al. A common 253-kb deletion involving VWF and TMEM16B in German and Italian patients with severe von Willebrand disease type 3. *J Thromb Haemost*. 2007;**5**(4):722-728.
  106. Acquila M, Bottini F, Di Duca M, Vijzelaar R, Molinari AC, Bicocchi MP. Multiplex ligation-dependent probe amplification to detect a large deletion within the von Willebrand gene. *Haemophilia*. 2009;**15**(6):1346-1348.
  107. Ngo KY, Glotz VT, Koziol JA, et al. Homozygous and heterozygous deletions of the von Willebrand factor gene in patients and carriers of severe von Willebrand disease. *Proc Natl Acad Sci U S A*. 1988;**85**(8):2753-2757.
  108. Mancuso DJ, Tuley EA, Westfield LA, et al. Human von Willebrand factor gene and pseudogene: structural analysis and differentiation by polymerase chain reaction. *Biochemistry*. 1991;**30**(1):253-269.
  109. Gupta PK, Saxena R, Adamtziki E, et al. Genetic defects in von Willebrand disease type 3 in Indian and Greek patients. *Blood Cells Mol Dis*. 2008;**41**(2):219-222.
  110. Kasatkar P, Shetty S, Ghosh K. Genetic heterogeneity in a large cohort of Indian type 3 von Willebrand disease patients. *PLoS One*. 2014;**9**(3):e92575.
  111. Gupta PK, Adamtziki E, Budde U, et al. Gene conversions are a common cause of von Willebrand disease. *Br J Haematol*. 2005;**130**(5):752-758.
  112. Tjernberg P, Castaman G, Vos HL, Bertina RM, Eikenboom JC. Homozygous C2362F von Willebrand factor induces intracellular retention of mutant von Willebrand factor resulting in autosomal recessive severe von Willebrand disease. *Br J Haematol*. 2006;**133**(4):409-418.
  113. Yin J, Ma Z, Su J, et al. Mutations in the D1 domain of von Willebrand factor impair their propeptide-dependent multimerization, intracellular trafficking and secretion. *J Hematol Oncol*. 2015;**8**:73.
  114. Baronciani L, Federici AB, Cozzi G, et al. Expression studies of missense mutations p.D141Y, p.C275S located in the propeptide of von Willebrand factor in patients with type 3 von Willebrand disease. *Haemophilia*. 2008;**14**(3):549-555.
  115. Solimando M, Baronciani L, La Marca S, et al. Molecular characterization, recombinant protein expression, and mRNA analysis of type 3 von Willebrand disease: Studies of an Italian cohort of 10 patients. *Am J Hematol*. 2012;**87**(9):870-874.
  116. Yadegari H, Driesen J, Pavlova A, et al. Insights into pathological mechanisms of missense mutations in C-terminal domains of von Willebrand factor causing qualitative or quantitative von Willebrand disease. *Haematologica*. 2013;**98**(8):1315-1323.
  117. Sanders YV, Groeneveld D, Meijer K, et al. von Willebrand factor propeptide and the phenotypic classification of von Willebrand disease. *Blood*. 2015;**125**(19):3006-3013.

## Supplemental information: Advanced literature search strategy

Search strategy was performed until 31 January 2017

Number of hits on PubMed: 1743

(((((“von Willebrand Diseases”[majr] OR “von Willebrand Disease”[ti] OR “von Willebrand Diseases”[ti] OR “vonwillebrand disease”[ti] OR “Willebrand disease”[ti] OR “Willebrand diseases”[ti] OR “willebrand’s disease”[ti] OR “willebrand’s diseases”[ti] OR “willebrands disease”[ti] OR “willebrands diseases”[ti] OR “VWD”[ti] OR “Von Willebrand’s Factor Deficiency”[ti] OR “Von Willebrand Factor Deficiency”[ti] OR “Von Willebrand Disorder”[ti] OR “von Willebrand Factor”[majr] OR “von Willebrand Factor”[ti] OR von Willebrand\*[ti] OR vonwillebrand\*[ti] OR willebrand\*[ti]) AND (“Mutation”[mesh] OR mutat\*[tw] OR “Allelic Imbalance”[tw] OR “Loss of Heterozygosity”[tw] OR “Chromosome Deletion”[tw] OR “Haploinsufficiency”[tw] OR “Base Pair Mismatch”[tw] OR “Chromosome Aberrations”[tw] OR “Abnormal Karyotype”[tw] OR “XYY Karyotype”[tw] OR “Aneuploidy”[tw] OR “Chimerism”[tw] OR “Chromosomal Instability”[tw] OR “Chromosome Fragility”[tw] OR “Chromosome Breakage”[tw] OR “Chromosome Duplication”[tw] OR “Tetrasomy”[tw] OR “Trisomy”[tw] OR “Chromosome Inversion”[tw] OR “Isochromosomes”[tw] OR “Chromosome-Defective Micronuclei”[tw] OR “Mosaicism”[tw] OR “Polyploidy”[tw] OR “Tetraploidy”[tw] OR “Triploidy”[tw] OR “Ring Chromosomes”[tw] OR “Sex Chromosome Aberrations”[tw] OR “Genetic Translocation”[tw] OR “Philadelphia Chromosome”[tw] OR “Uniparental Disomy”[tw] OR “Nonsense Codon”[tw] OR “DNA Repeat Expansion”[tw] OR “Trinucleotide Repeat Expansion”[tw] OR “Frameshift Mutation”[tw] OR “Gene Amplification”[tw] OR “Gene Duplication”[tw] OR “Genomic Instability”[tw] OR “Microsatellite Instability”[tw] OR “Germ-Line Mutation”[tw] OR “INDEL Mutation”[tw] OR “Insertional Mutagenesis”[tw] OR “Mutation Accumulation”[tw] OR “Mutation Rate”[tw] OR “Missense Mutation”[tw] OR “Point Mutation”[tw] OR “Sequence Deletion”[tw] OR “Chromosome Deletion”[tw] OR “Gene Deletion”[tw] OR “Sequence Inversion”[tw] OR “Chromosome Inversion”[tw] OR “Silent Mutation”[tw] OR “Genetic Suppression”[tw] OR “Polymorphism, Restriction Fragment Length”[mesh] OR “Polymorphism, Genetic”[mesh] OR Polymorphism\*[tw])) OR “von Willebrand Diseases/genetics”[majr] OR “von Willebrand Factor/genetics”[majr]) AND (english[la] OR dutch[la])) OR (((“von Willebrand Diseases”[mesh] OR “von Willebrand Disease”[ti] OR “von Willebrand Diseases”[ti] OR “vonwillebrand disease”[ti] OR “Willebrand disease”[ti] OR “Willebrand diseases”[ti] OR “willebrand’s disease”[ti] OR “willebrand’s diseases”[ti] OR “willebrands disease”[ti] OR “willebrands diseases”[ti] OR “VWD”[ti] OR “Von Willebrand’s Factor Deficiency”[ti] OR “Von Willebrand Factor Deficiency”[ti] OR “Von Willebrand Disorder”[ti] OR “von Willebrand Factor”[mesh] OR “von Willebrand Factor”[ti] OR von Willebrand\*[ti] OR vonwillebrand\*[ti] OR willebrand\*[ti]) AND (“Mutation”[majr] OR mutat\*[ti] OR “Allelic Imbalance”[ti] OR “Loss of Heterozygosity”[ti] OR “Chromosome Deletion”[ti] OR “Haploinsufficiency”[ti] OR “Base Pair Mismatch”[ti] OR “Chromosome Aberrations”[ti] OR “Abnormal Karyotype”[ti] OR “XYY Karyotype”[ti] OR “Aneuploidy”[ti] OR “Chimerism”[ti] OR “Chromosomal Instability”[ti] OR “Chromosome Fragility”[ti] OR “Chromosome Breakage”[ti] OR “Chromosome Duplication”[ti] OR “Tetrasomy”[ti] OR “Trisomy”[ti] OR “Chromosome Inversion”[ti] OR “Isochromosomes”[ti] OR “Chromosome-Defective Micronuclei”[ti] OR “Mosaicism”[ti] OR “Polyploidy”[ti] OR “Tetraploidy”[ti] OR “Triploidy”[ti] OR “Ring Chromosomes”[ti] OR “Sex Chromosome Aberrations”[ti] OR “Genetic Translocation”[ti] OR “Philadelphia Chromosome”[ti] OR “Uniparental Disomy”[ti] OR “Nonsense Codon”[ti] OR “DNA Repeat Expansion”[ti] OR “Trinucleotide Repeat Expansion”[ti] OR “Frameshift Mutation”[ti] OR “Gene Amplification”[ti] OR “Gene Duplication”[ti] OR “Genomic Instability”[ti] OR “Microsatellite Instability”[ti] OR “Germ-Line Mutation”[ti] OR “INDEL Mutation”[ti] OR “Insertional Mutagenesis”[ti] OR “Mutation Accumulation”[ti] OR “Mutation Rate”[ti] OR “Missense Mutation”[ti] OR “Point Mutation”[ti] OR “Sequence Deletion”[ti] OR “Chromosome Deletion”[ti] OR “Gene Deletion”[ti] OR “Sequence Inversion”[ti] OR “Chromosome Inversion”[ti] OR “Silent Mutation”[ti] OR “Genetic Suppression”[ti] OR “Polymorphism, Restriction Fragment Length”[majr] OR “Polymorphism, Genetic”[majr] OR Polymorphism\*[ti])) OR “von Willebrand Diseases/genetics”[majr] OR “von Willebrand Factor/genetics”[majr]) AND (english[la] OR dutch[la]))))





# 4

## **Correction of a dominant-negative von Willebrand factor multimerization defect by small interfering RNA-mediated allele-specific inhibition of mutant von Willebrand factor**

Annika de Jong

Richard Dirven

Josine Oud

Davy Tio

Bart van Vlijmen

Jeroen Eikenboom

*Journal of Thrombosis and Haemostasis (2018) 16(7):1357-1368*

## Abstract

**Background** Treatment of the bleeding disorder von Willebrand disease (VWD) focuses on increasing von Willebrand factor (VWF) levels by administration of desmopressin or VWF-containing concentrates. Both therapies leave the production of mutant VWF unhindered, which may have additional consequences, such as thrombocytopenia in patients with VWD type 2B, competition between mutant and normal VWF for platelet receptors, and the potential development of intestinal angiodysplasia. Most cases of VWD are caused by dominant negative mutations in VWF, and we hypothesize that diminishing expression of mutant VWF positively affects VWD phenotypes. **Objectives** To investigate allele-specific inhibition of VWF by applying small interfering RNAs (siRNAs) targeting common single-nucleotide polymorphisms (SNPs) in VWF. This approach allows allele-specific knockdown irrespective of the mutations causing VWD. **Methods** Four SNPs with a high predicted heterozygosity within VWF were selected, and siRNAs were designed against both alleles of the four SNPs. siRNA efficiency, allele specificity and siRNA-mediated phenotypic improvements were determined in VWF-expressing HEK293 cells. **Results** Twelve siRNAs were able to efficiently inhibit single VWF alleles in HEK293 cells that stably produce VWF. Transient cotransfections of these siRNAs with two VWF alleles resulted in a clear preference for the targeted allele over the untargeted allele for 11 siRNAs. We also demonstrated siRNA-mediated phenotypic improvement of the VWF multimerization pattern of the VWD type 2A mutation VWF p.Cys2773Ser. **Conclusions** Allele-specific siRNAs are able to distinguish VWF alleles on the basis of one nucleotide variation, and are able to improve a severe multimerization defect caused by VWF p.Cys2773Ser. This holds promise for the therapeutic application of allele-specific siRNAs in dominant negative VWD.

## Introduction

von Willebrand disease (VWD) is the most common inherited bleeding disorder caused by defects in von Willebrand factor (VWF), a large multimeric glycoprotein produced by endothelial cells and megakaryocytes. VWF is an important hemostatic protein with two main functions: adhesion and aggregation of platelets at sites of vascular damage, and protection of coagulation factor VIII from degradation in the bloodstream.<sup>1</sup> More than 90% of VWD cases are caused by dominant negative VWF mutations.<sup>2</sup> These dominant negative mutations can lead to either quantitative (VWD type 1) or qualitative (VWD types 2A, B, and M) defects in secreted VWF.<sup>2,3</sup>

VWD mainly leads to mucocutaneous or postoperative bleeding, and patients are generally treated on demand upon a bleeding event.<sup>4</sup> The mainstay of treatment is to increase circulating VWF levels by the administration of desmopressin (DDAVP) or VWF-containing concentrates.<sup>4</sup> Administration of DDAVP is the primary choice of treatment, and induces the release of VWF from its endothelial storage organelles, the Weibel-Palade bodies.<sup>5</sup> When DDAVP does not result in the secretion of VWF, or when the secreted VWF is non-functional, DDAVP may be ineffective. The release of mutant VWF may also result in adverse events such as the development of severe thrombocytopenia in patients with VWD type 2B, owing to spontaneous binding of mutant VWF to platelets. When DDAVP is ineffective or contraindicated, the preferred treatment is administration of VWF-containing concentrates.<sup>6,7</sup> Although normal exogenous VWF is administered, endogenous mutant VWF is still being produced and secreted, which might interfere with normal hemostasis. Therefore, administration of VWF-containing concentrates may correct the VWF deficiency, but cannot prevent secondary, negative effects caused by mutant VWF.

We hypothesize that reducing mutant VWF production, while preserving the production of normal VWF, has a positive effect on VWF function and VWD phenotypes. We aim to use allele-specific small interfering RNAs (siRNAs) to inhibit mutant *VWF* alleles. The use of allele-specific siRNAs in VWD has been reported before by Casari *et al.*, where siRNAs were designed against the breakpoint of the dominant negative partial VWF deletion p.Pro1127\_Cys1948delinsArg.<sup>8</sup> This approach may be effective, however, it is only applicable to patients harboring this specific deletion. Therefore, we choose an approach whereby siRNAs are designed against common single-nucleotide polymorphisms (SNPs) in *VWF*. When a patient is heterozygous for the specific SNP, one can target the SNP that is located on the same allele as the dominant negative *VWF* mutation causing VWD. The full complementarity of the siRNA with the targeted heterozygous *VWF* SNP allele will lead to siRNA-mediated degradation of the dominant negative *VWF* allele. The mismatch of the same siRNA with the other SNP allele is thought to maintain expression of the normal *VWF* allele (Fig. S1A). An approach in which siRNAs are designed against dominant negative mutations may be more straightforward, but

will not be feasible in a therapeutic perspective, because the existence of hundreds of VWD-related mutations.<sup>9</sup> Discrimination of *VWF* alleles by SNPs requires only a small set of SNPs with a high minor allele frequency (MAF) to cover a large group of patients with a wide range of *VWF* mutations.

In this study, we show the proof of principle of siRNA-mediated SNP-based allele-specific inhibition of *VWF*. We demonstrate that it is feasible to discriminate with siRNAs between two *VWF* alleles differing by only one nucleotide, and that this discrimination leads to a clear improvement of a dominant negative multimerization defect caused by *VWF* p.Cys2773Ser.

## Methods

### *Plasmid expression vectors*

Recombinant pcDNA3.1/Zeo (+) containing full-length human *VWF* (hVWF) cDNA was used and modified in this study. pcDNA3.1/Zeo (+) hVWF contained a *VWF* allele with the following nucleotides at the SNP positions: c.1451G (rs1800378), c.2365A (rs1063856), c.2385T (rs1063857), and c.2880G (rs1800380). Five new hVWF plasmids were generated to create opposite *VWF* alleles (c.1451A, c.2365G, c.2385C, c.2880A, and c.2365G/c.2880A). Both these nucleotide variations and *VWF* p.Cys2773Ser (c.8318C) were introduced into pcDNA3.1/Zeo (+) hVWF by use of the Q5 Site-Directed Mutagenesis Kit (New England Biolabs, Ipswich, MA, USA). HA and MYC peptide tags were used to distinguish *VWF* alleles at the protein level and at the mRNA level, and introduced at the C-terminal end of *VWF* by use of the Q5 Site-Directed Mutagenesis Kit. Tables S1 and S2 show an overview of the generated constructs. Primers for the substitutions and insertions were designed with NEBaseChanger (New England Biolabs). Plasmids were purified with the PureYield Plasmid Maxiprep system (Promega, Madison, WI, USA), and correctness of the sequences was verified by Sanger sequencing (BaseClear, Leiden, the Netherlands).

### *SNP selection and siRNA design and synthesis*

Four SNPs with a high MAF in the Caucasian population were selected from the 1000 Genomes Project.<sup>10</sup> On the basis of provided sequences, two or three siRNA oligonucleotides with the highest predicted efficiency and allele specificity were designed for both alleles of the four SNPs (Ambion, Life Technologies Europe BV, Bleiswijk, the Netherlands). Custom Silencer Select 21-mer siRNA oligonucleotides with a dTdT overhang at the 5' end of the sense strand were synthesized by Life Technologies (Ambion, Life Technologies Europe BV). Ambion Silencer Select Negative Control siRNA was used as a negative control (siNEG).



### **Cell culture and transfection**

Human embryonic kidney 293 (HEK293) cells (ATCC, Rockville, MD, USA) were cultured in Minimum Essential Medium Eagle  $\alpha$  (Sigma-Aldrich, St Louis, MO, USA) supplemented with 10% fetal bovine serum (GIBCO, Invitrogen, Carlsbad, CA, USA), 2 mM L-glutamine (Sigma-Aldrich), and 50  $\mu$ g/mL gentamicin (GIBCO, Invitrogen). HEK293 cells stably producing VWF were generated by transfection of hVWF plasmids with FuGENE HD transfection reagent (Promega). Cells stably producing VWF were selected by the use of Zeocin Selection Reagent (Life Technologies Europe BV).

For transient transfections, 100,000 cells were seeded on poly-D-lysine (5 mg/mL; Sigma-Aldrich) coated wells of 24 wells plates to reach 50-60% confluence the next day. Cells were transfected with plasmids and/or siRNA by the use of Lipofectamine 2000 Transfection Reagent (Thermo Fisher Scientific, Carlsbad, CA, USA). Each transfection was performed with 600 ng/mL plasmid and/or 0.5, 1, 5, 10 or 20 nM siRNA in 500  $\mu$ L of culture medium. Twenty-four hours after transfection, medium was refreshed with 500  $\mu$ L of culture medium. Conditioned medium and cell lysates were harvested 48 hours after transfection, when siRNAs were transfected into cells stably producing VWF, and 72 hours after transfection, when siRNA and VWF plasmids were cotransfected into transiently transfected cells. Cell lysates were generated by overnight incubation of HEK293 cells at 4 °C in 500  $\mu$ L of Passive Lysis buffer (Promega) supplemented with cComplete Protease Inhibitor Cocktail (Sigma-Aldrich).

### **Quantification of VWF protein levels**

VWF antigen (VWF:Ag), VWF-HA and VWF-MYC protein levels in conditioned medium and cell lysates were measured by ELISA. For VWF:Ag measurements, ELISA plates (Greiner, Frickenhausen, Germany) were coated overnight with polyclonal antibody rabbit anti-hVWF (A0082; Dako, Glostrup, Denmark) diluted in coating buffer (100 mM bicarbonate, 500 mM NaCl, pH 9.0). Samples were diluted in wash buffer (50 mM triethanolamine, 100 mM NaCl, 10 mM EDTA, 0.1% Tween-20), and incubated for 2 hours. Polyclonal antibody rabbit anti-hVWF coupled to horseradish peroxidase (HRP) (P0226; Dako) was used as the detecting antibody, and diluted in wash buffer. Wells were incubated with secondary antibody for 2 hours. O-phenylenediamine dihydrochloride (OPD) (Sigma-Aldrich) was used as substrate, and one tablet of OPD was dissolved in 24 mL of substrate buffer (22 mM citric acid, 51 mM phosphate, pH 5.0) plus 12  $\mu$ L of 30% H<sub>2</sub>O<sub>2</sub>. Wells were incubated with substrate solution, and the reaction was terminated by the addition of 2 M H<sub>2</sub>SO<sub>4</sub> after 15 minutes. Normal pooled plasma (NPP) was used as the reference.

To quantify VWF-HA protein levels, ELISA plates were coated overnight with a monoclonal antibody against hVWF (CLB-RAG35; Sanquin, Amsterdam, the Netherlands).<sup>11</sup> Plates were

blocked for 30 minutes in blocking buffer (phosphate-buffered saline [PBS], 3% bovine serum albumin, and 0.1% Tween-20). Samples were diluted in blocking buffer, and wells were incubated with diluted sample for 1.5 hour. Wells were incubated with rabbit anti-HA monoclonal antibody (Cell Signaling, Leiden, the Netherlands) diluted in blocking buffer for 1.5 hour. Goat anti-rabbit IgG (H+L)-HRP (Bio-Rad, Veenendaal, the Netherlands) diluted in blocking buffer was used as secondary antibody, and wells were incubated with secondary antibody for 1 hour. OPD conversion was performed as described above. Purified recombinant VWF-HA was used as the reference and normalized to VWF:Ag levels in NPP.

To quantify VWF-MYC protein levels, ELISA plates were coated overnight with rabbit anti-hVWF polyclonal antibody (Dako). Samples were diluted in blocking buffer, and plates were incubated with diluted sample for 2 hours. Wells were incubated with the secondary polyclonal antibody rabbit anti-c-Myc-tag-HRP (GenScript, Piscataway, NJ, USA) for 2 hours. OPD conversion was performed as described above, and the reaction was terminated after 10 minutes by the addition of 2 M  $\text{H}_2\text{SO}_4$ . Purified recombinant VWF-MYC was used as the reference, and normalized to VWF:Ag levels in NPP.

### ***RNA isolation and quantification of VWF mRNA***

RNA was generated from cell lysates harvested 72 hours after transfection by use of the RNeasy Micro Kit (Qiagen, Hilden, Germany). Plasmid and genomic DNA was removed with the TURBO DNA-free kit (Invitrogen). Complementary DNA was synthesized by the use of SuperScript II Reverse Transcriptase (Thermo Fisher Scientific) with poly(T) primers (Sigma-Aldrich). Quantitative PCR (qPCR) was performed with Sybr Select Master Mix (Thermo Fisher Scientific) in the ViiA 7 Real-Time PCR System (Thermo Fisher Scientific). Allele-specific qPCR primers amplifying the MYC or HA nucleotide sequence were used to distinguish the two *VWF* alleles. The glyceraldehyde-3-phosphate dehydrogenase gene was used as the endogenous reference gene, and analyzed within the same qPCR run. The comparative  $C_t$  method was used for analysis, with complementary DNA of HEK293 cells transfected with the two *VWF* alleles and siNEG being used as the control.<sup>12</sup>

### ***Immunofluorescent staining***

72 hours after transfection, HEK293 cells were fixed with 4% paraformaldehyde (Alfa Aesar, Karlsruhe, Germany) for 20 minutes. Cells were rinsed in PBS, and blocked and permeabilized for 20 minutes in blocking buffer (PBS, 5% normal goat serum [Dako]; 0.02% saponin [Sigma-Aldrich]). Primary antibodies (rabbit anti-HA and mouse anti-MYC; Cell Signaling) were diluted in blocking buffer, and cells were incubated with primary antibody for 45 minutes. Cells were incubated for 30 minutes with the secondary antibodies goat anti-rabbit IgG (H+L)

AF488 and goat anti-mouse IgG (H+L) AF594 (Thermo Fisher Scientific) diluted in blocking buffer. Coverslips were mounted by the use of ProLong Diamond Antifade Mountant (Thermo Fisher Scientific), and cells were visualized with a Leica TCS SP8 upright confocal microscope equipped with a 63x/1.40 numerical aperture Plan Apo oil immersion objective.

### **VWF multimer analysis**

Conditioned medium was collected 48 hours after refreshment of the medium and 72 hours after transfection. Conditioned medium samples were separated under non-reducing conditions on a 1.5% SeaKem HGT(P) agarose (Lonza, Rockland, ME, USA) separation gel containing 0.4% SDS, and visualized by western blotting with rabbit anti-hVWF polyclonal antibody (A0082; Dako) as described previously.<sup>13</sup> Densitometry images were generated with imageJ 1.51h (National Institutes of Health, Bethesda, MD, USA) to quantify high and intermediate molecular weight multimers. Densitometry images were divided into the five smallest bands and the rest (intermediate and large bands). First, the VWF large multimer ratio was determined by dividing the area of intermediate and large VWF multimers over the total area (Fig. S2). Then, the VWF large multimer index was calculated by dividing the VWF large multimer ratio of cells cotransfected with mutant and normal *VWF* with or without siRNA treatment by the VWF large multimer ratio of control cells (Fig. S2). This is a modified version of the VWF large multimer index described by Tamura *et al.*<sup>14</sup> We divided densitometry images into two instead of three segments because less high molecular weight VWF is produced in *in vitro* cell systems.

### **Statistics**

GraphPad prism version 7.00 (GraphPad Software, La Jolla, CA, USA) was used for graphics and statistical analyses. Error bars in the histograms represent one standard deviation. A two-tailed Mann-Whitney *U*-test was used to check for significance in siRNA allele specificity. For all statistical analyses, significance was set at  $P < 0.05$ .

## **Results**

### **SNP selection**

A set of four SNPs with a high MAF in the coding region of *VWF* was selected from the 1000 Genomes Project.<sup>10</sup> These SNPs include rs1800378 (c.1451G|A), rs1063856 (c.2365A|G), rs1063857 (c.2385T|C), and rs1800380 (c.2880G|A) (Table 1). rs1800378 results in a non-synonymous substitution (p.His484Arg) and has a MAF of 0.35 in the Caucasian population. rs1063856 also results in a non-synonymous substitution (p.Thr789Ala), and is in linkage

disequilibrium with rs1063857, which results in a synonymous substitution (p.Tyr795=). Both SNPs have a MAF of 0.37 in the Caucasian population. rs1800380 results in a synonymous substitution (p.Arg960=) and has a MAF of 0.26 in the Caucasian population. By counting the Caucasian individuals included in 1000 Genomes (N = 503) who are heterozygous for at least one of the four selected SNPs, we determined that 74% of this population are heterozygous for at least one of these SNPs (Table 1).<sup>10</sup>

**Table 1.** Single-nucleotide polymorphism (SNP) information in Caucasian population

SNP	cDNA location in <i>VWF</i>	Minor allele	MAF*	% heterozygous
rs1800378	c.1451G A	A	0.35	45.3
rs1063856	c.2365A G	G	0.37	46.5
rs1063857	c.2385T C	C	0.37	46.5
rs1800380	c.2880G A	A	0.26	38.1
<i>All 4 SNPs, at least one heterozygous</i>				74.0

\* Based on 1000 Genomes.<sup>10</sup> MAF, minor allele frequency; *VWF*, von Willebrand factor

***siRNA efficiency and allele specificity***

Two or three siRNAs per *VWF* allele were screened for their efficiency and allele specificity by siRNA transfections in HEK293 cells stably producing *VWF* generated for all eight *VWF* alleles (Fig. S1B; Table S1). Specific inhibition and non-specific inhibition were determined by *VWF*:Ag measurements in conditioned medium and cell lysates after transfection of each siRNA in cells expressing the targeted or untargeted *VWF* allele, respectively. We selected at least one siRNA per SNP allele according to their efficiency in inhibiting *VWF* and their ability to distinguish between the two *VWF* alleles (Fig. 1). These siRNAs included: si1451G-1, si1451G-2, si1451A-2, si1451A-3, si2365A-1, si2365G-2, si2385T-1 si2385T-2, si2385C-2, si2880G-3, si2880A-2 and si2880A-3. Although si2365G-2 did not efficiently inhibit the production of *VWF*, it was the most effective siRNA for this target and was therefore not excluded from further analyses.

In the normal human situation, two *VWF* alleles are coexpressed in the same cell. Competition between the two alleles might improve the allele specificity of the siRNAs. By using a coexpression system in which two *VWF* plasmids containing either a MYC or an HA peptide tag were cotransfected into HEK293 cells, we were able to distinguish and quantify the expression of the two respective *VWF* alleles. Although the peptide tags are located at the C-terminal end of *VWF*, they did not interfere with dimerization and multimerization of *VWF* (Fig. S3A). Staining of HEK293 cells cotransfected with two *VWF* plasmids showed coexpression of both conjugated proteins in most cells, confirming real coexpression in the system (Fig. S3B).

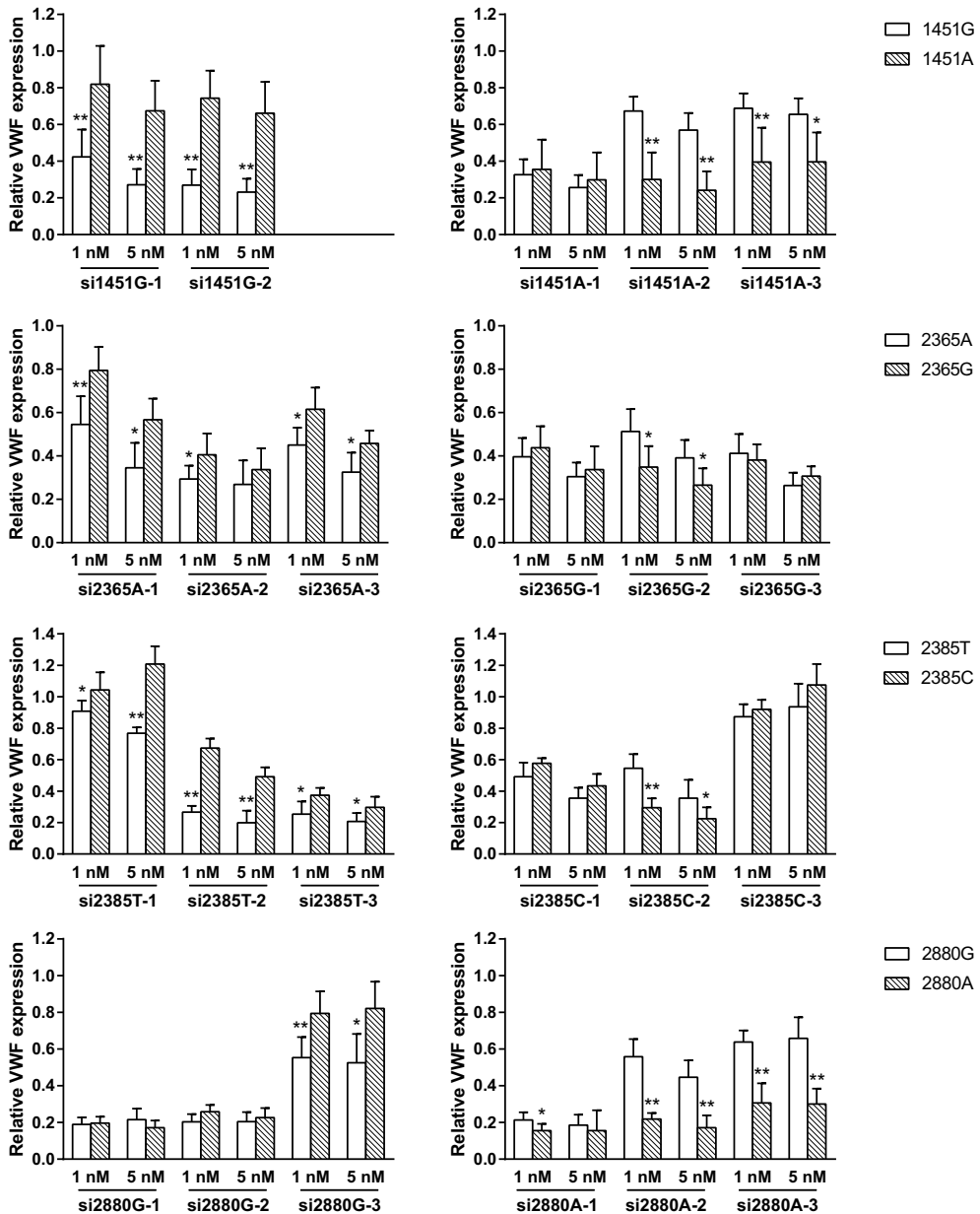


**Figure 1. Allele-specific inhibition of von Willebrand factor (VWF) in human embryonic kidney 293 (HEK293) cells stably producing VWF.** Normalized total VWF antigen (VWF:Ag) levels measured by ELISA in conditioned medium and cell lysates of HEK293 cells stably producing VWF transfected with allele-specific small interfering RNAs (siRNAs). Allele-specific siRNAs were transfected into HEK293 cells stably expressing either of the VWF alleles (Fig. S1B). Transfections were performed at siRNA concentrations of 1 nM and 5 nM, and the VWF:Ag levels measured by ELISA were normalized to the VWF:Ag levels measured in cells transfected with a negative control siRNA. Shown is the mean + one standard deviation of the compiled results of three independent experiments performed in duplicate (N = 6). Mann-Whitney (targeted versus untargeted allele), \* $P < 0.05$ , \*\* $P < 0.01$ .

Two VWF plasmids containing either of the *VWF* alleles were cotransfected with the 12 most potent siRNAs into HEK293 cells (Fig. S1C). The MYC peptide tag was incorporated in the plasmid containing the *VWF* allele: c.1451G, c.2365A, c.2385T, and c.2880G. The HA peptide tag was incorporated in plasmids containing the opposite *VWF* SNP alleles (Table S1). Coexpression of the siRNA with the two alleles of a SNP clearly led to increased efficiency and allele specificity for all siRNAs, except for si2385T-1, as compared with siRNA transfections in cells stably producing VWF (Figs 2A and S4). This was observed both at the protein level in conditioned medium and in cell lysates (Fig. 2A). Efficient and allele-specific inhibition was observed in a dose-dependent manner at all tested siRNA concentrations, with even upregulation of the untargeted allele being observed at the lowest siRNA concentrations (Fig. S4). These results were obtained reproducibly in two independent experiments. The optimal siRNA concentration was determined according to the lowest percentage of the targeted allele in the total sample, and was found to be 10 nM for si1451A-2, si1451A-3, and si2880A-2, and 5 nM for all other siRNAs (Fig. 2). The effect on mRNA level was determined for the 11 most effective siRNAs in a third independent experiment (Fig. 2B). We observed efficient inhibition of the targeted allele at the mRNA level, although with a lower degree of allele specificity than at the protein level measured in conditioned medium in the same experiment, with the relative mRNA expression of the targeted allele being approximately half that of the untargeted allele for most siRNAs (Fig. 2B).

### ***VWD phenotype improvement by siRNA-mediated allele-specific inhibition***

Eleven siRNAs proved to be highly efficient and allele-specific, and a remaining fraction of only 5% of the targeted allele in the whole sample was observed for the most optimal siRNA (data not shown). The presence of these low levels of targeted allele would predict a phenotype improvement in the presence of a dominant negative mutation. We selected a previously characterized VWD type 2A mutation, VWF p.Cys2773Ser, as a model mutation with which to study this hypothesis.<sup>15</sup> VWF plasmids containing all possible SNP alleles and VWF p.Cys2773Ser were generated to test this hypothesis (Table S2).

Transfection of normal VWF only into HEK293 cells leads to a VWF multimer pattern with a full range of VWF multimers (Fig. 3A, first lane). Cotransfection of normal VWF with increasing concentrations of VWF p.Cys2773Ser resulted in a progressively abnormal multimer pattern, with only monomers and dimers being present when only VWF p.Cys2773Ser was transfected (Fig. 3A, last lane).<sup>15</sup> The heterozygous state of the patient is mimicked by the cotransfection of equal amounts of normal and mutant VWF p.Cys2773Ser (Fig. 3A, middle lane). The heterozygous multimer pattern of the cotransfection of equal amounts of mutant and normal VWF (for set-up, see Fig. S1D) was improved towards a normal pattern by most siRNAs (Fig. 3B). The VWF large multimer index was calculated to quantify the increase in the amount of high molecular weight VWF (Table 2).

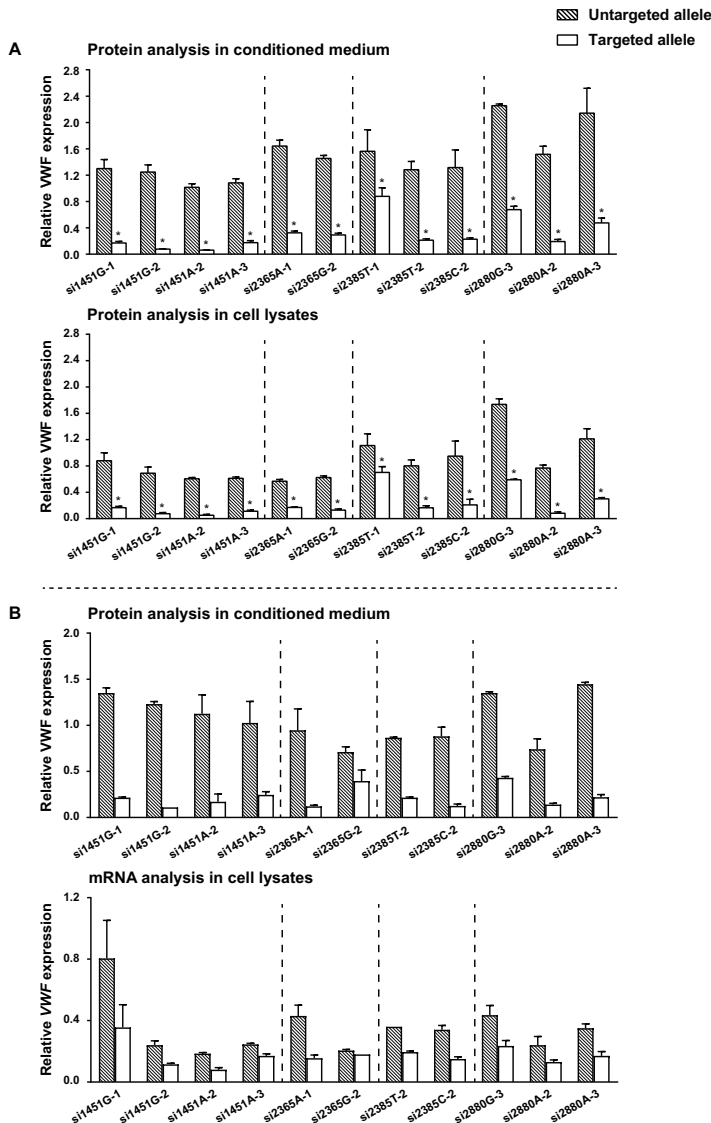


**Figure 2. Allele-specific inhibition of von Willebrand factor (VWF) in cotransfected human embryonic kidney 293 (HEK293) cells.** HEK293 cells were cotransfected with VWF-HA, VWF-MYC and allele-specific small interfering RNAs (siRNAs) at the optimal siRNA concentration, determined by the percentage of targeted allele in the whole sample. The optimal siRNA concentrations were determined to be 10 nM for si1451A-2, si1451A-3, and si2880A-2, and 5 nM for all other siRNAs. The untargeted and targeted alleles could be either VWF-HA or VWF-MYC, depending on the VWF allele (Table S1). VWF-HA and VWF-MYC protein and mRNA levels were normalized to the VWF-HA and VWF-MYC protein and mRNA levels measured in HEK293 cells cotransfected with the two VWF alleles and a negative control siRNA (Fig. S1C). (A) Normalized VWF-HA and VWF-MYC protein levels measured by ELISA in conditioned medium and cell lysates. Shown is the mean + one standard deviation (SD) of the compiled results of two independent experiments performed in duplicate (N = 4). (B) Normalized VWF-HA and VWF-MYC protein levels measured by ELISA in conditioned medium and, from the same experiment, the corresponding normalized VWF-HA and VWF-MYC mRNA levels determined by quantitative PCR on cDNA samples. Shown is the mean + 1 SD of the compiled results of one independent experiment performed in duplicate (N = 2). Mann-Whitney (targeted versus untargeted allele), \* $P < 0.05$ .

Cotransfection of normal and mutant VWF into HEK293 cells resulted in a large multimer index of  $50.1\% \pm 4.5\%$  as compared with cells transfected with only normal VWF (100%). Increases in the large multimer index were observed for most siRNAs, but were highest for cells treated with si1451G-2 and si2880G-3, at 82.8% and 85.3%, respectively (Table 2). Combining siRNAs to target different SNPs simultaneously could potentially increase the effect. A combination of two siRNAs targeting either c.2365A and c.2880G or c.2365G and c.2880A did not result in further improvement in multimerization patterns, and nor did the patterns deteriorate (Fig. 3C).

**Table 2.** VWF large multimer index calculated on densitometry images of multimer analysis

	VWF large multimer index (%)
Normal	100
Normal + mutant	$50.1 \pm 4.5$
Normal + mutant + si1451G-1	70.9
Normal + mutant + si1451G-2	82.8
Normal + mutant + si1451A-2	71.2
Normal + mutant + si1451A-3	66.8
Normal + mutant + si2365A-1	58.8
Normal + mutant + si2365G-2	48.4
Normal + mutant + si2385T-2	75.5
Normal + mutant + si2385C-2	70.9
Normal + mutant + si2880G-3	85.3
Normal + mutant + si2880A-2	59.8
Normal + mutant + si2880A-3	79.5

si1451G-1, indicates ‘small interfering RNA 1 against VWF c.1451G’, all siRNAs are indicated according to this principle; VWF, von Willebrand factor



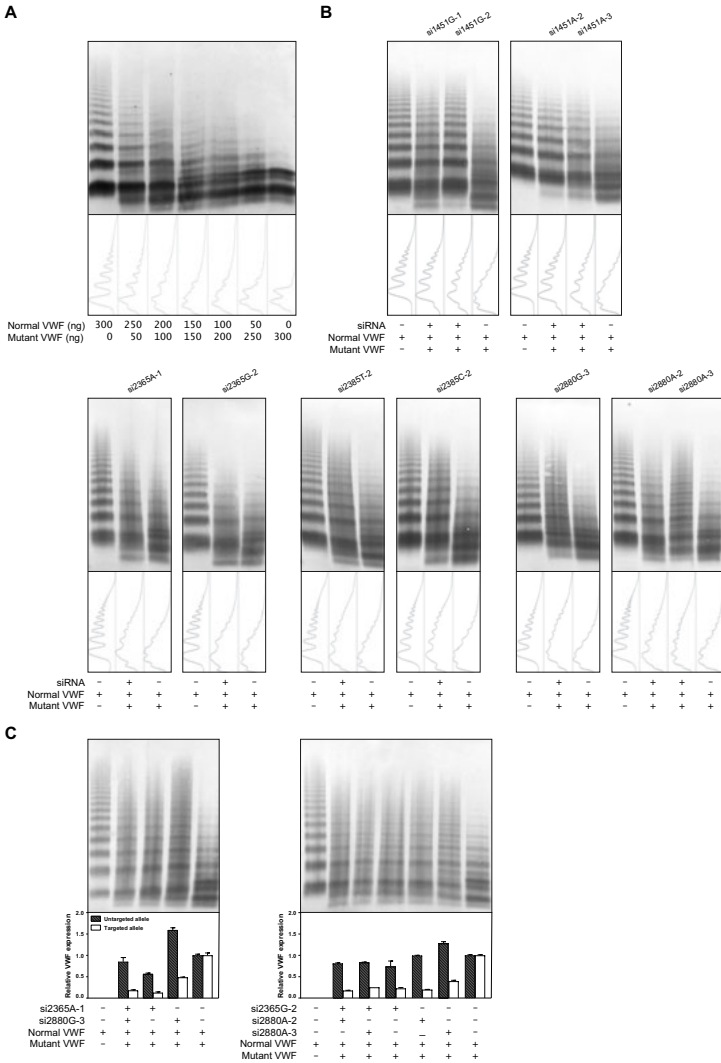


**Figure 3. Improvement of a multimerization defect by allele-specific small interfering RNAs (siRNAs).** von Willebrand factor (VWF) multimer analysis was performed on conditioned medium of human embryonic kidney 293 (HEK293) cells cotransfected with normal VWF and mutant (p.Cys2773Ser) VWF plasmids. Shown are conditioned medium samples 72 hours after transfection and 48 hours after refreshment of the medium, loaded on a 1.5% SDS-agarose gel. (A) HEK293 cells were transfected with different concentrations of normal and/or mutant VWF plasmids. Increasing concentrations of mutant VWF resulted in a severe dimerization and multimerization defect.<sup>15</sup> (B) HEK293 cells were transfected with only normal VWF or with normal and mutant VWF in a 1:1 ratio. Allele-specific siRNAs were transfected into HEK293 cells cotransfected with normal and mutant VWF (Fig. S1D). Addition of allele-specific siRNAs resulted in clear improvement of the VWF multimer patterns for several siRNAs. (C) HEK293 cells were transfected with only normal VWF or with normal and mutant VWF in a 1:1 ratio. A single siRNA or a combination of two siRNAs with different targets was transfected into HEK293 cells cotransfected with normal and mutant VWF. A combination of two siRNAs targeting c.2365A and c.2880G or c.2365G and c.2880A did not clearly improve the multimerization pattern as compared with single siRNA transfections. A slight improvement in allele-specific inhibition at the protein level was observed with combined targeting of c.2365A and c.2880G as compared with targeting of only c.2365A. This was not observed when siRNAs with the targets c.2365G and c.2880A were combined.

## Discussion

In this study, we selected a set of allele-specific siRNAs with the *in vitro* ability to mediate allele-specific inhibition of *VWF*. Inhibition of mutant *VWF* production, while preserving the production of normal *VWF*, improved the multimerization pattern of the dominant negative *VWF* mutation p.Cys2773Ser. This approach could improve several phenotypes caused by dominant negative *VWF* mutations, which are present in > 90% of the VWD population.<sup>2</sup>

Various studies have proven that siRNAs, microRNAs, antisense oligonucleotides and CRISPR-Cas9 can discriminate two alleles on the basis of one nucleotide variation.<sup>16-22</sup> This discrimination could be based on the dominant negative mutation itself, or on a SNP located on the same allele as the dominant negative mutation. For this study, we chose to use allele-specific siRNAs that target frequent SNPs in *VWF*. siRNAs were chosen to prove the feasibility of allele-specific inhibition in VWD, and because of their safe temporary effects. By the selection of four SNPs with a high MAF in *VWF*, it is possible to design a treatment applicable to a major part of the Caucasian population, as 74% will be heterozygous for at least one of these four SNPs. By increasing the number of SNPs, the population coverage can even be increased up to 93% (data not shown). A much larger number of siRNAs would be required to target each individual *VWF* mutation.

The proof of principle of allele-specific inhibition of *VWF* was tested by overexpression of *VWF* alleles in HEK293 cells. Two methods were used to screen for effective siRNAs. First, siRNAs were transfected into HEK293 cells stably producing *VWF*. This setting resembles a normal situation, in which there is continuous production of *VWF*. Using this experimental set-up, we selected at least one effective siRNA per SNP allele. However, the ratio of the targeted and untargeted allele was not yet optimal. We reasoned that discrimination between the two *VWF* alleles present in the heterozygous situation, as in patients, might improve allelic discrimination by siRNAs. To mimic the coexistence of two *VWF* alleles in one cell, we performed cotransfections of two *VWF* alleles and an siRNA targeting one of the two alleles in HEK293 cells. This did indeed lead to an increase in specificity of the siRNAs for the targeted allele. The increase in allele specificity suggests that competition between two alleles leads to preference of the siRNA for its specific target. Remarkably, we observed at the protein level, but not at the mRNA level, upregulation of the untargeted *VWF* allele for most siRNAs at the lowest siRNA concentrations (Figs S4 and 2B). This might have been caused by transfection of an excess of plasmids, which may lead to a maximum production capacity of the translational machinery. siRNA-mediated inhibition of the targeted allele may then provide greater access of the translational machinery to the untargeted allele, and enhance translation of the untargeted allele. An increase in the siRNA concentration would inhibit this process by increasing non-specific binding of the siRNA to the untargeted allele. Whether this upregulation also occurs in cells endogenously producing *VWF* could be studied in blood outgrowth endothelial cells (BOECs).<sup>23</sup> As BOECs are primary cells, they differ from heterologous cell systems in the

processing and maturation of pre-mRNA. Although siRNAs bind and process mature mRNA in the cytoplasm, differences in mRNA modifications between primary and heterologous cell systems should be kept in mind. We and others have shown the feasibility of isolating BOECs from VWD patients.<sup>24-27</sup> Genotyping patients and family members for the patients' mutation and the four selected SNPs will identify which SNPs the patient is heterozygous for, and which of the two SNP alleles is linked to the dominant negative mutation.

In this study, we investigated the effect of the most potent siRNAs on VWF p.Cys2773Ser, a fully characterized dominant negative mutation causing defective intracellular multimerization.<sup>15</sup> Cotransfection of normal VWF and VWF p.Cys2773Ser into HEK293 cells did indeed lead to a severe multimerization defect and a decrease in the amount of high molecular weight VWF. The addition of the most potent siRNAs resulted, for almost all siRNAs, in clear improvements in VWF multimerization. The multimer pattern could not be further improved by the simultaneous transfection of two siRNAs with different targets (Fig. 3C). Inhibition of mutant VWF as therapy for VWD is especially beneficial for VWD patients in whom the unhindered production of mutant VWF has detrimental effects that are not prevented by current therapies. The most clear example is the development of thrombocytopenia in VWD type 2B patients, which is often provoked by stress responses during surgery or pregnancy.<sup>28,29</sup> However, apart from those patients with a clear unmet clinical need, inhibition of mutant VWF might also benefit patients with other VWD phenotypes, e.g. patients with a very fast clearance rate or a severe secretion defect caused by intracellular retention. In those cases, inhibition of the mutant allele will increase circulating levels of normal VWF. Furthermore, recent findings suggest a role for VWF in angiogenesis, i.e. the formation of new blood vessels from existing vessels.<sup>30,31</sup> The negative regulation of VWF on the process of angiogenesis potentially results in increased blood vessel formation, and may lead to intestinal angiodysplasia and intractable intestinal bleeding in VWD patients.<sup>32,33</sup> As VWF is thought to have an intracellular and extracellular signaling function in the process of angiogenesis, mutant VWF itself may be responsible for maintaining the aberrant angiogenesis.<sup>31,32</sup> Inhibiting mutant VWF expression may attenuate all of these effects, and at the same time increase circulating levels of normal VWF.

Allele-specific siRNAs could be used in a prophylactic setting, either to prevent spontaneous bleeding or prior to scheduled interventions, or they could convert a DDAVP-unresponsive patient into a DDAVP-responsive patient. The exact application of allele-specific inhibition of VWF will depend, among other things, on the patient's phenotype and the duration of siRNA inhibition *in vivo*. *In vivo* use of siRNAs requires a delivery vehicle. Until now, delivery of siRNAs has been mainly focused on targeting the liver.<sup>34,35</sup> Recently, delivery vehicles targeting the endothelium have also shown positive results regarding inhibition of several endothelial genes.<sup>36,37</sup> These results are promising regarding the possibility of endothelium-targeted siRNA therapies for VWD.

Altogether, the recent developments in the field of siRNA delivery, the ability of the designed siRNAs to inhibit *VWF* in an allele-specific manner and the ability of these siRNAs to improve a severe VWD phenotype hold promise for the use of allele-specific siRNAs as therapy for dominant negative VWD.

## **Acknowledgements**

This study was financially supported by a research grant from the Landsteiner Foundation for Blood Transfusion Research (grant 1504). We would like to thank J. Voorberg from Sanquin (Amsterdam, the Netherlands) for the kind gift of the mAb against VWF, CLB-RAg35. We also would like to thank E. Weijers (LUMC, the Netherlands) for reviewing the paper.

## References

1. Leebeek FWG, Eikenboom JCJ. Von Willebrand's Disease. *N Engl J Med*. 2016;**375**(21):2067-2080.
2. Goodeve AC. The genetic basis of von Willebrand disease. *Blood Rev*. 2010;**24**(3):123-134.
3. Sadler JE, Budde U, Eikenboom JC, et al. Update on the pathophysiology and classification of von Willebrand disease: a report of the Subcommittee on von Willebrand Factor. *J Thromb Haemost*. 2006;**4**(10):2103-2114.
4. Curnow J, Pasalic L, Favaloro EJ. Treatment of von Willebrand Disease. *Semin Thromb Hemost*. 2016;**42**(2):133-146.
5. Mannucci PM, Ruggeri ZM, Pareti FI, Capitanio A. 1-Deamino-8-d-arginine vasopressin: a new pharmacological approach to the management of haemophilia and von Willebrands' diseases. *Lancet*. 1977;**1**(8017):869-872.
6. Franchini M, Mannucci PM. Von Willebrand factor (Vonvendi(R)): the first recombinant product licensed for the treatment of von Willebrand disease. *Expert Rev Hematol*. 2016;**9**(9):825-830.
7. Lillicrap D. von Willebrand disease: advances in pathogenetic understanding, diagnosis, and therapy. *Blood*. 2013;**122**(23):3735-3740.
8. Casari C, Pinotti M, Lancellotti S, et al. The dominant-negative von Willebrand factor gene deletion p.P1127\_C1948delinsR: molecular mechanism and modulation. *Blood*. 2010;**116**(24):5371-5376.
9. de Jong A, Eikenboom J. Von Willebrand disease mutation spectrum and associated mutation mechanisms. *Thromb Res*. 2017;**159**:65-75.
10. Auton A, Brooks LD, Durbin RM, et al. A global reference for human genetic variation. *Nature*. 2015;**526**(7571):68-74.
11. Romani de Wit T, Rondaij MG, Hordijk PL, Voorberg J, van Mourik JA. Real-time imaging of the dynamics and secretory behavior of Weibel-Palade bodies. *Arterioscler Thromb Vasc Biol*. 2003;**23**(5):755-761.
12. Wong ML, Medrano JF. Real-time PCR for mRNA quantitation. *Biotechniques*. 2005;**39**(1):75-85.
13. Tjernberg P, Vos HL, Castaman G, Bertina RM, Eikenboom JC. Dimerization and multimerization defects of von Willebrand factor due to mutated cysteine residues. *J Thromb Haemost*. 2004;**2**(2):257-265.
14. Tamura T, Horiuchi H, Imai M, et al. Unexpectedly High Prevalence of Acquired von Willebrand Syndrome in Patients with Severe Aortic Stenosis as Evaluated with a Novel Large Multimer Index. *J Atheroscler Thromb*. 2015;**22**(11):1115-1123.
15. Tjernberg P, Vos HL, Spaargaren-van Riel CC, et al. Differential effects of the loss of intrachain-versus interchain-disulfide bonds in the cystine-knot domain of von Willebrand factor on the clinical phenotype of von Willebrand disease. *Thromb Haemost*. 2006;**96**(6):717-724.
16. Miniarikova J, Zanella I, Huseinovic A, et al. Design, Characterization, and Lead Selection of Therapeutic miRNAs Targeting Huntingtin for Development of Gene Therapy for Huntington's Disease. *Mol Ther Nucleic Acids*. 2016;**5**:e297.
17. Novelli F, Lena AM, Panatta E, et al. Allele-specific silencing of EEC p63 mutant R304W restores p63 transcriptional activity. *Cell Death Dis*. 2016;**7**:e2227.

18. Miller VM, Xia H, Marrs GL, et al. Allele-specific silencing of dominant disease genes. *Proc Natl Acad Sci U S A*. 2003;**100**(12):7195-7200.
19. Pfister EL, Kennington L, Straubhaar J, et al. Five siRNAs targeting three SNPs may provide therapy for three-quarters of Huntington's disease patients. *Curr Biol*. 2009;**19**(9):774-778.
20. Skotte NH, Southwell AL, Ostergaard ME, et al. Allele-specific suppression of mutant huntingtin using antisense oligonucleotides: providing a therapeutic option for all Huntington disease patients. *PLoS One*. 2014;**9**(9):e107434.
21. Southwell AL, Skotte NH, Kordasiewicz HB, et al. In vivo evaluation of candidate allele-specific mutant huntingtin gene silencing antisense oligonucleotides. *Mol Ther*. 2014;**22**(12):2093-2106.
22. Yoshimi K, Kaneko T, Voigt B, Mashimo T. Allele-specific genome editing and correction of disease-associated phenotypes in rats using the CRISPR-Cas platform. *Nat Commun*. 2014;**5**:4240.
23. Martin-Ramirez J, Hofman M, van den Biggelaar M, Hebbel RP, Voorberg J. Establishment of outgrowth endothelial cells from peripheral blood. *Nat Protoc*. 2012;**7**(9):1709-1715.
24. Hawke L, Bowman ML, Poon MC, Scully MF, Rivard GE, James PD. Characterization of aberrant splicing of von Willebrand factor in von Willebrand disease: an underrecognized mechanism. *Blood*. 2016;**128**(4):584-593.
25. Wang JW, Bouwens EA, Pintao MC, et al. Analysis of the storage and secretion of von Willebrand factor in blood outgrowth endothelial cells derived from patients with von Willebrand disease. *Blood*. 2013;**121**(14):2762-2772.
26. Starke RD, Paschalaki KE, Dyer CE, et al. Cellular and molecular basis of von Willebrand disease: studies on blood outgrowth endothelial cells. *Blood*. 2013;**121**(14):2773-2784.
27. Selvam SN, Casey LJ, Bowman ML, et al. Abnormal angiogenesis in blood outgrowth endothelial cells derived from von Willebrand disease patients. *Blood Coagul Fibrinolysis*. 2017;**28**(7):521-533.
28. Hultin MB, Sussman II. Postoperative thrombocytopenia in type IIB von Willebrand disease. *Am J Hematol*. 1990;**33**(1):64-68.
29. Rick ME, Williams SB, Sacher RA, McKeown LP. Thrombocytopenia associated with pregnancy in a patient with type IIB von Willebrand's disease. *Blood*. 1987;**69**(3):786-789.
30. Groeneveld DJ, van Bakkum T, Dirven RJ, et al. Angiogenic characteristics of blood outgrowth endothelial cells from patients with von Willebrand disease. *J Thromb Haemost*. 2015;**13**(10):1854-1866.
31. Starke RD, Ferraro F, Paschalaki KE, et al. Endothelial von Willebrand factor regulates angiogenesis. *Blood*. 2011;**117**(3):1071-1080.
32. Castaman G, Federici AB, Tosetto A, et al. Different bleeding risk in type 2A and 2M von Willebrand disease: a 2-year prospective study in 107 patients. *J Thromb Haemost*. 2012;**10**(4):632-638.
33. Makris M. Gastrointestinal bleeding in von Willebrand disease. *Thromb Res*. 2006;**118 Suppl 1**:S13-17.
34. Pasi KJ, Rangarajan S, Georgiev P, et al. Targeting of Antithrombin in Hemophilia A or B with RNAi Therapy. *N Engl J Med*. 2017;**377**(9):819-828.

35. Heestermans M, van Vlijmen BJ. Oligonucleotides targeting coagulation factor mRNAs: use in thrombosis and hemophilia research and therapy. *Thromb J*. 2017;**15**:7.
36. Dahlman JE, Barnes C, Khan O, et al. In vivo endothelial siRNA delivery using polymeric nanoparticles with low molecular weight. *Nat Nanotechnol*. 2014;**9**(8):648-655.
37. Fehring V, Schaeper U, Ahrens K, et al. Delivery of therapeutic siRNA to the lung endothelium via novel Lipoplex formulation DACC. *Mol Ther*. 2014;**22**(4):811-820.

Supplemental data  
Figure S1

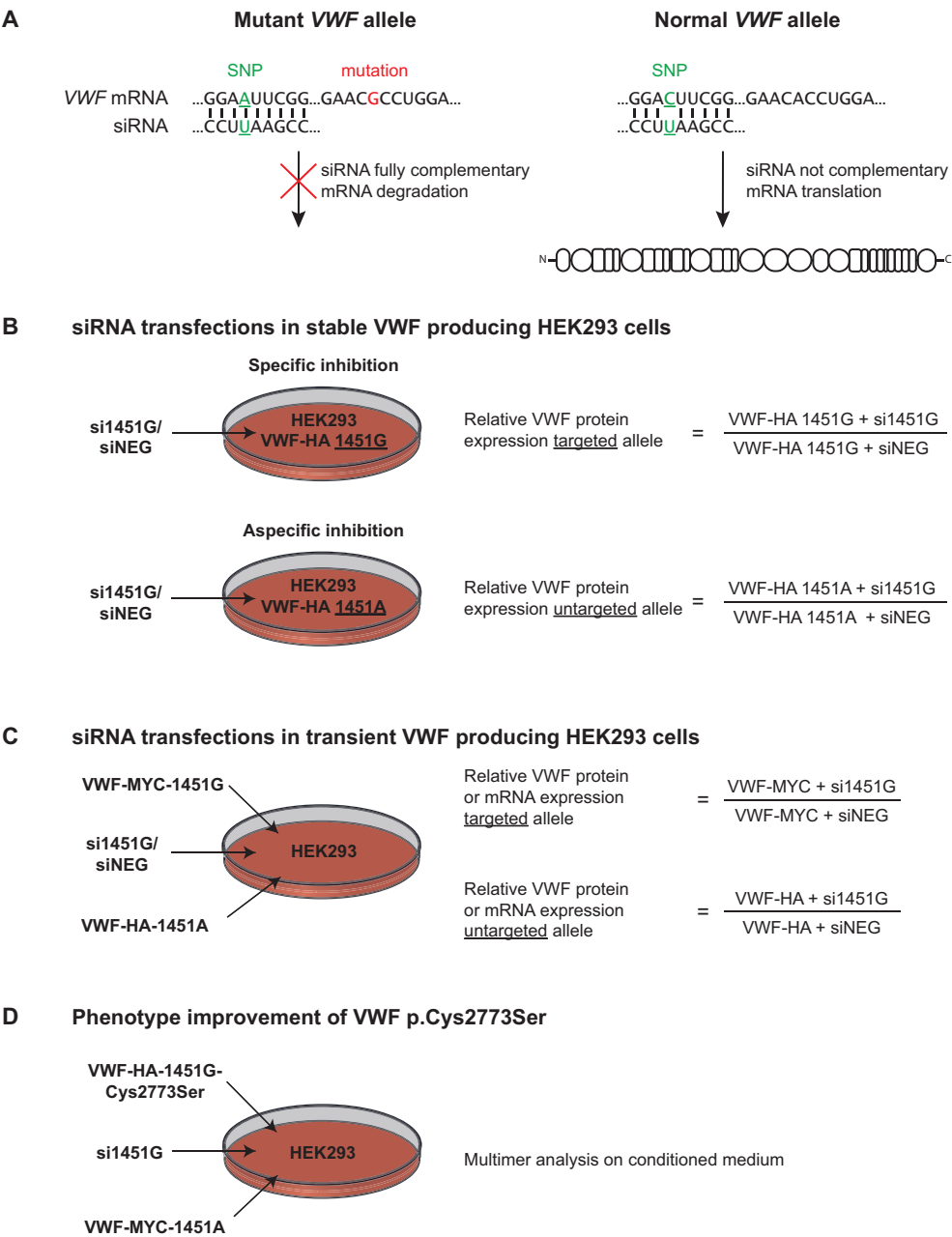
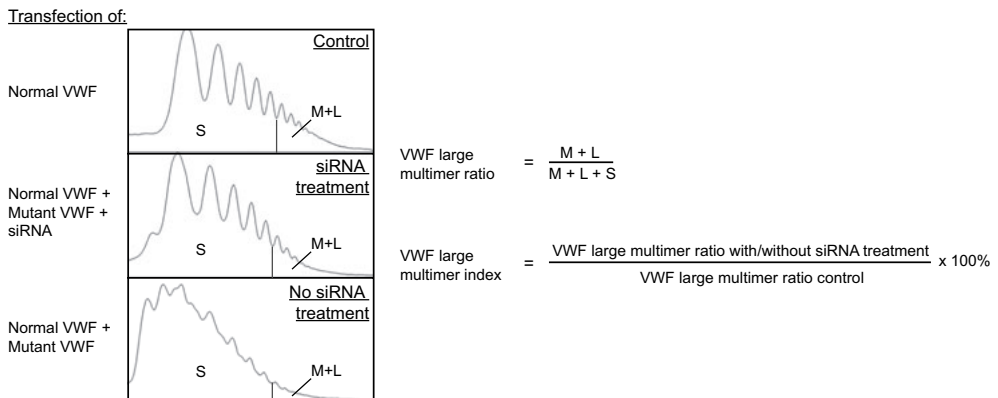


**Figure S1. Schematic representation of the hypothesis and experimental setup.** (A) siRNAs designed to target a heterozygous SNP (in this example an adenine, green) located on the same allele as the dominant-negative mutation (in this example a guanine, red) are expected to inhibit expression of the mutant *VWF*



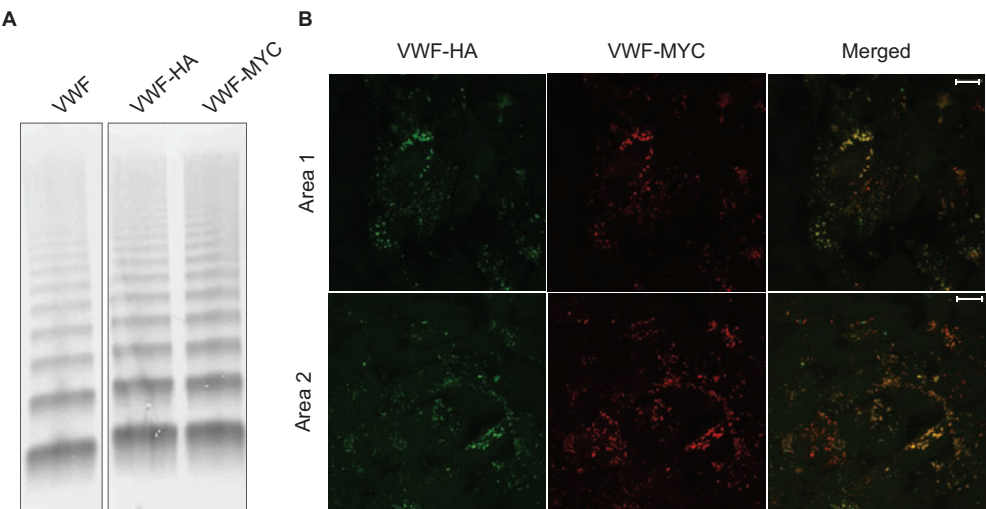
allele. The mismatch of the same siRNA with the other allele of the SNP (in this example a cytosine, green) is hypothesized to render the siRNA ineffective and therefore lead to normal mRNA translation. (B) Experimental setup of siRNA transfections to stable VWF producing HEK293 cells. siRNAs and siNEG were transfected to cells stably expressing the targeted *VWF* allele and to cells stably expressing the untargeted allele. Relative VWF expression was determined by dividing the VWF:Ag levels measured in conditioned medium and lysates of cells transfected with a specific siRNA (in this example si1451G) to cells transfected with siNEG. (C) Experimental setup of HEK293 cells cotransfected with siRNAs and two *VWF* alleles. siRNAs were transiently cotransfected to HEK293 cells with two *VWF* alleles containing either an HA or MYC peptide tag. Relative VWF expression of both alleles is determined by dividing the VWF-HA or VWF-MYC protein or mRNA levels measured in conditioned medium and lysates of cells transfected with a specific siRNA (in this example si1451G) to cells transfected with siNEG. (D) Experimental setup of HEK293 cells cotransfected with siRNA and two *VWF* alleles, of which the *VWF*-HA allele also contained the VWF p.Cys2773Ser mutation. Improvements in multimerization were determined by multimer analysis. VWF, von Willebrand factor; SNP, single-nucleotide polymorphism; siRNA, small interfering RNA; mRNA, messenger RNA; si1451G, indicates 'small interfering RNA against *VWF* c.1451G'

## Figure S2

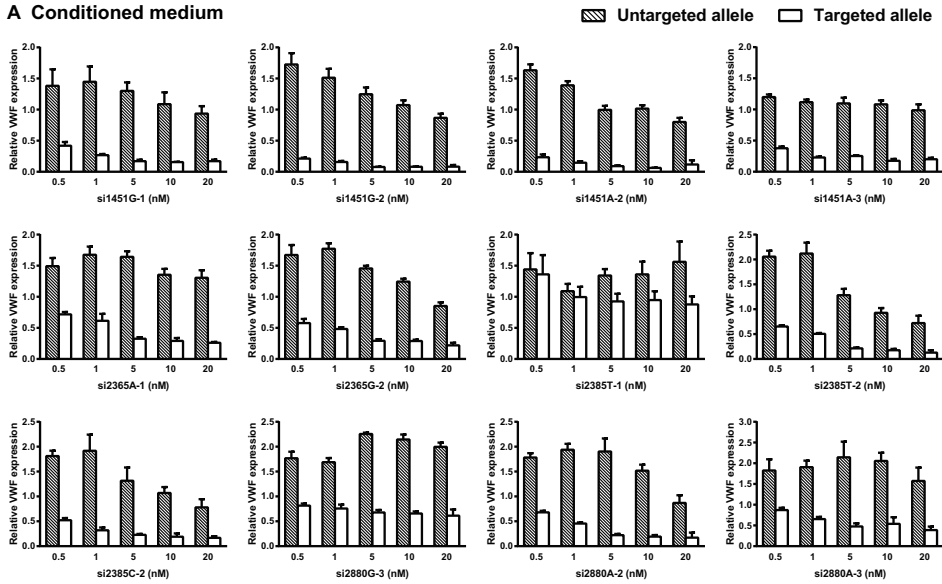
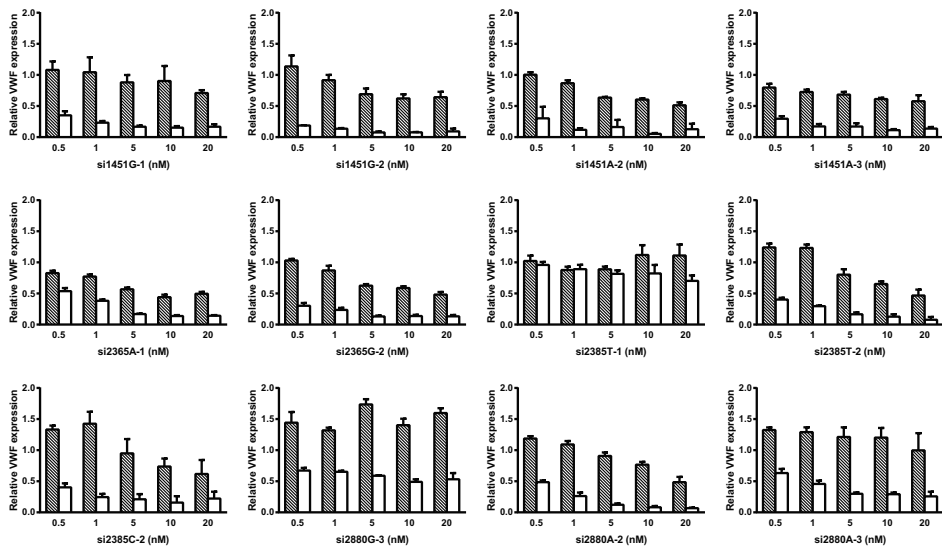


**Figure S2. Calculation of the VWF large multimer index.** Densitometry images are divided in the five smallest (S) bands and the rest (intermediate and large bands (M+L)). The VWF large multimer ratio is calculated for each densitometry image by dividing the area of intermediate and large VWF multimers (M+L) over the total area (M+L+S). The VWF large multimer index is calculated by dividing the VWF large multimer ratio of cells cotransfected with normal and mutant VWF (with or without siRNA treatment) over the VWF large multimer ratio of cells transfected with normal VWF only. VWF, von Willebrand factor; S, small multimers; M, intermediate multimers; L, large multimers

**Figure S3**



**Figure S3. Effect of HA and MYC peptide tags on VWF processing and transfection.** (A) VWF multimer analysis on conditioned medium of HEK293 cells transfected with VWF-HA, VWF-MYC or normal VWF plasmids. Shown are conditioned medium samples 72 hours after transfection and 48 hours after refreshing the medium, loaded on a 1.5% SDS-agarose gel. All three samples in the picture were run on the same gel. (B) Representative images of immunofluorescent staining of HEK293 cells cotransfected with VWF-HA (green) and VWF-MYC (red) plasmids. Most cells stain both VWF-HA and VWF-MYC, indicating a true coexpressing system. Bar represents 10  $\mu$ m. Images were taken with the Leica TCS SP8 upright confocal microscope with a 63x/1.40 NA Plan Apo oil immersion objective. VWF, von Willebrand factor

**Figure S4****A Conditioned medium****B Cell lysates**

**Figure S4. Dose response of allele-specific siRNAs cotransfected with two VWF alleles into HEK293 cells.** Normalized VWF-HA and VWF-MYC protein levels measured by ELISA in (A) conditioned medium and (B) cell lysates of HEK293 cells cotransfected with VWF-HA, VWF-MYC and allele-specific siRNAs at five different concentrations to determine the dose-response. The untargeted and targeted allele could either be VWF-HA or VWF-MYC, depending on the *VWF* allele (Table S1). VWF-HA and VWF-MYC protein levels were normalized to the VWF-HA and VWF-MYC protein levels measured in HEK293 cells cotransfected with the two *VWF* alleles and siNEG. Shown are the mean + 1 SD of the compiled results of two independent experiments performed in duplicate (N = 4). si1451G-1, indicates 'small interfering RNA-1 against *VWF* c.1451G', all siRNAs are indicated according to this principle; siRNA, small interfering RNA; VWF, von Willebrand factor; nM, nanomolar

**Table S1.** VWF plasmids used to determine efficiency and degree of allele-specificity in stable VWF producing HEK293 cells and transiently cotransfected HEK293 cells

pcDNA™3.1/Zeo (+)	rs1800378	rs1063856	rs1063857	rs1800380	Used for:
	c.1451G A	c.2365A G	c.2385T C	c.2880G A	
hVWF-HA	G	A	T	G	Stable cell line
hVWF-MYC	G	A	T	G	Cotransfection
hVWF-HA-1451A	A	A	T	G	Stable cell line/cotransfection
hVWF-HA-2365G	G	G	T	G	Stable cell line/cotransfection
hVWF-HA-2385C	G	A	C	G	Stable cell line/cotransfection
hVWF-HA-2880A	G	A	T	A	Stable cell line/cotransfection

VWF, von Willebrand factor

**Table S2.** VWF plasmids used for allele-specific inhibition of hVWF p.Cys2773Ser

	pcDNA™3.1/Zeo (+)	rs1800378	rs1063856	rs1063857	rs1800380	p.Cys2773Ser
		c.1451G A	c.2365A G	c.2385T C	c.2880G A	c.8318G C
To target c.1451G	hVWF-HA-Cys2773Ser	G	A	T	G	C
	hVWF-MYC-1451A	A	A	T	G	G
To target c.1451A	hVWF-HA-1451A-Cys2773Ser	A	A	T	G	C
	hVWF-MYC	G	A	T	G	G
To target c.2365A	hVWF-HA-Cys2773Ser	G	A	T	G	C
	hVWF-MYC-2365G	G	G	T	G	G
To target c.2365G	hVWF-HA-2365G-Cys2773Ser	G	G	T	G	C
	hVWF-MYC	G	A	T	G	G
To target c.2385T	hVWF-HA-Cys2773Ser	G	A	T	G	C
	hVWF-MYC-2385C	G	A	C	G	G
To target c.2385C	hVWF-HA-2385C-Cys2773Ser	G	A	C	G	C
	hVWF-MYC	G	A	T	G	G
To target c.2880G	hVWF-HA-Cys2773Ser	G	A	T	G	C
	hVWF-MYC-2880A	G	A	T	A	G
To target c.2880A	hVWF-HA-2880A-Cys2773Ser	G	A	T	A	C
	hVWF-MYC	G	A	T	G	G
To target c.2365A and c.2880G	hVWF-HA-Cys2773Ser	G	A	T	G	C
	hVWF-MYC-2365G/2880A	G	G	T	A	G
To target c.2365G and c.2880A	hVWF-HA-2365G/2880A-Cys2773Ser	G	G	T	A	C
	hVWF-MYC	G	A	T	G	G

VWF, von Willebrand factor







# 5

## Variability of von Willebrand factor-related parameters in endothelial colony forming cells

Annika de Jong  
Ester Weijers  
Richard Dirven  
Suzan de Boer  
Jasmin Streur  
Jeroen Eikenboom

*Journal of Thrombosis and Haemostasis* (2019) 17(9):1544-1554

## Abstract

**Background** Endothelial colony forming cells (ECFCs) are cultured endothelial cells derived from peripheral blood. ECFCs are a powerful tool to study pathophysiological mechanisms underlying vascular diseases, including von Willebrand disease. In prior research, however, large variations between ECFC lines were observed in, among others, von Willebrand factor (VWF) expression. **Objective** Understand the relation between phenotypic characteristics and VWF-related parameters of healthy control ECFCs. **Methods** ECFC lines (N = 16) derived from six donors were studied at maximum cell density. Secreted and intracellular VWF antigen were measured by ELISA. The angiogenic capacity of ECFCs was investigated by the Matrigel tube formation assay. Differences in expression of genes involved in angiogenesis, aging, and endothelial to mesenchymal transition (EndoMT) were measured by quantitative PCR. **Results** Different ECFC lines show variable morphologies and cell density at maximum confluency and cell lines with a low maximum cell density show a mixed and more mesenchymal phenotype. We identified a significant positive correlation between maximum cell density and VWF production, both at protein and mRNA level. Also, significant correlations were observed between maximum cell density and several angiogenic, aging and EndoMT parameters. **Conclusions** We observed variations in morphology, maximum cell density, VWF production, and angiogenic potential between healthy control ECFCs. These variations seem to be attributable to differences in aging and EndoMT. Because variations correlate with cell density, we believe that ECFCs maintain a powerful tool to study vascular diseases. It is however important to compare cell lines with the same characteristics and perform experiments at maximum cell density.



## Introduction

von Willebrand factor (VWF) is a large multimeric glycoprotein required for hemostasis. Generally, VWF is known as carrier protein for coagulation factor VIII and as mediator for platelet adhesion and aggregation at sites of vascular damage. More recently, other functions of VWF on the cellular level are described, for example in the process of angiogenesis.<sup>1</sup> Dysfunction or deficiencies of VWF lead to von Willebrand disease (VWD), the most common inherited bleeding disorder.<sup>2</sup> VWF is mainly synthesized in endothelial cells and stored in Weibel-Palade bodies.<sup>3</sup> A small proportion of VWF is produced in megakaryocytes, and stored in their alpha-granules.<sup>4</sup> The pathophysiology of VWD has historically been studied on a cellular level in heterologous cell systems by overexpression of VWF variants.<sup>5,6</sup> Yet, several aspects of VWF biology (i.e., the process of angiogenesis and VWF behavior under flow) can only be studied in endothelial cells. Moreover, because endothelial cells are the main source of VWF production, it is of utmost importance to study these cells in great detail to understand cellular defects in VWF to benefit VWD patients.

Obtaining endothelial cells from patients or healthy subjects used to be difficult because of the type of tissue needed for endothelial cell isolations. The source of endothelial cells mostly used is the umbilical vein, yielding human umbilical vein endothelial cells (HUVECs). However, the experimental use of HUVECs is limited because they cannot be obtained from subjects with specific clinical or genetic characteristics. Nowadays, endothelial cells can be isolated from the mononuclear cell fraction from peripheral blood and have the ability to expand *ex vivo*.<sup>7,8</sup> Cultured endothelial cells derived from peripheral blood have adopted different names in literature, such as blood outgrowth endothelial cells, late outgrowth endothelial cells or endothelial colony forming cells (ECFCs).<sup>9</sup> Recently, consensus was made to use the term ECFC and we will therefore adapt to this consensus. We would like to highlight that the ECFCs in this study are the same type of cells as the cells denoted as blood outgrowth endothelial cells used in prior studies published by us and most groups studying VWD pathophysiology.<sup>10-12</sup> In the past decade, multiple studies showed interesting results applying ECFCs to study VWD pathophysiology at the cellular level.<sup>10-15</sup> Unfortunately, these studies also showed a wide range of variation in the endothelial cells from VWD patients complicating interpretation and comparison of the results.<sup>16</sup> To confidently use ECFCs to study VWD pathophysiology, we need to understand the extent of these variations and their effects on VWF-related parameters; therefore we aim to understand the relation between the phenotypic characteristics and VWF-related parameters of ECFCs from healthy controls. We cultured ECFC lines and investigated their phenotypic characteristics in a standardized setup. The phenotypic characteristics of individual ECFC lines were correlated with VWF parameters and their angiogenic capacity. In addition, gene expression of specific pathways was investigated to unravel the potential underlying mechanism of ECFC variability.

## Materials and methods

### **ECFC isolation**

ECFCs were isolated according to Martin-Ramirez *et al* (2012).<sup>17</sup> In short, 30-80 mL peripheral blood was drawn in 10 mL trisodium citrate tubes (ECFCs 1 and 2; S-Monovette®#02.1067.001, Sarstedt, Nümbrecht, Germany) or 10 mL lithium heparin tubes (ECFCs 3-6; BD Biosciences Vacutainer #367880, BD, Erebodegem, Belgium). Peripheral blood was diluted 1:1 with phosphate-buffered saline (PBS) and blood components were separated by gradient centrifugation over Ficoll Paque (LUMC Pharmacy, Leiden, the Netherlands). The mononuclear cell fraction was isolated and washed 1x in PBS and 1x in 5 mL EGM-20 culture medium, consisting of 500 ml EBM™-2 medium (Lonza, Breda, the Netherlands) supplemented with the EGM™-2 BulletKit™ (Lonza), 100 mL fetal bovine serum (Gibco®, Invitrogen, Carlsbad, CA), and 7 mL Antibiotic Antimycotic solution (Sigma-Aldrich #A5955, St. Louis, MO). Cells were seeded on 48 wells Nunc™ Cell-Culture Treated Multidishes (Nunclon, Roskilde, Denmark) pre-coated with 50 µg/mL rat tail collagen type I (BD Biosciences). Medium was refreshed every other day. Cells were passaged according to the scheme in Fig. S1A.

The study protocol was approved by the Leiden University Medical Center ethics review board. Informed consent was obtained from all subjects in accordance with the Declaration of Helsinki.

### **ECFC culture**

ECFCs were cultured in EGM-20 culture medium, which was refreshed every other day. All experiments were performed on cells that were 3-5 days confluent. Cells were considered confluent when they stopped expanding as determined by the cell number per mm<sup>2</sup> (maximum cell density). Cell density was determined by the ITCN plug-in (v1.6) of Fiji, ImageJ (ImageJ 1.51r, Bethesda, MD) on bright-field images that were taken daily. Each single ECFC line at passage 5 was simultaneously subjected to fluorescence-activated cell sorting (FACS) analysis, gene expression analysis and tube formation analysis on Matrigel (Fig. S1B). Immunofluorescent staining and VWF antigen (VWF:Ag) measurements were performed in separate experiments (Fig. S1C). The characterization of each ECFC line was performed in two independent experiments, except for FACS analysis, which was performed once for each ECFC line.

### **FACS analysis**

Surface marker expression was detected with flow cytometry. ECFCs were pelleted and washed with FACS buffer (PBS; 1% bovine serum albumin [Sigma-Aldrich]; 0.01% sodium azide) and incubated on ice for 30 minutes with the following labeled primary antibodies or

isotype controls: CD14-FITC (BD Biosciences), CD31-FITC (PECAM1; BD Biosciences), CD45-Pacific Blue (BD Biosciences), CD144-PE (VE-cadherin; R&D), CD146-PerCp-Cy5 (MCAM, BD Biosciences), IgG1-FITC (R&D), IgG1-PE (BD Biosciences), IgG1-PerCp-Cy5, and IgG1-Pacific blue (all BD Biosciences). After antibody incubation, cells were washed in FACS buffer and run on the LSRII (BD Biosciences). Data were analyzed using FACSDiVa software (BD Biosciences).

### ***VWF:Ag measurements***

Basal VWF secretion was determined by the release of VWF over 24 hours in EGM-20 culture medium. For determination of intracellular VWF, cells were lysed overnight at 4°C in Opti-MEM™ I Reduced Serum Medium (Thermo Fisher Scientific, Carlsbad, CA) containing 0.1% Triton X-100 (Sigma-Aldrich) supplemented with cOmplete™ Protease Inhibitor Cocktail with EDTA (Roche Diagnostics, Mannheim, Germany). VWF:Ag levels were measured in conditioned medium and cell lysates by ELISA as previously described.<sup>18</sup>

### ***Confocal immunofluorescence microscopy***

ECFCs were plated on rat tail collagen (50 µg/mL) coated glass coverslips. Three different staining procedures were used to detect intra- and/or extracellular VWF. Solely intracellular VWF was visualized after fixation and permeabilization with ice-cold methanol, after which the cells were washed twice with PBS and blocked with PBS, 1% fetal bovine serum (Gibco) and 1% bovine serum albumin (Sigma-Aldrich). Intra- as well as extracellular VWF was visualized after fixation with 4% paraformaldehyde (Alfa Aesar, Karlsruhe, Germany), after which the cells were washed once and blocked and permeabilized with PBS, 5% normal goat serum (DAKO, Glostrup, Denmark) and 0.02% saponin (Sigma-Aldrich). Extracellular VWF was visualized after fixation with 4% paraformaldehyde, after which the cells were washed once and blocked with PBS and 5% normal goat serum (DAKO). Cells were stained for VWF with polyclonal antibody rabbit anti-hVWF (A0082, DAKO) and for VE-cadherin with purified mouse anti-human CD144 (BD Biosciences) diluted in the corresponding blocking buffer. Nuclear staining was performed with Hoechst (Thermo Fisher Scientific) diluted in PBS. Coverslips were mounted by ProLong® Diamond Antifade Mountant (Thermo Fisher Scientific) and cells were visualized by the Leica TCS SP8 X WLL converted confocal microscope equipped with a HC PL APO CS2 63x/1.40 OIL immersion objective.

### ***Matrigel tube formation***

Ninety-six wells plates were coated with 46 µL/well growth factor reduced Matrigel (BD Biosciences) for 1 hour at 37°C. ECFCs were seeded on the Matrigel at a concentration of 15,000 cells per well in EGM-2 medium. The culture plate was placed in a Leica DMI6000

inverted microscope with an environmental chamber for control of temperature (37°C) and CO<sub>2</sub> concentration (5%). Images were taken every 15 minutes with a 10x magnification using a LEICA DF350FX CCD camera until 24 hours after seeding cells. Analyses were performed with Fiji (ImageJ) using the Angiogenesis Analyzer plugin (version 1.0c). Two independent experiments were performed in triplicate for each ECFC line. Average values of triplicates were calculated for the tube length, number of branches, and number of meshes as characteristics of each ECFC line.

### ***Gene expression***

RNA was isolated using the RNeasy Micro Kit (Qiagen, Venlo, the Netherlands). Complementary DNA was synthesized using SuperScript™ II Reverse Transcriptase (Thermo Fisher Scientific) with poly(T) primers (Sigma-Aldrich). Quantitative PCR (qPCR) was performed using Sybr™ Select Master Mix (Thermo Fisher Scientific) in the CFX384 Touch instrument (Bio-Rad, Veenendaal, the Netherlands) with *GAPDH* as endogenous reference gene. Table S1 shows sequences of gene specific primers. The comparative Ct method was used as described by Wong and Medrano.<sup>19</sup>

### ***Statistics***

GraphPad Prism, version 7.00 (GraphPad Software, La Jolla, CA), was used for graphics and statistical analyses. Pearson correlation was used to determine the strength of association between cell density and all other measured parameters. Significance was set at  $P < 0.05$  (two-tailed).

## **Results**

### ***Phenotypic characterization***

ECFCs were isolated from six healthy donors which resulted in the outgrowth of 16 ECFC lines. In isolations of some donors, several clones appeared and these lines were cultured separately (for example, for donor 4, these multiple clones were named ECFC line 4A, 4B, etc.), so we could study both inter- and intra-donor variability. All ECFCs were positive for endothelial markers CD31 and CD146 and negative for leukocyte markers CD14 and CD45; however, a subset of ECFC lines showed decreased positivity for CD144 suggesting a mixed population (Fig. 1A, all histograms in Fig. S2). Furthermore, remarkable differences were observed between cell sizes at maximum confluency and morphology of the different lines (Fig. 1B and Fig. S3) and we observed that cell lines with bigger cell sizes have a more mesenchymal phenotype and could reach a lower cell density at maximum confluency. These “low cell density” ECFC lines

are the lines with decreased positivity for CD144 (Fig. 1C). Because we would like to show the characteristics of all cell populations that appear after ECFC isolation, we did not exclude cells for which the ECFC identity may be less clear because of lower CD144 positivity (i.e., ECFCs 1, 2, 6A, 6C, and 6E).

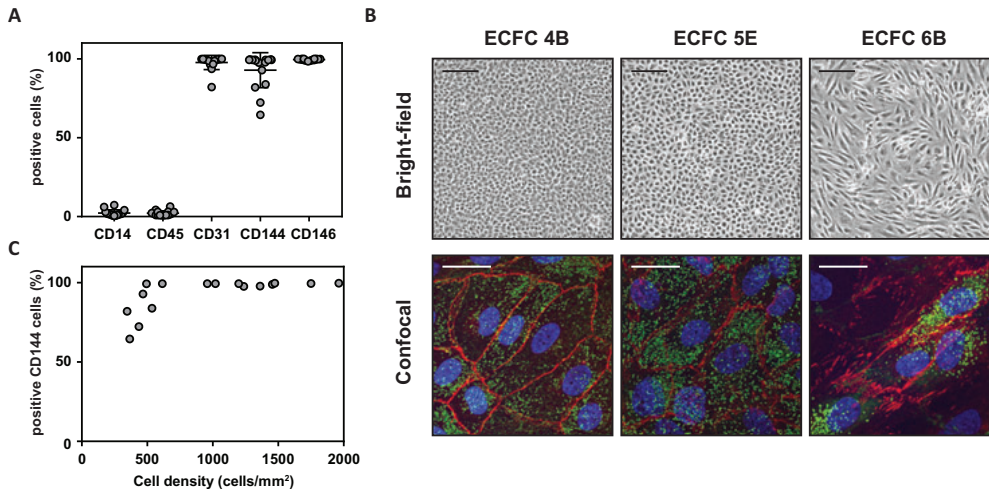


**Figure 1. ECFC surface marker expression and cell morphology.** (A) FACS analysis for surface markers CD14, CD31, CD45, CD144, and CD146 of all 16 ECFC lines derived from six healthy donors. All ECFC lines are negative for CD14 and CD45 and positive for CD31 and CD146. Variation is observed in CD144 expression. (B) Bright-field and confocal images of three representative ECFC lines with high, medium and low maximum cell densities 3-5 days after the cells stopped expanding. Bright-field images show clear morphological variation between ECFC lines. Scale bar in bright-field images represents 200  $\mu$ m. Confocal images show VWF (green) and VE-cadherin (red). Staining patterns clearly vary between ECFC lines, with VWF in Weibel-Palade bodies more at the periphery of the cell in lines with a high maximum cell density (ECFC 4B), VWF in elongated Weibel-Palade bodies dispersed throughout the whole cell in lines with an intermediate maximum cell density (ECFC 5E), and sparse VWF and more diffuse VE-cadherin staining in lines with a low maximum cell density (ECFC 6B). Scale bar in confocal images represents 10  $\mu$ m. (C) FACS analysis for CD144 in all 16 ECFC lines. Cells with a maximum cell density below 500 cells/mm<sup>2</sup> showed reduced positivity for CD144 (<500 cells/mm<sup>2</sup> 81.9 (64.5-99.2); >500 cells/mm<sup>2</sup> 99.3 (83.8-99.6), median (range),  $P = 0.0073$ , Mann-Whitney). ECFC, endothelial colony forming cell; FACS, fluorescence-activated cell sorting; VWF, von Willebrand factor

### VWF:Ag measurements

To evaluate the optimal timepoint to perform experiments, seven proliferative ECFC lines were subconfluently plated and followed over time for secreted VWF:Ag levels and cell density (bright-field images of three representative cell lines in Fig. S4). Maximum VWF:Ag levels were measured in conditioned medium 3-5 days after the ECFCs stopped expanding (maximum cell density). Both secreted VWF:Ag levels, and cell density remained constant after the maximum density was reached (Fig. 2A); therefore, all experiments in this study were performed at this stable phase, 3-5 days after the cells stopped expanding. The results for VWF secretion and cell density were comparable to observations in HUVECs.<sup>20,21</sup>

To determine differences in VWF:Ag secretion between the different ECFC lines, VWF:Ag levels released in 24 hours were measured in conditioned medium at maximum cell density. Interestingly, we observed a significant correlation between secreted VWF:Ag levels and maximum cell density, where cell lines with a high maximum cell density secreted more VWF than lines with a low maximum cell density ( $R^2 = 0.89$ ,  $P = 0.0001$ ; Fig. 2B). A correlation between secreted VWF:Ag levels and cell density is also observed in the days before maximum cell density; however, the slope of the lines is lower and increases until the day we measure highest VWF:Ag level. This slope remained constant from that moment on, just as the VWF:Ag levels did (data not shown). All separate clones were analyzed as independent data points, but a significant correlation between VWF:Ag secretion and maximum cell density was still present when all clones of a single donor were pooled. ECFC lines with a maximum cell density below 500 cells/mm<sup>2</sup> (ECFCs 1, 2, and 6A-E) had a VWF:Ag secretion below the lower limit of detection and were therefore excluded in the correlation analysis. The fold increase of VWF release in 1 hour after histamine stimulation over the release in 1 hour in unstimulated cells (the stimulation factor) was similar for all cell lines and was not related to maximum cell density (data not shown).

To exclude that cells with a high maximum cell density have a higher secretion rate and therefore lower intracellular VWF:Ag levels, we measured total VWF:Ag levels in conditioned medium and cell lysates. However, total VWF:Ag production also significantly correlated with maximum cell density ( $R^2 = 0.96$ ,  $P < 0.0001$ ; Fig. 2C). Because the total VWF:Ag level per individual cell was also higher in smaller cells, we excluded that higher VWF:Ag levels were measured because of the presence of a higher number of cells (Fig. 2D). Also, on the mRNA level, a significant correlation was observed between maximum cell density and VWF ( $R^2 = 0.63$ ,  $P = 0.0002$ ; Fig. 2E). Different clones that were isolated from individual donors also show variations in maximum cell density (Fig. 2F) and VWF:Ag expression (Fig. 2G) and we therefore subsequently analyzed all ECFC lines as individual clones.

Passaging of endothelial cells can result in morphological changes<sup>22</sup>; therefore, maximum cell density and VWF:Ag secretion at increasing passage numbers were studied. Two ECFC lines (4B and 5A) were passaged until they stopped proliferating at passage number 15 and 12, respectively. Both lines showed a decrease in maximum cell density with increasing passage number, which correlated with decreased secreted VWF:Ag levels (Fig. 2H and I). Furthermore, the ECFC line with the highest maximum cell density (4B) could be passaged until a higher passage number compared to the ECFC line with a lower maximum cell density (5A).

Overall, VWF production correlate with maximum ECFC density. This is observed both in cells at similar passage numbers and in cells with increasing passage numbers.

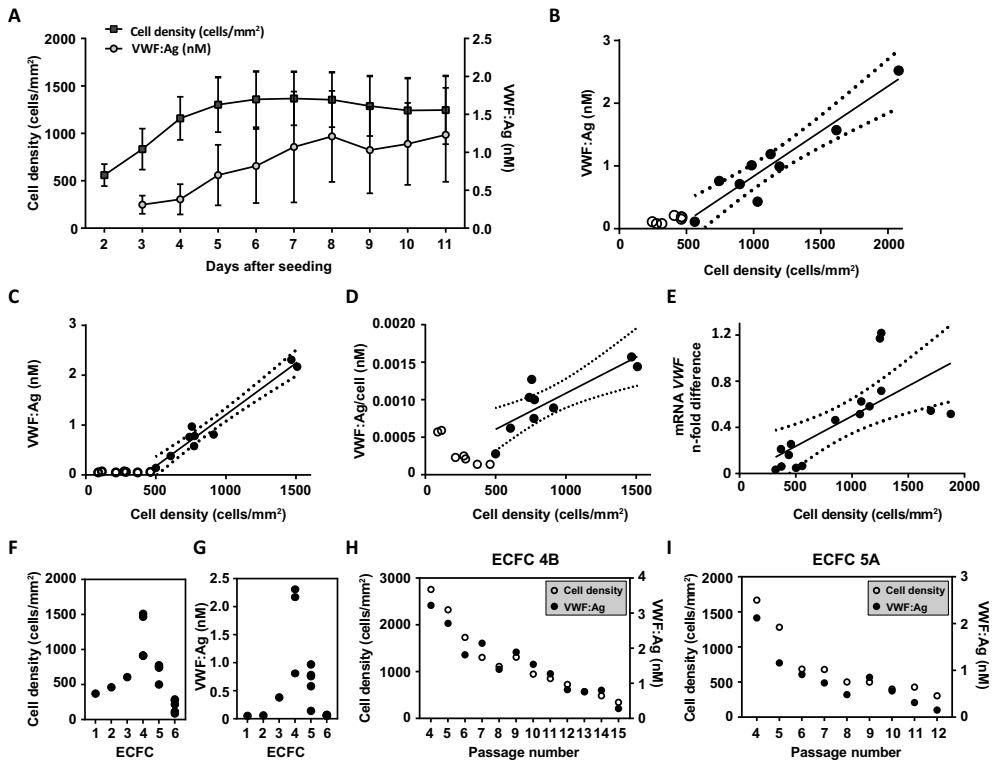


**Figure 2. VWF quantification and its relation to cell density.** (A) Average cell density and secreted VWF:Ag levels measured in conditioned medium that was harvested and refreshed every 24 hours in seven subconfluently plated ECFC lines. Highest VWF:Ag levels were identified 3-5 days after the cells stopped expanding. Both cell density and VWF:Ag production remained constant after the maximum was reached. (B) Secreted VWF:Ag levels measured in conditioned medium 24 hours after refreshing the medium showed a significant correlation with maximum cell density of ECFC lines with a maximum cell density of more than 500 cells/mm<sup>2</sup> ( $R^2 = 0.89$ ,  $P = 0.0001$ ). Open circles: maximum cell density <500 cells/mm<sup>2</sup>; closed circles: maximum cell density >500 cells/mm<sup>2</sup>. Each data point represents the average of two independent experiments. (C) Total VWF:Ag levels measured in conditioned medium and cell lysates 24 hours after refreshing the medium significantly correlate with maximum cell density of ECFC lines with a maximum cell density of more than 500 cells/mm<sup>2</sup> ( $R^2 = 0.96$ ,  $P < 0.0001$ ). Open circles: maximum cell density <500 cells/mm<sup>2</sup>; closed circles: maximum cell density >500 cells/mm<sup>2</sup>. (D) Total VWF:Ag levels per cell measured in conditioned medium and cell lysates 24 hours after refreshing the medium significantly correlate with maximum cell density of ECFC lines with a maximum cell density of more than 500 cells/mm<sup>2</sup> ( $R^2 = 0.71$ ,  $P = 0.0045$ ). Open circles: maximum cell density <500 cells/mm<sup>2</sup>; closed circles: maximum cell density >500 cells/mm<sup>2</sup>. (E) VWF mRNA levels measured by qPCR significantly correlate with maximum cell density ( $R^2 = 0.63$ ,  $P = 0.0002$ ). (F) Different ECFC lines per donor show variable cell densities at maximum confluency (G) Different ECFC lines per donor show variable VWF:Ag levels. (H) and (I) Maximum cell density and secreted VWF:Ag levels measured in conditioned medium 24 hours after refreshing the medium decrease with increasing passage number for ECFC lines 4B (H) and 5A (I). ECFC, endothelial colony forming cell; VWF, von Willebrand factor

### VWF localization

Endothelial cells store VWF in Weibel-Palade bodies.<sup>3</sup> To investigate whether the ECFC lines were able to store VWF in Weibel-Palade bodies, all ECFC lines were stained for VWF and endothelial marker VE-cadherin. Although all ECFC lines showed VWF in Weibel-Palade bodies,

large differences were observed in staining patterns (Fig. 1B for representative examples, all data in Fig. S3). ECFC lines with a very high maximum cell density (4A and 4B) showed mainly VWF staining closer to the cell membrane. Also, strings of released VWF were observed in some of these cell lines, whereas the cells were not extrinsically stimulated to secrete VWF (Fig. S3, stainings with PFA fixation). Cells with an intermediate maximum cell density and VWF production showed VWF staining in typical elongated Weibel-Palade bodies dispersed throughout the cell. Cells with a low maximum cell density showed only sparse VWF staining in a subset of cells. Interestingly, some ECFC lines with a low maximum cell density showed reduced VE-cadherin staining. This was in line with FACS results where cells with a maximum cell density below 500 cells/mm<sup>2</sup> showed decreased positivity for CD144 (Fig. 1B and C).

### **Matrigel tube formation**

Compared with the normal population, an increased number of VWD patients suffer from intestinal bleeding caused by angiodysplasia.<sup>23</sup> Several studies have shown a negative correlation of VWF and angiogenesis and VWF downregulation in an *in vitro* small interfering RNA knockdown assay resulted in increased angiogenic capacity.<sup>12,13,24</sup> We therefore reasoned that ECFC lines with low VWF production might have higher angiogenic potential than ECFC lines with high VWF production.<sup>24</sup>

The angiogenic properties of all 16 ECFC lines were investigated in an *in vitro* Matrigel tube formation assay. Herewith, the ability of endothelial cells to form tube-like structures was investigated, involving endothelial cell adhesion and migration. The formation of tube-like structures of all ECFC lines was followed for 24 hours. Although the angiogenic capacity clearly differed between ECFC lines (Fig. S3), the maximum tube length (Fig. 3A) and maximum number of branches, meshes, and junctions (data not shown) were mostly reached between 2 and 6 hours after seeding the cells. After maximum levels were reached, the cells migrated to form cell clumps for low maximum cell density ECFC lines or structures were destroyed in case of high maximum cell density ECFC lines; therefore, we used the average of the maximum value and the four adjacent values of each parameter in all analyses. Significant correlations with maximum cell density and maximum tube length ( $R^2 = 0.72$ ,  $P < 0.0001$ ; Fig. 3B), maximum number of meshes ( $R^2 = 0.60$ ,  $P < 0.001$ ; Fig. 3C) and maximum number of branches ( $R^2 = 0.75$ ,  $P < 0.0001$ ; Fig. 3D) were observed. Overall, the maximum cell density of ECFCs show a negative correlation with the angiogenic capacity.



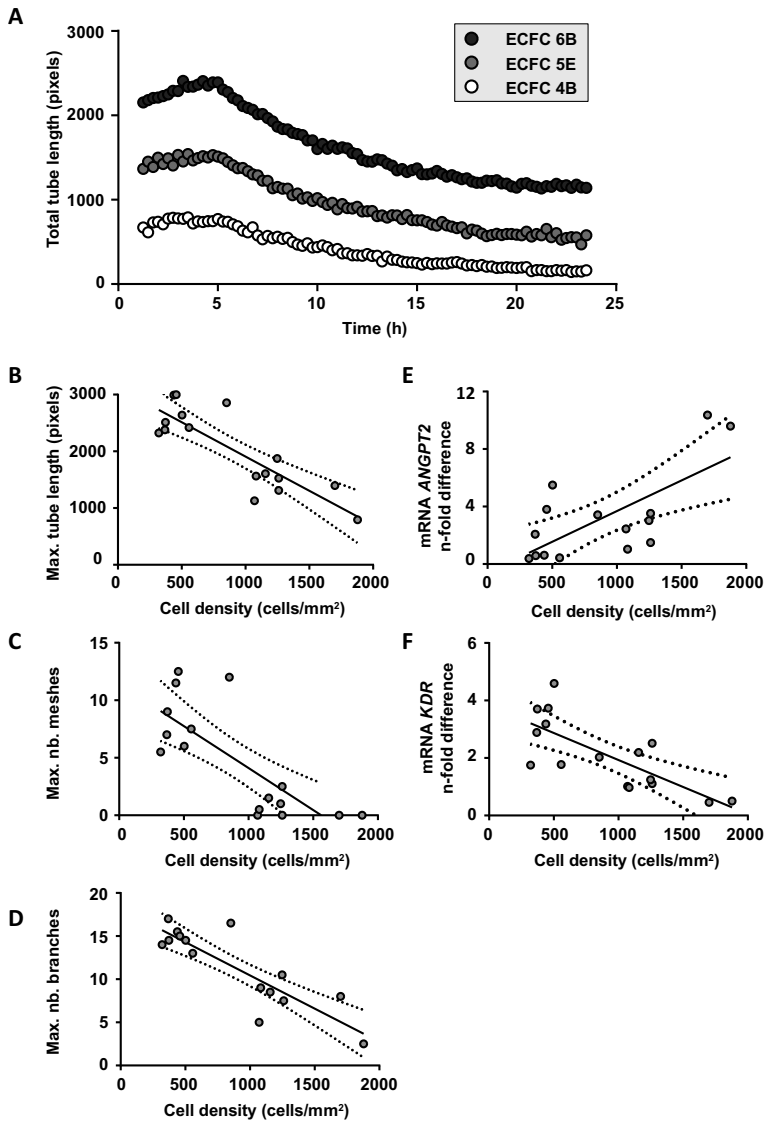


**Figure 3. Angiogenesis potential of ECFC lines and its relation to maximum cell density.** (A) The ability of ECFC lines to form tubes on Matrigel was followed for 24 hours. Plotted are the total tube length for three ECFC lines representative for low (ECFC 6B), medium (ECFC 5E), and high (ECFC 4B) maximum cell density. The maximum tube length was measured by the Angiogenesis Analyzer plugin of Fiji (ImageJ) and maximum tube length was reached between 2 and 6 hours after plating the cells. Highest tube length was observed in ECFC lines with a low maximum cell density. (B) The maximum tube length and the maximum number of (C) meshes and (D) branches that were measured in 24 hours were plotted against maximum cell density. Maximum tube length ( $R^2 = 0.72$ ,  $P < 0.0001$ ) and maximum number of meshes ( $R^2 = 0.60$ ,  $P < 0.001$ ) and branches ( $R^2 = 0.75$ ,  $P < 0.0001$ ) significantly correlated with maximum cell density. (E) Gene expression analysis of *ANGPT2* showed a significant positive correlation with maximum cell density ( $R^2 = 0.42$ ,  $P < 0.01$ ). (F) gene expression analysis of *KDR* showed a significant negative correlation with maximum cell density ( $R^2 = 0.66$ ,  $P = 0.0001$ ). (A-F) Each data point represents the average of two independent experiments. ANGPT2, Angiopoeitin-2; ECFC, endothelial colony forming cell; KDR, vascular endothelial growth factor receptor 2; VWF, von Willebrand factor

Gene expression of the angiogenic markers angiopoietin-2 (*ANGPT2*), *CD34*, *CD105* (endoglin), and VEGF receptor-2 (or kinase insert domain receptor, *KDR*) was evaluated to investigate the underlying mechanism for the observed variations. No correlation was detected between maximum cell density and *CD34* or *CD105* expression (data not shown). Interestingly, *ANGPT2* ( $R^2 = 0.42$ ,  $P < 0.01$ ; Fig. 3E) and *KDR* ( $R^2 = 0.66$ ,  $P = 0.0001$ ; Fig. 3F) expression significantly correlated with maximum cell densities, with higher levels of *ANGPT2* in cell lines with high maximum cell densities and higher levels of *KDR* in lines with lower maximum cell densities.

### **Gene expression of aging and endothelial to mesenchymal transition markers**

Gene expression analysis was performed on several pathways to better understand the mechanisms behind the variations between ECFC lines. Because passaging of cells resulted in decreased maximum cell density and lower VWF:Ag production (Fig. 2H and I), we reasoned that aging (cellular senescence) might underlie the observed variations. This was tested by gene expression analysis of SRY-Box 18 (*SOX18*) and C-X-C Motif Chemokine Ligand 8 (*CXCL8*). *SOX18* is described to be higher in early passage ECFCs, whereas *CXCL8* is higher in ECFCs close to their Hayflick limit.<sup>22</sup> *CXCL8* is also described as a modulator of senescence, and its gene expression significantly correlates with  $\beta$ -galactosidase and  $\gamma$ H2AX stainings.<sup>22</sup> We confirm the influence of aging on the variations seen in the ECFC lines by significant correlations between maximum cell density and gene expression of *CXCL8* ( $R^2 = 0.84$ ,  $P < 0.0001$ ; Fig. 4A) and *SOX18* ( $R^2 = 0.79$ ,  $P < 0.0001$ ; Fig. 4B). A lower expression of *CXCL8* and a higher expression of *SOX18* was detected in lines with a high maximum cell density. The inverse was true for lines with a low maximum cell density.

ECFC lines with a lower maximum cell density showed loss of cell-cell interactions and loss of the typical cobblestone morphology, observations that correlate with a mesenchymal-like phenotype. Transition of endothelial cells to a more mesenchymal phenotype is described as endothelial to mesenchymal transition (EndoMT). In EndoMT, gene expression of endothelial markers is reduced, whereas an induction in expression of extracellular matrix proteins becomes apparent.<sup>25,26</sup> We observed significant negative correlations between maximum cell density and mesenchymal marker  $\alpha$ -smooth muscle actin (*ACTA1*,  $R^2 = 0.81$ ,  $P < 0.0001$ ; Fig. 4C) and significant positive correlations between maximum cell density and endothelial basement membrane protein vimentin (*VIM*,  $R^2 = 0.59$ ,  $P < 0.001$ ; Fig. 4D). Collagen Type I Alpha 1 Chain (*COL1A1*; Fig. 4E) showed especially high expression levels in cell lines with a low maximum cell density (<500 cells/mm<sup>2</sup>). Increased EndoMT could be the result of increased shear stress, and although our cells are cultured under static conditions, we investigated gene expression of known shear stress markers Krüppel Like Factor 2 (*KLF2*) and Ephrin B2 (*EFNB2*) as well as *KLF2* downstream target thrombomodulin (*THBD*). Interestingly, ECFC density

significantly correlated with *KLF2* gene expression ( $R^2 = 0.79$ ,  $P < 0.0001$ ; Fig. 4F), wherein ECFC lines with smaller cells expressed higher levels of *KLF2*. The same was true when correlating ECFC density with *EFNB2* ( $R^2 = 0.86$ ,  $P < 0.0001$ ; Fig. 4G) and *THBD* ( $R^2 = 0.82$ ,  $P < 0.0001$ ; Fig. 4H).

Overall, gene expression of senescence and EndoMT markers negatively correlate with ECFC density, whereas shear stress markers positively correlate with ECFC density.

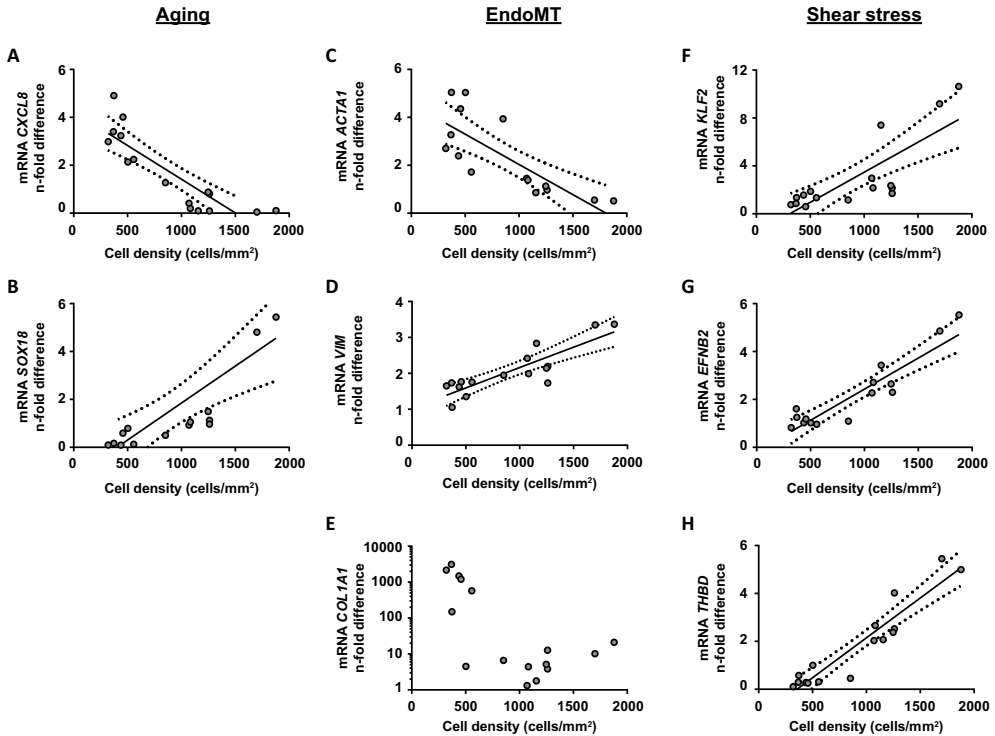


**Figure 4. ECFC gene expression analysis on genes related to aging, EndoMT and shear stress.** (A) Gene expression analysis of aging marker *CXCL8* show a negative correlation with maximum cell density ( $R^2 = 0.84$ ,  $P < 0.0001$ ). (B) Gene expression analysis of aging marker *SOX18* show a positive correlation with maximum cell density ( $R^2 = 0.79$ ,  $P < 0.0001$ ). (C) Gene expression analysis of EndoMT marker *ACTA1* show a negative correlation with maximum cell density ( $R^2 = 0.81$ ,  $P < 0.0001$ ). (D) Gene expression analysis of EndoMT marker *VIM* show a positive correlation with maximum cell density ( $R^2 = 0.59$ ,  $P < 0.001$ ). (E) Gene expression analysis of EndoMT marker *COL1A1* is strongly increased in cell lines with a low maximum cell density. (F) Gene expression analysis of shear stress marker *KLF2* shows a positive correlation with maximum cell density ( $R^2 = 0.79$ ,  $P < 0.0001$ ). (G) Gene expression analysis of shear stress marker *EFNB2* shows a positive correlation with maximum cell density ( $R^2 = 0.86$ ,  $P < 0.0001$ ). (H) Gene expression analysis of *THBD*, a downstream target of *KLF2*, shows a positive correlation with maximum cell density ( $R^2 = 0.82$ ,  $P < 0.0001$ ). (A-H) Each data point represents the average of two independent experiments. ACTA1, alpha smooth muscle actin; CXCL8, C-X-C Motif Chemokine Ligand 8; EFNB2, Ephrin B2; EndoMT, endothelial to mesenchymal transition; COL1A1, collagen Type 1 Alpha 1 Chain; KLF2, Krüppel-like Factor 2; SOX18, SRY-Box 18; THBD, Thrombomodulin; VIM, vimentin

## Discussion

ECFCs have been used in the past years to study pathophysiological effects of VWF mutations on a cellular level. Although knowledge on VWD pathophysiology has been improved by the use of ECFCs, high variations in ECFC morphology, VWF expression, and several other VWF-related parameters cannot be neglected. We have therefore studied the extent of variations in maximum cell density, VWF expression, VWF storage, and the capacity of ECFCs to form tubes on Matrigel in 16 ECFC lines derived from six healthy donors. Furthermore, we evaluated the mechanisms that could explain the variations by gene expression evaluation in the same set of ECFCs.

Although all ECFC lines used in this study were positive for endothelial markers CD31 and CD146 and negative for leukocyte markers CD14 and CD45, variations were observed in CD144 expression profile and the morphology of different ECFC lines. Especially cell density at maximum confluency was markedly different between the lines and this maximum cell density positively correlated with VWF production. Because maximum cell density correlates with VWF production (Fig. 2B-E), deviations from this line might indicate defective VWF secretion caused by, for example, retention in endoplasmic reticulum or Golgi. As a measure for cell density, we counted the cell number in bright-field images taken from the ECFCs immediately before performing the experiments. Although this is not a conventional method, this method does reflect the conditions at the moment of the experiment itself. Where cell count after trypsinization only informs on the cell count before plating the cells. However, cell count after trypsinization does correlate with cell count by ImageJ. In ECFC lines with a very low maximum cell density, we could not detect VWF by ELISA. We did not exclude these cells from most analyses because we aimed to show the characteristics of all cell lines that appear after the isolation procedure. However, it is questionable whether cells with a maximum cell density  $<500$  cells/mm<sup>2</sup> and decreased CD144 expression are true endothelial cells (even though these cells are CD14 and CD45 negative and CD31 and CD146 positive) or are a mixed population. We therefore suggest, based on the results shown in this study, not to use these cells in VWF/VWD research. However, when studying specific patients with a unique clinical phenotype, one may have to accept that the patient-derived ECFCs have a mixed phenotype. When “suboptimal” patient-derived clones with a mixed phenotype appear, it is then of utmost importance to compare these cell lines with an appropriate, and if necessary a mixed control.

The effects of passaging of ECFCs was determined in two ECFC lines and we observed a decrease in maximum cell density and VWF production every time a cell line was passaged. Furthermore, the ECFC line with the smallest cells and therefore highest maximum cell density (ECFC 4B) could reach a higher passage number than the ECFC line with the bigger cells and lower maximum cell density (ECFC 5A). The passage number indicates the number of times a cell line has been trypsinized and subcultured (Fig. S1), but is not to be confused

with the population doubling level, which is the number of times a cell has doubled since the primary isolation. Because ECFC 4B has a higher maximum cell density than ECFC 5A, the exact number of cell doublings that can be reached for ECFC 4B is even higher than the passage number indicates compared with ECFC 5A. Furthermore, passaging of cells also led to decreased maximum cell density and VWF production, which indicates that one single ECFC line can have different cellular characteristics.

An increased percentage of VWD patients compared to the normal population develop intestinal bleeding caused by angiodysplasia.<sup>27</sup> This is the result of increased angiogenesis, a process that *in vitro* can be simulated by a Matrigel tube formation assay. Although ECFCs proved to be a strong tool to study angiogenesis *ex vivo*, the exact role of VWF in angiogenesis remains unclear. Most importantly, small interfering RNA-mediated downregulation of VWF in HUVECs led to increased Matrigel tube formation.<sup>24</sup> We showed clear variations in angiogenic capacity between healthy control ECFCs with increased angiogenic capacity in lines with low VWF production compared with lines with high VWF production. It is important to acknowledge these inter-clonal variations in healthy control ECFCs, especially when drawing conclusions on patient-derived ECFCs. We showed decreased VWF production in cells with increased passage number, which might suggest that ECFCs at higher passage numbers show increased tube formation. This was however not observed by Groeneveld *et al*, where reduced tube formation was observed in late passage cells.<sup>12</sup> This indicates that other cell characteristics in aged cells are more important in *ex vivo* tube formation than VWF itself. One important remark is that ECFCs with a low maximum cell density have a bigger cell diameter upon seeding on Matrigel, compared with lines with a high maximum cell density; therefore, the distance between cells was smaller, which might affect tube formation. Different types of assays in which tube formation is followed from a monolayer of cells might give better insight in the angiogenic capacity of ECFCs.<sup>28,29</sup> But with these results, we address the presence of variations between ECFC lines on angiogenic potential. Several angiogenic markers that could explain the variations were measured by qPCR. Most important, we observed a significant correlation for maximum cell density and *KDR* with increased *KDR* expression in lines with a low maximum cell density. *KDR* is known to promote angiogenesis, which is in line with the observations seen in the studied ECFCs.

Variations between ECFC lines were observed in VWF production and tube formation on Matrigel. To understand the cause of the variations, we measured the expression of genes involved in two processes that might underlie these variations: aging and endoMT. Because cells age and increase in cell size with each passage number and ECFC lines with a high maximum cell density could reach a higher passage number, we reasoned that low maximum cell density ECFC lines are in a more senescent state than high maximum cell density ECFC lines, irrespective of the passage number or cell doubling level. Indeed, we found a significant

correlation between maximum cell density and senescence markers *CXCL8* and *SOX18*, suggesting that cell lines with a low maximum cell density are more senescent than cells with a high maximum cell density. This is an interesting observation because ECFCs with a low maximum cell density have bigger cells and therefore had less cell doublings in culture than ECFC lines with a high maximum cell density at the same passage number. A possible explanation could be that the cells from which the ECFC lines originate vary in their senescent state or that the cells have a different origin (i.e., tissue-specific or bone-marrow derived); however, more research is necessary to confirm this.<sup>30</sup> Although more markers are needed to fully define senescence, we highlight with these markers differences between cell lines.

EndoMT was studied as possible explanation for the variations because low maximum cell density lines had a more mesenchymal phenotype with loss in cell-cell contacts. We confirmed a more mesenchymal phenotype in low-density lines by gene expression analysis of mesenchymal markers *ACTA1*, *VIM*, and *COL1A1*. EndoMT could be induced by shear stress<sup>31</sup> and although all experiments are performed under static conditions, increased expression of shear stress markers *KLF2* and *EFNB2* was observed in high maximum cell density lines. This does not explain the mesenchymal phenotype observed in low maximum cell density lines, but opened up a possible different mechanism. The transcription factor *KLF2* is also described as transcriptional switch between quiescent and activated endothelial cells.<sup>32</sup> This suggests that cells from high maximum cell density lines are in a more activated state, which might explain the secreted VWF strings observed in immunofluorescent stainings of these lines. *VWF* and Thrombomodulin are both under the expression of *KLF2* and are both upregulated in high maximum cell density lines.

To conclude, we observed variations in morphology, maximum cell density, VWF:Ag production, and angiogenic capacity in ECFCs from healthy controls. And ECFC lines with a low maximum cell density are suggestive for a mixed population with a more mesenchymal cellular phenotype. The variations seem to be attributed to aging and endoMT; however, it remains unclear what exactly drives the variations in aging and endoMT. When investigating patient-derived ECFCs, these variations should always be acknowledged. Although clear variations are observed, we think that ECFCs maintain a powerful tool, especially when different conditions within one ECFC line are studied. When comparing patient-derived and control ECFCs, we suggest using cells with the same characteristics. Because there are limits to the clones that appear in patient-derived cells, it is suggested to have a large panel of healthy control ECFCs to match patient-derived ECFCs with control ECFCs. Also, it is important to take maximum cell density into account and to perform experiments 3-5 days after the cells stop expanding. We also suggest synchronization and standardization of the experiments between laboratories to fairly compare results. This is especially a necessity when sample sizes are small as they are in VWD research.

## Acknowledgements

This study was financially supported by a research grant from the Landsteiner Foundation for Blood Transfusion Research (grant 1504) and by a research grant from CSL Behring.

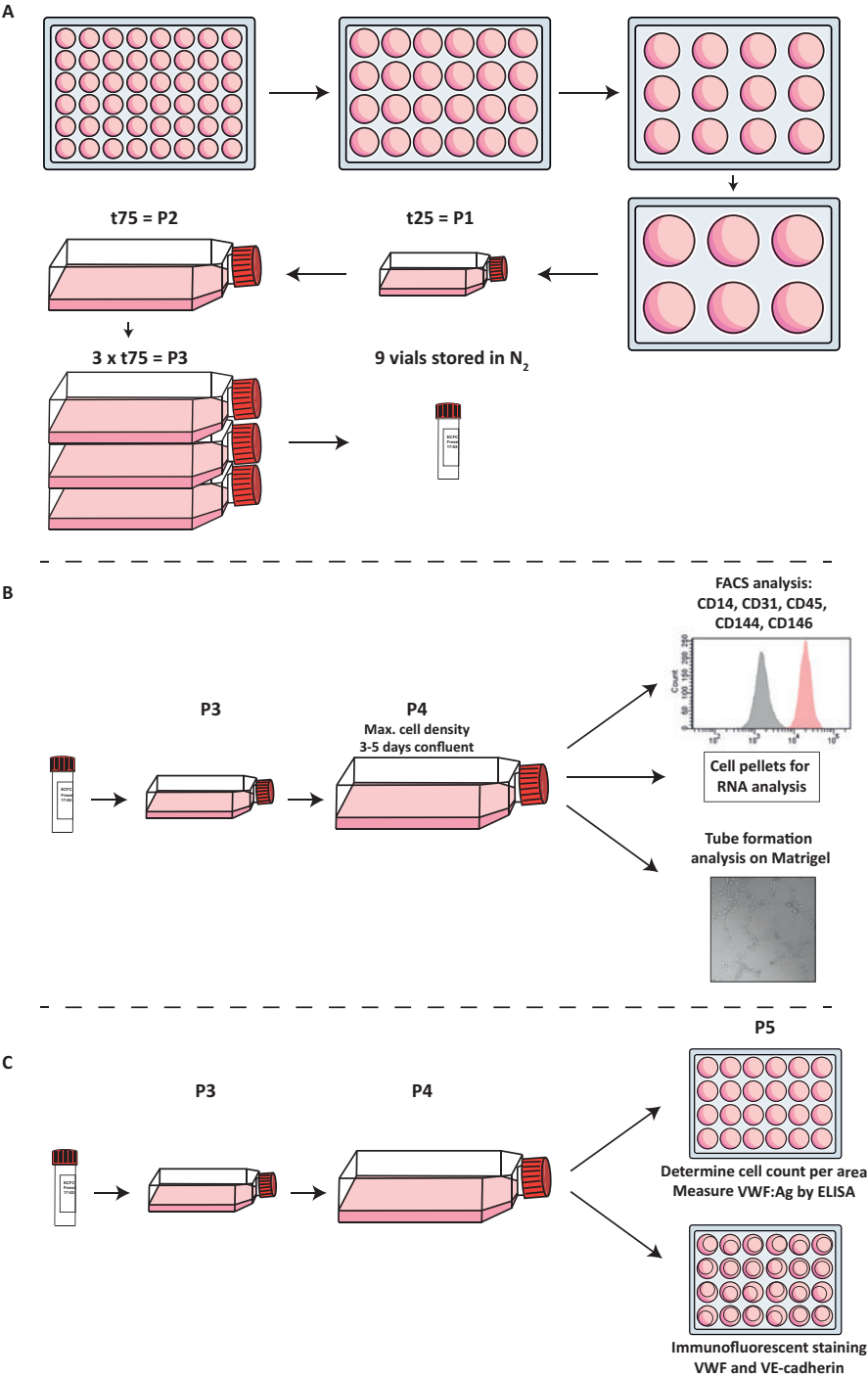
## References

1. Randi AM, Laffan MA. Von Willebrand factor and angiogenesis: basic and applied issues. *J Thromb Haemost.* 2017;**15**(1):13-20.
2. Leebeek FWG, Eikenboom JCJ. Von Willebrand's Disease. *N Engl J Med.* 2016;**375**(21):2067-2080.
3. Valentijn KM, Sadler JE, Valentijn JA, Voorberg J, Eikenboom J. Functional architecture of Weibel-Palade bodies. *Blood.* 2011;**117**(19):5033-5043.
4. McGrath RT, McRae E, Smith OP, O'Donnell JS. Platelet von Willebrand factor--structure, function and biological importance. *Br J Haematol.* 2010;**148**(6):834-843.
5. Wang JW, Groeneveld DJ, Cosemans G, et al. Biogenesis of Weibel-Palade bodies in von Willebrand's disease variants with impaired von Willebrand factor intrachain or interchain disulfide bond formation. *Haematologica.* 2012;**97**(6):859-866.
6. de Jong A, Eikenboom J. Von Willebrand disease mutation spectrum and associated mutation mechanisms. *Thromb Res.* 2017;**159**:65-75.
7. Ingram DA, Mead LE, Tanaka H, et al. Identification of a novel hierarchy of endothelial progenitor cells using human peripheral and umbilical cord blood. *Blood.* 2004;**104**(9):2752-2760.
8. Hirschi KK, Ingram DA, Yoder MC. Assessing identity, phenotype, and fate of endothelial progenitor cells. *Arterioscler Thromb Vasc Biol.* 2008;**28**(9):1584-1595.
9. Medina RJ, Barber CL, Sabatier F, et al. Endothelial Progenitors: A Consensus Statement on Nomenclature. *Stem Cells Transl Med.* 2017;**6**(5):1316-1320.
10. Starke RD, Paschalaki KE, Dyer CE, et al. Cellular and molecular basis of von Willebrand disease: studies on blood outgrowth endothelial cells. *Blood.* 2013;**121**(14):2773-2784.
11. Wang JW, Bouwens EA, Pintao MC, et al. Analysis of the storage and secretion of von Willebrand factor in blood outgrowth endothelial cells derived from patients with von Willebrand disease. *Blood.* 2013;**121**(14):2762-2772.
12. Groeneveld DJ, van Bekkum T, Dirven RJ, et al. Angiogenic characteristics of blood outgrowth endothelial cells from patients with von Willebrand disease. *J Thromb Haemost.* 2015;**13**(10):1854-1866.
13. Selvam SN, Casey LJ, Bowman ML, et al. Abnormal angiogenesis in blood outgrowth endothelial cells derived from von Willebrand disease patients. *Blood Coagul Fibrinolysis.* 2017;**28**(7):521-533.
14. Hawke L, Bowman ML, Poon MC, Scully MF, Rivard GE, James PD. Characterization of aberrant splicing of von Willebrand factor in von Willebrand disease: an underrecognized mechanism. *Blood.* 2016;**128**(4):584-593.
15. Bowman ML, Pluthero FG, Tuttle A, et al. Discrepant platelet and plasma von Willebrand factor in von Willebrand disease patients with p.Pro2808Leufs\*24. *J Thromb Haemost.* 2017;**15**(7):1403-1411.
16. Sadler JE. von Willebrand factor in its native environment. *Blood.* 2013;**121**(14):2583-2584.
17. Martin-Ramirez J, Hofman M, van den Biggelaar M, Hebbel RP, Voorberg J. Establishment of outgrowth endothelial cells from peripheral blood. *Nat Protoc.* 2012;**7**(9):1709-1715.



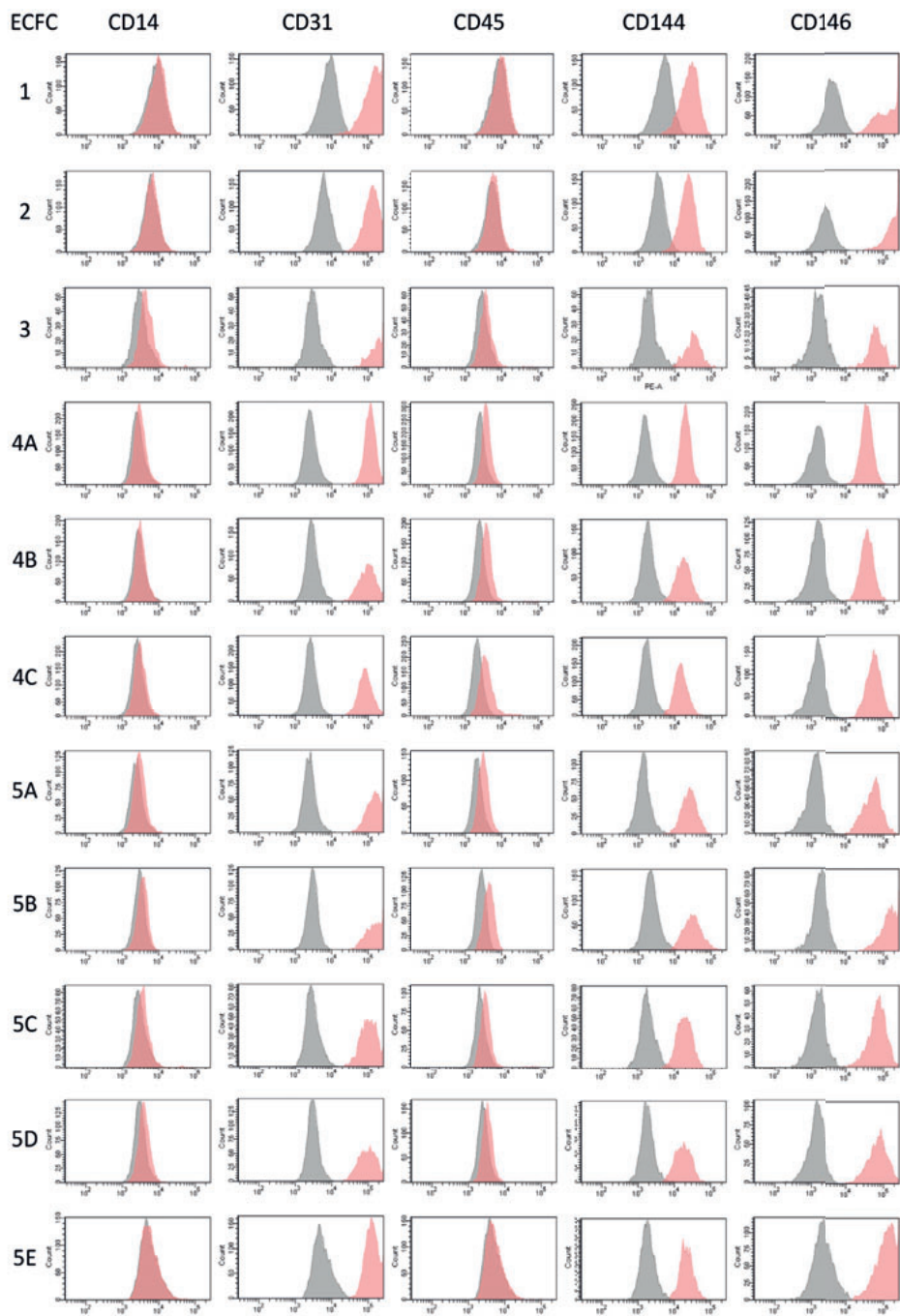
18. de Jong A, Dirven RJ, Oud JA, Tio D, van Vlijmen BJM, Eikenboom J. Correction of a dominant-negative von Willebrand factor multimerization defect by small interfering RNA-mediated allele-specific inhibition of mutant von Willebrand factor. *J Thromb Haemost.* 2018;**16**(7):1357-1368.
19. Wong ML, Medrano JF. Real-time PCR for mRNA quantitation. *Biotechniques.* 2005;**39**(1):75-85.
20. Howell GJ, Herbert SP, Smith JM, et al. Endothelial cell confluence regulates Weibel-Palade body formation. *Mol Membr Biol.* 2004;**21**(6):413-421.
21. Shahani T, Lavend'homme R, Luttun A, Saint-Remy JM, Peerlinck K, Jacquemin M. Activation of human endothelial cells from specific vascular beds induces the release of a FVIII storage pool. *Blood.* 2010;**115**(23):4902-4909.
22. Medina RJ, O'Neill CL, O'Doherty TM, et al. Ex vivo expansion of human outgrowth endothelial cells leads to IL-8-mediated replicative senescence and impaired vasoreparative function. *Stem Cells.* 2013;**31**(8):1657-1668.
23. Selvam S, James P. Angiodysplasia in von Willebrand Disease: Understanding the Clinical and Basic Science. *Semin Thromb Hemost.* 2017;**43**(6):572-580.
24. Starke RD, Ferraro F, Paschalaki KE, et al. Endothelial von Willebrand factor regulates angiogenesis. *Blood.* 2011;**117**(3):1071-1080.
25. Kalluri R, Weinberg RA. The basics of epithelial-mesenchymal transition. *J Clin Invest.* 2009;**119**(6):1420-1428.
26. Maleszewska M, Moonen JR, Huijkman N, van de Sluis B, Krenning G, Harmsen MC. IL-1beta and TGFbeta2 synergistically induce endothelial to mesenchymal transition in an NFkappaB-dependent manner. *Immunobiology.* 2013;**218**(4):443-454.
27. Castaman G, Federici AB, Tosetto A, et al. Different bleeding risk in type 2A and 2M von Willebrand disease: a 2-year prospective study in 107 patients. *J Thromb Haemost.* 2012;**10**(4):632-638.
28. Lopez JA, Zheng Y. Synthetic microvessels. *J Thromb Haemost.* 2013;**11 Suppl 1**:67-74.
29. van Duinen V, Zhu D, Ramakers C, van Zonneveld AJ, Vulto P, Hankemeier T. Perfused 3D angiogenic sprouting in a high-throughput in vitro platform. *Angiogenesis.* 2018;**22**(1):157-165.
30. Tura O, Skinner EM, Barclay GR, et al. Late outgrowth endothelial cells resemble mature endothelial cells and are not derived from bone marrow. *Stem Cells.* 2013;**31**(2):338-348.
31. Mahmoud MM, Serbanovic-Canic J, Feng S, et al. Shear stress induces endothelial-to-mesenchymal transition via the transcription factor Snail. *Sci Rep.* 2017;**7**(1):3375.
32. Dekker RJ, Boon RA, Rondaij MG, et al. KLF2 provokes a gene expression pattern that establishes functional quiescent differentiation of the endothelium. *Blood.* 2006;**107**(11):4354-4363.

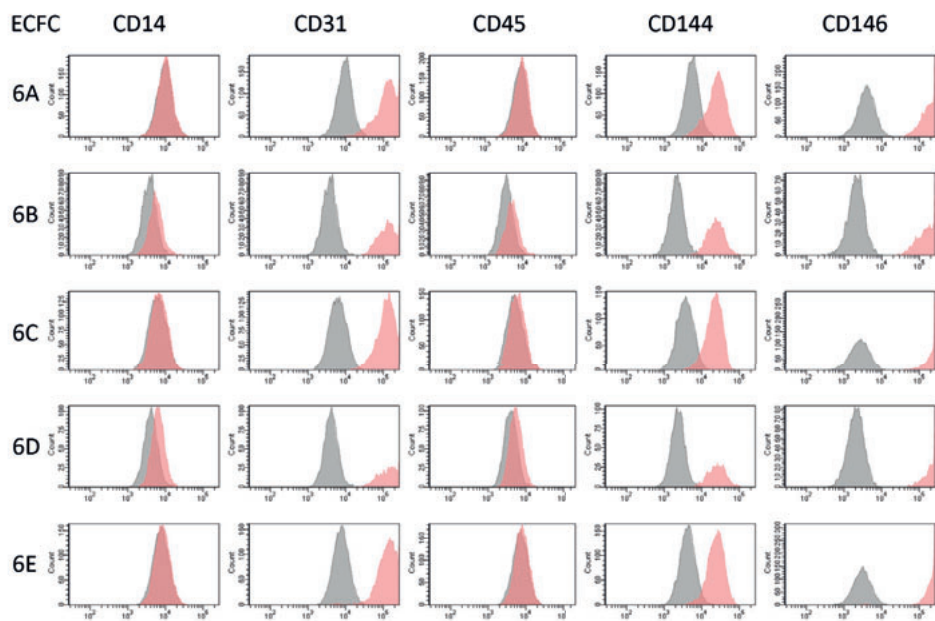
Supplemental data  
Figure S1



**Figure S1. Schematic overview of the experimental setup.** (A) peripheral blood mononuclear cells were plated in collagen coated 48 wells plates. ECFC lines appeared between days 13 and 27 after seeding. Individual lines were passaged from the 48 wells plate, to a 24 wells plate etc. Cells in a t25 culture flask were considered passage (P) 1 and cells were stored in nitrogen at P3. (B) Cells from the nitrogen storage were plated in a collagen coated t25 flask and passaged to a t75 flask. Bright-field images were taken every day and the number of cells in the images were determined by the ITCN plug-in of Fiji. Three to five days after the cells stopped expanding, cells were simultaneous subjected to FACS analysis, *in vitro* tube formation and gene expression analysis. (C) Cells from the nitrogen storage were plated in a collagen coated t25 flask and passaged to a t75 flask. From the t75 flask, cells were plated in 24 wells plates with or without coverslips. Bright-field images were taken every day from the 24 wells plates and the number of cells in the images was determined by the ITCN plug-in of Fiji. Three to five days after the cells stopped expanding, conditioned medium and protein lysates were harvested for VWF:Ag measurements and the coverslips were fixed and stained for VWF and VE-cadherin. ECFC, endothelial colony forming cell; FACS, fluorescence-activated cell sorting; VWF, von Willebrand factor

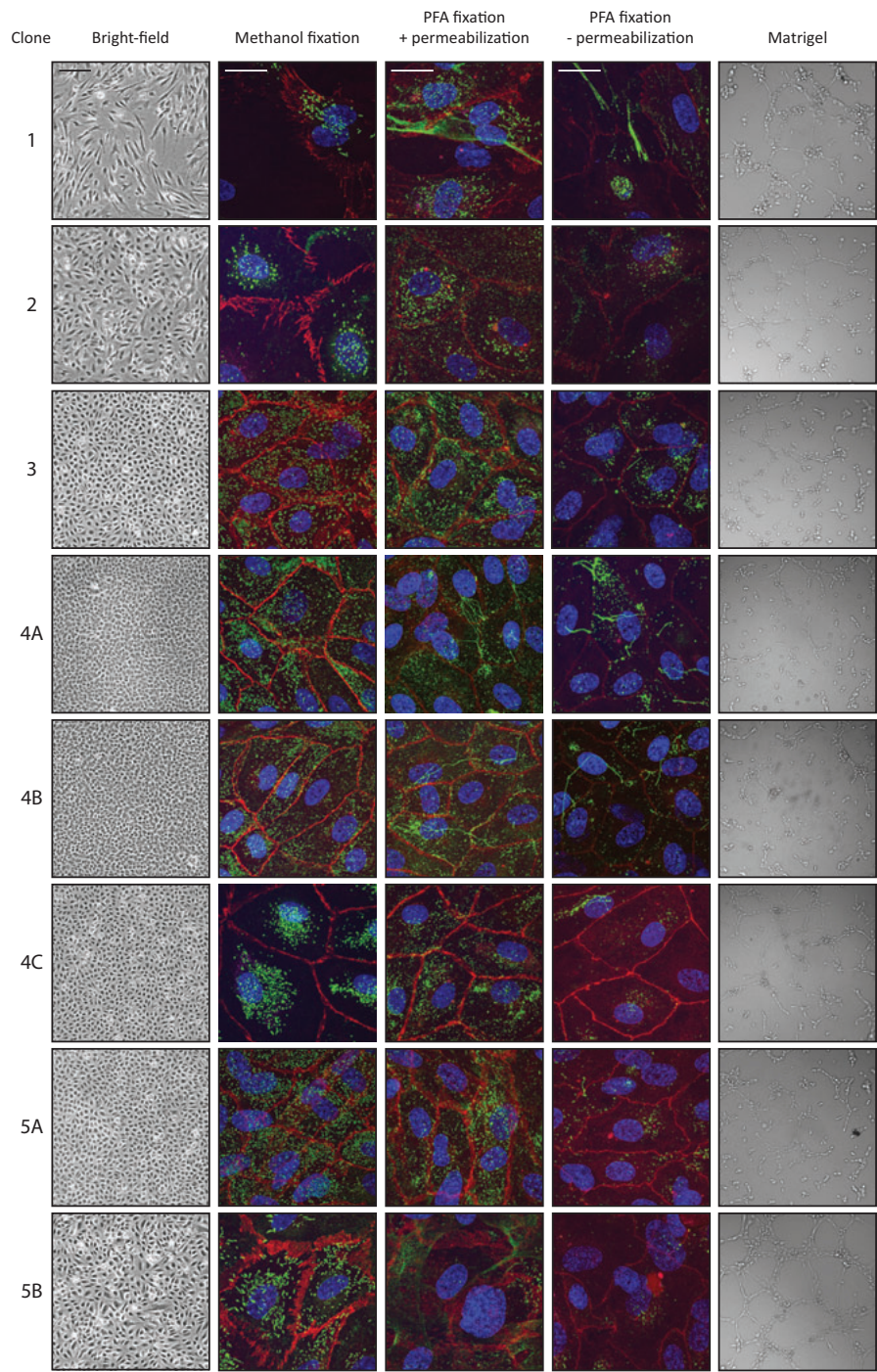
Figure S2





**Figure S2. FACS analysis histograms of CD14, CD31, CD45, CD144 and CD146.** FACS analysis for surface markers CD14, CD31, CD45, CD144 and CD146 of all 16 ECFC lines derived from six healthy donors. All ECFC lines are negative for CD14 and CD45 and positive for CD31 and CD146. Some ECFC lines have decreased positivity for CD144. ECFC, endothelial colony forming cell; FACS, fluorescence-activated cell sorting

Figure S3





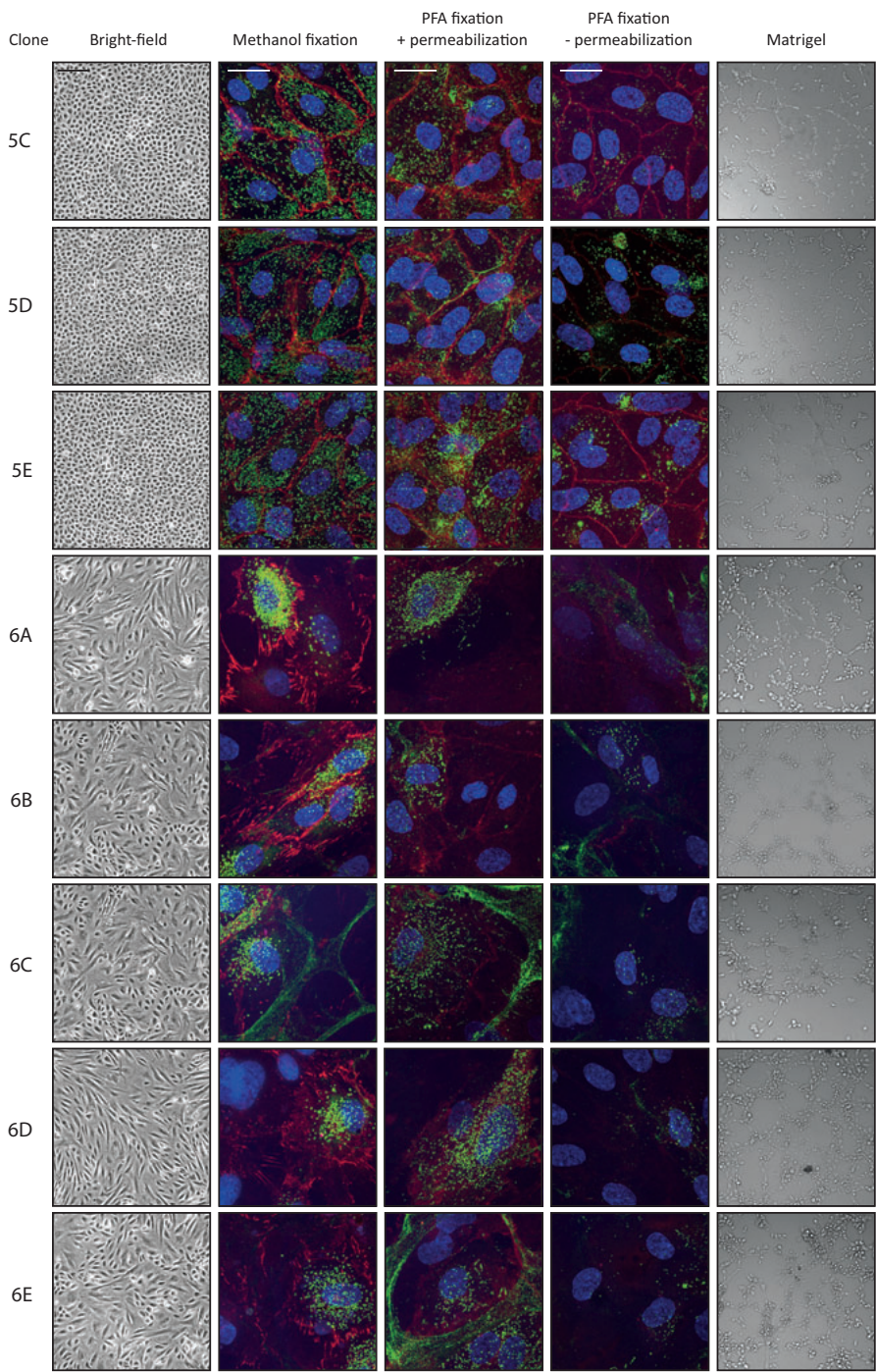


**Figure S3. Overview of bright-field, confocal and Matrigel images of all ECFC lines used in this study.** First panel: bright-field images of all ECFC lines three to five days after the cells stopped expanding. Bright-

field images show clear morphological variation between ECFC lines. Scale bar in bright-field images represent 200  $\mu\text{m}$ . Second, third and fourth panels: 2x zoom confocal images of all ECFC lines three to five days after the cells stopped expanding, stained for VWF (green) and VE-cadherin (red). Second panel shows intracellular VWF staining after methanol fixation. Third panel shows the intra- and extracellular VWF staining after PFA fixation with permeabilization. Fourth panel shows the extracellular VWF staining after PFA fixation without permeabilization. Scale bar in confocal images represent 10  $\mu\text{m}$ . Images were taken with the Leica TCS SP8 X WLL confocal microscope with a 63x/1.40 NA Plan Apo oil immersion objective. Fifth panel: Matrigel images of all ECFC lines. Images were taken with the Leica AF6000LX with a 10x magnification. ECFC, endothelial colony forming cell; PFA, paraformaldehyde; VWF, von Willebrand factor

**Figure S4**

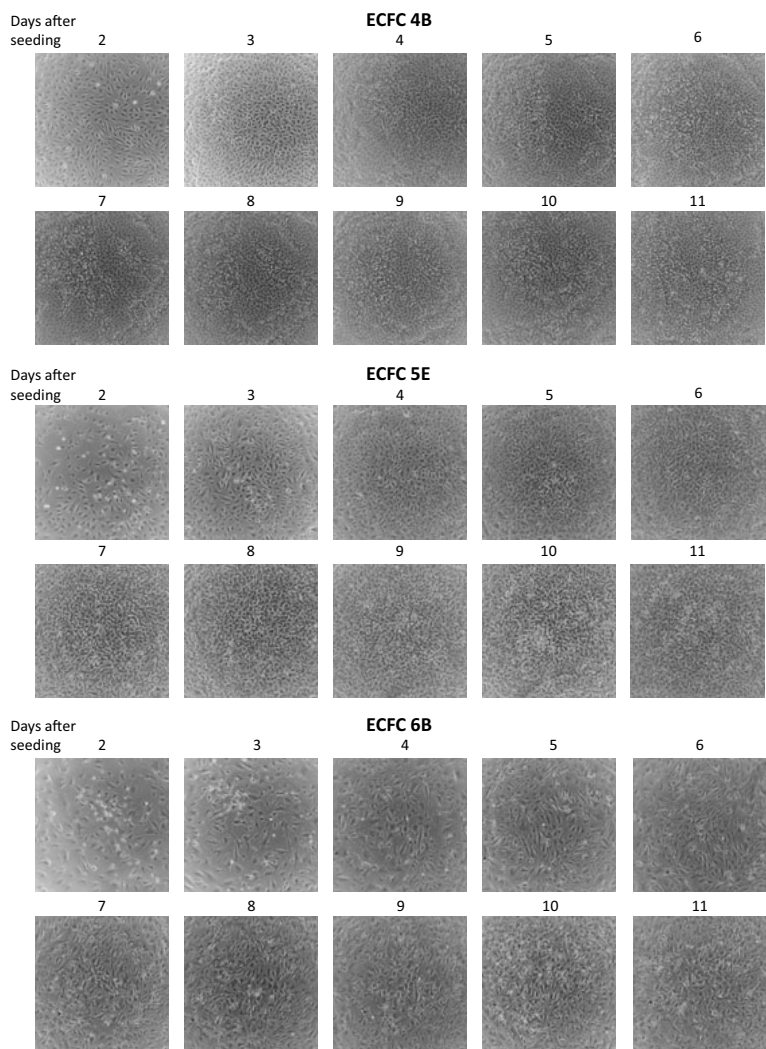


**Figure S4. Bright-field images of three representative cell lines followed for eleven days.** Bright-field images were taken from cells every day to follow the cell density and determine the optimal time-point to perform experiments. Three representative cell lines are shown, one with a very high (4B), one with an intermediate (5A) and one with a low maximum cell density (6B). ECFC, endothelial colony forming cell



**Table S1.** qPCR primer list

Primer	Sequence
GAPDH Fw	ACCATCTTCCAGGAGCGAGA
GAPDH Rv	GACTCCACGACGTACTCAGC
VWF Fw	TTGACGGGGAGGTGAATGTG
VWF Rv	ATGTCTGCTTCAGGACCACG
KDR Fw	TGGGAACCGGAACCTCACTATC
KDR Rv	GTCTTTTCCTGGGCACCTTCTATT
ANGPT2 Fw	GGGACAGCCGGCAAAATAAG
ANGPT2 Rv	AAACCACCAGCCTCCTGTTAG
CXCL8 Fw	ACCACCGGAAGGAACCATCT
CXCL8 Rv	AAAACTGCACCTTCACACAGAG
SOX18 Fw	GTGTGGGCAAAGGACGAG
SOX18 Rv	GTTTCAGCTCCTTCCACGCT
ACTA1 Fw	ACTGCCTTGGTGTGTGACAA
ACTA1 Rv	CACCATCACCCCTGATGTC
VIM Fw	GGCGAGGAGAGCAGGATTTC
VIM Rv	TGGGTATCAACCAGAGGGAGT
COL1A1 Fw	CAGCCGCTTCACCTACAGC
COL1A1 Rv	TTTGTATTCAATCACTGTCTTGCC
KLF2 Fw	CACACAGGTGAGAAGCCCTA
KLF2 Rv	ACATGTGCCGTTTCATGTGC
EFNB2 Fw	TGCTGGGGTGTTTTGATGGT
EFNB2 Rv	TCCAGGTAGAAATTTGGAGTTCG
THBD Fw	ACATCCTGGACGACGGTTTC
THBD Rv	CGCAGATGCACTCGAAGGTA

Fw, Forward; Rv, Reverse; ACTA1,  $\alpha$ -Smooth Muscle Actin; ANGPT2; angiopoietin-2; COL1A1, collagen Type 1 Alpha 1 Chain; CXCL8, C-X-C Motif Chemokine Ligand 8; EFNB2, Ephrin B2; GAPDH, Glyceraldehyde 3-phosphate dehydrogenase; KDR, Vascular endothelial growth factor receptor 2; KLF2, Krüppel-like Factor 2; SOX18, SRY-Box 18; THBD, Thrombomodulin; VIM, vimentin; VWF, von Willebrand factor





# 6

## **Defective von Willebrand factor multimerization in endothelial colony forming cells with low von Willebrand factor production**

Annika de Jong  
Richard Dirven  
Jeroen Eikenboom

*In preparation*

## Abstract

Von Willebrand factor (VWF) is a multimeric protein that is dimerized and multimerized in the endoplasmic reticulum and Golgi apparatus, respectively. After synthesis, VWF is either stored as large multimers in rod-shaped organelles, called Weibel-Palade bodies (WPBs), or VWF is constitutively released. Recent studies on cultured endothelial cells showed that constitutively released VWF is secreted faster and consists mainly of low molecular weight VWF. Furthermore, small interfering RNA (siRNA)-mediated downregulation of VWF in cultured endothelial cells resulted in shorter WPBs and increased secretion of VWF from the endothelial cells. The effects of VWF downregulation on the multimerization of VWF has never been studied and we hypothesized that downregulation of VWF not only results in shortening of the WPBs and increased VWF secretion, but also affects the VWF multimerization. This hypothesis was tested in endothelial colony forming cells (ECFCs) isolated from three healthy donors by downregulating the VWF synthesis with siRNAs against *VWF*. WPB quantification of confocal microscopy images confirmed that downregulation of VWF leads to shorter WPBs. The multimeric state of VWF was assessed in conditioned medium and protein lysates by VWF multimerization analysis and the VWF collagen binding assay. Remarkably, we observed in conditioned medium, but not in protein lysates, a decrease in high molecular weight VWF and an increase in the intensity of the VWF dimer. In addition, we confirmed increased VWF secretion from ECFCs treated with siRNA against *VWF* compared to cells treated with a negative control siRNA. Altogether, we show that VWF downregulation results in increased release of mainly low molecular weight VWF.

## Introduction

Von Willebrand factor (VWF) is a large multimeric hemostatic protein mainly produced by endothelial cells. The functionality of VWF in hemostasis is highly dependent on the multimeric size of VWF.<sup>1,2</sup> The process of VWF dimerization and multimerization is regulated in the endoplasmic reticulum and (trans)-Golgi network, respectively.<sup>3,4</sup> Large proportions of the VWF multimers are tightly packaged in the endothelial storage organelles, the Weibel-Palade bodies (WPBs).<sup>5-7</sup> Stimuli released after vascular damage, stress or inflammation enforces the WPBs to release their content.<sup>8</sup> Mediated by vascular shear, VWF multimers will unroll and form ultra-large VWF strings that attract platelets to sites of vascular damage. This process of secretion is called regulated or stimulated secretion and can be induced by amongst others thrombin or histamine that raise intracellular  $\text{Ca}^{2+}$  levels or epinephrine or vasopressin that raise intracellular cAMP levels.<sup>9</sup> Besides regulated secretion, WPBs also continuously secrete VWF without the aid of stimuli and this is known as basal secretion.<sup>10</sup> Furthermore, small proportions of VWF are not stored in WPBs, but directly secreted through the constitutive release pathway.<sup>11</sup> Although it has been known for years that constitutively released VWF mainly consists of low molecular weight (LMW) VWF<sup>12,13</sup>, it was recently described that constitutively released LMW VWF is mainly secreted at the basolateral side of the endothelial cells into the subendothelial matrix.<sup>14</sup> Basal and regulated secretion on the other hand, consists mainly of high molecular weight (HMW) VWF that is secreted at the apical side of the endothelial cells.<sup>14</sup>

Quantitative or qualitative defects in VWF leads to von Willebrand disease (VWD), the most common inherited bleeding disorder.<sup>15</sup> In the past decade, human umbilical vein endothelial cells (HUVECs) and endothelial colony forming cells (ECFCs, previously called blood outgrowth endothelial cells or BOECs) have been used to study VWD and VWF in more detail on a cellular level.<sup>16-20</sup> It was amongst others shown that siRNA-mediated downregulation of *VWF* in HUVECs led to increased secretion of VWF from the endothelial cells and a decrease in the number and length of WPBs.<sup>21,22</sup> Since downregulation of VWF led to decreased WPB size, we hypothesized that also the multimeric state of VWF is affected in VWF downregulated cells. In this study, we test this hypothesis in ECFCs isolated from three different healthy controls by downregulation of the VWF synthesis using siRNAs.

## Methods

### ***ECFC isolation***

ECFCs were isolated from three healthy donors as described before.<sup>23</sup> Peripheral blood was drawn in lithium heparin tubes (ECFCs C1 and C2; BD Biosciences, Erebodegem, Belgium) or in sodium heparin CPT™ Mononuclear Cell Preparation Tubes (C3; BD Biosciences). Blood was diluted 1:1 in phosphate buffered saline (PBS) and layered over Ficoll Paque (LUMC Pharmacy, Leiden, the Netherlands), followed by centrifugation. The mononuclear cell fraction was washed twice in PBS supplemented with 10% fetal bovine serum (FBS) after which cells were taken up in Lonza (ECFC C3) or PromoCell (ECFCs C1 and C2) endothelial culture medium. Lonza endothelial culture medium consisted of 500 ml EBM™-2 medium (Lonza, Breda, the Netherlands) supplemented with the EGM™-2 BulletKit™ (Lonza), 100 ml FBS (GIBCO®, Invitrogen, Carlsbad, CA, USA) and 7 ml Antibiotic Antimycotic solution (Sigma-Aldrich #A5955, st. Louis, MO, USA). PromoCell endothelial culture medium consisted of 500 ml Endothelial Cell Growth Medium 2 (PromoCell C-22111, Heidelberg, Germany), 50 ml FBS (GIBCO®) and 5 ml Antibiotic Antimycotic solution (Sigma-Aldrich). Mononuclear cells were plated in 48 wells plates (Nunc Cell-Culture Treated Multidishes (Nunclon, Roskilde, Denmark) or Sarstedt TS plates (Nümbrecht, Germany)) pre-coated with 50 µg/ml rat tail collagen type I (BD Biosciences). Medium was refreshed every other day until day 21. Passaging and usage of cells is performed as earlier described<sup>23</sup>, but with PromoCell culture medium.

The study was approved by the institutional ethical review board (study registered as NL54591.058.15). Informed consent was obtained from all healthy controls in accordance with the declaration of Helsinki.

### ***siRNA transfection***

For transfections, 100,000-125,000 cells per well were plated on rat tail collagen (50 µg/ml; BD biosciences) coated wells of a 24 wells plate. 24 hours after plating the cells, a negative control siRNA (siNEG, 4404020, Life Technologies Europe BV) or an siRNA against *VWF* (siVWF, s14834, Life Technologies Europe BV, Bleiswijk, the Netherlands) were transfected into ECFCs using DharmaFECT duo transfection reagent (Dharmacon, Lafayette, Colorado, USA). Before transfection, cells were washed twice with Hanks' Balanced Salt solution (Thermo Fisher Scientific, Carlsbad, CA, USA) and once with PromoCell EGM2 culture medium (without extra FBS). siRNAs and DharmaFECT duo were separately diluted in Optimem1 (Thermo Fisher Scientific) and mixed together by pipetting. After 20 minutes of incubation, the siRNA-DharmaFECT mixture was complemented with Optimem1 supplemented with 4% FBS. Cells were incubated with 150 µl transfection mixture containing a high concentration of siRNA for three hours. After the three hour incubation, 250 µl culture medium was added to obtain a final siRNA concentration of 20 nM. Medium was refreshed 24 hours after transfection and

every other day thereafter. Six days after transfection, the medium was harvested and cells were lysed with protein lysis buffer containing Optimem1, 0.1% triton X-100 (Sigma-Aldrich) and a tablet of cOmplete protease inhibitor cocktail with EDTA (Roche Diagnostics, Mannheim, Germany).

### **VWF analysis**

VWF antigen (VWF:Ag) and VWF collagen binding (VWF:CB) were simultaneously measured by ELISA in conditioned medium and protein lysate samples. The VWF:Ag ELISA was performed as described before<sup>24</sup>, with the only modification that samples were diluted in dilution buffer (PBS containing 1% bovine serum albumin). For VWF:CB analysis, ELISA plates were coated with 0.3% bovine collagen type I (95%) and III (5%) (StemCell technologies, Cologne, Germany) in PBS. Samples were diluted in dilution buffer and incubated for 2 hours. To increase the signal of the ELISA, biotin (Sigma-Aldrich) was conjugated to rabbit anti-VWF-IgG (A0082; DAKO, Glostrup, Denmark) to generate rabbit anti-VWF-IgG-biotin. ELISA plates were incubated with rabbit anti-VWF-IgG-biotin diluted in dilution buffer for one hour. Thereafter, ELISA plates were incubated with Streptavidin-(POLY) horseradish peroxidase (Thermo Fisher Scientific) diluted in dilution buffer for one hour. O-phenylenediamine dihydrochloride (Sigma-Aldrich) was used as substrate and dissolved in 11 ml substrate buffer (22 mM citric acid, 51 mM phosphate, pH 5.0) with addition of 11  $\mu$ l 30% H<sub>2</sub>O<sub>2</sub>. The enzymatic reaction was terminated using 2M H<sub>2</sub>SO<sub>4</sub>. Normal pooled plasma was used as reference.

VWF multimers were analyzed under non-reducing conditions by agarose gel electrophoresis and subsequent western blotting as described before.<sup>24</sup> ECL Western Blotting Substrate (Promega, Madison, WI, USA) was used to detect the VWF multimers. Densitometry images were generated by ImageJ (ImageJ 1.51h, Bethesda, MD, USA).<sup>24</sup> Equal concentrations of VWF:Ag were loaded in each lane of a gel.

### **Immunofluorescent analysis and WPB quantification**

ECFCs were plated on rat tail collagen coated coverslips and transfected as described above. Six days after transfection, cells were fixed using ice-cold methanol for 10 minutes and stained for VWF, VE-cadherin and nuclei as described before.<sup>23</sup> Per cell line, 10 to 13 images were randomly taken (focused on nuclei staining) using the Leica TCS SP8 X WLL converted confocal microscope with an HC PL APO CS2 63x/1.40 OIL immersion objective. The number of cells and number and size of WPBs were quantified using CellProfiler software (v.8.1.3).<sup>25</sup> Using a self-created pipeline, channels (VWF, VE-cadherin and nuclei) were split and converted into black and white images. First, the number of cells were determined by Hoechst positive objects. Then, the interior of a cell was determined by the area that was

surrounded by VE-cadherin positive staining. Lastly, the number and length of the WPBs were determined per cell by analysis of VWF positive objects. WPBs were only analyzed for cells that were completely visible.

### **Statistical analysis**

Graphical images and statistical analyses were performed using GraphPad Prism 8 (GraphPad Software, La Jolla, CA, USA). The Mann-Whitney *U* test was used to assess significance between siNEG and siVWF treated cells. For all analyses, a  $P < 0.05$  was considered significant.

## **Results and discussion**

Previous findings showed that downregulation of the production of VWF in HUVECs by siRNA nucleofection leads to decreased WPB length.<sup>21,22</sup> To investigate whether downregulation of VWF by liposomal siRNA transfection also leads to decreased WPB length in ECFCs, we transfected three proliferative healthy control ECFC lines with either siNEG or siVWF. Transfected cell lines were stained for VWF and VE-cadherin, after which the number and length of WPBs per image were quantified (Fig. 1A). Quantification of the length and number of WPBs confirmed that downregulation of VWF results in a decreased size of WPBs as well as a decreased number of WPBs per cell (Fig. 1B and 1C). For all three cell lines, the median number of WPBs per cell in siNEG treated cells was comparable and around 280 (Fig. 1B). The median length of a WPB in siNEG treated cells slightly varied per cell line from 1.33  $\mu\text{m}$  for C2, to 1.44  $\mu\text{m}$  for C3 (Fig. 1C). WPB length ranged in all cell lines from 0.6 - 5  $\mu\text{m}$  (data not shown), which is in line with previous findings.<sup>6,7,21,22</sup> Here, the images for quantification are generated by a maximum projection of the z-stacks of a frame. However, since most WPBs do not perfectly align with the plain, it is likely that we underestimate the actual length of the WPBs, especially for the larger WPBs. The actual difference in WPB length between siNEG and siVWF could therefore be bigger than is indicated in the graphs (Fig. 1C). The effects of siVWF on the length and number of WPBs depended on the efficiency of siVWF to inhibit VWF, and this varied between the three cell lines (Table 1). E.g. downregulation of VWF in C2 was less efficient, which translated in the less reduction in WPB length. Furthermore, not all areas on the coverslips showed the same degree of VWF downregulation. In some images of siVWF treated cells, cells with normal WPBs were observed, which suggests that the siRNA has not been internalized in these cells. When these cells divide, larger areas with untransfected cells are visible. Fig. S1 shows all images that were taken from the cells. Indeed, some images taken from siVWF treated cells show normal WPBs. This is also clearly indicated in the bar graphs where the median length of WPBs per image was unchanged for some areas (Fig. 1C, especially ECFC C3).



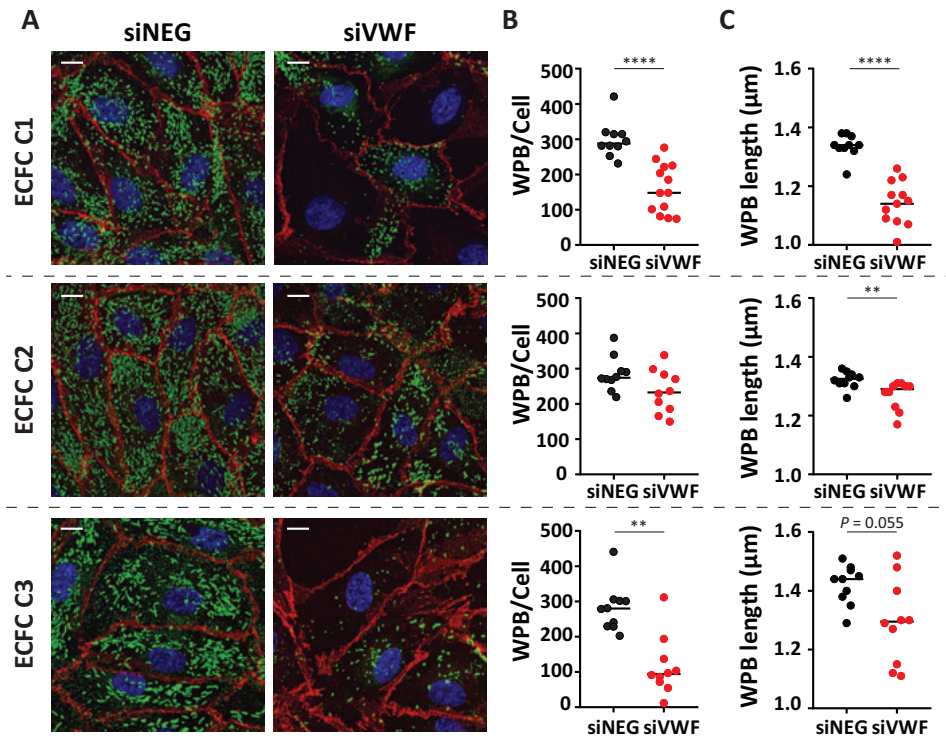


**Figure 1. Quantification of number and length of WPBs in three healthy control ECFCs.** (A) Confocal images of ECFC C1, C2, and C3 treated with siNEG or siVWF. Cells were stained for VWF (green), VE-cadherin (red) and nuclei (blue). Scale bar represents 10  $\mu$ m (B) Quantification of the number of WPBs per cell. Downregulation of VWF by siVWF resulted in a decreased number of WPBs per cell for ECFC C1 and C3. Mann-Whitney, \*\*  $P < 0.01$ , \*\*\*\*  $P < 0.0001$  (C) Quantification of the WPB length. Downregulation of VWF resulted in a significant decrease in the length of WPBs for ECFCs C1 and C2. A trend towards a significant decrease in WPB length was observed for ECFC C3. Mann-Whitney, \*\*  $P < 0.01$ , \*\*\*\*  $P < 0.0001$ . For all bar graphs: each dot represents the median number of WPBs or the median WPB length per image. ECFC, endothelial colony forming cells; siNEG, negative control siRNA; siVWF, siRNA against VWF; VWF, von Willebrand factor; WPB, Weibel-Palade body

**Table 1.** VWF:Ag concentration measured in conditioned medium or protein lysates of ECFCs treated with either siNEG or siVWF

VWF:Ag (mU)	Conditioned medium			Protein lysates		
	ECFC C1	ECFC C2	ECFC C3	ECFC C1	ECFC C2	ECFC C3
siNEG	15.4 $\pm$ 1.9	12.3 $\pm$ 3.2	6.2 $\pm$ 1.5	44.6 $\pm$ 11.0	38.9 $\pm$ 10.5	27.5 $\pm$ 9.2
siVWF	1.9 $\pm$ 0.3	2.8 $\pm$ 0.6	1.4 $\pm$ 0.2	3.8 $\pm$ 0.7	7.6 $\pm$ 1.1	3.1 $\pm$ 0.6
% VWF downregulation	89%	77%	78%	92%	81%	89%

ECFC, endothelial colony forming cells; mU, milli-units; siNEG, negative control siRNA; siVWF, siRNA against VWF; VWF, von Willebrand factor; VWF:Ag, VWF antigen

Since mainly HMW VWF is stored in the WPBs<sup>14</sup>, we questioned whether downregulation of VWF not only affects the length of the WPBs, but also the multimeric state of VWF. The multimeric state of VWF was first assessed by the VWF:CB assay. The VWF:CB assay is able to detect multimerization defects, since HMW VWF binds collagen more efficiently than LMW VWF.<sup>26</sup> Conditioned medium and protein lysate samples were simultaneously subjected to VWF:Ag and VWF:CB ELISAs. Interestingly, we observed a significant decrease in VWF:CB/VWF:Ag in conditioned medium samples of cell lines transfected with siVWF compared to siNEG treated cells ( $P < 0.001$ , Fig. 2Ai). On the other hand, the VWF:CB/VWF:Ag in protein lysates was unaltered in siVWF treated ECFCs (Fig. 2Bi). To confirm that the multimeric state of VWF is indeed altered in siVWF treated cells and to assess the exact VWF multimerization pattern, we performed a VWF multimerization assay on all three cell lines transfected with either siNEG or siVWF. In conditioned medium samples of ECFCs treated with siVWF, we clearly observed an increase in intensity of the dimer band and decrease of HMW VWF (Fig. 2Aii). In the protein lysates, the difference between siNEG and siVWF treated cells is less apparent (Fig. 2Bii). However, also in protein lysates a slight decrease in HMW VWF, but also a slight decrease in the intensity of the dimer band, seems notable in siVWF treated cells (Fig. 2Bii). Furthermore, as was observed previously<sup>22</sup>, we noted an increase in the percentage of secreted VWF in siVWF treated cells compared to siNEG treated cells in 24 hours ( $P < 0.05$ , Fig. 2C). This suggests that VWF is secreted faster in cells with low VWF production.

Altogether, we show that VWF downregulation results in a decrease in the number and length of the WPBs and increased secretion of mainly LMW VWF. Since mainly LMW VWF is secreted through the constitutive release pathway, and secretion of VWF through this pathway is faster than secretion through basal release, it is possible that relatively more VWF is secreted through the constitutive release pathway in siVWF treated cells. In our experimental set-up, we could not discriminate between constitutively and basal released VWF. Studies in which the distribution of VWF secretion is determined, by for example Transwell membranes, are needed to confirm this hypothesis.

Whether the effects of VWF downregulation on the multimerization of VWF can be translated to the human body are unknown. To our knowledge, only a small percentage of patients are known to develop VWD because of reduced VWF production. These patients have either one null allele or mutations in the promotor region of *VWF*.<sup>27</sup> These patients, however, do not show affected plasma multimers. Furthermore, our group recently published on the use of allele-specific siRNAs as a therapeutic approach to correct dominant negative VWD. With these studies we aim to inhibit the production of the mutant *VWF* allele only, and thereby correct for VWD phenotypes. This approach would ultimately lead to a VWF production of 50% compared to normal, similar to VWD patients with one null allele. Although these patients do not show affected multimerization, awareness of this *ex vivo* data is critical when studying the effects of allele-specific siRNAs in preclinical VWD models.

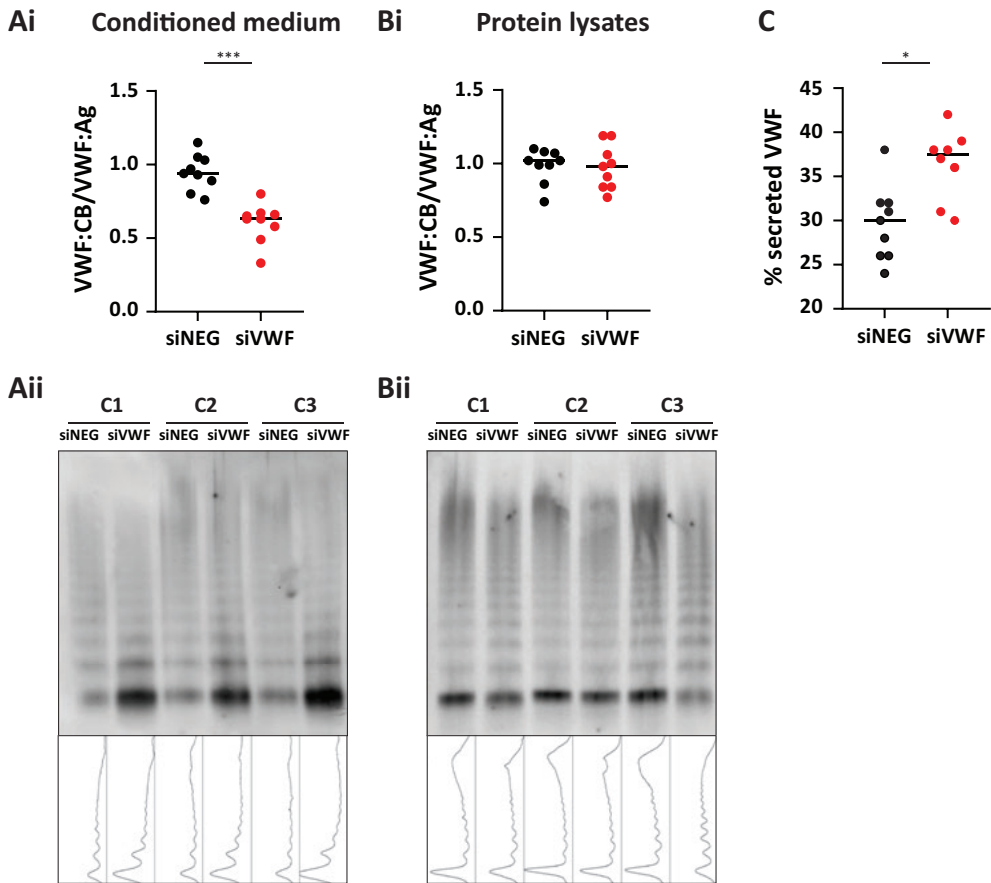


**Figure 2. Effects of VWF downregulation on the multimerization and secretion of VWF.** (Ai) Downregulation of VWF production results in a significant decrease in VWF:CB/VWF:Ag in conditioned medium compared to siNEG treated cells. (Aii) VWF multimerization analysis of conditioned medium samples obtained from ECFC C1, C2, and C3 treated with siNEG or siVWF. Downregulation of VWF production by siVWF resulted in a decrease of high molecular weight VWF and an increase in the intensity of the dimer band. (Bi) Downregulation of VWF production did not alter the VWF:CB/VWF:Ag in protein lysates. (Bii) VWF multimerization analysis of protein lysate samples obtained from ECFC C1, C2, and C3 treated with siNEG or siVWF. A small decrease of high molecular weight VWF seem apparent in siVWF treated cell lines. Also a slight decrease in the intensity of the dimer band is observed. (C) Downregulation of VWF production by siVWF leads to an increase in VWF secretion in 24 hours. (A-C) Graphs show the combined data of VWF:CB and VWF:Ag measurements of ECFC C1, C2, and C3. Transfection experiments were performed three times in duplicate. Every dot represents the average of the duplicate experiment. Mann-Whitney, \*  $P < 0.05$ , \*\*\*  $P < 0.001$ . ECFC, endothelial colony forming cell; siNEG, negative control siRNA; siVWF, siRNA against VWF; VWF, von Willebrand factor; VWF:CB, VWF collagen binding; VWF:Ag, VWF antigen

## References

1. Sporn LA, Marder VJ, Wagner DD. von Willebrand factor released from Weibel-Palade bodies binds more avidly to extracellular matrix than that secreted constitutively. *Blood*. 1987;**69**(5):1531-1534.
2. Federici AB, Bader R, Pagani S, Colibretti ML, De Marco L, Mannucci PM. Binding of von Willebrand factor to glycoproteins Ib and IIb/IIIa complex: affinity is related to multimeric size. *Br J Haematol*. 1989;**73**(1):93-99.
3. Wagner DD, Marder VJ. Biosynthesis of von Willebrand protein by human endothelial cells: processing steps and their intracellular localization. *J Cell Biol*. 1984;**99**(6):2123-2130.
4. Zhou YF, Eng ET, Nishida N, Lu C, Walz T, Springer TA. A pH-regulated dimeric bouquet in the structure of von Willebrand factor. *EMBO J*. 2011;**30**(19):4098-4111.
5. Valentijn KM, Eikenboom J. Weibel-Palade bodies: a window to von Willebrand disease. *J Thromb Haemost*. 2013;**11**(4):581-592.
6. Mourik MJ, Faas FG, Zimmermann H, Voorberg J, Koster AJ, Eikenboom J. Content delivery to newly forming Weibel-Palade bodies is facilitated by multiple connections with the Golgi apparatus. *Blood*. 2015;**125**(22):3509-3516.
7. Weibel ER, Palade GE. New cytoplasmic components in arterial endothelia. *J Cell Biol*. 1964;**23**:101-112.
8. Schillemans M, Karampini E, Kat M, Bierings R. Exocytosis of Weibel-Palade bodies: how to unpack a vascular emergency kit. *J Thromb Haemost*. 2019;**17**(1):6-18.
9. Rondaij MG, Bierings R, Kragt A, van Mourik JA, Voorberg J. Dynamics and plasticity of Weibel-Palade bodies in endothelial cells. *Arterioscler Thromb Vasc Biol*. 2006;**26**(5):1002-1007.
10. Giblin JP, Hewlett LJ, Hannah MJ. Basal secretion of von Willebrand factor from human endothelial cells. *Blood*. 2008;**112**(4):957-964.
11. Sporn LA, Marder VJ, Wagner DD. Differing polarity of the constitutive and regulated secretory pathways for von Willebrand factor in endothelial cells. *J Cell Biol*. 1989;**108**(4):1283-1289.
12. Sporn LA, Marder VJ, Wagner DD. Inducible secretion of large, biologically potent von Willebrand factor multimers. *Cell*. 1986;**46**(2):185-190.
13. Tsai HM, Nagel RL, Hatcher VB, Seaton AC, Sussman, II. The high molecular weight form of endothelial cell von Willebrand factor is released by the regulated pathway. *Br J Haematol*. 1991;**79**(2):239-245.
14. Lopes da Silva M, Cutler DF. von Willebrand factor multimerization and the polarity of secretory pathways in endothelial cells. *Blood*. 2016;**128**(2):277-285.
15. Leebeek FW, Eikenboom JC. Von Willebrand's Disease. *N Engl J Med*. 2016;**375**(21):2067-2080.
16. Wang JW, Bouwens EA, Pintao MC, et al. Analysis of the storage and secretion of von Willebrand factor in blood outgrowth endothelial cells derived from patients with von Willebrand disease. *Blood*. 2013;**121**(14):2762-2772.
17. Groeneveld DJ, van Bekkum T, Dirven RJ, et al. Angiogenic characteristics of blood outgrowth endothelial cells from patients with von Willebrand disease. *J Thromb Haemost*. 2015;**13**(10):1854-

- 1866.
18. Selvam SN, Casey LJ, Bowman ML, et al. Abnormal angiogenesis in blood outgrowth endothelial cells derived from von Willebrand disease patients. *Blood Coagul Fibrinolysis*. 2017;**28**(7):521-533.
  19. Starke RD, Ferraro F, Paschalaki KE, et al. Endothelial von Willebrand factor regulates angiogenesis. *Blood*. 2011;**117**(3):1071-1080.
  20. Starke RD, Paschalaki KE, Dyer CE, et al. Cellular and molecular basis of von Willebrand disease: studies on blood outgrowth endothelial cells. *Blood*. 2013;**121**(14):2773-2784.
  21. Ferraro F, Mafalda Lopes da S, Grimes W, et al. Weibel-Palade body size modulates the adhesive activity of its von Willebrand Factor cargo in cultured endothelial cells. *Sci Rep*. 2016;**6**(1):32473.
  22. Ferraro F, Kriston-Vizi J, Metcalf DJ, et al. A two-tier Golgi-based control of organelle size underpins the functional plasticity of endothelial cells. *Dev Cell*. 2014;**29**(3):292-304.
  23. de Jong A, Weijers E, Dirven R, de Boer S, Streur J, Eikenboom J. Variability of von Willebrand factor-related parameters in endothelial colony forming cells. *J Thromb Haemost*. 2019;**17**(9):1544-1554.
  24. de Jong A, Dirven RJ, Oud JA, Tio D, van Vlijmen BJM, Eikenboom J. Correction of a dominant-negative von Willebrand factor multimerization defect by small interfering RNA-mediated allele-specific inhibition of mutant von Willebrand factor. *J Thromb Haemost*. 2018;**16**(7):1357-1368.
  25. McQuin C, Goodman A, Chernyshev V, et al. CellProfiler 3.0: Next-generation image processing for biology. *PLOS Biology*. 2018;**16**(7):e2005970.
  26. Flood VH, Gill JC, Friedman KD, et al. Collagen Binding Provides a Sensitive Screen for Variant von Willebrand Disease. *Clinical Chemistry*. 2013;**59**(4):684-691.
  27. de Jong A, Eikenboom J. Von Willebrand disease mutation spectrum and associated mutation mechanisms. *Thromb Res*. 2017;**159**:65-75.

Supplemental Figure

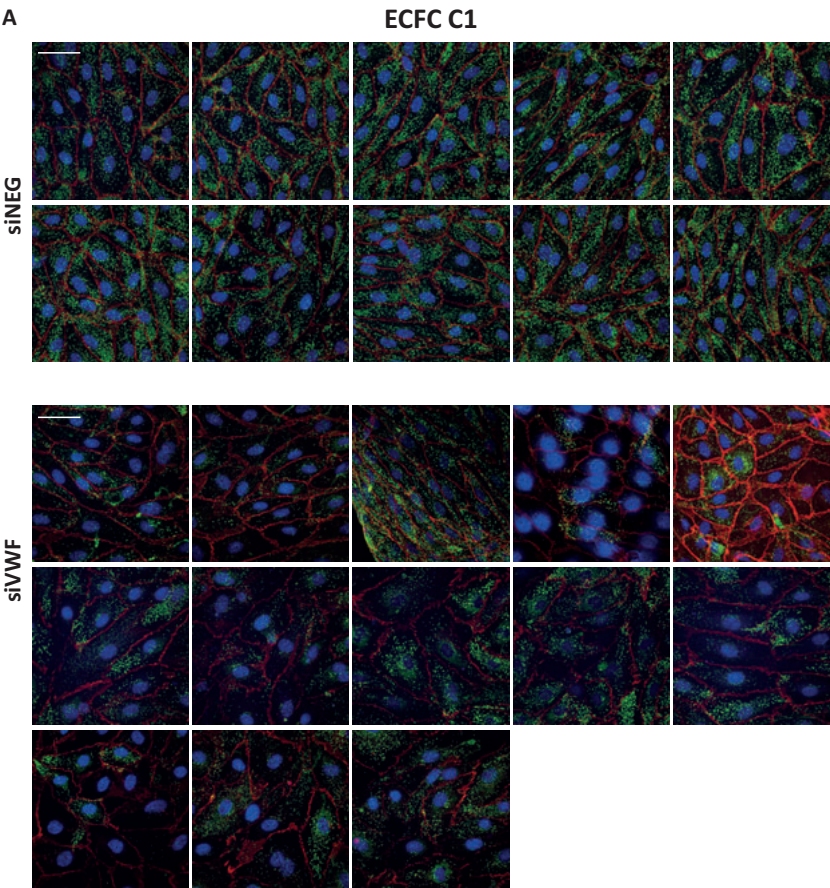
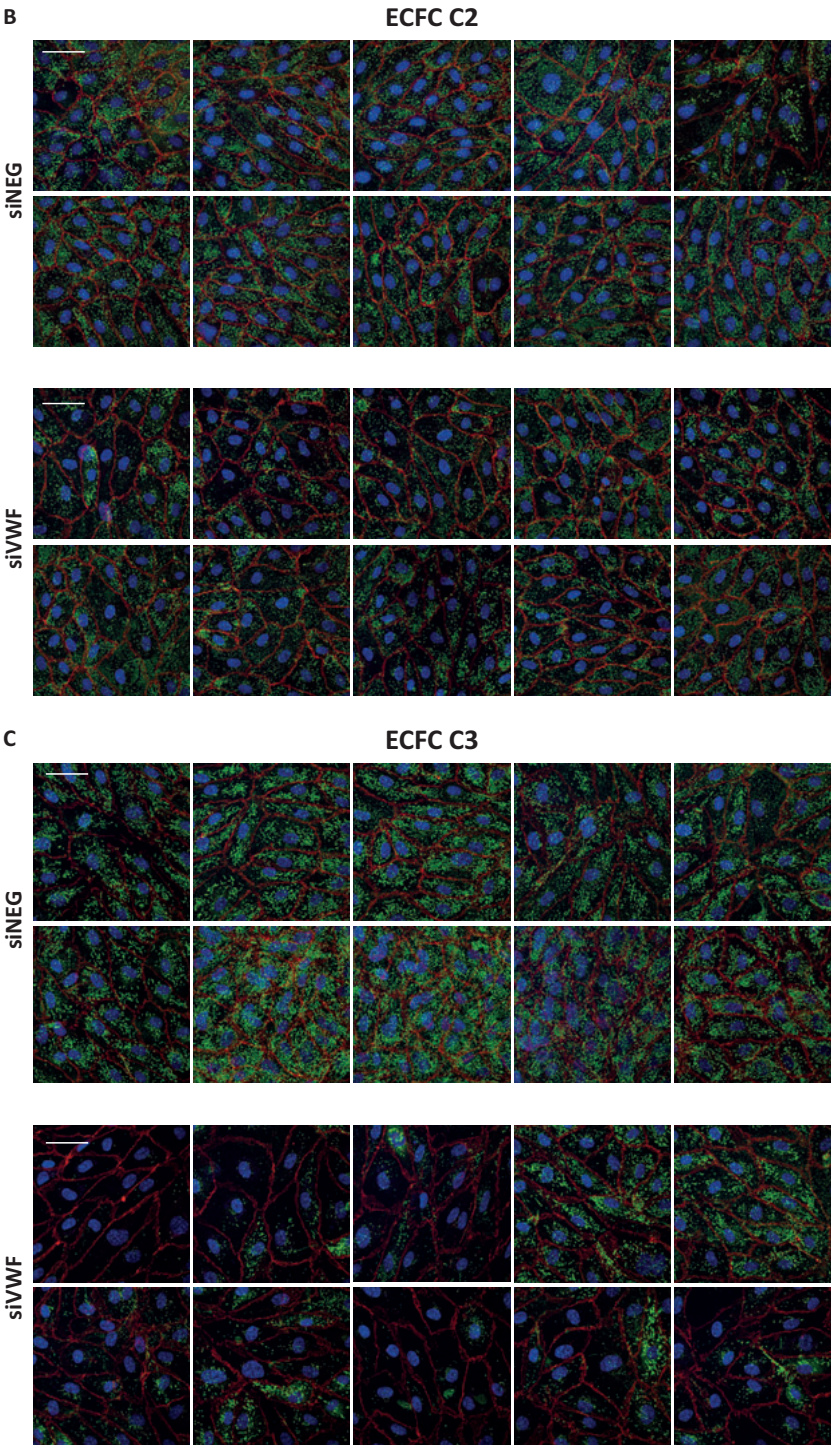


**Figure S1. Effects of VWF downregulation on WPB formation. Confocal images of ECFC C1 (A), C2 (B), and C3 (C) treated with siNEG or siVWF.** ECFCs were stained for VWF (green) and VE-cadherin (red). Per condition, 10-13 images were taken. Scale bar represents 50  $\mu$ m. ECFC, endothelial colony forming cell; siNEG, negative control siRNA; siVWF, siRNA against *VWF*; VWF, von Willebrand factor









# 7

## ***Ex vivo* improvement of a von Willebrand disease type 2A phenotype using an allele-specific small interfering RNA**

Annika de Jong  
Richard Dirven  
Johan Boender  
Ferdows Atiq  
Seyed Yahya Anvar  
Frank Leebeek  
Bart van Vlijmen  
Jeroen Eikenboom

***Submitted***

## Abstract

Von Willebrand disease (VWD) is the most common inherited bleeding disorder and is mainly caused by dominant negative mutations in the multimeric protein von Willebrand factor (VWF). These mutations may either result in quantitative or qualitative defects in VWF. VWF is an endothelial protein that is secreted to the circulation upon endothelial activation. Once secreted, VWF multimers bind platelets and chaperone coagulation factor VIII in the circulation. Treatment of VWD focuses on increasing VWF plasma levels, but production and secretion of mutant VWF remains uninterrupted. Presence of circulating mutant VWF might, however, still affect normal hemostasis or functionalities of VWF beyond hemostasis. We hypothesized that inhibition of the production of mutant VWF improves the function of VWF overall and ameliorates VWD phenotypes. We have previously proposed the use of allele-specific small interfering RNAs (siRNAs) that target frequent *VWF* SNPs to inhibit mutant *VWF*. The aim of this study is to prove the functionality of these allele-specific siRNAs in endothelial colony forming cells (ECFCs). We have been able to isolate ECFCs from a VWD type 2A patient with an intracellular multimerization defect, reduced VWF collagen binding and a defective processing of proVWF to VWF. After transfection of an allele-specific siRNA that specifically inhibited expression of mutant VWF, we showed amelioration of the laboratory phenotype, with normalization of the VWF collagen binding, improvements in VWF multimers, and enhanced VWF processing. Altogether, we prove that allele-specific inhibition of the production of mutant VWF by siRNAs is a promising therapeutic strategy to improve VWD phenotypes.

## Introduction

Von Willebrand disease (VWD) is the most common inherited bleeding disorder that clinically affects around 1 in 10,000 people.<sup>1</sup> VWD is mainly characterized by mucocutaneous bleeding, like nose bleeding or menorrhagia.<sup>2</sup> Also, surgical or dental procedures might lead to critical bleeding events. VWD is caused by quantitative or qualitative defects in von Willebrand factor (VWF), a large multimeric glycoprotein produced by endothelial cells and megakaryocytes.<sup>3</sup> VWF primarily functions in hemostasis, where ultra-large VWF strings that are secreted from the endothelial cells attract platelets to sites of vascular damage. Furthermore, in the circulation VWF acts as chaperone for coagulation factor VIII (FVIII), thereby extending the half-life of FVIII.<sup>4</sup> In the past years, also roles of VWF beyond hemostasis have been described. Examples are roles of VWF in inflammation, angiogenesis and wound healing.<sup>5-7</sup>

Treatment of VWD is focused on raising VWF plasma levels, most often on demand after a bleeding event, or prior to a planned surgery or dental procedure. Plasma VWF levels can be raised by administration of desmopressin (DDAVP) or VWF-containing concentrates.<sup>8-11</sup> DDAVP provokes the release of endogenous VWF from the endothelial cells and is the primary choice of treatment in most patients with VWD type 1 and some patients with VWD type 2. DDAVP is, however, contra-indicated in VWD type 2B where released mutant VWF might lead to dangerously deep thrombocytopenia caused by the enhanced binding of mutant VWF to platelets.<sup>12</sup> Also, some patients are unresponsive to DDAVP treatment.<sup>9</sup> Those patients that do not respond to DDAVP or for which DDAVP is contra-indicated, can be treated with VWF-containing concentrates.<sup>11</sup> Although DDAVP or VWF-containing concentrates are usually sufficient to stop or prevent bleeding, they have only short-term effects and they do not cope with the continuous release of mutant VWF. Circulating mutant VWF might cause thrombocytopenia in VWD type 2B that cannot be prevented by administration of VWF-containing concentrates. Furthermore, presence of mutant VWF might affect processes beyond hemostasis in which VWF plays a role. An example is the development of intestinal angiodysplasia (as a result of disturbed angiogenesis) resulting in severe intestinal bleeding. This diathesis is more common among VWD patients than the normal population and is suggested to be caused by long-term exposure to mutant VWF that affects angiogenesis.<sup>13,14</sup> VWD patients with recurrent gastrointestinal bleeding are often treated with repeated dosing of VWF-containing concentrates, which is a burden and does not always solve the gastrointestinal bleeding.<sup>15</sup>

Since most VWD is caused by dominant negative mutations in VWF, we and others previously hypothesized that inhibition of the production of only mutant VWF might overcome the abovementioned shortcomings of the current treatment modalities.<sup>16,17</sup> Inhibition of mutant VWF only might be accomplished by small interfering RNAs (siRNAs) that discriminate between two alleles based on one nucleotide mismatch. We recently published the proof of principle

of this approach in human embryonic kidney (HEK) 293 cells overexpressing *VWF* alleles.<sup>16</sup> We showed that allele-specific siRNAs that target a heterozygous single-nucleotide polymorphism (SNP) located on the same allele as a dominant negative VWD type 2A mutation corrects for the VWD type 2A phenotype.<sup>16</sup> For this approach, various siRNAs have been selected to target four frequent SNPs in *VWF*. It was calculated that 74% of the patient population will be heterozygous for at least one of these four SNPs and thus might be a candidate for this approach of allele-specific *VWF* silencing.

HEK293 cells are a good model to prove the principle of allele-specific *VWF* inhibition and select for efficient and specific siRNA candidates, however HEK293 cells do not endogenously produce *VWF*. We therefore aim in this study to test the approach of allele-specific *VWF* inhibition by SNP-targeted siRNAs in endothelial colony forming cells (ECFCs, previously called blood outgrowth endothelial cells or BOECs). ECFCs are cultured endothelial cells that can be isolated from peripheral blood.<sup>18,19</sup> We show that siRNAs are able to selectively inhibit *VWF* alleles in healthy control ECFCs and that allele-specific siRNAs can improve the VWD phenotype of ECFCs that were isolated from a VWD type 2A patient with the *VWF* p.Cys1190Tyr mutation.

## Methods

### *Patients and controls*

A VWD type 2A patient with the *VWF* p.Cys1190Tyr (c.3569G>A) mutation and five healthy control subjects were included in the study. Blood was drawn from all subjects for ECFC, plasma and genomic DNA isolation. The patient's plasma was analyzed for *VWF* antigen (*VWF*:Ag), *VWF* activity and FVIII activity. *VWF*:Ag in plasma was determined using the STA LIA *VWF*:Ag test (Stago, Leiden, the Netherlands) and was analyzed on the Sta-R Max analyzer (Stago) with a commercial STA *VWF*:Ag calibrator (STA Unicalibrator, Stago) as reference. *VWF* activity was determined with the *VWF* ristocetin-triggered GPIb binding assay (*VWF*:GPIbR) with HemosIL AcuStar *VWF*:RCo reagent (Werfen IL, Breda, the Netherlands). Samples were analyzed on the BIO-FLASH (Werfen) and a commercial calibrator (supplied with the HemosIL AcuStar *VWF*:RCo) was used as reference. The FVIII activity was determined using an automated one-stage clotting assay on the STA-R MAX analyzer (Stago) with Sta-immunodef VIII (Stago) and STA-CK Prest 5 (APTT) (Stago) reagents. Commercial normal pool plasma (STA Unicalibrator, Stago) was used as reference. Genomic DNA was used to confirm the mutation in the VWD patient and to determine the genotypes in all subjects for four *VWF* SNPs: rs1800378, rs1063856, rs1063857 and rs1800380. Genotypes were determined using the Taqman SNP genotyping assays (Thermo Fisher Scientific, Carlsbad, CA, USA).

The study protocol was approved by the institutional ethical review board (study registered as NL54591.058.15). Informed consent was obtained from all subjects in accordance with the declaration of Helsinki.

### ***SNP phasing***

PacBio long read single molecule sequencing was used for linkage analysis of the heterozygous SNP and the p.Cys1190Tyr mutation. RNA was isolated from an ECFC cell pellet from the VWD type 2A patient using the RNeasy Micro Kit (Qiagen, Venlo, the Netherlands). Complementary DNA (cDNA) was synthesized using SuperScript™ II Reverse Transcriptase (Thermo Fisher Scientific) with primers designed to span a region of 2.8 kb (Forward primer: CACCTTCAGTGGGATCTGCC; Reverse primer: TTCAAGACCTCGCTGGTGG). *VWF*-specific products were amplified using the KAPA HiFi HotStart ReadyMix PCR kit (Roche Diagnostics, Mannheim, Germany). Amplicons were barcoded and SMRTbell adapters were added using the SMRTbell Barcoded Adapter Complete Prep Kit (Pacific Biosciences, Menlo Park, CA, USA). Barcoded amplicons were sequenced using a P6-C4 SMRT cell on a Pacific Biosciences RSII sequencer. Error-free circular consensus reads were mapped to the reference, followed by variant calling and resolution of variants phase using WhatsHap suit.

### ***ECFC isolation and culture***

ECFCs were isolated as described in Chapter 6 of this thesis. Peripheral blood was drawn in lithium heparin tubes (ECFC C1, C2 and C4; BD Biosciences, Erebodegem, Belgium) or in sodium heparin CPT™ Mononuclear Cell Preparation Tubes (ECFC C3, C5 and 2A; BD Biosciences).

siRNA transfections were performed in ECFCs as described in Chapter 6 of this thesis with Custom Silencer Select siRNAs (Ambion, Life Technologies, Bleiswijk, the Netherlands), an siRNA against *VWF* (siVWF, s14834, Life Technologies), or a negative control siRNA (siNEG, 4404020, Life Technologies). siRNAs were transfected into ECFCs in a concentration of 20 nM, unless otherwise stated. RNA lysates were generated 48 hours after transfection. Conditioned medium and protein lysates were harvested six days after transfection, and 24 hours after refreshing the medium. Protein lysates were generated by an overnight incubation of ECFCs in OptiMem1 (Thermo Fisher Scientific), 0.1% triton X-100 (Sigma-Aldrich) and a tablet of cOmplete protease inhibitor cocktail with EDTA (Roche Diagnostics)

### ***VWF protein analysis***

VWF:Ag levels in conditioned medium and protein lysates were measured by ELISA as described before<sup>16</sup>, with the modification that samples were diluted in phosphate-buffered

saline containing 0.1% tween (PBS-tween), or in PBS containing 1% BSA when the VWF:Ag ELISA was performed simultaneous with the VWF collagen binding (VWF:CB) assay. The VWF:CB assay is performed as described in Chapter 6 of this thesis.

Quantification of unprocessed proVWF in protein lysates was performed by a sandwich ELISA. ELISA plates were coated with rabbit anti-VWF (Dako) in 100 mM bicarbonate, 500 mM NaCl at pH 9.0. ELISA plates were incubated with protein lysates diluted in PBS-tween. Mouse anti-VWFpp conjugated to horseradish peroxidase (CLB-Pro 14.3, Sanquin, Amsterdam, the Netherlands) was used as detection antibody and ELISA plates were incubated with detection antibody diluted in PBS-tween. OPD was used as substrate and dissolved in substrate buffer (22 mM citric acid, 51 mM phosphate, pH 5.0) with addition of 11  $\mu$ l 30% H<sub>2</sub>O<sub>2</sub>. The enzymatic reaction was followed kinetically for 5 minutes. The ratio of unprocessed VWF over the total VWF:Ag levels was used as a measure for the processing of VWF. The average of control samples was set to one.

VWF multimers were visualized using agarose gel electrophoresis under non-reducing conditions as described before.<sup>16</sup> VWF multimers were visualized using ECL Western Blotting Substrate (Promega, Madison, WI, USA).

VWF monomers were visualized by western blot under reducing conditions. Protein lysates were reduced using 50 mM NuPAGE™ Sample Reducing Agent (Thermo Fisher Scientific) and proteins were separated on a 4-12% Bis-Tris gel (Thermo Fisher Scientific). Proteins were transferred to a PVDF membrane (BioRad, Veenendaal, the Netherlands) using a Trans-Blot Turbo Transfer System (BioRad, 1.5A, 15 minutes). Rabbit anti-VWF conjugated to horseradish peroxidase (DAKO, P0226) was used as detection antibody. The membrane was incubated with detection antibody diluted in PBS-tween containing 5% non-fat milk (Nutricia, Zoetermeer, the Netherlands). ECL Western Blotting Substrate was used to visualize VWF. Densitometry images were generated and quantified by ImageJ (ImageJ 1.51h, Bethesda, MD, USA).

### **RNA analysis**

RNA isolation, cDNA synthesis and qPCR analysis with *GAPDH* as endogenous reference gene were performed as described before.<sup>19</sup> Quantitative PCR (qPCR) was performed to quantify *VWF*, but also separate *VWF* alleles. Allele-specific qPCR primers were designed, containing the SNPs on the second last position of the forward primer. Primer sequences and annealing temperatures are shown in Table S1.

## Immunofluorescent staining

ECFCs were fixated using ice-cold methanol and stained as described before.<sup>19</sup> Rabbit anti-VWF (DAKO) and mouse anti-protein disulphide isomerase (PDI, Stressgen biotechnologies, San diego, CA, USA) were used as primary antibodies.

## Statistical analysis

Graphical images and statistical analysis were performed using GraphPad Prism 8 (GraphPad Software, La Jolla, CA, USA). Mann-Whitney *U* tests were performed to determine significance between specific and aspecific inhibition. One-way ANOVA with Dunnett's multiple comparisons test was used to determine significance between three or four groups.  $P < 0.05$  was considered significant.

## Results

### Time course of VWF inhibition by siRNAs in ECFCs

siRNAs are used in this study to inhibit *VWF* (alleles) in ECFCs. To assess the moment of strongest VWF inhibition by siRNAs on protein level, but also the duration of VWF inhibition, we transfected ECFCs with siVWF or siNEG and followed the VWF secreted in 24 hours for 28 days. Strongest VWF inhibition was observed in conditioned medium, six days after transfection of siVWF (Fig. 1). Furthermore, only after 28 days the VWF levels in siVWF transfected ECFCs were at the same level as ECFCs transfected with siNEG (Fig. 1). Since the strongest effects were observed six days after transfection, we decided to consistently measure the effects of the siRNAs on protein level, six days after transfection.

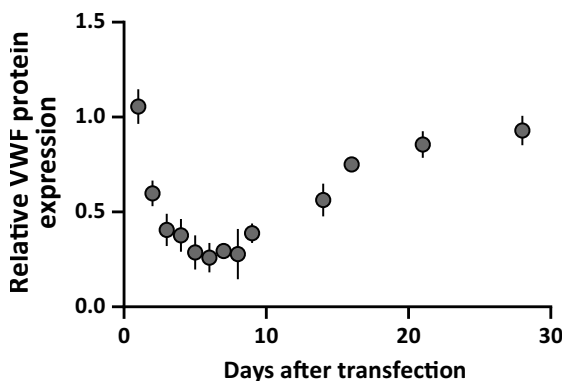


**Figure 1. Time course of VWF inhibition by siRNAs in ECFCs.** ECFC C3 was transfected with siVWF or siNEG at a concentration of 10 nM. 24 hour medium was taken at the time points indicated in the figure. Shown are the VWF:Ag levels measured in cells transfected with siVWF, normalized to the VWF:Ag levels measured in cells transfected with siNEG. Lowest relative VWF:Ag protein expression was observed six days after transfection. At this day the relative VWF:Ag expression was 26 percent. 28 days after siRNA transfection, the relative VWF:Ag expression was 93 percent and almost back to baseline. The experiment under these conditions was performed three times in duplicate. For some time points, a sample was only taken once.

Similar results were observed with different siRNA concentrations (data not shown). ECFC, endothelial colony forming cell; nM, nanomolar; siNEG, negative control siRNA; siVWF, siRNA against *VWF*; VWF, von Willebrand factor; VWF:Ag, VWF antigen

Allele-specific siRNA inhibition in healthy control ECFCs

We previously tested the efficiency and specificity of allele-specific siRNAs that target four common *VWF* SNPs in *VWF* overexpressing HEK293 cells.<sup>16</sup> For the current study, we selected the most effective allele-specific siRNA per SNP-target from the previous study. To evaluate the efficiency and specificity of the selected allele-specific siRNAs on a protein level in ECFCs, siRNAs were transfected in ECFCs that were homozygous for specific SNPs (ECFCs used per SNP-target are shown in Table 1). For example, an siRNA that is designed to target *VWF* c.1451G (si1451G) was tested for its efficiency in ECFC C1, an ECFC line that is homozygous for *VWF* c.1451G (Fig. 2A). si1451G was tested for its specificity in ECFC C3, an ECFC line that is homozygous for *VWF* c.1451A (Fig. 2A). The same ECFCs were used to assess the efficiency and specificity of si1451A. For all siRNAs tested, no or only minor reduction of the production of the untargeted *VWF* allele was observed as is shown by the relative *VWF* expression in ECFCs that did not harbor the SNP variant corresponding to the transfected siRNA (Fig. 2B, untargeted allele). On the other hand, a strong *VWF* knockdown of the targeted allele was observed in ECFCs that contained the SNP variant corresponding to the transfected siRNA (Fig. 2B, targeted allele). Knockdown was especially strong and efficient for si1451A and si1451G.

**Table 1.** Genotypes of subjects of ECFCs included in this study. The grey cells indicate the SNPs that were targeted per ECFC line

	rs1800378 c.1451A G		rs1063856 c.2365A G		rs1063857 c.2385T C		rs1800380 c.2880G A	
ECFC C1	G	G	A	A	T	T	G	G
ECFC C2	G	A	G	G	C	C	G	A
ECFC C3	A	A	A	A	T	T	G	G
ECFC C4	G	G	G	G	C	C	A	A
ECFC C5	G	A	G	A	T	C	G	A
ECFC 2A	G	A	A	A	T	T	G	G

ECFC, endothelial colony forming cell

The allele-specific siRNAs have been designed with the aim to target heterozygous SNPs located on the same allele as a dominant negative mutation and thereby ultimately correct for a disease phenotype. The ability of the selected siRNAs to inhibit *VWF* alleles in heterozygous ECFCs could, however, only be assessed on RNA level. We therefore tested the allele-specific siRNAs in an ECFC line that is heterozygous for all four SNPs (ECFC C5) and performed allele-specific qPCR to determine the relative RNA expression of either of the *VWF* alleles (Fig. 2C). On RNA level, a stronger overall knockdown of *VWF* was observed compared to what was observed on protein level, both for the targeted and untargeted allele (Fig. 2D). However, for most siRNAs clear specificity for its targeted allele remained. Only si2365A and si2365G showed minor specificity for its targeted allele. This is in line with results observed in HEK293 cells.<sup>16</sup>



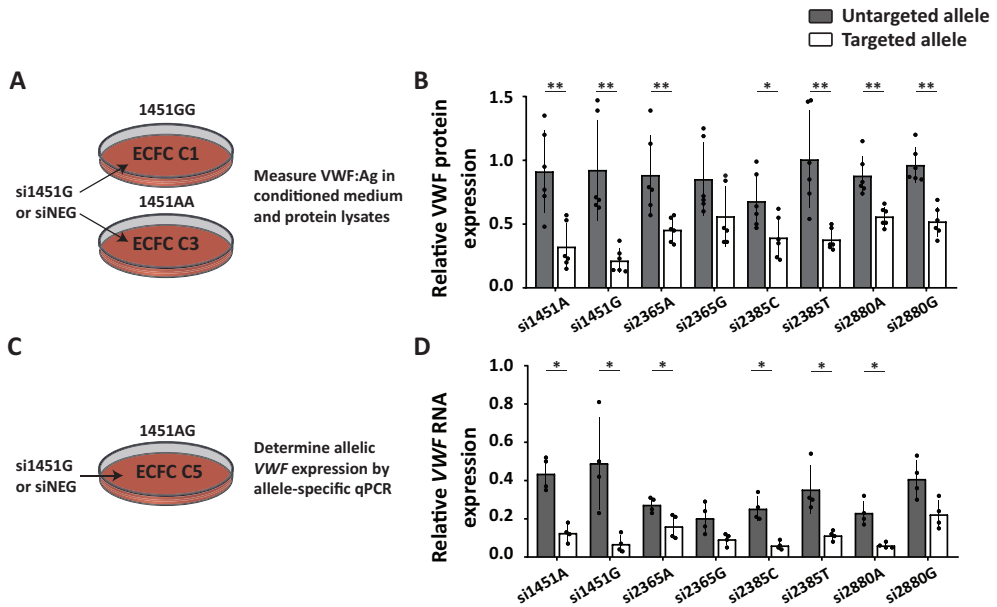


**Figure 2. Allele-specific inhibition of VWF in healthy control ECFCs.** (A) Experimental set-up of siRNA transfections in ECFCs that were homozygous for specific SNPs to test the efficiency and specificity of allele-specific siRNAs on protein level. As an example, si1451G or siNEG were transfected in ECFC C1 (homozygous for *VWF* c.1451G) and in ECFC C3 (homozygous for *VWF* c.1451A). The efficiency of si1451G is determined by the degree of VWF inhibition in ECFC C1. The specificity of si1451G is determined by the degree of VWF inhibition in ECFC C3. VWF:Ag levels were measured in 24 hour conditioned medium and protein lysates harvested six days after transfection. (B) Relative VWF protein expression of the untargeted (grey bars) and targeted allele (white bars) of ECFCs transfected with allele-specific siRNAs. si1451A and si1451G were tested for their efficiency and specificity in ECFC C1 and ECFC C3. si2365A, si2365G, si2385C and si2385T were tested for their efficiency and specificity in ECFC C2 and ECFC C3. si2880A and si2880G were tested for their efficiency and specificity in ECFC C1 and ECFC C4. Shown are the total VWF:Ag levels (conditioned medium + protein lysates) measured in ECFCs transfected with specific siRNAs, normalized to the total VWF:Ag levels measured in the same ECFCs transfected with siNEG. Shown are the mean  $\pm$  1 SD of three independent experiments performed in duplicate. Mann-Whitney, \* $P < 0.05$ , \*\* $P < 0.01$  (C) Experimental set-up of siRNA transfections in ECFC C5 (heterozygous for all four *VWF* SNPs), to test the efficiency and specificity of allele-specific siRNAs on RNA level. As an example, si1451G or siNEG were transfected in ECFC C5. RNA lysates were generated 48 hours after transfection and the allelic VWF expression was determined by allele-specific qPCR. (D) Relative *VWF* RNA expression of the untargeted (grey bars) and targeted allele (white bars) of ECFC C5 transfected with allele-specific siRNAs. Shown are the RNA expression levels of *VWF* alleles of ECFC C5 transfected with specific siRNAs, normalized to the expression level of the same allele measured in ECFC C5 transfected with siNEG. Shown are the mean  $\pm$  1 SD of two independent experiments performed in duplicate. Mann-Whitney, \* $P < 0.05$ . ECFC, endothelial colony forming cell; nM, nanomolar; qPCR, quantitative PCR; siNEG, negative control siRNA; siVWF, siRNA against *VWF*; VWF, von Willebrand factor; VWF:Ag, VWF antigen

### Correction of a VWD type 2A multimerization phenotype by an allele-specific siRNA

After proving that allele-specific siRNAs can discriminate between *VWF* alleles in healthy control ECFCs, we investigated whether allele-specific VWF inhibition could also correct a VWD phenotype in ECFCs. ECFCs from a VWD type 2A patient with the *VWF* p.Cys1190Tyr mutation were successfully isolated (ECFC 2A). This patient is clinically characterized by

normal VWF:Ag levels (1.07 IU/mL) and FVIII activity (0.78 IU/mL), but with a reduced VWF activity (0.27 IU/mL). Also, reduced high molecular weight (HMW) VWF is observed in the patient's plasma. Heterozygous SNPs are essential for allele-specific inhibition of the mutant allele, and genotyping of genomic DNA revealed that the patient is heterozygous for one of the four selected SNPs, *VWF* c.1451A|G. PacBio long read sequencing was performed to identify the phasing of this SNP, and showed that *VWF* c.1451A was located on the same allele as the dominant negative mutation p.Cys1190Tyr (c.3569A) (Fig. 3A). Therefore, ECFCs should be transfected with si1451A to inhibit the mutant allele and correct for the VWD type 2A phenotype. On the other hand, treatment of ECFC 2A with si1451G should reduce expression of the wild type allele and is expected to deteriorate the phenotype. Treatment of ECFC 2A with either si1451A or si1451G resulted in allele-specific *VWF* inhibition, as is shown by the allelic *VWF* expression in Fig. 3B. The *VWF* p.Cys1190Tyr mutation is associated with defective plasma multimers, and a defective intracellular multimerization defect was demonstrated for another mutation at the same amino acid (*VWF* p.Cys1190Arg).<sup>20,21</sup> We first subjected protein lysates and conditioned medium to the VWF:CB assay, an assay that is able to detect VWF multimerization defects.<sup>22</sup> As expected, we observed both in protein lysates and in conditioned medium of ECFC 2A a lower VWF:CB/VWF:Ag ratio compared to samples derived from healthy control ECFCs (VWF:CB/VWF:Ag in protein lysates of ECFC 2A  $0.70 (\pm 0.14)$  versus  $0.98 (\pm 0.15)$  in healthy control ECFCs, and in conditioned medium of ECFC 2A  $0.64 (\pm 0.04)$  versus  $0.89 (\pm 0.16)$  in healthy control ECFCs; Fig. 3Ci and 3Di) This VWF:CB defect was almost corrected in protein lysates of ECFC 2A transfected with si1451A. Contrarily, inhibition of expression of the wild type allele by si1451G clearly worsened the VWF:CB phenotype (Fig. 3Ci). Remarkably, in conditioned medium of ECFC 2A transfected with si1451A, no correction of the VWF:CB defect was observed. Nevertheless, inhibition of the wild type allele by si1451G did result in significantly lower VWF:CB/VWF:Ag as compared to siNEG transfected ECFC 2A (Fig. 3Di). We wondered why inhibition of mutant VWF did not result in correction of VWF:CB/VWF:Ag in conditioned medium as it did in the protein lysates. We hypothesized that downregulation of VWF in general leads to reduced VWF:CB/VWF:Ag in conditioned medium. To assess this hypothesis, VWF:CB/VWF:Ag was determined in conditioned medium and protein lysates of ECFC C1, C2 and C3 transfected with allele-specific siRNAs, siNEG and siVWF. We observed in conditioned medium, but not in protein lysates, that inhibition of the production of VWF by (allele-specific) siRNAs resulted in a gradual decrease of VWF:CB/VWF:Ag ( $N = 6$  for each siRNA in control ECFCs; Fig. 3Cii and 3Dii). When the VWF:CB/VWF:Ag of ECFC 2A transfected with siNEG, si1451A or si1451G were plotted against the VWF:CB/VWF:Ag ratios of healthy control ECFCs, we observed that the VWF:CB/VWF:Ag of ECFC 2A transfected with si1451A (inhibition of mutant allele) shifted towards the reference line of the healthy control ECFCs ( $N = 9$  for ECFC 2A). Whereas inhibition of the normal allele by si1451G resulted in further deterioration of the VWF:CB/VWF:Ag ratio (in conditioned medium as well as in protein lysates, Fig. 3Cii and 3Dii).

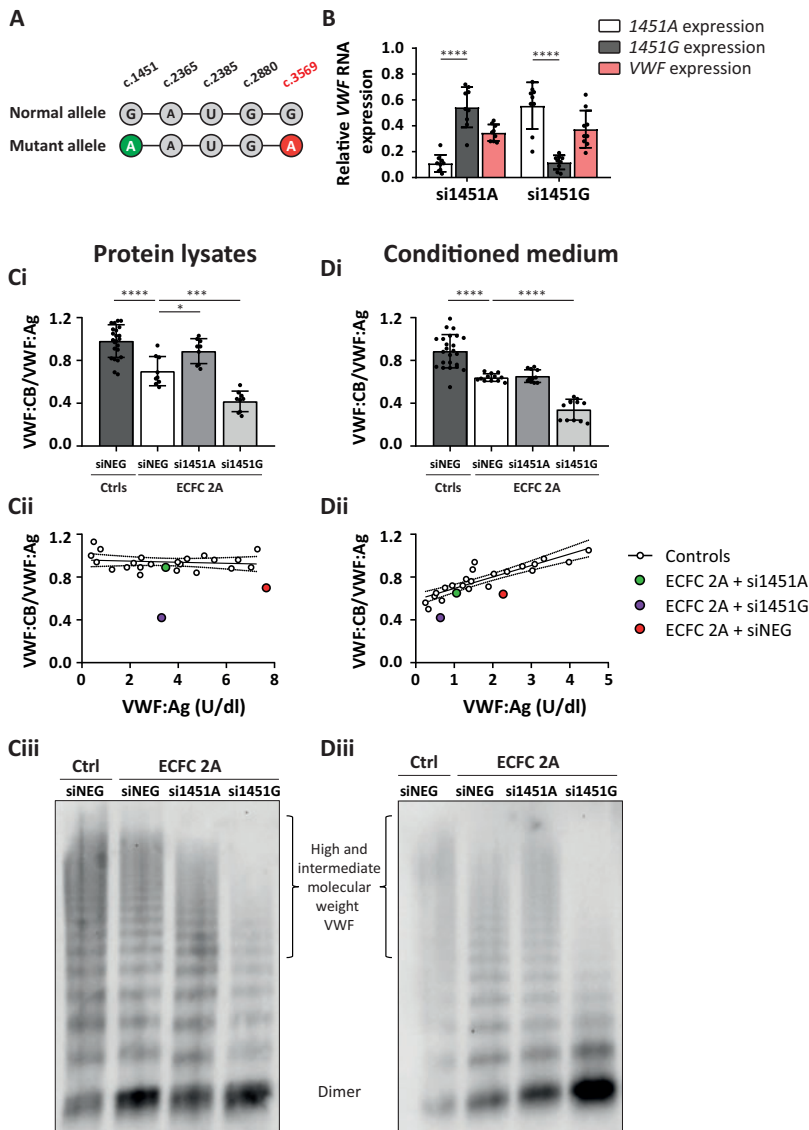


**Figure 3. Correction of the VWF multimerization defect in ECFC 2A.** (A) Phasing of the heterozygous SNP, VWF c.1451A|G, with the dominant negative mutation VWF p.Cys1190Tyr (c.3569A). PacBio sequencing revealed that VWF c.1451A is located on the same allele as VWF c.3569A. (B) Relative VWF RNA expression of ECFC 2A transfected with 20 nM si1451A or si1451G. Shown are the RNA expression levels of VWF alleles c.1451A and c.1451G as well as the total VWF expression. Expression levels were determined in RNA lysates of ECFCs transfected with si1451A or si1451G, normalized to the expression level of the same allele measured in ECFCs transfected with siNEG. Shown are the mean  $\pm$  1 SD of three independent experiments performed in triplicate. Mann-Whitney (c.1451A versus c.1451G expression), \*\*\*\*  $P < 0.0001$ . VWF:CB/VWF:Ag determined in (Ci) protein lysates and (Di) conditioned medium of ECFC C1, C2 and C3, transfected with siNEG and ECFC 2A transfected with siNEG, si1451A and si1451G. Shown are the mean  $\pm$  1 SD of three independent experiments performed in triplicate for ECFC 2A and the mean  $\pm$  1 SD of three independent experiments performed in duplicate for ECFC C1, C2 and C3. One-way ANOVA, \*  $P < 0.05$ , \*\*\*  $P < 0.001$ , \*\*\*\*  $P < 0.0001$ . Normal reference line of VWF:CB/VWF:Ag

plotted against the VWF:Ag levels measured in (Cii) protein lysates and (Dii) conditioned medium of ECFC C1, C2 and C3 transfected with siNEG, siVWF and various allele-specific siRNAs. Every white dot represents the average of three independent experiments performed in duplicate of an ECFC line transfected with a specific siRNA. Included in the graphs are the average of VWF:CB/VWF:Ag of three experiments performed in triplicate in which ECFC 2A was transfected with si1451A (green), si1451G (purple) or siNEG (red). VWF multimerization analysis of (Ciii) protein lysates and (Diii) conditioned medium harvested from a healthy control ECFC line transfected with siNEG and ECFC 2A transfected with si1451A, si1451G and siNEG. ECFC, endothelial colony forming cell; qPCR, quantitative PCR; siNEG, negative control siRNA; siVWF, siRNA against VWF; VWF, von Willebrand factor; VWF:Ag, VWF antigen; VWF:CB, VWF collagen binding

Although multimerization defects can be detected with the VWF:CB ELISA, the assay gives no information on the exact multimerization pattern. To assess the multimerization pattern, conditioned medium and protein lysate samples were subjected to the VWF multimer analysis. In conditioned medium, a slight decrease of HMW VWF was observed in the patient-derived ECFCs compared to control ECFCs (Fig. 3Diii). Inhibition of production of mutant VWF resulted in a slight increase in HMW VWF. Inhibition of production of wild type VWF clearly worsened the multimerization pattern in conditioned medium (Fig. 3Diii). No clear decrease of HMW VWF was observed in protein lysates of ECFC 2A compared to protein lysates of healthy control ECFCs. However, a clear increase in the intensity of the dimer band was apparent (Fig. 3Ciii). Also, a slight change in running pattern is visible, i.e. VWF from ECFC 2A seem to migrate a bit slower than VWF from the control ECFC. When the mutant allele was inhibited by si1451A, the intensity of the dimer band clearly decreased, however this coincided with a small decrease in HMW VWF. Furthermore, VWF migration shifted towards the pattern of the control ECFC. When the wild type allele was inhibited by si1451G, the multimerization pattern deteriorated with a decrease in HMW VWF and an increase in the intensity of the dimer band.

### ***Improved VWF processing after allele-specific inhibition of mutant VWF in ECFC 2A***

The multimerization pattern of protein lysates of ECFC 2A showed an increase in the intensity of the dimer band. This suggests that the processing of VWF into VWF multimers is affected. Dimerization of VWF takes place in the endoplasmic reticulum (ER).<sup>23</sup> To test whether VWF might be retained in the ER, we performed a costaining of VWF and the ER marker PDI. Indeed, a clear overlap of VWF and PDI staining is observed in ECFC 2A, indicating ER retention (Fig. 4A, ECFC 2A + siNEG, second column). This was not observed in control ECFCs (Fig. 4A, control, first column). When the mutant allele was inhibited by si1451A, retention of VWF in the ER was clearly decreased (best observed in greyscale image) and many cells showed no ER retention at all (Fig. 4A, ECFC 2A + si1451A, third column). Inhibition of the wild type allele by si1451G resulted in a rather severe cellular phenotype, with increased retention of VWF in the ER suggesting increase in severity of the cellular phenotype (Fig. 4A, ECFC 2A + si1451G, fourth column).

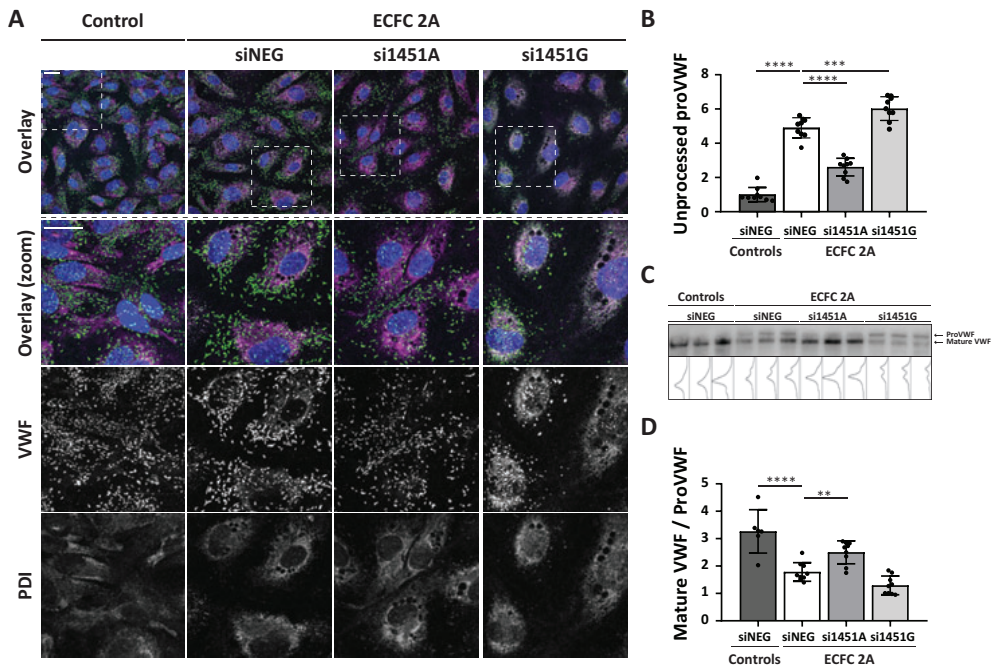


**Figure 4. Correction of the VWF processing defect in ECFC 2A.** (A) Confocal images of an untreated healthy control ECFC line and ECFC 2A transfected with siNEG, si1451A and si1451G. ECFCs were stained for VWF (green), PDI (magenta) and nuclei (blue). The upper row shows an overview image with VWF (green), PDI (magenta) and nuclei (blue). The second row shows a zoom-in of the upper image. Colocalization between VWF and PDI is shown in grey. The third and fourth rows show greyscale images of VWF and PDI staining, respectively. Scale bar represents 20  $\mu$ m. (B) Quantification of unprocessed proVWF measured by ELISA in protein lysates of control ECFCs transfected with siNEG or ECFC 2A transfected with siNEG, si1451A or si1451G. Shown are the mean  $\pm$  1 SD of three independent experiments performed in triplicate for ECFC 2A and the mean  $\pm$  1 SD of nine randomly selected protein samples of ECFC C1, C2 and C3. The average of the control ECFCs is set to one. One-way ANOVA, \*\*\*  $P < 0.001$ , \*\*\*\*  $P < 0.0001$ . (C) Western blot of protein lysates of control ECFCs transfected with siNEG or ECFC 2A transfected with siNEG, si1451A or si1451G. Protein lysates were run under reduced conditions on a 4-12% Bis-Tris gel. Shown are protein lysates of ECFC C1, C2 and C3 transfected with siNEG and the three samples of a triplicate experiment for ECFC 2A transfected with siNEG, si1451A and si1451G. (D) Quantification of the western blot shown in panel C. Shown is the mean  $\pm$  1 SD of quantified western blots performed on protein lysates of three independent experiments performed in triplicate for ECFC 2A and the mean  $\pm$  1 SD of six protein lysate samples of ECFC C1, C2 and C3. One-way ANOVA, \*\*  $P < 0.01$ , \*\*\*\*  $P < 0.0001$ . ECFC, endothelial colony forming cell; PDI, protein disulphide isomerase; siNEG, negative control siRNA; siVWF, siRNA against VWF; VWF, von Willebrand factor; VWF:Ag, VWF antigen; VWF:CB, VWF collagen binding

VWF is produced as proVWF that is dimerized in the ER. After dimerization of proVWF in the ER, VWF is translocated to the Golgi where the propeptide is cleaved from VWF by furin.<sup>24</sup> Increased ER retention of VWF results in an increased amount of unprocessed proVWF in the cells. This can be quantified by an ELISA that measures the amount of propeptide that is still bound to VWF. Protein lysates of ECFC 2A showed a 4.9 fold higher level of unprocessed VWF compared to protein lysates of control ECFCs. This was decreased 1.9 fold after inhibition of production of the mutant allele by si1451A (Fig. 4B). Compared to control ECFCs, 6 fold

more unprocessed VWF was present in ECFC 2A in which the wild type allele was inhibited by si1451G (Fig. 4B).

A western blot in which the samples are run under reducing conditions can be used as an alternative method to identify defects in the processing of VWF. In this western blot, an increase in the intensity of the unprocessed proVWF band was detected in protein lysates of ECFC 2A compared to control ECFCs (Fig. 4C). The intensity of the unprocessed proVWF band decreased after inhibition of the mutant allele by si1451A. An increase in the intensity of the unprocessed proVWF band was observed when the wild type allele was inhibited by si1451G (Fig. 4C). Quantification of the western blot confirms the defective processing of VWF and correction of the phenotype after transfection of si1451A that inhibited expression of the mutant allele (Fig. 4D).

## Discussion

Allele-specific siRNAs may be used to selectively inhibit mutant alleles to improve disease phenotypes. Previously, we have shown that allele-specific siRNAs that distinguish two *VWF* alleles based on one nucleotide mismatch of SNPs can specifically inhibit *VWF* alleles in HEK293 cells, and that these siRNAs can improve a VWD phenotype. Here, we aimed to extend the proof of concept of allele-specific VWF inhibition to an *ex vivo* setting by the use of patient-derived and healthy control ECFCs. In this study, we prove that allele-specific siRNAs can inhibit single *VWF* alleles based on one nucleotide mismatch *ex vivo* in healthy control ECFCs. This was shown both on protein and RNA level. Also, inhibition of the mutant allele in ECFCs isolated from a VWD type 2A patient resulted in clear improvements in the patient's cellular phenotype.

ECFCs are used in this study as *ex vivo* cell model for VWD. ECFCs are the only source of proliferative endothelial cells that can be isolated from patients by a peripheral blood venepuncture.<sup>25</sup> The use of ECFCs has the advantage that the cells are proliferative, have generally a high VWF production and are easy to transfect.<sup>26</sup> However, also clear variations between various ECFC cell lines emerges.<sup>19</sup> Most important, clear variations in VWF expression exists between ECFC lines and it was therefore suggested to be cautious when comparing different ECFC lines. When allele-specific siRNAs are tested in (patient-derived) ECFCs, the effects are determined in ECFCs transfected with either an allele-specific siRNA or a negative control siRNA. Cells are therefore used as their own internal control, and do not have to be compared to control ECFCs. To assess the efficiency and specificity of the allele-specific siRNAs on a protein level, we had no choice but to compare different healthy control ECFC lines (Fig. 2A). And although the ECFC lines in this study were carefully selected based on their proliferative state and VWF production, differences between ECFC lines could not be avoided.

This was also reflected in variations in the efficiency of siVWF to inhibit VWF production in ECFCs. For example, we reproducibly observed a stronger relative VWF inhibition by siVWF in ECFC C1 compared to ECFC C2 (data not shown). No firm conclusions can therefore be drawn on the efficiency and specificity of the allele-specific siRNAs on protein level that have been tested in the different healthy control ECFC lines (Fig. 2B).

SNPs in *VWF* with a high minor allele frequency have been used in this study as target to inhibit *VWF* alleles. This approach was chosen since with only a small number of SNPs, a large percentage of the patient population can be reached. It was for example calculated that 74% of the Caucasian population is heterozygous for at least one of the four SNPs used in this study.<sup>16</sup> From this study it became evident that especially si1451A and si1451G have high potency as allele-specific siRNAs, and both siRNAs proved, depending on the allele targeted, successful to, respectively correct or deteriorate a VWD type 2A phenotype *ex vivo*. Whether the other siRNAs have the same ability to correct for VWD phenotypes, remains to be unanswered. It is however highly unlikely that si2365A or si2365G will have similar effects as si1451A or si1451G. Fortunately, exclusion of si2365A and si2365G does not reduce the fraction of the patient population that can be reached, since *VWF* c.2365A|G is in almost complete linkage disequilibrium with *VWF* c.2385C|T.<sup>27</sup> Furthermore, the efficacy of the allele-specific siRNAs in this study may still be improved by for example alternating the chemical modification of the siRNAs.<sup>28</sup> Also, more SNP-targets could be tested to increase the percentage of the targeted patient population.

The ability of the allele-specific siRNAs to correct a VWD phenotype was tested in ECFCs isolated from a VWD type 2A patient with the *VWF* p.Cys1190Tyr mutation. This mutation is characterized by a clearly defined laboratory phenotype with reduced HMW multimers and reduced VWF collagen binding.<sup>20</sup> Inhibition of the mutant allele by si1451A resulted in clear improvements in the processing of VWF and the VWF:CB/VWF:Ag in protein lysates. Remarkably, no increase of VWF:CB/VWF:Ag was observed in conditioned medium of ECFC 2A in which expression of the mutant allele was inhibited by si1451A (Fig. 3Di). It appeared, however, that also a reduced VWF:CB/VWF:Ag was observed in healthy control ECFCs transfected with siRNAs that reduced the overall expression of VWF (Fig. 3Dii). When the VWF:CB/VWF:Ag of ECFC 2A transfected with si1451A was plotted against the normal reference line, the VWF:CB/VWF:Ag was almost normalized. Also, the multimerization pattern of VWF in conditioned medium showed an increase in HMW VWF in ECFCs transfected with si1451A compared to siNEG transfected cells. The reason for discrepancy between de VWF:CB assay and the VWF multimer analysis remains uncertain. It might be possible that the VWF:CB is sensitive for altered ratios between HMW and low molecular weight VWF. Further *in vivo* studies should reveal whether reduced VWF:CB after downregulation of VWF is also apparent *in vivo* and what the potential consequences of this effect are.

The use of siRNAs as a therapeutic application requires persistence of the siRNA activity over a longer period of time. Clinical trials with siRNAs that target liver-expressed genes showed persistent siRNA-mediated downregulation of several genes for more than a month.<sup>29-31</sup> In ECFCs, downregulation of VWF was observed for up to 28 days, even though the cells were still proliferating in the first week after transfection. Furthermore, siRNA-mediated inhibition of *Icam2* and *Tie2* in mice by siRNAs that were complexed in polymeric nanoparticles or a cationic lipoplex delivery system, respectively, resulted in persistent, and around 80 percent, *Icam2* and *Tie2* inhibition for more than 21 days after a single dose.<sup>32,33</sup> These results of long-term gene inhibition are promising for further developments of siRNA therapeutics for endothelial genes, like VWF. For VWD patients, long-term correction of VWF may especially be beneficial for selected patients with a severe bleeding phenotype that currently require repeated dosing with VWF-containing concentrates.

To conclude, we show that allele-specific siRNAs are effective in the inhibition of single VWF alleles in ECFCs. Inhibition of expression of the mutant allele in ECFCs isolated from a VWD type 2A patient with the VWF p.Cys1190Tyr mutation resulted in clear improvements of the cellular phenotype. Further studies in VWD mouse models are needed to translate the positive *ex vivo* results to an *in vivo* model, and to show whether the allele-specific siRNAs are able to correct a bleeding phenotype.

## Acknowledgements

This study was financially supported by a research grant from the Landsteiner Foundation for Blood Transfusion Research (grant 1504). We would like to thank Petra Noordijk and Lejla Mahic (LUMC, department of internal medicine, Clinical Epidemiology, the Netherlands) for performing DNA isolations, and Suzan de Boer (LUMC, department of internal medicine, Thrombosis and Hemostasis, the Netherlands) for ECFC isolations. We also would like to thank Emile de Meijer (LUMC, Human Genetics, the Netherlands) for PacBio sequencing sample preparation.



## References

1. Leebeek FW, Eikenboom JC. Von Willebrand's Disease. *N Engl J Med*. 2016;**375**(21):2067-2080.
2. Tosetto A, Rodeghiero F, Castaman G, et al. A quantitative analysis of bleeding symptoms in type 1 von Willebrand disease: results from a multicenter European study (MCMDM-1 VWD). *J Thromb Haemost*. 2006;**4**(4):766-773.
3. Springer TA. von Willebrand factor, Jedi knight of the bloodstream. *Blood*. 2014;**124**(9):1412-1425.
4. Weiss HJ, Sussman II, Hoyer LW. Stabilization of factor VIII in plasma by the von Willebrand factor. Studies on posttransfusion and dissociated factor VIII and in patients with von Willebrand's disease. *J Clin Invest*. 1977;**60**(2):390-404.
5. Kawecki C, Lenting PJ, Denis CV. von Willebrand factor and inflammation. *J Thromb Haemost*. 2017;**15**(7):1285-1294.
6. Starke RD, Ferraro F, Paschalaki KE, et al. Endothelial von Willebrand factor regulates angiogenesis. *Blood*. 2011;**117**(3):1071-1080.
7. Ishihara J, Ishihara A, Starke RD, et al. The heparin binding domain of von Willebrand factor binds to growth factors and promotes angiogenesis in wound healing. *Blood*. 2019;**133**(24):2559-2569.
8. Mannucci PM, Ruggeri ZM, Pareti FI, Capitanio A. 1-Deamino-8-d-arginine vasopressin: a new pharmacological approach to the management of haemophilia and von Willebrands' diseases. *Lancet*. 1977;**1**(8017):869-872.
9. Castaman G, Lethagen S, Federici AB, et al. Response to desmopressin is influenced by the genotype and phenotype in type 1 von Willebrand disease (VWD): results from the European Study MCMDM-1VWD. *Blood*. 2008;**111**(7):3531-3539.
10. Franchini M, Mannucci PM. Von Willebrand factor (Vonvendi(R)): the first recombinant product licensed for the treatment of von Willebrand disease. *Expert Rev Hematol*. 2016;**9**(9):825-830.
11. Peyvandi F, Kouides P, Turecek PL, Dow E, Berntorp E. Evolution of replacement therapy for von Willebrand disease: From plasma fraction to recombinant von Willebrand factor. *Blood Rev*. 2019;**38**:100572.
12. Kruse-Jarres R, Johnsen JM. How I treat type 2B von Willebrand disease. *Blood*. 2018;**131**(12):1292-1300.
13. Selvam S, James P. Angiodysplasia in von Willebrand Disease: Understanding the Clinical and Basic Science. *Semin Thromb Hemost*. 2017;**43**(6):572-580.
14. Franchini M, Mannucci PM. Gastrointestinal angiodysplasia and bleeding in von Willebrand disease. *Thromb Haemost*. 2014;**112**(3):427-431.
15. deWee EM, Sanders YV, Mauser-Bunschoten EP, et al. Determinants of bleeding phenotype in adult patients with moderate or severe von Willebrand disease. *Thromb Haemost*. 2012;**108**(4):683-692.
16. de Jong A, Dirven RJ, Oud JA, Tio D, van Vlijmen BJM, Eikenboom J. Correction of a dominant-negative von Willebrand factor multimerization defect by small interfering RNA-mediated allele-

- specific inhibition of mutant von Willebrand factor. *J Thromb Haemost.* 2018;**16**(7):1357-1368.
17. Casari C, Pinotti M, Lancellotti S, et al. The dominant-negative von Willebrand factor gene deletion p.P1127\_C1948delinsR: molecular mechanism and modulation. *Blood.* 2010;**116**(24):5371-5376.
  18. Ingram DA, Mead LE, Tanaka H, et al. Identification of a novel hierarchy of endothelial progenitor cells using human peripheral and umbilical cord blood. *Blood.* 2004;**104**(9):2752-2760.
  19. de Jong A, Weijers E, Dirven R, de Boer S, Streur J, Eikenboom J. Variability of von Willebrand factor-related parameters in endothelial colony forming cells. *J Thromb Haemost.* 2019;**17**(9):1544-1554.
  20. Schneppenheim R, Michiels JJ, Obser T, et al. A cluster of mutations in the D3 domain of von Willebrand factor correlates with a distinct subgroup of von Willebrand disease: type 2A/IIIE. *Blood.* 2010;**115**(23):4894-4901.
  21. de Jong A, Eikenboom J. Von Willebrand disease mutation spectrum and associated mutation mechanisms. *Thromb Res.* 2017;**159**:65-75.
  22. Flood VH, Gill JC, Friedman KD, et al. Collagen Binding Provides a Sensitive Screen for Variant von Willebrand Disease. *Clinical Chemistry.* 2013;**59**(4):684-691.
  23. Lippok S, Kolsek K, Lof A, et al. von Willebrand factor is dimerized by protein disulfide isomerase. *Blood.* 2016;**127**(9):1183-1191.
  24. van de Ven WJ, Voorberg J, Fontijn R, et al. Furin is a subtilisin-like proprotein processing enzyme in higher eukaryotes. *Mol Biol Rep.* 1990;**14**(4):265-275.
  25. Martin-Ramirez J, Hofman M, van den Biggelaar M, Hebbel RP, Voorberg J. Establishment of outgrowth endothelial cells from peripheral blood. *Nat Protoc.* 2012;**7**(9):1709-1715.
  26. Medina RJ, Barber CL, Sabatier F, et al. Endothelial Progenitors: A Consensus Statement on Nomenclature. *Stem Cells Transl Med.* 2017;**6**(5):1316-1320.
  27. Auton A, Brooks LD, Durbin RM, et al. A global reference for human genetic variation. *Nature.* 2015;**526**(7571):68-74.
  28. Malek-Adamian E, Fakhoury J, Arnold AE, Martinez-Montero S, Shoichet MS, Damha MJ. Effect of Sugar 2',4'-Modifications on Gene Silencing Activity of siRNA Duplexes. *Nucleic Acid Ther.* 2019;**29**(4):187-194.
  29. Pasi KJ, Rangarajan S, Georgiev P, et al. Targeting of Antithrombin in Hemophilia A or B with RNAi Therapy. *N Engl J Med.* 2017;**377**(9):819-828.
  30. Ray KK, Landmesser U, Leiter LA, et al. Inclisiran in Patients at High Cardiovascular Risk with Elevated LDL Cholesterol. *N Engl J Med.* 2017;**376**(15):1430-1440.
  31. Adams D, Gonzalez-Duarte A, O'Riordan WD, et al. Patisiran, an RNAi Therapeutic, for Hereditary Transthyretin Amyloidosis. *N Engl J Med.* 2018;**379**(1):11-21.
  32. Dahlman JE, Barnes C, Khan O, et al. In vivo endothelial siRNA delivery using polymeric nanoparticles with low molecular weight. *Nat Nanotechnol.* 2014;**9**(8):648-655.
  33. Fehring V, Schaeper U, Ahrens K, et al. Delivery of therapeutic siRNA to the lung endothelium via novel Lipoplex formulation DACC. *Mol Ther.* 2014;**22**(4):811-820.







# 8

## **Amelioration of the murine von Willebrand disease type 2B phenotype using an allele-specific small interfering RNA**

Annika de Jong  
Caterina Casari  
Richard Dirven  
Bart van Vlijmen  
Peter Lenting  
Cécile Denis  
Jeroen Eikenboom

*In preparation*

## Abstract

Von Willebrand disease (VWD) type 2B is caused by dominant negative mutations in the platelet binding site within von Willebrand factor (VWF), resulting in an increase in VWF that circulates in its 'activated' state (active VWF), spontaneous platelet binding and subsequent thrombocytopenia. Since small interfering RNAs (siRNAs) can distinguish two *VWF* alleles by only one nucleotide, we hypothesized that an siRNA that inhibits production of the dominant negative VWD type 2B mutation VWF p.Val1316Met, but not wild type VWF, could correct the VWD type 2B phenotype. In this study we aim to prove the concept of allele-specific *VWF* inhibition in a heterozygous VWD type 2B mouse model via siRNA-mediated allele-specific inhibition. VWF deficient mice hydrodynamically injected with both wild type and mutant mouse *Vwf* (m*Vwf*) p.Val1316Met cDNA were used. We show that these mice recapitulate the human VWD type 2B phenotype with low platelet counts and an increase in active mVWF. An *in vitro* siRNA screen in HEK293 cells overexpressing m*Vwf* alleles resulted in the selection of an siRNA that selectively inhibited production of the mutant allele with minor inhibition of the wild type allele. Injection of this siRNA in heterozygous VWD type 2B mice resulted in strong VWF downregulation where the siRNA had a higher ability to inhibit the mutant allele over the wild type allele. This resulted in clear improvements in the platelet phenotype. Altogether, we showed that allele-specific siRNAs are capable of correcting a VWD type 2B phenotype in mice. These results are promising for further developments of RNA-targeted therapies for VWD.

## Introduction

Von Willebrand disease (VWD) is the most common inherited bleeding disorder and is in most cases caused by dominant negative mutations in von Willebrand factor (VWF).<sup>1</sup> VWF is a large multimeric glycoprotein that is secreted from endothelial cells upon vascular damage. Once secreted, vascular shear unfolds VWF into ultra large VWF strings that are attached to the exposed collagen.<sup>2</sup> The elongated structure of VWF allows binding of platelets via their glycoprotein Iba receptor to the A1 domain of VWF, starting platelet adhesion and subsequent platelet activation and aggregation at sites of vascular damage.<sup>3</sup>

Several types of VWD can be distinguished due to either qualitative or quantitative defects in VWF. VWD type 2B is one of the qualitative VWD types and is caused by dominant negative gain-of-function mutations in the platelet's glycoprotein Iba binding site in the A1 domain of VWF.<sup>4</sup> These mutations cause a conformational change of the VWF A1 domain and therefore allow platelets to bind VWF without activation of VWF by vascular shear for example.<sup>5,6</sup> Furthermore, the VWF-platelet complexes are cleared rapidly and most VWD type 2B patients present with low platelet counts, either at steady state or in situations of increased VWF release.<sup>7,8</sup>

Mutations at a few locations within the A1 domain of VWF are responsible for VWD type 2B.<sup>4</sup> VWF p.Val1316Met leads to one of the most severe VWD type 2B phenotypes and patients with this mutation present with a very low platelet count, decreased VWF plasma levels and giant platelets.<sup>9</sup> Treatment of VWD type 2B can in some situations be problematic. Desmopressin, which mediates short-term release of VWF from endothelial cells, is generally contra-indicated because increased release of mutant VWF leads to an even further drop in platelet count. VWF-containing concentrates, on the other hand, are able to correct for the bleeding phenotype in most situations.<sup>10</sup> However, pregnancy, surgery or inflammation may lead to stress-induced release of endogenously produced mutant VWF from endothelial cells.<sup>9-12</sup> This may lead to a deep thrombocytopenia which cannot be prevented by administration of an exogenous source of VWF-containing concentrates and may even require platelet transfusion.<sup>13</sup>

We hypothesize that specific inhibition of the production of mutant VWF, without affecting the production of normal VWF, will have a positive effect on VWF function and might be a solution for VWD patients with an unmet clinical need, such as the VWD type 2B patients described above.<sup>14,15</sup> We previously showed that allele-specific siRNAs that target frequent single-nucleotide polymorphisms within *VWF* are able to distinguish two *VWF* alleles based on one nucleotide variation.<sup>14</sup> Targeting a heterozygous SNP located on the same allele as the dominant negative mutation has already proven successful *in vitro* (HEK293 cells<sup>14</sup>) and *ex vivo* (endothelial colony forming cells<sup>16</sup>). Here, we extend this proof of concept of allele-specific *VWF* inhibition to a mouse model of heterozygous VWD type 2B. Since in-bred mice do not contain (human) heterozygous variations, we cannot discriminate between *VWF* alleles

with the SNP-targeted approach in mice. Therefore, instead of targeting a heterozygous SNP linked to the dominant negative mutation, we have designed siRNAs that target the dominant negative mouse VWD type 2B mutation, p.Val1316Met, itself. Heterozygous VWD type 2B mice were generated by hydrodynamic injection of both wild type mouse *Vwf* (m*Vwf*) and mutant m*Vwf* p.Val1316Met cDNA in VWF deficient ( $^{-/-}$ ) mice. Injection of an siRNA that targets the m*Vwf* p.Val1316Met cDNA sequence in heterozygous VWD type 2B mice resulted in strong inhibition of the mutant allele and correction of the VWD type 2B platelet phenotype.

## Methods

### **Plasmid expression vectors**

Full length mouse *Vwf* (m*Vwf*) cDNA was obtained by NotI and XbaI restriction of pLIVE®-m*Vwf*.<sup>17</sup> Both restriction sites were introduced in the pLIVE® plasmid by the Q5® Site-Directed Mutagenesis Kit (New England Biolabs, Ipswich, MA, USA). The obtained m*Vwf* cDNA was ligated into pcDNA™3.1/Zeo (+) using the DNA Ligation Kit for Long Fragments (Takara, Saint-Germain-en-Laye, France). The mVWF p.Val1316Met mutation (c.3946G>A) was introduced in pcDNA™3.1/Zeo (+) m*Vwf* by the Q5® Site-Directed Mutagenesis Kit to obtain pcDNA™3.1/Zeo (+) m*Vwf*-p.Val1316Met. A Myc peptide tag was introduced at the C-terminal end of mVWF to create pcDNA™3.1/Zeo (+) m*Vwf*/Myc and was used to distinguish wild type mVWF from mVWF-p.Val1316Met on a protein level *in vitro*. For *in vivo* experiments, we ligated m*Vwf*/Myc and m*Vwf*-p.Val1316Met back into pLIVE®, and introduced an HA tag at the C-terminal end of m*Vwf*-p.Val1316Met to create m*Vwf*-p.Val1316Met/HA. Plasmids for *in vivo* application were purified using NucleoBond® PC 2000 EF (Macherey-Nagel, Düren, Germany).

### **siRNA design**

Four custom Silencer® Select 21-mer siRNA oligonucleotides (Ambion, Life Technologies Europe BV) with a dTdT overhang at the 5' end of the sense strand were designed to fully complement the m*Vwf* p.Val1316Met mutation (c.3946A) and therefore have one mismatch with the wild type allele (c.3946G). To create more specific siRNAs (i.e. decreased potency for the untargeted allele), nine siRNAs were designed that contain one extra mismatch next to the mutation. siRNA sequences are summarized in Fig. 1A. For *in vitro* siRNA screening, we used custom synthesized Silencer Select siRNAs with standard purification (Thermo Fisher Scientific, Carlsbad, CA, USA: 4390827) and Ambion® Silencer® Select Negative Control siRNA (Thermo Fisher Scientific: 4404020) as negative control (siNEG). For *in vivo* experiments, we used custom synthesized Silencer Select siRNAs with HPLC purification (Thermo Fisher Scientific: 4390831).



### **Cell culture and transfection**

siRNA and plasmid transfections in Human Embryonic Kidney 293 (HEK293) cells (ATCC, Rockville, MD, USA) were performed as described before.<sup>14</sup> Screening of the designed siRNAs for efficiency and specificity was performed by cotransfection of *mVwf*/Myc or *mVwf*-p.Val1316Met plasmid with 2 nM siRNA in separate wells. *In vitro* improvements in the function of mVWF was investigated in HEK293 cells cotransfected with *mVwf*/Myc, *mVwf*-p.Val1316Met and siRNA in the same well. *mVwf* plasmids were always transfected in a total plasmid concentration of 600 ng/mL.

### **Mouse experiments**

Hydrodynamic gene transfer of *mVwf* plasmids was performed in 8-12 weeks old male/female VWF<sup>-/-</sup> mice on a C57BL/6 background as described before.<sup>17</sup> In short, a total amount of 40 or 50 µg plasmid (indicated per experiment) was diluted in 0.9% sodium chloride in a volume that is equivalent to 10% of the body weight. Diluted plasmid was injected through the tail vein in approximately 5 seconds. To generate heterozygous VWD type 2B mice, equal quantities of pLIVE<sup>®</sup> *mVwf*/Myc and pLIVE<sup>®</sup> *mVwf*-p.Val1316Met/HA were injected. Five days after plasmid injections, siRNAs in a final concentration of 0.5 or 1 mg/kg were injected through the tail vein and directed to the liver by the use of InvivoFectamine 3.0 Reagent (Thermo Fisher Scientific) following the manufacturer's instructions. At indicated time points, blood was drawn in 10% EDTA (final concentration: 50 mM) or citrate (final concentration: 13.8 mM) from the retro-orbital plexus under isoflurane anesthesia. All animal experiments were performed with approval of the local ethical committee CEEA26 under the number APAFIS#20037-2019032714308918 v3.

### **Blood analysis**

Platelet count and platelet volume were determined in whole EDTA blood using a veterinary cell counter (Scil Vet ABC Plus, Horiba Medical, France), except for one experiment in which flow cytometry was used. For flow cytometry analysis, whole blood was diluted 20 times in phosphate-buffered saline (PBS). Platelets in diluted blood were stained for 15 minutes with a FITC labeled rat anti-mouse CD41 antibody (cat: 553848, BD Pharmingen, San Jose, CA, USA) at room temperature. Samples were directly analyzed with an Accuri C6 flow cytometer (BD Biosciences, Le Pont de Claix, France).

### **Staining of blood smears and liver sections**

Blood smears were prepared from EDTA blood and stained using Kwik-DIFF (Thermo Fisher Scientific) and imaged using the 3DHitech Panoramic 250 slide scanner.

Whole livers were embedded in Tissue-Tek O.C.T. (Sakura, Alphen aan den Rijn, The Netherlands) and snap frozen. 5  $\mu\text{m}$  cryosections were fixed by ethanol containing 5% acetic acid (ice-cold) and blocked with PBS supplemented with 10% normal goat serum (Dako, Glostrup, Denmark). Rabbit anti-HA (Cell signaling, Leiden, the Netherlands), rat anti-Myc (Chromotek, Martinsried, Germany) or isotype controls were diluted in blocking buffer and liver sections were incubated with primary antibodies for 45 minutes. Liver sections were incubated with secondary antibodies goat anti-rat IgG (H+L) AF488 and goat anti-rabbit IgG (H+L) AF594 (Thermo Fisher Scientific) diluted in blocking buffer for 30 minutes. Stained sections were mounted using ProLong Gold (Life Technologies) and imaged using the 3DHistech Panoramic 250 slide scanner.

### ***VWF quantification and functional assays***

Total mVWF, mVWF/Myc and mVWF/HA protein levels were measured in plasma, and total mVWF and mVWF/Myc protein levels were measured in conditioned medium as described before<sup>14</sup> with the modification that sheep anti-VWF (ab11713; Abcam, Cambridge, United Kingdom) was used as coating antibody for the mVWF/HA ELISA. A pool of normal mouse plasma (NMP) from wild type C57BL/6J mice was used as a reference for the mVWF:Ag ELISA. NMP was prepared the same as the plasma samples of individual mice. Recombinant mVWF/Myc and mVWF/HA produced by HEK293 cells was used as reference in the mVWF/Myc and mVWF/HA ELISA and normalized to mVWF:Ag levels measured in NMP. All antigen data is represented as percentage of NMP.

Active mVWF was measured using the AU/VWFA-11 nanobody that captures only mVWF in which the A1 domain is in its open conformation.<sup>5</sup> This nanobody was a kind gift of Dr. Rolf Urbanus (Utrecht Medical Center, Utrecht, the Netherlands). ELISA plates were coated with the AU/VWFA-11 nanobody diluted in coating buffer (100 mM bicarbonate, 500 mM sodium chloride, pH 9.0) overnight at 4°C. Wells were blocked thereafter with PBS containing 3% bovine serum albumin (BSA; Sigma-Aldrich, St Louis, MO, USA) for 30 minutes at 37°C. Samples (conditioned medium or plasma) were diluted in PBS containing 3% BSA in 3 mVWF:Ag concentrations (5.0, 3.4 and 1.7 percent of NMP) and incubated for 2 hours at 37°C. To increase the signal in the ELISA, we conjugated biotin (Sigma-Aldrich) to rabbit anti-VWF-IgG (A0082; Dako) to create rabbit anti-VWF-IgG-biotin. Wells were incubated with rabbit anti-VWF-IgG-biotin diluted in PBS containing 3% BSA for 1 hour at 37°C. Streptavidin-(POLY) horseradish peroxidase (Thermo Fisher Scientific) in PBS containing 3% BSA was used as detecting antibody and wells were incubated with detecting antibody for 1 hour at 37°C. Wells were incubated with 1 tablet of O-phenylenediamine dihydrochloride (Sigma-Aldrich) dissolved in 11 ml substrate buffer (22 mM citric acid, 51 mM phosphate, pH 5.0) and 11  $\mu\text{l}$  30%  $\text{H}_2\text{O}_2$ . The enzymatic reaction was stopped using 2M  $\text{H}_2\text{SO}_4$ . Slopes were calculated per sample from the extinctions obtained

from the three dilutions that were plated per sample. The mVWF activation factor of a plasma sample was calculated by dividing the slope of a plasma sample over the average of the slopes of plasma from mice injected with (wild type) mVwf/Myc cDNA only. The mVWF activation factor of conditioned medium samples was calculated by dividing the slope of a conditioned medium sample over the average of the slopes of conditioned media from cells transfected with wild type mVwf/Myc only.

### Statistical analysis

Graphic illustrations were generated using GraphPad Prism 8.0.1 (GraphPad Software, La Jolla, CA, USA). The Mann-Whitney *U* or Kruskal-Wallis test was used to investigate significance between two or three groups, respectively. Wilcoxon matched-pairs signed rank test or Friedman test was used to assess significance between before and after siRNA treatment. *P* < 0.05 was considered statistically significant. All data is represented as the median with the range, unless otherwise stated.

## Results

### *In vitro* selection of efficient and allele-specific siRNAs

Four siRNAs were designed to be fully complementary with mutant mVwf p.Val1316Met, and therefore had one mismatch with the wild type allele (Fig. 1A). Cotransfection of these siRNAs with either wild type mVwf/Myc or mutant mVwf-p.Val1316Met plasmids in HEK293 cells revealed that siRNA-1 efficiently inhibited total mVWF, but was not specific to the mutant allele. siRNA-2, -3 and -4 on the other hand were neither efficient nor very specific (Fig. 1B). It was previously shown that addition of one extra mismatch in an allele-specific siRNA might improve the specificity of the siRNA.<sup>18-20</sup> We therefore designed nine variations on siRNA-1 with additional mismatches at different positions of the siRNA (Fig. 1A) and transfected these siRNAs with either mVwf/Myc or mVwf-p.Val1316Met plasmids. Two of the newly designed siRNAs (siRNA-1-14G and siRNA-1-10U) were clearly more specific for the mutant allele, while retaining efficiency (Fig. 1B). These two siRNAs were selected for further experiments.

Cotransfections of mVwf/Myc and mVwf-p.Val1316Met plasmids with either siRNA-1-14G or siRNA-1-10U were performed to investigate whether competition between both alleles increases the specificity of the siRNAs and to observe whether the siRNAs could correct for a VWD type 2B phenotype *in vitro*. Clear inhibition of mutant mVWF-p.Val1316Met was already observed for both siRNAs at an siRNA concentration of 0.5 nM with no inhibition of wild type mVWF/Myc. Also at higher siRNA concentrations, we observed minor inhibition of mVWF/Myc, especially for siRNA-1-10U (Fig. 1C and 1D). Improvements in the VWD type 2B phenotype

were assessed in conditioned medium using the active mVWF ELISA that detects the open conformation of the mVWF A1 domain. Compared to siNEG treated cells, both siRNA-1-14G and siRNA-1-10U treated cells showed a decrease in the presence of dysfunctional mVWF by a decrease in the mVWF activation factor. siRNA-1-10U was superior over siRNA-1-14G. We therefore chose siRNA-1-10U as our lead compound for the *in vivo* experiments.

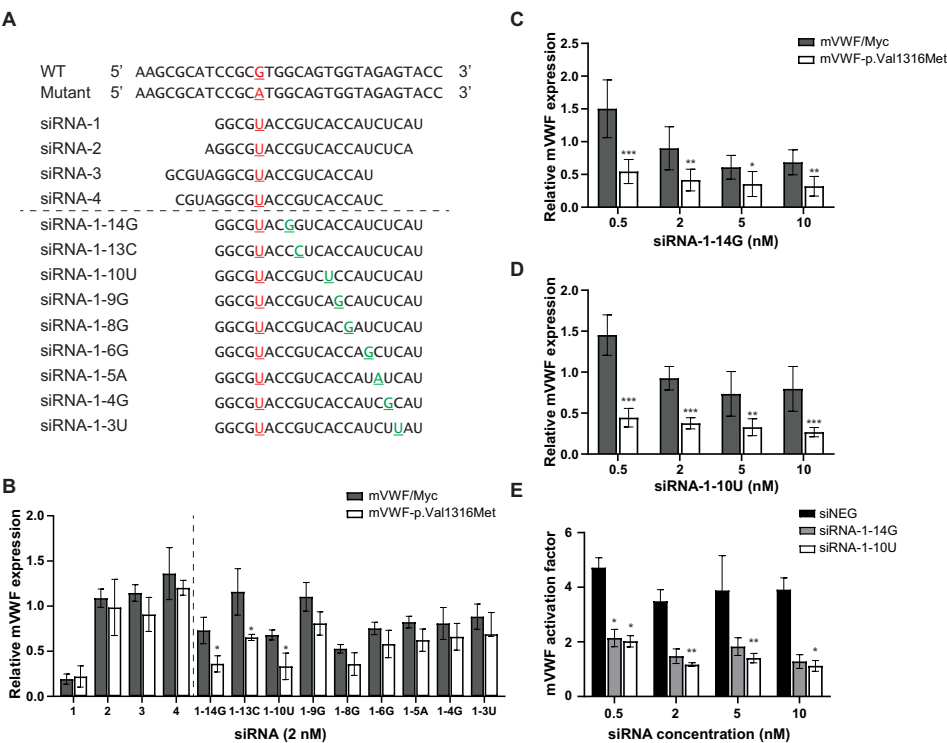


**Figure 1. *In vitro* siRNA screen in HEK293 cells.** (A) mRNA sequences of the wild type (WT) and mutant allele surrounding the nucleotide responsible for the p.Val1316Met mutation and the sequences of the antisense strand of siRNAs designed to target the p.Val1316Met mutation in mice. The red nucleotide in the siRNAs indicates the nucleotide that is complementary to the mutant allele, but is mismatched with the wild type allele. The green nucleotides indicate an extra mismatch that was incorporated in siRNA-1 to make the siRNA more specific to inhibit the mutant allele only. (B) siRNA screen in HEK293 cells. Bars represent mVWF levels measured in conditioned medium of HEK293 cells cotransfected with either mVwf/Myc or mVwf-p.Val1316Met plasmids and 2 nM siRNA, normalized to mVWF levels measured in conditioned medium of HEK293 cells cotransfected with either mVwf/Myc or mVwf-p.Val1316Met and a negative control siRNA (siNEG). Shown are the mean  $\pm$  1 SD of two independent experiments performed in duplicate, except for siRNA-1 that was tested three times in duplicate. Mann-Whitney, \*  $P < 0.05$  (C, D) Normalized mVWF/Myc and mVWF-p.Val1316Met protein levels measured in conditioned medium of HEK293 cells cotransfected with mVwf/Myc, mVwf-p.Val1316Met and (C) siRNA-1-14G or (D) siRNA-1-10U. siRNAs were transfected at concentrations of 0.5, 2, 5 and 10 nM and protein levels were normalized to the mVWF/Myc and mVWF-p.Val1316Met protein levels measured in conditioned medium of HEK293 cells cotransfected with mVwf/Myc, mVwf-p.Val1316Met and siNEG. Shown are the mean  $\pm$  1 SD of four independent experiments performed in duplicate. Mann-Whitney, \*  $P < 0.05$ , \*\*  $P < 0.01$ , \*\*\*  $P < 0.001$  (E) The mVWF activation factor measured in conditioned medium of HEK293 cells cotransfected with mVwf/Myc, mVwf-p.Val1316Met and siRNA-1-14G, siRNA-1-10U or siNEG. Shown are the mean  $\pm$  1 SD of two independent experiments performed in duplicate. Kruskal-Wallis, \*  $P < 0.05$ , \*\*  $P < 0.01$ . HEK293, Human Embryonic Kidney 293; mVWF, mouse von Willebrand factor; nM, nanomolar; siRNA, small interfering RNA; WT, wild type

### Generation of a heterozygous mouse model for VWD type 2B

Hydrodynamic gene transfer of mutant *mVwf* cDNA in *VWF<sup>-/-</sup>* mice has frequently been used to study phenotypic effects of known VWD mutations.<sup>17,21</sup> Most of these studies inject solely mutant *mVwf* cDNA, however in our approach of allele-specific inhibition of mutant *mVwf* we require a heterozygous model.<sup>22</sup> A heterozygous VWD type 2B mouse model was therefore generated by hydrodynamic injection of equal amounts of both *mVwf/Myc* and *mVwf-p.Val1316Met/HA* cDNA in *VWF<sup>-/-</sup>* mice. Four days after hydrodynamic injection, we observed equal expression of both products in plasma for all mice (Fig. 2A). This resulted in a deep drop in platelet count in five out of six mice as compared to mice expressing *mVWF/Myc* only ( $P = 0.052$ , Fig. 2B). No decreased platelet count was observed in one mouse, however, the total *mVWF:Ag* levels in this mouse were relative low (111%), which might have been insufficient to induce the VWD type 2B platelet phenotype. Furthermore, injection of both *mVwf/Myc* and *mVwf-p.Val1316Met/HA* cDNA in *VWF<sup>-/-</sup>* mice resulted in a significant increase in dysfunctional *mVWF* as represented by the increased *mVWF* activation factor, compared to *VWF<sup>-/-</sup>* mice injected with *mVwf/Myc* cDNA only ( $P < 0.01$ , Fig. 2C). This increase in the *mVWF* activation factor was also observed for the mouse without a decreased platelet count. The VWD type 2B platelet phenotype was confirmed by analysis of blood smears from the heterozygous VWD type 2B mice. These smears contained only small numbers of platelets, which were usually observed in aggregates (Fig. 2D). Liver sections were stained for *mVWF/Myc* and *mVWF-p.Val1316Met/HA* using anti-Myc and anti-HA antibodies to investigate the distribution of both gene products in the liver. Interestingly, the hepatocytes that internalized plasmid, always internalized both plasmids as represented by the colocalization of anti-Myc and anti-HA staining (Fig. 2E). Altogether, this indicates that the model used represents a true heterozygous mouse model for VWD.

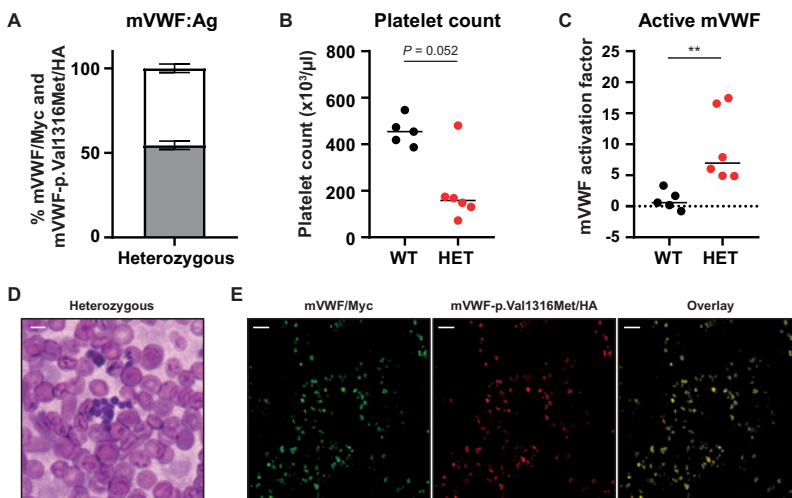


**Figure 2. Characteristics of heterozygous VWD type 2B mice.** (A) Distribution of *mVWF/Myc* (white bar) and

mVWF-p.Val1316Met/HA (grey bar) in plasma of VWF<sup>-/-</sup> mice four days after injection of equal quantities (25 µg) of both plasmids. Expression of both plasmids is approximately equal. (B) Platelet count and (C) mVWF activation factor of VWF<sup>-/-</sup> mice, four days after injection of mVwf/Myc (WT) cDNA only or co-injection of mVwf-p.Val1316Met/HA and mVwf/Myc (HET) cDNA. The horizontal lines in the graphs show the median and the dots represent single mice. Mann-Whitney, \*\*  $P < 0.01$  (D) Representative blood smear of a heterozygous VWD type 2B mouse, four days after injection of both mVwf/Myc and mVwf-p.Val1316Met/HA cDNA in VWF<sup>-/-</sup> mice. Platelet aggregates are observed. Bar represents 5 µm. (E) Staining of mVWF/Myc and mVWF-p.Val1316Met/HA in liver sections (5 µm thickness) generated from livers harvested from VWF<sup>-/-</sup> mice, four days after injection of both mVwf/Myc and mVwf-p.Val1316Met/HA. Stainings were performed using antibodies directed to Myc (green) and HA (red). Clear co-expression of both alleles is observed in all hepatocytes that express mVWF (colocalization in yellow). No hepatocytes are observed with mVWF/Myc or mVWF-p.Val1316Met/HA only. Bar represents 100 µm. HET, heterozygous; mVWF, mouse von Willebrand factor; WT, wild type

### ***In vivo correction of the VWD type 2B phenotype***

The heterozygous VWD type 2B mice showed a clear phenotype, four days after hydrodynamic injection of both mVwf/Myc and mVwf-p.Val1316Met/HA cDNA. To investigate whether the *in vitro* selected siRNA against mVwf p.Val1316Met (siRNA-1-10U) could correct the *in vivo* type 2B phenotype, we injected siRNA-1-10U in a concentration of 1 mg/kg, five days after hydrodynamic injection (N = 6). Two days after injection of siRNA-1-10U, a strong 88% knockdown of total mVWF was observed with a relative specificity of siRNA-1-10U towards the mutant allele (Table 1). Of note, also untreated heterozygous VWD type 2B mice showed on average 44% reduced mVWF:Ag levels at this day (Table 1). Specificity of siRNA-1-10U to inhibit the mutant allele is clearly indicated by the percentage of mVWF-p.Val1316Met/HA in plasma that decreased from 57% (55%-58%) to 32% (25%-42%) of total plasma mVWF ( $P < 0.05$ ; Fig. 3A). This coincided with a strong increase in platelet count ( $P = 0.063$ ; Fig. 3B). Platelet count was not increased for one mouse after siRNA-1-10U treatment. Another mouse did not show a decrease in platelet count after hydrodynamic injection, precluding the possibility of correction. Platelet size is known to be increased in mice injected with mVwf-p.Val1316Met cDNA.<sup>17,23</sup> The forward scatter in flow cytometry measurements could be used as an estimation of the platelet size. Previous work showed a platelet forward scatter of  $1.3 \times 10^5$  for VWF<sup>-/-</sup> mice injected with wild type mVwf cDNA.<sup>23</sup> In this study, heterozygous VWD type 2B mice showed a platelet forward scatter of  $4.1 \times 10^5$ . Injection of siRNA-1-10U did, however, not result in a decrease of the platelet forward scatter (Fig. 3C). The mVWF activation factor was decreased 1.6 fold after siRNA-1-10U injection, indicating a decrease of the presence of mutant constitutively active mVWF (N = 4; Fig. 3D). mVWF:Ag levels after siRNA injection were too low for two mice to determine the mVWF activation factor. One of these two mice was the mouse with a normal starting platelet count. The other mouse had a low starting platelet count that was increased after siRNA injection. Interestingly, the mouse without correction of the platelet count, did show amelioration in active mVWF with a 1.6 fold decrease in the mVWF activation factor.

**Table 1.** total mVWF, mVWF/Myc and mVWF-p.Val1316Met/HA antigen levels measured in plasma from VWF<sup>-/-</sup> mice hydrodynamically injected with mVwf/Myc and mVwf-p.Val1316Met/HA cDNA

siRNA	Concentration	Sex	Total mVWF (Myc+HA) (% of NMP)				mVWF/Myc (% of NMP)				mVWF-p.Val1316Met/HA (% of NMP)			
			Day -1	Day +2	Day +4	Day +7	Day -1	Day +2	Day +4	Day +7	Day -1	Day +2	Day +4	Day +7
siRNA-1-10U	1 mg/kg	M	1270	196			568	146			702	50		
siRNA-1-10U	1 mg/kg	F	472	22			198	13			274	9		
siRNA-1-10U	1 mg/kg	F	599	42			257	31			342	12		
siRNA-1-10U	1 mg/kg	F	2908	205			1230	140			1677	66		
siRNA-1-10U	1 mg/kg	F	1915	566			864	329			1051	238		
siRNA-1-10U	1 mg/kg	F	1364	151			577	101			787	50		
-	-	M	1284	1497			529	681			755	816		
-	-	M	253	136			101	61			153	75		
-	-	M	415	171			188	81			227	90		
-	-	F	1524	393			737	181			788	213		
-	-	F	2270	1422			1042	628			1228	795		
siRNA-1-10U	0.5 mg/kg	M	4091	830	418	336	1870	525	318	227	2220	305	100	109
siRNA-1-10U	0.5 mg/kg	M	2753	473	257	35	1333	369	209	28	1420	104	48	8
siRNA-1-10U	0.5 mg/kg	M	2888	449	307	401	1455	341	245	301	1433	109	61	100
siRNA-1-10U	0.5 mg/kg	M	1025	114	60	104	573	88	52	89	453	26	7	16
siRNA-1-10U	0.5 mg/kg	F	2849	256	132	209	1422	197	105	166	1427	59	27	43
-	-	M	4675	3263	3274	1151	2172	1539	1612	540	2503	1724	1663	610
-	-	F	380	78	77	90	192	45	40	43	188	33	36	47

F, female; M, male; mg/kg, milligram per kilogram; mVWF, mouse von Willebrand factor; NMP, normal mouse plasma; siRNA, small interfering RNA

Injections of 1 mg/kg siRNA-1-10U resulted in a deep knockdown of total mVWF and most mice had a mVWF expression of less than 200%, two days after siRNA-1-10U injection. It is therefore questionable whether the increase in platelet count after siRNA-1-10U injection was the result of decreased presence of mutant mVWF or that the total levels of mVWF were so low after siRNA-1-10U injection that the level of mutant type 2B VWF was too low to induce the VWD type 2B platelet phenotype. Therefore, we performed a second independent experiment where we injected heterozygous VWD type 2B mice with a lower dose of siRNA-1-10U (0.5 mg/kg; N = 5). A lower siRNA dose may not only lead to reduced inhibition of total mVWF, but potentially also improve specificity for the mutant allele. In this experiment, mice were followed for seven days after siRNA injection to assess the duration of siRNA-1-10U efficacy. Injection of 0.5 mg/kg siRNA-1-10U again led to a clear decrease in total mVWF plasma levels two days after siRNA injection, but the total mVWF:Ag levels were slightly higher (449%) than the total mVWF:Ag levels after injections of 1 mg/kg siRNA-1-10U (197%; Table 1). The percentage of mutant mVWF in plasma of the heterozygous VWD type 2B mice, one day before siRNA-1-10U injection was 50% (44%-54%). This decreased to 23% (22%-37%), 20% (12%-24%) and 21% (15%-33%),

two, four and seven days after siRNA-1-10U injection, respectively (Fig. 3E). Like with the 1 mg/kg dose, platelet counts increased two days after siRNA-1-10U injection (Fig. 3F). Remarkably, a further increase in platelet count was noted four and seven days after siRNA-1-10U injection ( $P < 0.01$ ; Fig. 3F). Also, as was observed after injection of 1 mg/kg siRNA-1-10U, we did not observe a decrease in platelet size two days after 0.5 mg/kg siRNA-1-10U injection. But a statistically significant decrease in platelet size was observed seven days after siRNA-1-10U injection ( $P < 0.01$ ; Fig. 3G). These beneficial effects in platelet phenotype coincided with a strong decrease in active VWF as represented by the decrease in the mVWF activation factor ( $P < 0.01$ ; Fig. 3H). Altogether, comparable results were obtained with siRNA doses of 1 and 0.5 mg/kg and these data indicate that allele-specific siRNAs can improve the VWD type 2B phenotype in mice.

## Discussion

Previously we have shown that allele-specific siRNAs are able to inhibit the production of mutant VWF with minor inhibition of wild type VWF *in vitro* and *ex vivo*.<sup>14-16</sup> In this study, we extended the proof of concept of allele-specific VWF inhibition to a heterozygous VWD type 2B mouse model. Heterozygous VWD type 2B mice were generated by hydrodynamic injection of both wild type and mutant *mVwf* cDNA (*mVwf*/Myc and *mVwf*-p.Val1316Met/HA). These mice phenotypically resemble human VWD type 2B with low platelet counts, increased platelet size and an increase in active mVWF. Clear phenotypic improvements were observed after injection of an siRNA that reduced the production of mVWF-p.Val1316Met/HA but had less affinity to inhibit the production of wild type mVWF/Myc.

As a model for the proof of principle of allele-specific inhibition of mutant mVWF *in vivo* we used VWF<sup>-/-</sup> mice hydrodynamically injected with mutant and wild type *mVwf* cDNA. Hydrodynamic gene transfer of *mVwf* cDNA results in hepatic VWF expression while VWF normally is produced in the endothelium and platelets.<sup>17,21</sup> Albeit artificial, hepatic VWF expression has the advantage that it can easily be targeted by siRNAs using InvivoFectamine, a commercially available liposomal formula suited for hepatic siRNA delivery.<sup>24</sup> The proof of concept of allele-specific inhibition in an *in vivo* setting can therefore easily be assessed. Drawback of the model is that hydrodynamic injection may result in supraphysiologic mVWF plasma levels and a wide range in expression levels (Table 1). This, however, did not seem to affect the siRNA efficacy, since the percentage of mutant mVWF after siRNA injection was comparable for all mice, irrespective of starting plasma mVWF levels (Fig. 3A, 3E).



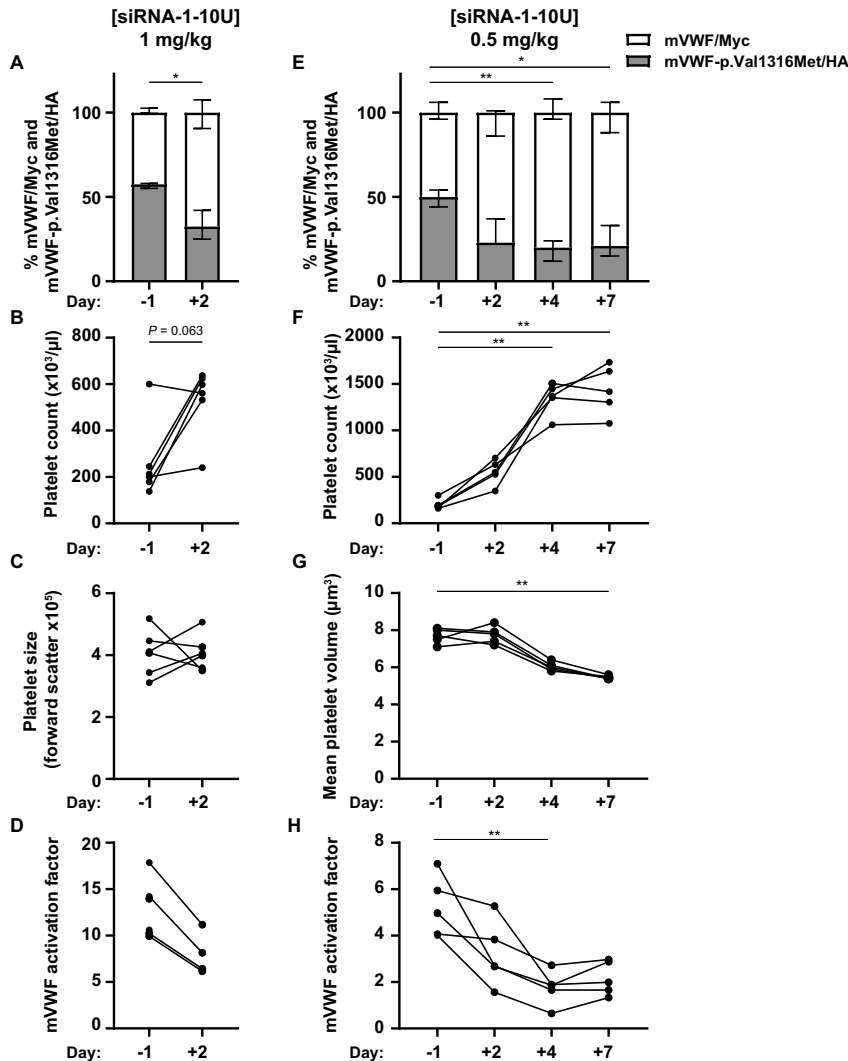


**Figure 3. Correction of the VWD type 2B phenotype.** (A-D) Phenotype improvement of heterozygous VWD type 2B mice injected with 1 mg/kg siRNA-1-10U. (A) Percentage of wild type mVWF/Myc (white bars) and mutant mVWF-p.Val1316Met/HA (grey bars) one day before and two days after siRNA-1-10U injection. Wilcoxon test, \*  $P < 0.05$ . (B) Platelet count measured in mice one day before and two days after siRNA-1-10U injection increased for four out of six mice. One mouse did not respond to siRNA treatment and one mouse had a high starting platelet count, which maintained constant. Wilcoxon test,  $P = 0.063$ . (C) Platelet size, estimated by the forward scatter determined by flow cytometry analysis, was unchanged two days after siRNA-1-10U treatment. (D) A decrease in the mVWF activation factor was observed two days after siRNA-1-10U treatment for four out of six mice. Two mice had too low total mVWF plasma levels to determine the mVWF activation factor. (E-H) Phenotype improvement of heterozygous VWD type 2B mice injected with 0.5 mg/kg siRNA-1-10U. (E) Percentage of wild type mVWF/Myc (white bars) and mutant mVWF-p.Val1316Met/HA (grey bars) one day before and two, four and seven days after siRNA-1-10U injection. Friedman test, \*  $P < 0.05$ , \*\*  $P < 0.01$ . (F) Platelet count increased for all mice after injection of siRNA-1-10U. Friedman test, \*\*  $P < 0.01$ . (G) Platelet size, determined by the veterinary cell counter, was not decreased two days after siRNA injection compared to one day before siRNA injection. Decreased platelet size was observed four and seven days after siRNA-1-10U injection. Friedman test, \*\*  $P < 0.01$ . (H) The mVWF activation factor decreased after siRNA-1-10U injection. Friedman test, \*\*  $P < 0.01$ . mg/kg, milligram per kilogram; mVWF, mouse von Willebrand factor; siRNA, small interfering RNA

Two independent experiments were performed in which siRNAs were injected in heterozygous VWD type 2B mice. With these experiments we aimed to investigate the siRNA concentration needed for allele-specific *mVwf* inhibition in our heterozygous mouse model. In a first experiment, mice were injected with 1 mg/kg siRNA-1-10U. This resulted in rather low total mVWF plasma levels, two days after siRNA injection. Although the plasma levels were rather low, all siRNA-injected mice showed improvements in the ratio of wild type over mutant mVWF and the mVWF activation factor. Furthermore, also platelet count was clearly increased for four out of six mice. It is, however, not possible to confirm that the increase in platelet count was the result of low levels of mutant mVWF or low levels of total mVWF. Especially since a heterozygous VWD type 2B mouse with low total mVWF levels (111%) showed a comparable platelet count to mice injected with wild type *mVwf* cDNA exclusively (Fig. 2B). Even though successful hydrodynamic injection was confirmed in this mouse by expression of both wild type mVWF (43%) and mutant mVWF-p.Val1316Met/HA (57%) and a 4.9 fold increase in the mVWF activation factor.

In a second experiment, we lowered the siRNA dose to 0.5 mg/kg to induce a less strong inhibition of mVWF. Decreasing the siRNA concentration might also lead to better discrepancy between wild type and mutant mVWF, since it is reasoned that a decreased siRNA concentration will first reduce binding of the siRNA to the untargeted allele. Although the sample size is too low to draw definite conclusions, the lower siRNA dose seemed to induce a slightly less strong inhibition of total mVWF and a slight increase in the ratio of wild type mVWF over mutant mVWF-p.Val1316Met compared to mice injected with 1 mg/kg siRNA (Table 1). We also reproduced the increase in platelet count with 0.5 mg/kg siRNA-1-10U. The increase in platelet count is observed in mice with total mVWF:Ag levels above 300%, which is sufficient to induce low platelet counts in *VWF*<sup>-/-</sup> mice injected with mutant *mVwf*-p.Val1316Met cDNA only. However, we have no evidence yet which VWF concentration is sufficient to induce low platelet counts in our heterozygous VWD type 2B mouse model and whether the increase in platelet count after injection of 0.5 mg/kg is indeed caused by a decrease in mutant mVWF and not by a decrease in total mVWF.

Interestingly, a striking increase in platelet count was observed four and seven days after siRNA-1-10U injection, which coincided with normal platelet size values. Platelet counts were even higher than generally is observed in mice hydrodynamically injected with wild type *mVwf* cDNA only.<sup>17,21</sup> This interesting result suggests that there is an increased platelet production, and that these platelets are not cleared through VWF-platelet complexes when there is less mutant VWF present. Besides the increase in platelet count, also a significant decrease in platelet size was observed four and seven days after siRNA injection. This was not observed two days after siRNA injection, which could be explained by the life-time of platelets in mice, which is about four to five days.<sup>25</sup> It might therefore be possible that the persistent increased

platelet size observed two days after siRNA injection, is representative of the large platelets that were still circulating from before the siRNA injection.

A limitation of this study is that we did not include a negative control siRNA in the mouse experiments. Inclusion of a negative control siRNA, preferably a mismatch control, is recommended to prove that the phenotypic improvements are caused by direct effects of the siRNA and to exclude possible off-target effects.<sup>26,27</sup> It is however unlikely that the phenotypic improvements in VWF itself, i.e. decreased mVWF activation factor, are due to an siRNA off-target effect. Also, the allele-specific knockdown effects are unlikely due to off-target effects. However, future studies with a mismatch negative control siRNA should prove that the correction of platelet count and size is indeed the effect of the allele-specific siRNA.

Although siRNA-1-10U has a higher affinity for mutant mVWF, we also observed downregulation of wild type mVWF/Myc *in vitro* and *in vivo*. The most ideal allele-specific siRNA should, however, not be able to inhibit wild type mVWF, even at a high siRNA concentration. Different chemical modification of the siRNA might improve siRNA specificity. In this study, siRNAs with the Locked Nucleic Acid (LNA) modifications were used. LNA is known to stabilize the siRNA and therefore makes the siRNA more potent to its target.<sup>28</sup> Different modifications, like 2' fluoro or 2' O-methyl ribose modifications, might further improve specificity.<sup>29</sup>

In this study, a VWD mouse model with hepatic expression of mVWF was used. This model provided support for the concept of allele-specific VWF inhibition to correct for VWD phenotypes. Extra-hepatic siRNA delivery, including endothelial siRNA delivery, is more challenging. Fortunately, recent studies have shown promising results in downregulation of several endothelial genes by lipid or polymeric nanoparticles.<sup>30-32</sup> Future studies in which these nanoparticles are used to target VWF mutations in recently developed knock-in VWD mouse models are needed to prove that the approach of allele-specific VWF inhibition to correct VWD phenotypes is also promising in a model where mutant VWF is expressed in endothelial cells instead of the hepatocytes.<sup>33</sup>

Altogether we have shown that injection of an allele-specific siRNA that targets liver-expressed mVwf-p.Val1316Met in a heterozygous VWD type 2B mouse model, leads to correction of the VWD type 2B platelet phenotype. Decreased percentage of mutant mVWF in plasma after siRNA injection was noted, which coincided with an increase in platelet count and a decrease in platelet size and the mVWF activation factor. These results are promising for further studies on RNA-targeted therapies for VWD. It is, however, important to show that no off-target effects are induced. This should be proven by an experiment in which a mismatch negative control is taken along. Furthermore, future studies in endothelial knock-in models for VWD are needed to further elucidate the impact of allele-specific *Vwf* inhibition *in vivo*.

## References

1. Goodeve AC. The genetic basis of von Willebrand disease. *Blood Rev.* 2010;**24**(3):123-134.
2. De Ceunynck K, De Meyer SF, Vanhoorelbeke K. Unwinding the von Willebrand factor strings puzzle. *Blood.* 2013;**121**(2):270-277.
3. Leebeek FW, Eikenboom JC. Von Willebrand's Disease. *N Engl J Med.* 2016;**375**(21):2067-2080.
4. de Jong A, Eikenboom J. Von Willebrand disease mutation spectrum and associated mutation mechanisms. *Thromb Res.* 2017;**159**:65-75.
5. Hulstein JJ, de Groot PG, Silence K, Veyradier A, Fijnheer R, Lenting PJ. A novel nanobody that detects the gain-of-function phenotype of von Willebrand factor in ADAMTS13 deficiency and von Willebrand disease type 2B. *Blood.* 2005;**106**(9):3035-3042.
6. Blenner MA, Dong X, Springer TA. Structural basis of regulation of von Willebrand factor binding to glycoprotein Ib. *J Biol Chem.* 2014;**289**(9):5565-5579.
7. Casari C, Du V, Wu YP, et al. Accelerated uptake of VWF/platelet complexes in macrophages contributes to VWD type 2B-associated thrombocytopenia. *Blood.* 2013;**122**(16):2893-2902.
8. Casonato A, Gallinaro L, Cattini MG, et al. Reduced survival of type 2B von Willebrand factor, irrespective of large multimer representation or thrombocytopenia. *Haematologica.* 2010;**95**(8):1366-1372.
9. Federici AB, Mannucci PM, Castaman G, et al. Clinical and molecular predictors of thrombocytopenia and risk of bleeding in patients with von Willebrand disease type 2B: a cohort study of 67 patients. *Blood.* 2009;**113**(3):526-534.
10. Kruse-Jarres R, Johnsen JM. How to treat type 2B von Willebrand disease. *Blood.* 2018;**131**(12):1292-1300.
11. Casonato A, Sartori MT, Bertomoro A, Fede T, Vasoin F, Girolami A. Pregnancy-induced worsening of thrombocytopenia in a patient with type IIB von Willebrand's disease. *Blood Coagul Fibrinolysis.* 1991;**2**(1):33-40.
12. Hultin MB, Sussman II. Postoperative thrombocytopenia in type IIB von Willebrand disease. *Am J Hematol.* 1990;**33**(1):64-68.
13. Ranger A, Manning RA, Lyall H, Laffan MA, Millar CM. Pregnancy in type 2B VWD: a case series. *Haemophilia.* 2012;**18**(3):406-412.
14. de Jong A, Dirven RJ, Oud JA, Tio D, van Vlijmen BJM, Eikenboom J. Correction of a dominant-negative von Willebrand factor multimerization defect by small interfering RNA-mediated allele-specific inhibition of mutant von Willebrand factor. *J Thromb Haemost.* 2018;**16**(7):1357-1368.
15. Casari C, Pinotti M, Lancellotti S, et al. The dominant-negative von Willebrand factor gene deletion p.P1127\_C1948delinsR: molecular mechanism and modulation. *Blood.* 2010;**116**(24):5371-5376.
16. de Jong A, Dirven RJ, de Boer CM, et al. Allele-specific Inhibition of VWF p.Cys1190Tyr in Patient-Derived Endothelial Colony Forming Cells Corrects the von Willebrand Disease Type 2A Phenotype. *Res Pract Thromb Haemost.* 2019;**3**(Suppl S1 (OC56.2)):113.
17. Rayes J, Hollestelle MJ, Legendre P, et al. Mutation and ADAMTS13-dependent modulation of disease severity in a mouse model for von Willebrand disease type 2B. *Blood.* 2010;**115**(23):4870-4877.

18. Miller VM, Xia H, Marrs GL, et al. Allele-specific silencing of dominant disease genes. *Proc Natl Acad Sci U S A*. 2003;**100**(12):7195-7200.
19. Noguchi S, Ogawa M, Kawahara G, Malicdan MC, Nishino I. Allele-specific Gene Silencing of Mutant mRNA Restores Cellular Function in Ullrich Congenital Muscular Dystrophy Fibroblasts. *Mol Ther Nucleic Acids*. 2014;**3**:e171.
20. Ohnishi Y, Tamura Y, Yoshida M, Tokunaga K, Hohjoh H. Enhancement of allele discrimination by introduction of nucleotide mismatches into siRNA in allele-specific gene silencing by RNAi. *PLoS One*. 2008;**3**(5):e2248.
21. Golder M, Pruss CM, Hegadorn C, et al. Mutation-specific hemostatic variability in mice expressing common type 2B von Willebrand disease substitutions. *Blood*. 2010;**115**(23):4862-4869.
22. Legendre P, Navarrete AM, Rayes J, et al. Mutations in the A3 domain of von Willebrand factor inducing combined qualitative and quantitative defects in the protein. *Blood*. 2013;**121**(11):2135-2143.
23. Casari C, Paul DS, Susen S, et al. Protein kinase C signaling dysfunction in von Willebrand disease (p.V1316M) type 2B platelets. *Blood Adv*. 2018;**2**(12):1417-1428.
24. Eguchi A, De Mollerat Du Jeu X, Johnson CD, Nektaria A, Feldstein AE. Liver Bid suppression for treatment of fibrosis associated with non-alcoholic steatohepatitis. *J Hepatol*. 2016;**64**(3):699-707.
25. Odell TT, McDonald TP. Life span of mouse blood platelets. *Proc Soc Exp Biol Med*. 1961;**106**:107-108.
26. Gagnon KT, Corey DR. Guidelines for Experiments Using Antisense Oligonucleotides and Double-Stranded RNAs. *Nucleic Acid Ther*. 2019;**29**(3):116-122.
27. Heestermans M, de Jong A, van Tilburg S, et al. Use of “C9/11 Mismatch” Control siRNA Reveals Sequence-Related Off-Target Effect on Coagulation of an siRNA Targeting Mouse Coagulation Factor XII. *Nucleic Acid Ther*. 2019;**29**(4):218-223.
28. Singh SK, Nielsen P, Koshkin AA, Wengel J. LNA (locked nucleic acids): synthesis and high-affinity nucleic acid recognition. *Chem Commun*. 1998(4):455-456.
29. Malek-Adamian E, Fakhoury J, Arnold AE, Martinez-Montero S, Shoichet MS, Damha MJ. Effect of Sugar 2',4'-Modifications on Gene Silencing Activity of siRNA Duplexes. *Nucleic Acid Ther*. 2019;**29**(4):187-194.
30. Dahlman JE, Barnes C, Khan O, et al. In vivo endothelial siRNA delivery using polymeric nanoparticles with low molecular weight. *Nat Nanotechnol*. 2014;**9**(8):648-655.
31. Khan OF, Kowalski PS, Doloff JC, et al. Endothelial siRNA delivery in nonhuman primates using ionizable low-molecular weight polymeric nanoparticles. *Sci Adv*. 2018;**4**(6):eaar8409.
32. Fehring V, Schaeper U, Ahrens K, et al. Delivery of therapeutic siRNA to the lung endothelium via novel Lipoplex formulation DACC. *Mol Ther*. 2014;**22**(4):811-820.
33. Adam F, Casari C, Prevost N, et al. A genetically-engineered von Willebrand disease type 2B mouse model displays defects in hemostasis and inflammation. *Sci Rep*. 2016;**6**:26306.



# 9

## General discussion and perspectives



This thesis described the proof of concept of allele-specific siRNA-mediated inhibition of dominant negative von Willebrand factor (VWF) alleles as a potential therapeutic approach for dominant negative von Willebrand disease (VWD). The main aim was to show that allele-specific siRNAs can efficiently inhibit the production of a mutant VWF allele, with no or minor inhibition of the wild type allele, and to show that this positively affects VWF function and VWD phenotypes. The potential of this approach was demonstrated in this thesis *in vitro* in Human Embryonic Kidney 293 cells (HEK293; Chapter 4), *ex vivo* in endothelial colony forming cells (ECFCs; Chapter 7) and *in vivo* in a VWD mouse model (Chapter 8). Also, the applicability of ECFCs as a valid model for VWD has been described in this thesis (Chapters 5 and 6).

## A new treatment approach for VWD

### ***Reasoning behind an alternative treatment strategy for VWD***

VWD is caused by qualitative or quantitative defects in VWF.<sup>1,2</sup> VWF is known as an important player in hemostasis, where VWF attracts platelets to sites of vascular damage, but also chaperones coagulation factor VIII in the circulation.<sup>3,4</sup> Current treatment options for VWD focus on increasing the levels of VWF in plasma, either by administration of DDAVP or VWF-containing concentrates.<sup>5,6</sup> Both treatment options are generally sufficient to stop or prevent bleeding after trauma or before a planned surgery. However, both DDAVP and VWF-containing concentrates do not address the source of the problem: production of mutant VWF subunits. The production and, subsequently secretion of mutant VWF, may be problematic in a subgroup of VWD patients. Especially these patients have a clinical unmet need and would benefit from a new treatment strategy that blocks the production of mutant VWF only.

The first group of patients with a clear clinical unmet need are VWD type 2B patients. VWD type 2B is caused by dominant negative mutations in the A1 domain of VWF.<sup>2</sup> These mutations result in a conformational change of the A1 domain allowing spontaneous platelet binding, even when VWF is in its closed conformation.<sup>7-9</sup> Because of the enhanced platelet binding, but also because of increased clearance of the VWF-platelet complex, patients develop variable degrees of thrombocytopenia.<sup>10</sup> Treatment of VWD type 2B with DDAVP results in an increased concentration of circulating mutant VWF that captures circulating platelets and induces a further decrease in platelet count.<sup>11,12</sup> Whereas, the VWF present in VWF-containing concentrates will perform normal hemostasis, but will not prevent the removal of platelets by mutant endogenous VWF. Stimuli that are released in certain stress situations, for example during infection, pregnancy or surgery, lead to an increased release of mutant VWF that may induce a deep thrombocytopenia with bleeding as a consequence.<sup>10,13-16</sup> In case of bleeding, patients may need platelet transfusion in addition to VWF-containing concentrates.<sup>13</sup>



A second group of VWD patients that would benefit from a new treatment strategy, are patients that develop severe intestinal bleeding, mainly caused by angiodysplasia (vascular malformations). This diathesis is more common in VWD patients than in the normal population.<sup>17,18</sup> Especially VWD patients with a complete absence of VWF or VWD patients lacking high molecular weight (HMW) VWF multimers have a higher chance of developing gastrointestinal bleeding.<sup>18-20</sup> Severe blood loss from the gastrointestinal tract may result in decreased hemoglobin which sometimes require transfusion of packed red blood cells.<sup>21,22</sup> In the past decade, it became evident that VWF plays a role in angiogenesis, the formation of new blood vessels, which explained the increased patient population that suffer from these severe intestinal bleeding.<sup>23</sup> However, the exact mechanism on how VWF affects angiogenesis and why especially patients that lack HMW VWF are prone to this diathesis remains to be elucidated. Bleeding from the gastrointestinal tract are not easily resolved by on demand treatment with VWF-containing concentrates.<sup>22,24</sup> Probably because the VWF-containing concentrates do not target the source of the problem: deficient or dysfunctional intracellular VWF and long-term exposure to mutant VWF. Long-term prophylaxis of VWF-containing concentrates does reduce the frequency of gastrointestinal bleeding, but comes along with the burden of frequent injections and a reduced quality of life.<sup>21,25-27</sup> A recent report on a small number of VWD patients suggests long-term use of Lenalidomide, a thalidomide analog with anti-angiogenic properties.<sup>28</sup> Although this proved relative successful in this group of patients, it again does not address the causative factor: mutant VWF. Also, another study in which thalidomide was used did not show any effects in the treatment of gastrointestinal bleeding.<sup>20</sup> In short, there is no clear-cut solution for treatment of angiodysplasia-related gastrointestinal bleeding.

Above, two groups of patients are described with a clear clinical unmet need. However, long-term correction of VWF is expected to also benefit patients without a clinical unmet need. Although the current treatment modalities are able to prevent or stop bleeding during surgery or after trauma, patients continuously live with the knowledge that bleeding can suddenly occur. Also, an ongoing bleed affects the patients daily life, and may require a hospital visit. This results in an overall reduced quality of life in VWD patients.<sup>29-32</sup>

### ***Expected effects of allele-specific inhibition of mutant VWF for VWD patients***

The expected effects of allele-specific inhibition of mutant VWF depends per type of VWD. Allele-specific inhibition of mutant VWF to correct VWD will only correct VWD caused by heterozygous dominant negative mutations, i.e. VWD types 1, 2A, 2B and 2M.<sup>33</sup> Both VWD type 2N and VWD type 3 result from homozygous mutations and will therefore not be corrected using our approach of allele-specific VWF inhibition.<sup>34</sup>

VWD type 1 is associated with decreased VWF plasma concentration that is the consequence of decreased VWF production, defective VWF secretion or an increased clearance of VWF.<sup>2</sup> A decreased VWF production is often the result of a heterozygous null allele, and cannot be corrected by allele-specific inhibition of mutant *VWF*.<sup>35</sup> Allele-specific inhibition of *VWF* in VWD type 1 patients with decreased VWF secretion is expected to improve the secretion of VWF from the endothelial cells.<sup>36-38</sup> When the secretion defect is severe, correction of this secretion defect by allele-specific siRNAs might even result in an overall increase in circulating VWF, even though the overall production of VWF is roughly halved after inhibition of the mutant allele. Allele-specific inhibition of mutant *VWF* in VWD type 1 patients with enhanced VWF clearance is expected to increase the survival of VWF.<sup>39</sup> When the clearance effect of a dominant negative mutation is strong, downregulation of the dominant negative allele might increase the overall VWF plasma concentration, irrespective of the reduced VWF production after siRNA inhibition.

VWD type 2A is associated with reduced HMW VWF, caused by either an intracellular multimerization defect or enhanced cleavage of VWF by ADAMTS13.<sup>2,40,41</sup> Inhibition of mutant VWF in both situations is expected to increase the concentration of the largest VWF multimers in the circulation. Since especially HMW VWF has the highest hemostatic activity, it is expected that downregulation of mutant VWF in VWD type 2A results in improved hemostatic function of VWF and amelioration of the patient's bleeding phenotype. In this thesis, we indeed proved in HEK293 cells (Chapter 4) and in ECFCs (Chapter 7) that inhibition of mutant VWF results in an increase in HMW VWF for two different mutations associated with an intracellular multimerization defect.<sup>42</sup> Whether this also results in improved hemostatic function remains to be answered from preclinical VWD models. Angiodysplasia-related intestinal bleeding are also common among VWD type 2A patients. Downregulation of the expression of mutant VWF is expected to have two advantages. First, it is thought to positively affect the process of angiogenesis and thereby reducing the chance of developing angiodysplasia. Second, inhibition of mutant VWF increases the hemostatic function of VWF and thus reduce the possibility to develop severe bleeding. It is however expected that a continuous correction of VWF is required to correct for the defective angiogenesis. Dysfunctional VWF does not only result in intestinal angiodysplasia, but also in vascular malformations elsewhere, like in the nailfold.<sup>43</sup> Long-term correction of dysfunctional VWF is therefore also expected to correct for vascular malformations at other sides than the intestine.

VWD type 2B is associated with reduced VWF survival, a decrease in HMW VWF, and variable degrees of thrombocytopenia.<sup>7,44</sup> The reduced VWF survival in VWD type 2B is suggested to be (at least partly) caused by an increased binding affinity of mutant VWF to the clearance receptor lipoprotein receptor-related protein 1 (LRP1) on macrophages.<sup>45,46</sup> Inhibition of mutant VWF is expected to result in decreased binding affinity of VWF to LRP1, thereby increasing the

survival of VWF. The decrease in HMW VWF is the result of increased clearance of the larger VWF multimers, but also by enhanced sensitivity of mutant VWF to proteolysis by ADAMTS13.<sup>47</sup> Inhibition of mutant VWF is expected to correct for both aspects. The thrombocytopenia in VWD type 2B is the consequence of increased clearance of the VWF-platelet complex, but also by modified megakaryocytopoiesis and affected platelet production.<sup>46,48,49</sup> Inhibition of mutant VWF is expected to reduce the binding of VWF to platelets, thereby reducing the elimination of circulating platelets. Indeed, in this thesis we show that inhibition of mutant VWF in a heterozygous VWD type 2B mouse model results in correction of decreased platelet counts (Chapter 8). Besides low platelet counts in VWD type 2B, also enlarged platelets and platelet aggregates are observed in VWD type 2B patients.<sup>49</sup> Furthermore, binding of mutant VWF to the platelets glycoprotein Ib $\alpha$  (GPIb $\alpha$ ) receptor was recently shown to affect platelet function by altered platelet signaling.<sup>50,51</sup> Inhibition of mutant VWF is therefore expected to increase platelet function as well. siRNA-targeting to the megakaryocytes and platelets is yet impossible, and therefore we do not expect to correct for defects caused by mutant VWF that is produced in the megakaryocytes/platelets. It is, however, unclear what the relative effects of megakaryocytes/platelet produced mutant VWF on platelet function and production are. We do know that VWF<sup>-/-</sup> mice expressing the VWD type 2B mutation mVWF p.Val1316Met after hydrodynamic injection show an increase in platelet size, while these mice do not express platelet mVWF.<sup>52</sup> We were able to reduce the platelet size after allele-specific inhibition of the production of mVWF p.Val1316Met (Chapter 8), which suggests that mainly circulating VWF, and not platelet VWF, is responsible for the affected platelet size and production.

VWD type 2M is caused by heterozygous mutations in the A1 domain of VWF that decreases the binding affinity of VWF to platelets GPIb $\alpha$  or collagen.<sup>2</sup> Inhibition of mutant VWF by allele-specific siRNAs are likely to improve the VWF activity. However, since less VWF will be produced and secreted, it is uncertain whether this will also result in increased platelet binding and improvements in the hemostatic function of VWF. Flow experiments on the platelet-binding activity in ECFCs derived from a VWD type 2M patient treated with allele-specific siRNA might reveal whether inhibition of mutant VWF in VWD type 2M improves the platelet binding capacity.

Besides the role of VWF in hemostasis, several additional roles for VWF have been elucidated in the past years. Examples are roles of VWF in inflammation, wound healing, and smooth muscle cell proliferation.<sup>53-55</sup> Although the consequences of mutant VWF on these processes are yet unknown, it is likely that it somehow affects VWD patients. Therefore, it is expected that inhibition of mutant VWF will not only improve the hemostatic function of VWF, but also roles of VWF beyond hemostasis.

### ***Clinical application of allele-specific siRNAs***

How siRNA-mediated therapeutics for VWD might be implemented in the clinic depends on the indication and the duration of siRNA efficacy. So far, there is no clinical data on the efficacy of siRNAs in the endothelium. However, recent data shows long-term efficacy of siRNAs in the human liver and in mouse endothelium.<sup>56-58</sup> Even though merely speculative, we assume a long-term siRNA efficacy when we envision the application of siRNA therapeutics in the clinic.

The most important indication for RNA therapeutics in VWD are surgery or dental procedures. An injection of allele-specific siRNA prior to a planned surgery is expected to prevent excessive bleeding during surgery, but could also help in the healing process after surgery.<sup>54</sup> Injection of an allele-specific *VWF* siRNA might be accompanied by administration of DDAVP. This would result in a short-term increase of fully functional VWF, enough to cover a planned intervention. In VWD type 2B patients, DDAVP could then safely be administered without the fear of provoking thrombocytopenia.<sup>12</sup> The approach would also allow the use of DDAVP in patients that are normally unresponsive to DDAVP, for example patients with a severe secretion defect.<sup>59</sup> These patients otherwise require replacement therapy.

Another important indication, also discussed above, are angiodysplasia-related gastrointestinal bleeding. Since administration of VWF-containing concentrates is usually not sufficient to stop bleeding and only long-term prophylaxis reduces the change of developing a gastrointestinal bleed<sup>21,24</sup>, it is expected that only long-term correction of VWF by allele-specific siRNAs would reduce the risk of developing angiodysplasia-related gastrointestinal bleeding.

When a VWD patient develops a bleed that requires replacement therapy, the patient is generally referred to a hospital for an injection with VWF-containing concentrates. In the Netherlands, patients are referred to specific hemophilia treatment centers, which are in a relative short distance for most people.<sup>60</sup> However, a visit to a hospital could be more complicated when living in a rural area or when on holidays. Long-term correction of VWF by allele-specific siRNAs might be a solution for those patients that normally would require regular monitoring but live in more rural areas, but also when a patient plans a holiday to a less accessible location.

## **RNA therapeutics**

We currently live at an exciting time with respect to siRNA therapeutics. In 2018, exactly 20 years after the first publication of RNA interference by Mello and Fire, the first siRNA drug (Patisiran) was approved by the U.S. Food and Drug administration.<sup>56</sup> Patisiran is an siRNA, encapsulated

in a lipid nanoparticle, that effectively target transthyretin (*TTR*) in the liver and ameliorates hereditary transthyretin amyloidosis. Clinical trials show effective *TTR* knockdown using an every-three week dosing regimen. Besides Patisiran, many other siRNA drugs have made it to clinical trials, and new approvals are to be expected in the coming years.<sup>61</sup> The most important results from these clinical trials for our work is the long-term efficacy of siRNAs after a single dose. For example, a single dose of Fitusiran, an N-acetylgalactosamine (GalNAC)-conjugated siRNA against antithrombin, anticipated as an alternative therapy for prevention of bleeding in hemophilia A and B patients, resulted in strong antithrombin inhibition for at least 30 days.<sup>62</sup> And even more remarkably, a single dose of Inclisiran, a GalNAC-conjugated siRNA against protease proprotein convertase subtilisin/kexin type 9 (*PCSK9*), anticipated for use in familial hypercholesterolemia patients, resulted in a very strong knockdown of *PCSK9*.<sup>63</sup> With even after 180 days, a *PCSK9* knockdown that ranged between 47.9 and 59.3%.<sup>63</sup> These are a few examples of the current successes in siRNA therapeutics and highlights the potential of this class of drugs in the treatment of genetic disorders, like VWD.

### ***Allele-specific siRNA target selection for diseases caused by dominant negative mutations***

siRNAs degrade mRNA sequences based on full complementarity. The cleavage ability of an siRNA might be disrupted when a mismatch is present between the siRNA and the mRNA.<sup>64</sup> This feature allows the design of allele-specific siRNAs: siRNAs that inhibit the production of one allele of a gene without affecting the other allele. Allele-specific inhibition requires nucleotide variations between two alleles of a gene. These variations can be a heterozygous dominant negative mutation, but also heterozygous single-nucleotide polymorphisms (SNPs) that are linked to the dominant negative mutation.<sup>65-68</sup> The use of a heterozygous dominant negative mutation as a target for an allele-specific siRNA is an ideal approach for diseases that result from a single mutation. However, VWD, and also many other diseases, result from many different mutations.<sup>2</sup> Therefore, to develop a treatment approach for dominant negative VWD that is to be applied to a large patient population and not only to individual patients, we have chosen for a SNP-based approach. SNPs are nucleotide substitutions that are present in the human genome.<sup>69</sup> Most of these SNPs are harmless and are not associated with disease. Also, some SNPs are common, meaning that in a population many people are heterozygous for these SNPs. We have made use of very common SNPs in the coding sequence of *VWF* and selected four SNPs for which about 74 percent of the Caucasian population is heterozygous.<sup>42</sup> The percentage of the population that is heterozygous for at least one of the four SNPs was only calculated for the Caucasian population, however also in other populations investigated in the 1000 genomes project, a high minor allele frequency was found for the same four SNPs.<sup>69</sup> An important remark is that two of the four selected SNPs, c.2365A|G and c.2385C|T, have been associated with *VWF* levels.<sup>70-72</sup> However, since the effects of the SNPs are minimal in

comparison to the effects of the dominant negative mutations that cause VWD, it is expected that allele-specific inhibition of these SNPs will have minor effect on the correction of the phenotype.

### ***Design of allele-specific siRNAs***

For the studies described in this thesis, siRNAs have been designed against both alleles of the four selected SNPs. In our studies, 21 nucleotide siRNAs with a dTdT overhang at the 3' end of the sense strand were used. Therefore, 21 siRNA designs are possible that include the SNP in the antisense strand. Ideally, all of these siRNAs are tested to identify the most efficient and allele-specific siRNA candidate. This is however a costly procedure. Fortunately, the twenty year experience in siRNA design resulted in algorithms that may predict the efficiency of siRNAs.<sup>73,74</sup> Therefore, only the three siRNAs with the highest predicted efficacy were designed and tested per SNP target (siRNA designs were done by Life Technologies).<sup>42</sup> Besides the requirement that the designed siRNAs should be efficient, the siRNAs should also be specific for its SNP target. Over the past two decades, many studies applied allele-specific inhibition and used SNPs or mutations to discriminate between two alleles, of which some examples can be observed in the following references.<sup>65,66,75-78</sup> Based on these studies, many thoughts have been generated on what factors are important in the discriminatory effect of siRNAs. Recently, also an online algorithm was published that should help in the design of allele-specific siRNAs (<http://crdd.osdd.net/servers/aspsirna/index.php>).<sup>79</sup> General ideas of discriminatory elements of allele-specific siRNAs are: (1) highest discrimination is observed when the mismatch is located in the center of the siRNA<sup>80,81</sup>, (2) the mismatch should not be located in the seed sequence<sup>80</sup>, (3) and better discrimination is observed when the mismatch involves a purine/purine mismatch between the siRNA and the target mRNA (i.e. adenine/guanine mismatch).<sup>80,82</sup> Interestingly, although most siRNAs that proved effective in our studies had their mismatch located in the center of the siRNA, we also observed effective allele-specific inhibition for siRNAs where the mismatch was not located in the center. Furthermore, none of our siRNA/mRNA interactions involved a purine/purine mismatch, nevertheless we observed a very good discrimination for several of our designed siRNAs. Especially siRNAs that target either *VWF* c.1451A or *VWF* c.1451G were very effective, while they create a pyrimidine/purine mismatch between the siRNA and mRNA sequence. Differences between our observations and previous observations may result from differences in the chemical modification of the siRNAs. We used siRNAs with a locked nucleic acid (LNA) modification that is known to increase the specificity of the siRNAs.<sup>83</sup> Furthermore, every mRNA sequence has a different secondary structure, which is likely to affect the binding of an siRNA to the mRNA. It is therefore difficult to predict the specificity of an allele-specific siRNA and it is suggested to test multiple allele-specific siRNA candidates for their effectiveness and not fully rely on prediction tools.

### **Previous work on allele-specific siRNAs**

In the past two decades, several *in vitro*, *ex vivo* and *in vivo* studies have been performed on the applicability of allele-specific siRNA-mediated inhibition of mutant alleles to improve disease phenotypes, and many with great success.<sup>65,66,75-78</sup> However, only one has made it to a clinical trial (NCT00716014), and this trial only involved one patient.<sup>84</sup> Although the trial was relative successful, no further studies have been reported on this treatment. Speculation can be done on the reason of this lack in progress. First of all, further development of drugs and start of clinical trials are expensive and will in general require a sponsor, most often a company. But, allele-specific inhibition of mutant alleles is a highly personalized treatment, and is only applicable to patients that harbor the specific mutation/SNP where the siRNA was designed for. For example, as for the only clinical trial that has been performed so far, the specific siRNA was applicable to only three patients.<sup>84</sup> The costs for further development will be excessive, and will never be reimbursed. Another complication of allele-specific siRNAs is that appropriate animal models are often unavailable to perform preclinical studies on. The chance that the sequence around a SNP or mutation is similar in mice and monkeys than it is in humans is small. Therefore, it is difficult to study the specific effects of siRNA-mediated inhibition in a preclinical model, unless humanized disease models are generated and used.<sup>85,86</sup> The last reason is the difficulty in the delivery of siRNAs to specific cell types. Naked unmodified siRNAs are cleared within 5 minutes from the body by the kidney, liver and spleen, and delivery vehicles are needed to get the siRNA to the desired cell type.<sup>87,88</sup> Targeting the hepatocytes of the liver is known to be relatively easy using lipid nanoparticles, or GalNAC conjugates.<sup>88,89</sup> However, the development of delivery vehicles to extra-hepatic organs remains challenging, and it is only for the last few years that effective delivery vehicles have been described and tested in preclinical models.<sup>57,58</sup> It is therefore expected that clinical trials using these delivery vehicles are not far from happening.

### **Extra-hepatic delivery of siRNAs**

Most successes of siRNA therapeutics so far use liver-targeted siRNAs. Hepatic siRNA targeting is relatively easy and is mainly achieved by complexation of siRNAs in liposomes, or conjugation of an internalizing peptide to the siRNA. Therefore, for the *in vivo* proof of concept of allele-specific inhibition of mutant *VWF* as a potential treatment approach for VWD, we choose a VWD mouse model with liver-expressed *VWF* (Chapter 8). Using Invivofectamine (Thermo Fisher Scientific, Carlsbad, CA, USA), a commercial available liposomal formula, we successfully inhibited *VWF* in the liver, and proved that allele-specific inhibition of mutant *VWF* in a heterozygous VWD type 2B mouse model improves the disease phenotype. Next, it is important to translate these results to a VWD model where mutant *VWF* is expressed in a physiological fashion, i.e. a mouse model with endothelial produced mutant *VWF*. The first challenge to overcome: how to get the siRNA into the endothelium. Fortunately, recent

developments show promising results in this respect. The most successful approaches that have been described use cationic lipids, polymeric nanoparticles or lipid-conjugated siRNAs.

The first studies that successfully achieved endothelial targeting by siRNAs used cationic lipids.<sup>58,90-96</sup> siRNAs are complexed in cationic lipids by electrostatic interactions between the negative siRNA and the cationic lipid.<sup>58</sup> An example of a cationic lipid is ActuFECT01, which showed good distribution to the endothelium.<sup>91-95</sup> ActuFECT01 has been used in the lipoplex formulation of Atu027, a lipoplex containing an siRNA that targets protein kinase N3. Atu027 even made it to a phase I clinical trial (NCT00938574) in the treatment of solid tumors.<sup>97</sup> A second phase I/II trial (NCT01808638) has been completed in March 2016, however no data have been presented on the results thus far. Although effective knockdown of endothelial genes was achieved, repeated dosing was needed to achieve robust *in vivo* knockdown and the siRNA also internalized in resident macrophages.<sup>96</sup> Changes in the composition of lipoplexes containing the cationic lipid ActuFECT01, resulted in the development of a novel lipoplex formulation: DACC.<sup>58</sup> DACC showed especially in the lung vasculature robust knockdown of several endothelial genes, and importantly, one dose of siRNA against *Tie2* resulted in *Tie2* knockdown for up to 21 days.<sup>58</sup> However, since the first report in 2014, no new data have been published on the use of DACC. The mechanism of internalization of cationic lipids is so far unknown. Fehring *et al* speculate that electrostatic interactions between the positively charged lipoplex and the negatively charged endothelium might result in internalization of these lipoplexes into the endothelium.<sup>58</sup>

A second class of endothelial targeted compounds are polymeric nanoparticles. Instead of cationic lipids, polymer lipids are used and siRNAs are complexed within a polymeric nanoparticle by multivalent interactions. Dahlman *et al* describe the formulation of 7C1, an ionizable low-molecular weight polymeric nanoparticles, and show that 7C1 forms stable siRNA/lipid particles.<sup>57</sup> 7C1 is especially effective in targeting lung endothelium, without targeting hepatocytes or immune cells. Robust knockdown of several endothelial genes was proven and siRNA-mediated inhibition of *ICAM2* was even retained for a period of 21 days after a single siRNA injection.<sup>57</sup> Follow-up studies showed effective endothelial gene knockdown by siRNAs encapsulated in 7C1 in lung endothelium, but also in tumor endothelium.<sup>98-100</sup> Also, effective delivery of microRNAs or antisense oligonucleotides against microRNAs (antimiR) was proven by the use of 7C1.<sup>101,102</sup> Furthermore, simultaneous inhibition of 5 genes was even feasible using multiplex 7C1 complexation.<sup>103,104</sup> Translation of the use of 7C1 from mouse models to non-human primates was recently reported.<sup>105</sup> Non-human primates were injected with an siRNA against *Tie2* and a strong downregulation of *Tie2* was observed on RNA level in the lung and the heart. This, however, did not result in reduced Tie2 protein levels. However, only three animals were used in the treatment group and the animals were sacrificed 48 hours after treatment, which might have been too early to observe effects on protein level. Most



importantly, no acute signs of toxicity were found after siRNA injection in the primates.<sup>105</sup>

Both cationic lipids and polymeric nanoparticles show highest internalizing capability in the lung endothelium. For our studies this is highly advantageous, since the lung endothelium is responsible for a large part of the VWF production.<sup>106</sup> The mechanism why especially the lung endothelium is targeted remains unknown.

The last strategy of endothelial targeting discussed here is lipid-conjugated siRNAs.<sup>87</sup> A recent study by Biscans *et al* show the biodistribution of a diverse panel of lipid-conjugated siRNAs to extra-hepatic tissues.<sup>107</sup> Several conjugates show, amongst others, distribution to the lungs and heart. This study did not look specifically into endothelial genes, and the potential of downregulation of genes in the lung and liver were yet limited. However, knowledge of the type of lipid conjugate that is internalized in the lungs and heart is a start for further research to the engineering of lipid conjugates that are internalized by endothelial cells. A limitation of lipid conjugates is that they do not specifically target a tissue and large parts of the injected lipid is cleared by the liver, kidney and spleen.<sup>107</sup> This increases the chance of off-target effects, however since VWF is only synthesized in the endothelium and megakaryocytes, this is unlikely to be a serious problem.

Altogether, serious progress has been made in the development of compounds to deliver siRNAs into the endothelium. Especially cationic lipids and polymeric nanoparticles show robust and long-term inhibition of endothelially genes *in vivo*, especially in the lung vasculature. These results are promising for future studies on RNA-targeted therapies for VWD.

### ***Improvements in siRNA modifications to make them more effective***

The siRNAs used in studies reported in this thesis are chemically modified by LNA modifications.<sup>83</sup> LNA is a modification in which the 2' oxygen and 4' carbon of the ribose are linked through an extra bridge. This extra bridge enforces the ribose in the 3'-endo conformation, which gives it a higher affinity to its target. It is also known for its strong ability to discriminate between nucleotides.<sup>108</sup> Besides LNA modifications, many more functional modifications were proven effective in siRNA design. Examples of widely used modifications are 2'-O-methyl, or 2'-fluoro modifications of the ribose ring. Testing siRNAs with different modifications might even lead to the improvements in the functionality of allele-specific siRNA candidates.<sup>109</sup>

### ***Alternatives to siRNA therapeutics***

As approach to inhibit mutant *VWF* alleles as an alternative treatment approach for dominant negative VWD, we have chosen to use allele-specific siRNAs. Allelic discrimination could, however, also be achieved by different approaches that target either mRNA or DNA. These approaches include the use of amongst others antisense oligonucleotides (AONs), miRNAs, CRISPR/Cas9 or Zinc Finger nucleases.<sup>86,110-112</sup> Application of AONs and Crispr/Cas9 will be discussed below.

AONs are short single-stranded DNA molecules that have the ability to target the pre-mRNA in the nucleus, or the mRNA in the cytoplasm.<sup>113</sup> The mechanism of action of antisense oligonucleotides depends on the modification of the AON sugar ring.<sup>114</sup> Unmodified AONs are rapidly degraded by nucleases.<sup>115</sup> Backbone chemistries are therefore necessary to limit nuclease degradation.<sup>115</sup> Furthermore, sugar ring modifications enhance the binding capacity of the AON to the (pre)-mRNA target.<sup>116</sup> mRNA cleavage after AON targeting is facilitated by RNase H, but this is not possible when all the nucleotide sugar rings are chemically modified. Therefore so-called ‘gapmers’ have been designed that contain fully modified outer nucleotides, but have an unmodified DNA core of eight to ten nucleotides.<sup>116</sup> This allows strong binding of the AON to the (pre)-mRNA, but may still facilitate RNase H dependent cleavage.<sup>114</sup> RNase H-mediated cleavage can take place both in the cytoplasm and in the nucleus, which allows the use of gapmers to target intronic sites as well.<sup>117</sup> Since many SNPs are located in intronic regions, more targets can be reached by gapmers than by siRNAs. Furthermore, chemically modified AON backbones are more easily taken up by a variety of cells in the body and can therefore be injected without the requirement of a delivery vehicle (naked delivery).<sup>118</sup> It is, however, questionable how much is internalized by the endothelium. Therefore, AON conjugation to an internalizing peptide or complexation of an AON in a lipid or polymeric nanoparticle might nevertheless be necessary for endothelial uptake. An allele-specific gapmer that targets a SNP in the 3' UTR of Huntingtin has made it to an ongoing Phase I/II clinical trial (NCT03225833). Preclinical data using this gapmer in a humanized Huntington's disease mouse model showed persistent AON activity for several weeks.<sup>86</sup> Also other clinical trials using non allele-specific AONs show long-term efficacy.<sup>85,119</sup> It is not possible to predict which of the two are superior, AONs or siRNAs. This can only be identified by experimental investigations. Difficulty with AON testing, however, is that thousands of different AONs with variable lengths and chemistries can be designed per target, and that algorithms that predict the efficacy of AONs are unavailable.<sup>114</sup> This is a costly investigation, and practically impossible to be investigated in an academic setting.

Both siRNAs and AONs target the mRNA or pre-mRNA and the effects they have on protein expression are therefore transient. Repeated dosing is necessary to maintain a sustained correction of the defective protein. In the past years, a tremendous amount of work has been

performed on the CRISPR/Cas9 (clustered regularly interspaced short palindromic repeats) system to modulate the genome.<sup>120</sup> The mechanism of CRISPR/Cas9 is based on a single guide RNA (sgRNA) designed to complement a DNA sequence and that directs Cas9 to the DNA. Cas9 is an endonuclease that induces a double-strand break in the DNA, which is repaired by non-homologous end joining, one of the cell's repair mechanisms. However, non-homologous end joining is an error-prone repair system, and often results in disrupted genetic sequences.<sup>121</sup> When an sgRNA is designed to target a dominant negative mutation or a SNP that is linked to a dominant negative mutation, allele-specific gene disruption may be accomplished.<sup>111,122,123</sup> One requirement is that Cas9 needs a PAM (Protospacer adjacent motif) sequence on the DNA to achieve DNA cleavage.<sup>120</sup> When this sequence is not present around the SNP or mutation, allele-specific CRISPR/Cas is not possible. However, recent investigations in different or modified Cas9 proteins have resulted in Cas9 proteins that can recognize different PAM sequences, thereby increasing the number of Cas9 targets.<sup>124,125</sup> An important and often discussed aspect of CRISPR/Cas9 are off-target effects.<sup>126,127</sup> Since CRISPR/Cas9 alters the DNA, off-target effects may have serious consequences. Good target selection and sgRNA design is therefore a crucial step in developing CRISPR/Cas9 therapeutics. However, allele-specific genome editing is restricted to sites of heterozygous variations, which limits the possibility for specific sgRNA designs and increases the chance of off-target effects. Another difficulty with the CRISPR system is the delivery of both a sgRNA and an mRNA encoding Cas9 or a Cas9 protein into endothelial cells.<sup>128</sup> Viral delivery might be possible, but does not selectively target endothelial cells. Recently, a polymeric nanoparticle was described that was able to deliver both the Cas9 mRNA and an sgRNA into endothelial cells. These results are promising and may have clinical potential.<sup>129</sup>

Altogether, besides siRNAs, several other approaches may successfully be used as alternative treatment approach for dominant negative VWD. Since the effects of siRNAs and AONs are transient, it is thought to be a more safe approach than CRISPR/Cas9 that permanently edits the DNA. Since VWD is not associated with a very low quality of life or a high mortality, permanent correction of VWD by CRISPR/Cas9 might not outweigh the potential risk of off-target effects. On the other hand, developments in CRISPR/Cas9 quickly emerge and it might therefore be possible that safe usage and specific delivery of CRISPR/Cas 9 is feasible in a few years from now.

## Cellular and animal models to study VWD

In this thesis, several different cellular and animal models have been used to study the effects of allele-specific siRNAs against *VWF*. First, siRNAs have been tested for their efficacy in VWF overexpressing HEK293 cells.<sup>42</sup> HEK293 cells do not endogenously produce VWF, but the cells

are easily transfected with VWF constructs, resulting in a functional VWF protein. HEK293 are commonly used cells in VWD research, since they are one of the only cells that are able to store VWF in pseudo-WPBs.<sup>130</sup> Many disease-causing mechanisms have thus been revealed by HEK293 cells that were transfected with mutant VWF constructs.<sup>131-133</sup> Since HEK293 cells are easy to transfect, they are also commonly used for the screening of siRNA candidates. To test the efficacy of the allele-specific siRNAs in our study, siRNAs were transfected in HEK293 cells together with two full-length VWF constructs that contained either of a SNP allele. To discriminate between the two gene products on protein level, Myc and HA peptide tags were added to the constructs. This allowed quantification of protein expression of both constructs separately by ELISA. Using this method, we successfully selected a set of siRNAs that discriminate between two *VWF* alleles.<sup>42</sup> A different and often used method to screen for effective siRNAs is to make use of reporter constructs containing a minigene.<sup>134-136</sup> These reporter constructs contain only part of the gene, for example one exon, and a luminescent gene. Cotransfection of the siRNA with two constructs containing either of an allelic variant and a different luminescent gene allows high-throughput screening of siRNA candidates. Although this is a fast approach to screen for siRNA candidates, it does not guarantee that the selected siRNAs are also effective when the full-length cDNA is present. This is probably due to a different secondary mRNA structure of the gene product of the minigene that affects the binding of the siRNA to the mRNA.<sup>137</sup> Although the process is slower, it is therefore suggested to screen the siRNAs in a system containing full-length *VWF* cDNA.

HEK293 cells proved a good model for the selection of siRNA candidates. However, they do not endogenously produce VWF. It was therefore important to translate the results from HEK293 cells to an endothelial cell line. As *ex vivo* endothelial disease model, we have chosen to use endothelial colony forming cells (ECFCs) that were isolated from a VWD patient and several healthy controls. ECFCs have proven a good *ex vivo* endothelial model to study VWD in the past years, and several disease causing mechanisms have been studied using these cells.<sup>38,138-141</sup> Although ECFCs are an interesting cell model to study disease-causing mechanisms, there are also many limitations associated with the use of these cells. First of all, the success rate of obtaining proliferative ECFC clones is low. A recent report stated a success rate of 70-75 percent<sup>142</sup>, however in our lab this success rate is somewhat lower and is just below 50 percent (unreported data). The reported success rate may be biased because many reports do not state the number of unsuccessful isolations. Also, when it is possible to isolate ECFCs from a specific donor, there is a high chance that this donor will consistently yield successful ECFC isolations. Repeated isolation from the same donor would increase the success rate of a lab. The success rate from our lab may be lower, since it does not include many repeated isolations. Then, ECFC lines that are successfully isolated show a large variation in morphology, proliferation rate, and VWF-related parameters.<sup>143,144</sup> Work described in this thesis indicate the isolation of sixteen ECFC colonies from six healthy donors and show that all cell lines

show a different cell density when they are at their maximum confluency.<sup>144</sup> This cell density significantly correlated with the VWF production of the cells. Since there is a clear variation observed between ECFC lines, it is impossible to compare two cell lines with each other that have completely different cellular characteristics. Care should therefore be taken to match a patient-derived ECFC line with a control ECFC line with the same cellular characteristics. Healthy control ECFCs have been used in this thesis to study the efficacy of allele-specific siRNAs against *VWF* SNPs. We show a good correlation of the effects of the allele-specific siRNAs in HEK293 cells and in ECFCs. This also validates that full-length VWF overexpressing HEK293 cells is a solid cell model to screen for siRNA candidates. Allele-specific siRNAs have also been tested for their ability to correct a VWD phenotype. In this experimental set-up, the effects of an allele-specific siRNA on a patient-derived ECFC line are compared to the effects seen in the same patient-derived ECFC line transfected with a negative control siRNA. ECFCs are thus used as their own internal control in this situation, and do not have to be compared to other ECFC lines with possible different cellular characteristics. For this thesis, allele-specific siRNAs have been tested on one patient-derived ECFC line. Unfortunately, several attempts to isolate ECFCs from other patients were not successful. Since the success rate of ECFC isolation is low, an alternative approach to obtain patient-specific cells is desirable. An alternative source of endothelial cells are induced pluripotent stem cells (iPSCs) differentiated to endothelial cells.<sup>145,146</sup> iPSCs can be generated from several cell types, amongst others urine, fibroblasts or peripheral blood mononuclear cells, with a much higher success rate than ECFC isolations.<sup>147,148</sup> Especially the increased success rate of obtaining endothelial cells from an easily accessible cell source is highly advantageous. However, the suitability of iPSC-derived endothelial cells as a model for VWD has yet to be proven.

For the *in vivo* proof of principle studies, a VWD mouse model with hepatic VWF expression was used. This well-established mouse model is generated by hydrodynamic injection of *Vwf* cDNA in *VWF*<sup>-/-</sup> mice on a C57BL/6J background.<sup>52</sup> Hydrodynamic injection of mutant *Vwf* cDNA have repeatedly proven to result in a phenotype resembling that of VWD patients.<sup>52,149</sup> Heterozygous VWD type 2B mice were generated by injection of both wild type and mutant *Vwf* cDNA. This resulted in a VWD type 2B phenotype resembling that of VWD type 2B patients. Delivery of siRNAs to induce allele-specific inhibition of mutant *VWF* was facilitated by Invivofectamine, a commercially available lipid nanoparticle that efficiently delivers siRNAs to the hepatocytes.<sup>150,151</sup> This proved to be a very successful method for the proof of principle of allele-specific inhibition of *VWF* to correct the VWD type 2B phenotype. However, to become clinically relevant, the effects of allele-specific siRNAs to ameliorate VWD phenotypes should be tested in a more physiological model with endothelial expressed mutant VWF. So far, only two VWD knock-in mouse models have been described.<sup>152,153</sup> One of these VWD knock-in mouse models harbour the mouse VWF p.Val1316Met mutation<sup>152</sup>, and it would be of great interest to investigate our siRNA designed to target the mouse VWF p.Val1316Met in

this mouse model using one of the recently developed endothelial delivery vehicles.<sup>57,58</sup> This allows to investigate the efficiency of (allele-specific) siRNAs to inhibit VWF in endothelial cells *in vivo*. Furthermore, it would be possible to test the effects of inhibition of mutant *VWF* on the hemostatic capacity of these mice, by for example a bleeding assay.<sup>152</sup> Unfortunately, these knock-in mouse models do not allow to test the SNP-targeted allele-specific siRNAs. This can only be achieved by (humanized) heterozygous mouse models containing the human SNPs, but also the human sequence around the SNPs.

## Concluding remarks

Inhibition of mutant *VWF* alleles by allele-specific siRNAs was proven in this thesis to be a promising strategy to correct for VWD phenotypes. Proof of principle studies were performed in HEK293 cells, ECFCs and a VWD mouse model with hepatic VWF production, and in all of these disease models a correction of VWD phenotypes was observed after transfection or injection of allele-specific siRNAs. The field of RNA therapeutics has made a tremendous progress in the past years with respect to siRNA design and endothelial siRNA delivery. These developments are promising regarding our approach of RNA therapeutics to correct VWD phenotypes. Studies in (humanized) preclinical models should further elucidate the potency of allele-specific siRNAs as alternative treatment approach for dominant negative VWD.

## References

1. Leebeek FW, Eikenboom JC. Von Willebrand's Disease. *N Engl J Med*. 2016;**375**(21):2067-2080.
2. de Jong A, Eikenboom J. Von Willebrand disease mutation spectrum and associated mutation mechanisms. *Thromb Res*. 2017;**159**:65-75.
3. Weiss HJ, Sussman II, Hoyer LW. Stabilization of factor VIII in plasma by the von Willebrand factor. Studies on posttransfusion and dissociated factor VIII and in patients with von Willebrand's disease. *J Clin Invest*. 1977;**60**(2):390-404.
4. Savage B, Saldivar E, Ruggeri ZM. Initiation of platelet adhesion by arrest onto fibrinogen or translocation on von Willebrand factor. *Cell*. 1996;**84**(2):289-297.
5. Mannucci PM, Ruggeri ZM, Pareti FI, Capitanio A. 1-Deamino-8-d-arginine vasopressin: a new pharmacological approach to the management of haemophilia and von Willebrands' diseases. *Lancet*. 1977;**1**(8017):869-872.
6. Peyvandi F, Kouides P, Turecek PL, Dow E, Berntorp E. Evolution of replacement therapy for von Willebrand disease: From plasma fraction to recombinant von Willebrand factor. *Blood Rev*. 2019;**38**:100572.
7. Ruggeri ZM, Pareti FI, Mannucci PM, Ciavarella N, Zimmerman TS. Heightened interaction between platelets and factor VIII/von Willebrand factor in a new subtype of von Willebrand's disease. *N Engl J Med*. 1980;**302**(19):1047-1051.
8. Hulstein JJ, de Groot PG, Silence K, Veyradier A, Fijnheer R, Lenting PJ. A novel nanobody that detects the gain-of-function phenotype of von Willebrand factor in ADAMTS13 deficiency and von Willebrand disease type 2B. *Blood*. 2005;**106**(9):3035-3042.
9. Blenner MA, Dong X, Springer TA. Structural basis of regulation of von Willebrand factor binding to glycoprotein Ib. *J Biol Chem*. 2014;**289**(9):5565-5579.
10. Federici AB, Mannucci PM, Castaman G, et al. Clinical and molecular predictors of thrombocytopenia and risk of bleeding in patients with von Willebrand disease type 2B: a cohort study of 67 patients. *Blood*. 2009;**113**(3):526-534.
11. Holmberg L, Nilsson IM, Borge L, Gunnarsson M, Sjorin E. Platelet aggregation induced by 1-desamino-8-D-arginine vasopressin (DDAVP) in Type IIB von Willebrand's disease. *N Engl J Med*. 1983;**309**(14):816-821.
12. Kruse-Jarres R, Johnsen JM. How I treat type 2B von Willebrand disease. *Blood*. 2018;**131**(12):1292-1300.
13. Hultin MB, Sussman II. Postoperative thrombocytopenia in type IIB von Willebrand disease. *Am J Hematol*. 1990;**33**(1):64-68.
14. Casonato A, Sartori MT, Bertomoro A, Fede T, Vasoin F, Girolami A. Pregnancy-induced worsening of thrombocytopenia in a patient with type IIB von Willebrand's disease. *Blood Coagul Fibrinolysis*. 1991;**2**(1):33-40.
15. Ranger A, Manning RA, Lyall H, Laffan MA, Millar CM. Pregnancy in type 2B VWD: a case series. *Haemophilia*. 2012;**18**(3):406-412.
16. Sato K, Kuroda S, Kobayashi T, et al. A case report on the successful perioperative management

- of hepatectomy for hepatocellular carcinoma in a patient with von Willebrand disease. *Int J Surg Case Rep.* 2018;**44**:131-134.
17. Tsagianni A, Comer DM, Yabes JG, Ragni MV. Von Willebrand disease and gastrointestinal bleeding: A national inpatient sample study. *Thromb Res.* 2019;**178**:119-123.
  18. Fressinaud E, Meyer D. International survey of patients with von Willebrand disease and angiodysplasia. *Thromb Haemost.* 1993;**70**(3):546.
  19. Castaman G, Federici AB, Tosi A, et al. Different bleeding risk in type 2A and 2M von Willebrand disease: a 2-year prospective study in 107 patients. *J Thromb Haemost.* 2012;**10**(4):632-638.
  20. Makris M, Federici AB, Mannucci PM, et al. The natural history of occult or angiodysplastic gastrointestinal bleeding in von Willebrand disease. *Haemophilia.* 2015;**21**(3):338-342.
  21. Zanon E, Vianello F, Casonato A, Girolami A. Early transfusion of factor VIII/von Willebrand factor concentrates seems to be effective in the treatment of gastrointestinal bleeding in patients with von Willebrand type III disease. *Haemophilia.* 2001;**7**(5):500-503.
  22. Botero JP, Pruthi RK. Refractory bleeding from intestinal angiodysplasias successfully treated with danazol in three patients with von Willebrand disease. *Blood Coagul Fibrinolysis.* 2013;**24**(8):884-886.
  23. Starke RD, Ferraro F, Paschalaki KE, et al. Endothelial von Willebrand factor regulates angiogenesis. *Blood.* 2011;**117**(3):1071-1080.
  24. Berntorp E, Windyga J. Treatment and prevention of acute bleedings in von Willebrand disease - efficacy and safety of Wilate, a new generation von Willebrand factor/factor VIII concentrate. *Haemophilia.* 2009;**15**(1):122-130.
  25. Federici AB, Castaman G, Franchini M, et al. Clinical use of Haemate P in inherited von Willebrand's disease: a cohort study on 100 Italian patients. *Haematologica.* 2007;**92**(7):944-951.
  26. Berntorp E, Petrini P. Long-term prophylaxis in von Willebrand disease. *Blood Coagul Fibrinolysis.* 2005;**16 Suppl 1**:S23-26.
  27. Abshire TC, Federici AB, Alvarez MT, et al. Prophylaxis in severe forms of von Willebrand's disease: results from the von Willebrand Disease Prophylaxis Network (VWD PN). *Haemophilia.* 2013;**19**(1):76-81.
  28. Khatir NV, Patel B, Kohli DR, Solomon SS, Bull-Henry K, Kessler CM. Lenalidomide as a novel therapy for gastrointestinal angiodysplasia in von Willebrand disease. *Haemophilia.* 2018;**24**(2):278-282.
  29. Atiq F, Mauser-Bunschoten EP, Eikenboom J, et al. Sports participation and physical activity in patients with von Willebrand disease. *Haemophilia.* 2019;**25**(1):101-108.
  30. de Wee EM, Fijnvandraat K, de Goede-Bolder A, et al. Impact of von Willebrand disease on health-related quality of life in a pediatric population. *J Thromb Haemost.* 2011;**9**(3):502-509.
  31. de Wee EM, Mauser-Bunschoten EP, Van Der Bom JG, et al. Health-related quality of life among adult patients with moderate and severe von Willebrand disease. *J Thromb Haemost.* 2010;**8**(7):1492-1499.
  32. Barr RD, Sek J, Horsman J, et al. Health status and health-related quality of life associated with



- von Willebrand disease. *Am J Hematol*. 2003;**73**(2):108-114.
33. Goodeve AC. The genetic basis of von Willebrand disease. *Blood Rev*. 2010;**24**(3):123-134.
  34. Allen S, Abuzenadah AM, Blagg JL, et al. Two novel type 2N von Willebrand disease-causing mutations that result in defective factor VIII binding, multimerization, and secretion of von Willebrand factor. *Blood*. 2000;**95**(6):2000-2007.
  35. Goodeve A, Eikenboom J, Castaman G, et al. Phenotype and genotype of a cohort of families historically diagnosed with type 1 von Willebrand disease in the European study, Molecular and Clinical Markers for the Diagnosis and Management of Type 1 von Willebrand Disease (MCMDM-1VWD). *Blood*. 2007;**109**(1):112-121.
  36. White-Adams TC, Ng CJ, Jacobi PM, Haberichter SL, Di Paola JA. Mutations in the D'D3 region of VWF traditionally associated with type 1 VWD lead to quantitative and qualitative deficiencies of VWF. *Thromb Res*. 2016;**145**:112-118.
  37. Groeneveld DJ, Wang JW, Mourik MJ, et al. Storage and secretion of naturally occurring von Willebrand factor A domain variants. *Br J Haematol*. 2014;**167**(4):529-540.
  38. Wang JW, Bouwens EA, Pintao MC, et al. Analysis of the storage and secretion of von Willebrand factor in blood outgrowth endothelial cells derived from patients with von Willebrand disease. *Blood*. 2013;**121**(14):2762-2772.
  39. Haberichter SL, Castaman G, Budde U, et al. Identification of type 1 von Willebrand disease patients with reduced von Willebrand factor survival by assay of the VWF propeptide in the European study: molecular and clinical markers for the diagnosis and management of type 1 VWD (MCMDM-1VWD). *Blood*. 2008;**111**(10):4979-4985.
  40. Tjernberg P, Vos HL, Castaman G, Bertina RM, Eikenboom JC. Dimerization and multimerization defects of von Willebrand factor due to mutated cysteine residues. *J Thromb Haemost*. 2004;**2**(2):257-265.
  41. Hassenpflug WA, Budde U, Obser T, et al. Impact of mutations in the von Willebrand factor A2 domain on ADAMTS13-dependent proteolysis. *Blood*. 2006;**107**(6):2339-2345.
  42. de Jong A, Dirven RJ, Oud JA, Tio D, van Vlijmen BJM, Eikenboom J. Correction of a dominant-negative von Willebrand factor multimerization defect by small interfering RNA-mediated allele-specific inhibition of mutant von Willebrand factor. *J Thromb Haemost*. 2018;**16**(7):1357-1368.
  43. Koscielny JK, Latza R, Mursdorf S, et al. Capillary microscopic and rheological dimensions for the diagnosis of von Willebrand disease in comparison to other haemorrhagic diatheses. *Thromb Haemost*. 2000;**84**(6):981-988.
  44. Casonato A, Daidone V, Galletta E, Bertomoro A. Type 2B von Willebrand disease with or without large multimers: A distinction of the two sides of the disorder is long overdue. *PLoS One*. 2017;**12**(6):e0179566.
  45. Wohner N, Legendre P, Casari C, Christophe OD, Lenting PJ, Denis CV. Shear stress-independent binding of von Willebrand factor-type 2B mutants p.R1306Q & p.V1316M to LRP1 explains their increased clearance. *J Thromb Haemost*. 2015;**13**(5):815-820.
  46. Casari C, Du V, Wu YP, et al. Accelerated uptake of VWF/platelet complexes in macrophages

- contributes to VWD type 2B-associated thrombocytopenia. *Blood*. 2013;**122**(16):2893-2902.
47. Rayes J, Hommais A, Legendre P, et al. Effect of von Willebrand disease type 2B and type 2M mutations on the susceptibility of von Willebrand factor to ADAMTS-13. *J Thromb Haemost*. 2007;**5**(2):321-328.
  48. Nurden P, Debili N, Vainchenker W, et al. Impaired megakaryocytopoiesis in type 2B von Willebrand disease with severe thrombocytopenia. *Blood*. 2006;**108**(8):2587-2595.
  49. Nurden P, Gobbi G, Nurden A, et al. Abnormal VWF modifies megakaryocytopoiesis: studies of platelets and megakaryocyte cultures from patients with von Willebrand disease type 2B. *Blood*. 2010;**115**(13):2649-2656.
  50. Casari C, Paul DS, Susen S, et al. Protein kinase C signaling dysfunction in von Willebrand disease (p.V1316M) type 2B platelets. *Blood Adv*. 2018;**2**(12):1417-1428.
  51. Casari C, Berrou E, Lebreton M, et al. von Willebrand factor mutation promotes thrombocytopathy by inhibiting integrin  $\alpha$ IIb $\beta$ 3. *J Clin Invest*. 2013;**123**(12):5071-5081.
  52. Rayes J, Hollestelle MJ, Legendre P, et al. Mutation and ADAMTS13-dependent modulation of disease severity in a mouse model for von Willebrand disease type 2B. *Blood*. 2010;**115**(23):4870-4877.
  53. Kaweck i C, Lenting PJ, Denis CV. von Willebrand factor and inflammation. *J Thromb Haemost*. 2017;**15**(7):1285-1294.
  54. Ishihara J, Ishihara A, Starke RD, et al. The heparin binding domain of von Willebrand factor binds to growth factors and promotes angiogenesis in wound healing. *Blood*. 2019;**133**(24):2559-2569.
  55. Worou M, Didelot M, Muczynski V, et al. von Willebrand Factor Induces Human Vascular Smooth Muscle Cells Proliferatio through Low Density Lipoprotein-related Receptor Protein 4 and  $\alpha$ v $\beta$ 3 Integrin. *Res Pract Thromb Haemost*. 2019;**3**(Suppl S1 (OC67.3)):44.
  56. Adams D, Gonzalez-Duarte A, O'Riordan WD, et al. Patisiran, an RNAi Therapeutic, for Hereditary Transthyretin Amyloidosis. *N Engl J Med*. 2018;**379**(1):11-21.
  57. Dahlman JE, Barnes C, Khan O, et al. In vivo endothelial siRNA delivery using polymeric nanoparticles with low molecular weight. *Nat Nanotechnol*. 2014;**9**(8):648-655.
  58. Fehring V, Schaeper U, Ahrens K, et al. Delivery of therapeutic siRNA to the lung endothelium via novel Lipoplex formulation DACC. *Mol Ther*. 2014;**22**(4):811-820.
  59. Castaman G, Lethagen S, Federici AB, et al. Response to desmopressin is influenced by the genotype and phenotype in type 1 von Willebrand disease (VWD): results from the European Study MCMDM-1VWD. *Blood*. 2008;**111**(7):3531-3539.
  60. de Wee EM, Leebeek FW, Eikenboom JC. Diagnosis and management of von Willebrand disease in The Netherlands. *Semin Thromb Hemost*. 2011;**37**(5):480-487.
  61. Setten RL, Rossi JJ, Han SP. The current state and future directions of RNAi-based therapeutics. *Nat Rev Drug Discov*. 2019;**18**(6):421-446.
  62. Pasi KJ, Rangarajan S, Georgiev P, et al. Targeting of Antithrombin in Hemophilia A or B with RNAi Therapy. *N Engl J Med*. 2017;**377**(9):819-828.

63. Ray KK, Landmesser U, Leiter LA, et al. Inclisiran in Patients at High Cardiovascular Risk with Elevated LDL Cholesterol. *N Engl J Med*. 2017;**376**(15):1430-1440.
64. Kunne T, Swarts DC, Brouns SJ. Planting the seed: target recognition of short guide RNAs. *Trends Microbiol*. 2014;**22**(2):74-83.
65. Lee JS, Chang EH, Koo OJ, et al. Pmp22 mutant allele-specific siRNA alleviates demyelinating neuropathic phenotype in vivo. *Neurobiol Dis*. 2017;**100**:99-107.
66. Leachman SA, Hickerson RP, Hull PR, et al. Therapeutic siRNAs for dominant genetic skin disorders including pachyonychia congenita. *J Dermatol Sci*. 2008;**51**(3):151-157.
67. Pfister EL, Kennington L, Straubhaar J, et al. Five siRNAs targeting three SNPs may provide therapy for three-quarters of Huntington's disease patients. *Curr Biol*. 2009;**19**(9):774-778.
68. Lombardi MS, Jaspers L, Spronkmans C, et al. A majority of Huntington's disease patients may be treatable by individualized allele-specific RNA interference. *Exp Neurol*. 2009;**217**(2):312-319.
69. Auton A, Brooks LD, Durbin RM, et al. A global reference for human genetic variation. *Nature*. 2015;**526**(7571):68-74.
70. Mufti AH, Ogiwara K, Swystun LL, et al. The common VWF single nucleotide variants c.2365A>G and c.2385T>C modify VWF biosynthesis and clearance. *Blood Adv*. 2018;**2**(13):1585-1594.
71. Smith NL, Chen MH, Dehghan A, et al. Novel associations of multiple genetic loci with plasma levels of factor VII, factor VIII, and von Willebrand factor: The CHARGE (Cohorts for Heart and Aging Research in Genome Epidemiology) Consortium. *Circulation*. 2010;**121**(12):1382-1392.
72. van Schie MC, de Maat MP, Isaacs A, et al. Variation in the von Willebrand factor gene is associated with von Willebrand factor levels and with the risk for cardiovascular disease. *Blood*. 2011;**117**(4):1393-1399.
73. Dar SA, Gupta AK, Thakur A, Kumar M. SMEpred workbench: A web server for predicting efficacy of chemically modified siRNAs. *RNA Biol*. 2016;**13**(11):1144-1151.
74. Vert JP, Foveau N, Lajaunie C, Vandenbrouck Y. An accurate and interpretable model for siRNA efficacy prediction. *BMC Bioinformatics*. 2006;**7**:520.
75. Novelli F, Lena AM, Panatta E, et al. Allele-specific silencing of EEC p63 mutant R304W restores p63 transcriptional activity. *Cell Death Dis*. 2016;**7**:e2227.
76. Nishimura AL, Shum C, Scotter EL, et al. Allele-specific knockdown of ALS-associated mutant TDP-43 in neural stem cells derived from induced pluripotent stem cells. *PLoS One*. 2014;**9**(3):e91269.
77. Courtney DG, Atkinson SD, Allen EH, et al. siRNA silencing of the mutant keratin 12 allele in corneal limbal epithelial cells grown from patients with Meesmann's epithelial corneal dystrophy. *Invest Ophthalmol Vis Sci*. 2014;**55**(5):3352-3360.
78. Loy RE, Lueck JD, Mostajo-Radji MA, Carrell EM, Dirksen RT. Allele-specific gene silencing in two mouse models of autosomal dominant skeletal myopathy. *PLoS One*. 2012;**7**(11):e49757.
79. Monga I, Qureshi A, Thakur N, Gupta AK, Kumar M. ASPsiRNA: A Resource of ASP-siRNAs Having Therapeutic Potential for Human Genetic Disorders and Algorithm for Prediction of Their Inhibitory Efficacy. *G3 (Bethesda)*. 2017;**7**(9):2931-2943.
80. Schwarz DS, Ding H, Kennington L, et al. Designing siRNA that distinguish between genes that

- differ by a single nucleotide. *PLoS Genet.* 2006;**2**(9):e140.
81. Miller VM, Xia H, Marrs GL, et al. Allele-specific silencing of dominant disease genes. *Proc Natl Acad Sci U S A.* 2003;**100**(12):7195-7200.
  82. Huang H, Qiao R, Zhao D, et al. Profiling of mismatch discrimination in RNAi enabled rational design of allele-specific siRNAs. *Nucleic Acids Res.* 2009;**37**(22):7560-7569.
  83. Singh SK, Nielsen P, Koshkin AA, Wengel J. LNA (locked nucleic acids): synthesis and high-affinity nucleic acid recognition. *Chem Commun.* 1998(4):455-456.
  84. Leachman SA, Hickerson RP, Schwartz ME, et al. First-in-human mutation-targeted siRNA phase Ib trial of an inherited skin disorder. *Mol Ther.* 2010;**18**(2):442-446.
  85. Ackermann EJ, Guo S, Benson MD, et al. Suppressing transthyretin production in mice, monkeys and humans using 2nd-Generation antisense oligonucleotides. *Amyloid.* 2016;**23**(3):148-157.
  86. Southwell AL, Skotte NH, Kordasiewicz HB, et al. In vivo evaluation of candidate allele-specific mutant huntingtin gene silencing antisense oligonucleotides. *Mol Ther.* 2014;**22**(12):2093-2106.
  87. Osborn MF, Khvorova A. Improving siRNA Delivery In Vivo Through Lipid Conjugation. *Nucleic Acid Ther.* 2018;**28**(3):128-136.
  88. Kulkarni JA, Witzigmann D, Chen S, Cullis PR, van der Meel R. Lipid Nanoparticle Technology for Clinical Translation of siRNA Therapeutics. *Acc Chem Res.* 2019;**52**(9):2435-2444.
  89. Springer AD, Dowdy SF. GalNAc-siRNA Conjugates: Leading the Way for Delivery of RNAi Therapeutics. *Nucleic Acid Ther.* 2018;**28**(3):109-118.
  90. Miyawaki-Shimizu K, Predescu D, Shimizu J, Broman M, Predescu S, Malik AB. siRNA-induced caveolin-1 knockdown in mice increases lung vascular permeability via the junctional pathway. *Am J Physiol Lung Cell Mol Physiol.* 2006;**290**(2):L405-413.
  91. Santel A, Aleku M, Keil O, et al. RNA interference in the mouse vascular endothelium by systemic administration of siRNA-lipoplexes for cancer therapy. *Gene Ther.* 2006;**13**(18):1360-1370.
  92. Santel A, Aleku M, Keil O, et al. A novel siRNA-lipoplex technology for RNA interference in the mouse vascular endothelium. *Gene Ther.* 2006;**13**(16):1222-1234.
  93. Aleku M, Schulz P, Keil O, et al. Atu027, a liposomal small interfering RNA formulation targeting protein kinase N3, inhibits cancer progression. *Cancer Res.* 2008;**68**(23):9788-9798.
  94. Aleku M, Fisch G, Mopert K, et al. Intracellular localization of lipoplexed siRNA in vascular endothelial cells of different mouse tissues. *Microvasc Res.* 2008;**76**(1):31-41.
  95. Santel A, Aleku M, Roder N, et al. Atu027 prevents pulmonary metastasis in experimental and spontaneous mouse metastasis models. *Clin Cancer Res.* 2010;**16**(22):5469-5480.
  96. Kaufmann J, Ahrens K, Santel A. RNA interference for therapy in the vascular endothelium. *Microvasc Res.* 2010;**80**(2):286-293.
  97. Schultheis B, Strumberg D, Santel A, et al. First-in-human phase I study of the liposomal RNA interference therapeutic Atu027 in patients with advanced solid tumors. *J Clin Oncol.* 2014;**32**(36):4141-4148.
  98. Yu Q, Tai YY, Tang Y, et al. BOLA (Bola Family Member 3) Deficiency Controls Endothelial Metabolism and Glycine Homeostasis in Pulmonary Hypertension. *Circulation.* 2019;**139**(19):2238-2255.

99. Jung K, Heishi T, Khan OF, et al. Ly6Clo monocytes drive immunosuppression and confer resistance to anti-VEGFR2 cancer therapy. *J Clin Invest*. 2017;**127**(8):3039-3051.
100. Koga JI, Nakano T, Dahlman JE, et al. Macrophage Notch Ligand Delta-Like 4 Promotes Vein Graft Lesion Development: Implications for the Treatment of Vein Graft Failure. *Arterioscler Thromb Vasc Biol*. 2015;**35**(11):2343-2353.
101. White K, Lu Y, Annis S, et al. Genetic and hypoxic alterations of the microRNA-210-ISCU1/2 axis promote iron-sulfur deficiency and pulmonary hypertension. *EMBO Mol Med*. 2015;**7**(6):695-713.
102. Wilson R, Espinosa-Diez C, Kanner N, et al. MicroRNA regulation of endothelial TREX1 reprograms the tumour microenvironment. *Nat Commun*. 2016;**7**:13597.
103. Sager HB, Dutta P, Dahlman JE, et al. RNAi targeting multiple cell adhesion molecules reduces immune cell recruitment and vascular inflammation after myocardial infarction. *Sci Transl Med*. 2016;**8**(342):342ra380.
104. Sager HB, Hulsmans M, Lavine KJ, et al. Proliferation and Recruitment Contribute to Myocardial Macrophage Expansion in Chronic Heart Failure. *Circ Res*. 2016;**119**(7):853-864.
105. Khan OF, Kowalski PS, Doloff JC, et al. Endothelial siRNA delivery in nonhuman primates using ionizable low-molecular weight polymeric nanoparticles. *Sci Adv*. 2018;**4**(6):eaar8409.
106. Yamamoto K, de Waard V, Fearn C, Loskutoff DJ. Tissue distribution and regulation of murine von Willebrand factor gene expression in vivo. *Blood*. 1998;**92**(8):2791-2801.
107. Biscans A, Coles A, Haraszti R, et al. Diverse lipid conjugates for functional extra-hepatic siRNA delivery in vivo. *Nucleic Acids Res*. 2019;**47**(3):1082-1096.
108. Lundin KE, Gissberg O, Smith CIE, Zain R. Chemical Development of Therapeutic Oligonucleotides. *Methods Mol Biol*. 2019;**2036**:3-16.
109. Malek-Adamian E, Fakhoury J, Arnold AE, Martinez-Montero S, Shoichet MS, Damha MJ. Effect of Sugar 2',4'-Modifications on Gene Silencing Activity of siRNA Duplexes. *Nucleic Acid Ther*. 2019;**29**(4):187-194.
110. Zeitler B, Froelich S, Marlen K, et al. Allele-selective transcriptional repression of mutant HTT for the treatment of Huntington's disease. *Nat Med*. 2019;**25**(7):1131-1142.
111. Yoshimi K, Kaneko T, Voigt B, Mashimo T. Allele-specific genome editing and correction of disease-associated phenotypes in rats using the CRISPR-Cas platform. *Nat Commun*. 2014;**5**:4240.
112. Miniarikova J, Zanella I, Huseinovic A, et al. Design, Characterization, and Lead Selection of Therapeutic miRNAs Targeting Huntingtin for Development of Gene Therapy for Huntington's Disease. *Mol Ther Nucleic Acids*. 2016;**5**:e297.
113. Wurster CD, Ludolph AC. Antisense oligonucleotides in neurological disorders. *Ther Adv Neurol Disord*. 2018;**11**:1756286418776932.
114. Shen X, Corey DR. Chemistry, mechanism and clinical status of antisense oligonucleotides and duplex RNAs. *Nucleic Acids Res*. 2018;**46**(4):1584-1600.
115. Dirin M, Winkler J. Influence of diverse chemical modifications on the ADME characteristics and toxicology of antisense oligonucleotides. *Expert Opin Biol Ther*. 2013;**13**(6):875-888.
116. DeVos SL, Miller TM. Antisense oligonucleotides: treating neurodegeneration at the level of RNA.

- Neurotherapeutics*. 2013;**10**(3):486-497.
117. Carroll JB, Warby SC, Southwell AL, et al. Potent and selective antisense oligonucleotides targeting single-nucleotide polymorphisms in the Huntington disease gene / allele-specific silencing of mutant huntingtin. *Mol Ther*. 2011;**19**(12):2178-2185.
  118. Godfrey C, Desviat LR, Smedsrod B, et al. Delivery is key: lessons learnt from developing splice-switching antisense therapies. *EMBO Mol Med*. 2017;**9**(5):545-557.
  119. Gaudet D, Brisson D, Tremblay K, et al. Targeting APOC3 in the familial chylomicronemia syndrome. *N Engl J Med*. 2014;**371**(23):2200-2206.
  120. Anders C, Niewoehner O, Duerst A, Jinek M. Structural basis of PAM-dependent target DNA recognition by the Cas9 endonuclease. *Nature*. 2014;**513**(7519):569-573.
  121. Jiang F, Doudna JA. CRISPR-Cas9 Structures and Mechanisms. *Annu Rev Biophys*. 2017;**46**:505-529.
  122. Courtney DG, Moore JE, Atkinson SD, et al. CRISPR/Cas9 DNA cleavage at SNP-derived PAM enables both in vitro and in vivo KRT12 mutation-specific targeting. *Gene Ther*. 2016;**23**(1):108-112.
  123. Monteys AM, Ebanks SA, Keiser MS, Davidson BL. CRISPR/Cas9 Editing of the Mutant Huntingtin Allele In Vitro and In Vivo. *Mol Ther*. 2017;**25**(1):12-23.
  124. Esvelt KM, Mali P, Braff JL, Moosburner M, Yaung SJ, Church GM. Orthogonal Cas9 proteins for RNA-guided gene regulation and editing. *Nat Methods*. 2013;**10**(11):1116-1121.
  125. Kleinstiver BP, Prew MS, Tsai SQ, et al. Engineered CRISPR-Cas9 nucleases with altered PAM specificities. *Nature*. 2015;**523**(7561):481-485.
  126. Hsu PD, Scott DA, Weinstein JA, et al. DNA targeting specificity of RNA-guided Cas9 nucleases. *Nat Biotechnol*. 2013;**31**(9):827-832.
  127. Lin Y, Cradick TJ, Brown MT, et al. CRISPR/Cas9 systems have off-target activity with insertions or deletions between target DNA and guide RNA sequences. *Nucleic Acids Res*. 2014;**42**(11):7473-7485.
  128. Liu C, Zhang L, Liu H, Cheng K. Delivery strategies of the CRISPR-Cas9 gene-editing system for therapeutic applications. *J Control Release*. 2017;**266**:17-26.
  129. Sago CD, Lokugamage MP, Paunovska K, et al. High-throughput in vivo screen of functional mRNA delivery identifies nanoparticles for endothelial cell gene editing. *Proc Natl Acad Sci U S A*. 2018;**115**(42):E9944-e9952.
  130. Michaux G, Hewlett LJ, Messenger SL, et al. Analysis of intracellular storage and regulated secretion of 3 von Willebrand disease-causing variants of von Willebrand factor. *Blood*. 2003;**102**(7):2452-2458.
  131. Tjernberg P, Castaman G, Vos HL, Bertina RM, Eikenboom JC. Homozygous C2362F von Willebrand factor induces intracellular retention of mutant von Willebrand factor resulting in autosomal recessive severe von Willebrand disease. *Br J Haematol*. 2006;**133**(4):409-418.
  132. Castaman G, Giacomelli SH, Jacobi P, et al. Homozygous type 2N R854W von Willebrand factor is poorly secreted and causes a severe von Willebrand disease phenotype. *J Thromb Haemost*.

- 2010;**8**(9):2011-2016.
133. Yadegari H, Driesen J, Pavlova A, et al. Insights into pathological mechanisms of missense mutations in C-terminal domains of von Willebrand factor causing qualitative or quantitative von Willebrand disease. *Haematologica*. 2013;**98**(8):1315-1323.
  134. Hohjoh H. Allele-specific silencing by RNA interference. *Methods Mol Biol*. 2010;**623**:67-79.
  135. Giorgio E, Lorenzati M, Rivetti di Val Cervo P, et al. Allele-specific silencing as treatment for gene duplication disorders: proof-of-principle in autosomal dominant leukodystrophy. *Brain*. 2019;**142**(7):1905-1920.
  136. Courtney DG, Atkinson SD, Moore JE, et al. Development of allele-specific gene-silencing siRNAs for TGFBI Arg124Cys in lattice corneal dystrophy type I. *Invest Ophthalmol Vis Sci*. 2014;**55**(2):977-985.
  137. Noguchi S, Ogawa M, Kawahara G, Malicdan MC, Nishino I. Allele-specific Gene Silencing of Mutant mRNA Restores Cellular Function in Ullrich Congenital Muscular Dystrophy Fibroblasts. *Mol Ther Nucleic Acids*. 2014;**3**:e171.
  138. Starke RD, Paschalaki KE, Dyer CE, et al. Cellular and molecular basis of von Willebrand disease: studies on blood outgrowth endothelial cells. *Blood*. 2013;**121**(14):2773-2784.
  139. Groeneveld DJ, van Bekkum T, Dirven RJ, et al. Angiogenic characteristics of blood outgrowth endothelial cells from patients with von Willebrand disease. *J Thromb Haemost*. 2015;**13**(10):1854-1866.
  140. Selvam SN, Casey LJ, Bowman ML, et al. Abnormal angiogenesis in blood outgrowth endothelial cells derived from von Willebrand disease patients. *Blood Coagul Fibrinolysis*. 2017;**28**(7):521-533.
  141. Bowman ML, Pluthero FG, Tuttle A, et al. Discrepant platelet and plasma von Willebrand factor in von Willebrand disease patients with p.Pro2808Leufs\*24. *J Thromb Haemost*. 2017;**15**(7):1403-1411.
  142. Smadja DM, Melero-Martin JM, Eikenboom J, Bowman M, Sabatier F, Randi AM. Standardization of methods to quantify and culture endothelial colony-forming cells derived from peripheral blood: Position paper from the International Society on Thrombosis and Haemostasis SSC. *J Thromb Haemost*. 2019;**17**(7):1190-1194.
  143. Sadler JE. von Willebrand factor in its native environment. *Blood*. 2013;**121**(14):2583-2584.
  144. de Jong A, Weijers E, Dirven R, de Boer S, Streur J, Eikenboom J. Variability of von Willebrand factor-related parameters in endothelial colony forming cells. *J Thromb Haemost*. 2019;**17**(9):1544-1554.
  145. Hu S, Zhao MT, Jahanbani F, et al. Effects of cellular origin on differentiation of human induced pluripotent stem cell-derived endothelial cells. *JCI Insight*. 2016;**1**(8).
  146. Orlova VV, Drabsch Y, Freund C, et al. Functionality of endothelial cells and pericytes from human pluripotent stem cells demonstrated in cultured vascular plexus and zebrafish xenografts. *Arterioscler Thromb Vasc Biol*. 2014;**34**(1):177-186.
  147. Staerk J, Dawlaty MM, Gao Q, et al. Reprogramming of human peripheral blood cells to induced

- pluripotent stem cells. *Cell Stem Cell*. 2010;**7**(1):20-24.
148. Raab S, Klingenstein M, Liebau S, Linta L. A Comparative View on Human Somatic Cell Sources for iPSC Generation. *Stem Cells Int*. 2014:768391.
149. Golder M, Pruss CM, Hegadorn C, et al. Mutation-specific hemostatic variability in mice expressing common type 2B von Willebrand disease substitutions. *Blood*. 2010;**115**(23):4862-4869.
150. Safdar H, Cheung KL, Salvatori D, et al. Acute and severe coagulopathy in adult mice following silencing of hepatic antithrombin and protein C production. *Blood*. 2013;**121**(21):4413-4416.
151. Eguchi A, De Mollerat Du Jeu X, Johnson CD, Nektaria A, Feldstein AE. Liver Bid suppression for treatment of fibrosis associated with non-alcoholic steatohepatitis. *J Hepatol*. 2016;**64**(3):699-707.
152. Adam F, Casari C, Prevost N, et al. A genetically-engineered von Willebrand disease type 2B mouse model displays defects in hemostasis and inflammation. *Sci Rep*. 2016;**6**:26306.
153. Sanda N, Suzuki N, Suzuki A, et al. Vwf K1362A resulted in failure of protein synthesis in mice. *Int J Hematol*. 2018;**107**(4):428-435.



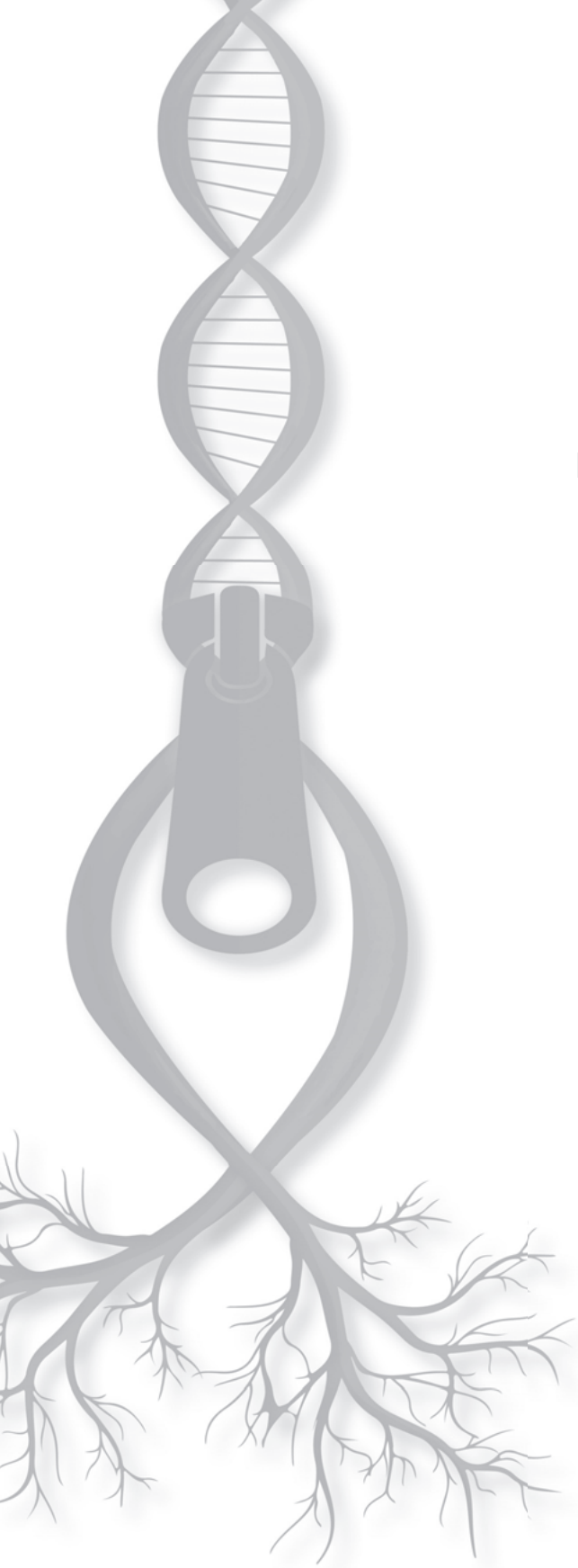




# 10

English summary

Nederlandse samenvatting



## English summary

Von Willebrand disease (VWD) is the most common inherited bleeding disorder that clinically affects around 1 in 10,000 people. Patients mainly develop mucocutaneous bleeding, i.e. bruises, epistaxis, gum bleeding and menorrhagia. The more severely affected patients may also develop joint bleeding, or bleeding from the gastrointestinal tract. Also, trauma, surgery or dental procedures may lead to critical bleeding events. VWD-related bleeding are caused by defects in von Willebrand factor (VWF), and these defects can be quantitative or qualitative of nature. VWF is a large multimeric protein that is produced by endothelial cells and megakaryocytes. In the endothelial cells, VWF multimers are generated by C-terminal dimerization of two VWF monomers in the endoplasmic reticulum, followed by N-terminal multimerization in the (trans)-Golgi network. The produced VWF multimers are subsequently stored in storage organelles, the Weibel-Palade bodies (WPBs), or constitutively secreted from the endothelial cells. Vascular damage triggers the release of VWF from the WPBs into the circulation. At sites of vascular injury VWF multimers attach to the exposed collagen, and the presence of shear in the circulation results in the elongation of VWF into ultra-large VWF strings. The primary function of VWF in hemostasis is the attraction of platelets to sites of vascular damage. These platelets can adhere via their glycoprotein Ib alpha receptors to the VWF A1 domain when it is in its open conformation. This subsequently results in platelet activation and platelet plug formation. The ultra-large VWF multimers are cleaved in the A2 domain of VWF by the metalloprotease ADAMTS13, leaving VWF multimers with variable sizes in the circulation. In the circulation, VWF is bound to coagulation factor VIII (FVIII), thereby enhancing the FVIII half-life. VWD can be the result of defects in all mechanisms described above. Patients with a partial VWF deficiency are categorized among VWD type 1. This partial deficiency may result from defective production, reduced secretion or enhanced clearance of VWF. VWD type 2A patients are associated with affected VWF multimers in the circulation, which may result from an intracellular dimerization or multimerization defect, or enhanced cleavage of VWF by ADAMTS13. The binding of VWF to platelets is affected in VWD type 2B and 2M, with enhanced VWF-platelet binding in VWD type 2B, and reduced VWF-platelet binding in VWD type 2M. VWD type 2N results from a decreased binding of VWF to coagulation FVIII. Lastly, VWD type 3 is associated with a complete absence of VWF.

VWD is a heterogeneous disease, and diagnosis of VWD can therefore be challenging. The workflow of VWD diagnosis is reviewed in **Chapter 2** of this thesis. Diagnosis starts with a questionnaire into the bleeding and family history. When a bleeding disorder is suspected, several general tests are performed to exclude different bleeding disorders. When these tests hint towards VWD, several VWD specific diagnostic tests are performed, which can confirm or exclude VWD. These include VWF:Ag, VWF activity, and FVIII activity measurements. When VWD is confirmed, specific tests are performed to correctly classify patients to the right VWD type. VWF multimerization, VWF-FVIII binding, VWF collagen binding, ristocetin induced

platelet aggregation (RIPA), and VWF propeptide measurements are examples of these subtyping tests.

VWD is mainly caused by mutations in VWF, and VWD-associated mutations have been described in literature since the beginning of the 1990s. An overview of all VWF mutations that have been described in literature until the beginning of 2017 have been reviewed in **Chapter 3**. In total, around 750 different variations have been described to be associated with VWD. From these variations, the disease-causing mechanism was proven for approximately 220 variants. The disease-causing mechanisms have been identified using cellular or animal disease models. These include transfection of mutant VWF constructs in heterologous cell systems, like Human Embryonic Kidney 293 (HEK293), COS-7 and AtT-20, or the use of hydrodynamic gene transfer of VWF plasmids in VWF deficient mice. Most mutations that cause VWD types 1, 2A, 2B and 2M are dominant negative mutations. This means that only one *VWF* allele has to be affected to cause VWD. VWD types 2N and 3 on the other hand are caused by recessive mutations.

Since most VWD is caused by dominant negative mutations in VWF, we hypothesized that inhibition of the mutant *VWF* allele only, without affecting the wild type *VWF* allele, would improve the function of VWF and ameliorate VWD phenotypes. And that this concept may be a new therapeutic approach for a subgroup of VWD patients for which the current treatment modalities are insufficient. As a tool to inhibit specific *VWF* alleles, we made use of small interfering RNAs (siRNAs). siRNAs are small double stranded RNA molecules that can be designed to complement mRNA sequences. Full complementarity between the siRNA and the mRNA will lead to mRNA degradation. A mismatch between the siRNA and the mRNA may preclude the possibility of mRNA degradation by the siRNA, and result in normal translation of this mRNA into protein. siRNAs can be designed to target the nucleotide variation causing the dominant negative mutation itself, or a single-nucleotide polymorphisms (SNP) that is linked to the dominant negative mutation. We have chosen for a SNP-based approach. SNPs as target were chosen since the ultimate goal is to develop a new treatment strategy for VWD, and it is not feasible to design and test siRNAs for the hundreds of mutations that cause VWD. Therefore, four SNPs with a high minor allele frequency in *VWF* have been selected and siRNAs have been designed to target both alleles of the four SNPs. With these four SNPs it is possible to target 74 percent of the population. In **Chapter 4**, we used VWF overexpressing HEK293 cells, as *in vitro* cell model to prove the concept of allele-specific inhibition of *VWF*. Using this cell model, we selected allele-specific siRNAs that efficiently inhibited the targeted allele, but were not or less efficient in inhibiting the untargeted allele. When these siRNAs targeted a *VWF* allele that also contained the dominant negative VWD type 2A mutation, p.Cys2773Ser, clear improvements were made in the VWF multimerization pattern.

Studies in HEK293 cells resulted in the selection of allele-specific siRNAs that were efficient and specific in inhibiting single *VWF* alleles. However, HEK293 cells do not produce VWF endogenously, and therefore we aimed to prove the concept of allele-specific *VWF* inhibition in a more physiologic disease model. Endothelial colony forming cells (ECFCs) are cultured endothelial cells that can be isolated from the mononuclear cell fraction of peripheral blood. These cells harbour the typical endothelial cobble stone morphology, and are positive for CD31 and CD146, and negative for CD14 and CD45. Since these cells can be isolated from patients, they are an interesting disease model to test the effectiveness of the allele-specific siRNAs to improve VWD phenotypes in a patient-specific environment. In **Chapter 5**, we optimized this model by characterization of 16 ECFC lines derived from six different ECFC isolations for several VWF-related parameters. We observed clear variations between the cell lines with respect to cell morphology and VWF production. Most importantly, we showed that all cell lines had a different cell density at maximum confluency and that this cell density at maximum confluency positively correlated with VWF production. Furthermore, the tube formation capacity in Matrigel, as a measure for the angiogenic potential, was higher in cells with a low maximum cell density and low VWF production. The possible underlying mechanism behind the variations in ECFCs was investigated by gene expression analysis of several aging and endothelial to mesenchymal transition (EndoMT) genes. ECFCs with a low maximum cell density showed higher expression of both aging and EndoMT markers. It is important to acknowledge the variations between ECFC lines and it is suggested to compare ECFC lines only when they have the same cellular characteristics. When investigating, for example, the effects of siRNA treatment in patient-derived ECFCs, the treated patient-derived ECFCs are compared to the same ECFCs treated with a negative control siRNA. In these situations, ECFCs are used as their own internal control, and can therefore be confidently used.

Before investigating (allele-specific) siRNA treatment in patient-derived ECFCs, it is important to first investigate the overall effects of siRNA-mediated downregulation of VWF on the function and processing of VWF in control ECFCs. Especially since it has been reported that siRNA-mediated inhibition of VWF in human umbilical vein endothelial cells result in shorter WPBs and enhanced secretion of VWF from the endothelial cells. We reproduced these previous findings in **Chapter 6**, but also showed that siRNA-mediated downregulation of VWF resulted in enhanced secretion of mainly low molecular weight VWF. These are important changes in VWF processing and multimerization to keep in mind when performing siRNA treatments in patient-derived ECFCs.

The ability of the allele-specific siRNAs that were selected from the screen in HEK293 cells (in Chapter 4) to also induce allele-specific *VWF* inhibition in ECFCs was investigated in **Chapter 7**. The siRNAs that were selected in Chapter 4 were also effective in ECFCs, which was proven both on protein and RNA level. Furthermore, we successfully isolated ECFCs from

a VWD type 2A patient with the VWF p.Cys1190Tyr mutation. These ECFCs showed decreased VWF collagen binding, defective VWF multimerization and defective processing of proVWF into VWF. Genotyping of this patient revealed that the patient is heterozygous for one of the four selected SNPs and downregulation of the mutant allele by targeting the associated SNP resulted in improvements in VWF collagen binding, VWF multimerization and the processing of VWF.

The effects of the allele-specific siRNAs were promising *in vitro* (HEK293) and *ex vivo* (ECFCs), but several aspects of VWD physiology cannot be investigated in these static cell systems. The last step of this research, discussed in **Chapter 8** of this thesis, was to investigate the effects of allele-specific inhibition of mutant *VWF* in a heterozygous VWD mouse model. Heterozygous VWD type 2B mice were generated by hydrodynamic injection of wild type and mutant mouse *Vwf* cDNA in VWF deficient mice. As a model mutation, the VWD type 2B mutation VWF p.Val1316Met, was chosen. This mutation is associated in men and mice with decreased platelet count, increased platelet size and an increase in VWF that circulates in its active conformation. Inhibition of the mutant allele only by an siRNA that targets the dominant negative mutation p.Val1316Met itself, resulted in clear phenotypic improvements, with correction of platelet count, normalization of platelet size and a decrease in VWF that circulated in its activated conformation.

Altogether, work described in this thesis proved that allele-specific inhibition of the production of mutant VWF by siRNAs results in improvements of several VWD phenotypes in HEK293 cells, in ECFCs and in a VWD mouse model. These results are promising for further development of allele-specific siRNAs as a new treatment strategy for VWD.

## Nederlandse samenvatting

De ziekte van von Willebrand is de meest voorkomende erfelijke bloedingsziekte met een prevalentie van ongeveer één patiënt op elke 10.000 mensen. Patiënten ontwikkelen voornamelijk blauwe plekken, bloedneuzen of tandvleesbloedingen. Vrouwen hebben vaak ook hevig menstrueel bloedverlies en sommige patiënten die ernstiger zijn aangedaan kunnen gewrichtsbloedingen of darmbloedingen ontwikkelen. Bloedingen na verwondingen zullen minder snel stoppen. Ook kunnen ernstige bloedingen ontstaan tijdens een operatie of kiesextractie. Bloedingen bij de ziekte van von Willebrand worden veroorzaakt door een defect in de von Willebrand factor (VWF). VWF is een groot multimeereiwit dat wordt aangemaakt in endotheelcellen, de cellen die de vaatwand bekleden, en in megakaryocyten, cellen van waaruit de bloedplaatjes worden aangemaakt. In dit proefschrift bespreken we alleen de rol van VWF dat in het endotheel wordt geproduceerd. Na synthese van VWF monomeren in het endotheel worden in het endoplasmatisch reticulum twee VWF monomeren aan elkaar gekoppeld, zodat er een VWF dimeer wordt gevormd. Vervolgens zullen de dimeren aan elkaar worden gekoppeld in het Golgicomplex en zo een groot VWF multimeer vormen. Deze VWF multimeren worden opgeslagen in endotheelcellen in langgerekte opslagorganellen, de zogenoemde Weibel-Palade-lichaampjes. Op het moment van vaatschade zullen signalen ervoor zorgen dat VWF uit het endotheel wordt uitgescheiden. Door de aanwezigheid van stroming in de bloedvaten zal het VWF zich uitrollen tot hele lange VWF strengen. Door het uitrollen van VWF kunnen bloedplaatjes binden, waardoor de bloedstelping start. VWF wordt vervolgens geknipt waardoor VWF vrij gaat circuleren in het bloed. In de circulatie heeft VWF nog een belangrijke functie: het binden van het stollingseiwit factor VIII. Doordat VWF en factor VIII gebonden aan elkaar zijn, zal factor VIII langer in het bloed kunnen blijven circuleren. De ziekte van von Willebrand kan worden veroorzaakt door een defect in alle mechanismen die hierboven beschreven zijn en patiënten worden aan de hand van het specifieke defect ingedeeld in verschillende typen van de ziekte van von Willebrand; types 1, 2A, 2B, 2M, 2N en 3. Patiënten met de ziekte van von Willebrand type 1 hebben een verlaagde concentratie van VWF in het bloed. Dit kan worden veroorzaakt door een verlaagde productie, maar ook door een defect in het uitscheiden van VWF uit het endotheel of doordat het VWF te snel door het lichaam wordt afgebroken. Patiënten met de ziekte van von Willebrand type 2A hebben afwijkende VWF multimeren. Dit kan worden veroorzaakt doordat het proces van dimerizatie of multimerizatie in de cellen zelf defect is, maar ook doordat de VWF multimeren te snel worden afgebroken. Bij de ziekte van von Willebrand type 2B en 2M is er een defect in het binden van VWF aan bloedplaatjes, met in type 2B een verhoogde binding aan bloedplaatjes, en in type 2M een verlaagde binding aan bloedplaatjes. Een verminderde binding van VWF aan stollingsfactor VIII is het onderliggende probleem in patiënten met de ziekte van von Willebrand type 2N. Als laatste, patiënten met type 3 van de ziekte van von Willebrand hebben een volledige afwezigheid van VWF in het bloed.



De ziekte van von Willebrand is een erg diverse ziekte, waardoor de diagnose lastig kan zijn. Het stappenplan in de diagnostiek van de ziekte van von Willebrand staat beschreven in **hoofdstuk 2** van dit proefschrift. Allereerst wordt de patiënt gevraagd naar de persoonlijke bloedingsgeschiedenis en of bloedingen ook veelvuldig voorkomen in de familie. Wanneer de mogelijkheid bestaat dat de patiënt een bloedingsziekte heeft, zullen er een aantal standaard testen worden afgenomen om andere bloedingsziekten uit te sluiten. Als de diagnose van de ziekte van von Willebrand aannemelijk is, zullen ziektespecifieke testen worden afgenomen. In deze testen wordt de VWF concentratie en VWF en factor VIII activiteit in het plasma van de patiënt bepaald. Als de diagnose van de ziekte van von Willebrand is gesteld, zullen nog een aantal extra testen worden afgenomen om de specifieke type van de ziekte te bepalen. Voorbeelden van deze testen zijn het analyseren van de VWF multimeren en de binding van VWF aan factor VIII en collageen.

De ziekte van von Willebrand wordt in de meeste gevallen veroorzaakt door mutaties in VWF. Al vanaf het begin van de jaren 90 van de vorige eeuw zijn mutaties in VWF beschreven in de literatuur. In **hoofdstuk 3** is een overzicht gemaakt van alle mutaties in VWF die beschreven zijn tot het begin van 2017. In totaal zijn er ongeveer 750 verschillende variaties in VWF gekoppeld aan de ziekte van von Willebrand. Van deze variaties is voor 220 mutaties daadwerkelijk bewezen dat deze tot de ziekte van von Willebrand leiden. Bewijs hiervoor is geleverd door het bestuderen van deze mutaties in ziektemodellen. Veelvuldig gebruikte ziektemodellen zijn cellen waarin het mutant VWF tot expressie wordt gebracht. Ook is er in de literatuur gebruik gemaakt van VWF deficiënte muizen waarin het VWF tot expressie werd gebracht. De meeste mutaties die de ziekte van von Willebrand type 1, 2A, 2B en 2M veroorzaken zijn dominant negatieve mutaties. Dit betekent dat maar 1 van de 2 VWF allelen defect hoeft te zijn om de ziekte te veroorzaken. De ziekte van von Willebrand type 2N en 3 wordt veroorzaakt door recessieve mutaties. In het geval van recessieve mutaties moeten beide VWF allelen zijn aangedaan om de ziekte te krijgen.

Aangezien de ziekte van von Willebrand meestal wordt veroorzaakt door dominant negatieve mutaties, hadden we als hypothese dat het remmen van het mutante VWF allel, zonder het gezonde 'wild type' allel te remmen, een positief effect heeft op de functie van VWF en dat daarbij ook het fenotype van de ziekte van von Willebrand zou kunnen verbeteren. Dit idee zou een eventuele nieuwe therapeutische benadering zijn voor een populatie van patiënten met de ziekte van von Willebrand die onvoldoende baat hebben bij de huidige therapieën. Voor het remmen van specifiek het mutante VWF allel hebben we in dit proefschrift gebruik gemaakt van zogenoemde 'small interfering' RNAs (siRNAs). siRNAs zijn korte dubbelstrengs RNA moleculen die ontworpen worden volledig complementair aan een 'messenger' RNA (mRNA) sequentie. Volledige complementariteit van het siRNA aan een mRNA zal leiden tot afbraak van het mRNA. Hierdoor zal er geen eiwit geproduceerd kunnen worden. Echter kan

een ‘mismatch’ tussen een siRNA en mRNA ervoor zorgen dat de siRNA niet goed kan binden, waardoor de siRNA zijn functie niet goed kan uitvoeren. Hierdoor kan het mRNA normaal worden omgezet in eiwit. Om onderscheid te maken tussen het mutante en gezonde *VWF* allel moet een siRNA worden ontworpen tegen een heterozygote variatie in het *VWF* gen. Dit zou de genetische variatie kunnen zijn die leidt tot de dominant negatieve mutatie zelf, aangezien de patiënt altijd heterozygoot is voor deze mutatie. Een andere mogelijkheid is om gebruik te maken van heterozygote ‘single nucleotide variaties’ (SNPs). SNPs zijn genetische variaties die van nature voorkomen in ons DNA, maar die niet perse geassocieerd zijn met ziekten. Sommige van deze SNPs komen heel vaak voor, wat betekent dat veel personen in een populatie heterozygoot zijn voor deze SNPs. Door een siRNA te gebruiken tegen een heterozygote SNP die op hetzelfde allel ligt als de dominant negatieve mutatie, zou het dus ook mogelijk kunnen zijn om de productie van het mutante allel te remmen. In dit proefschrift is gekozen om siRNAs te ontwerpen tegen deze veelvoorkomende SNPs, aangezien we met een gering aantal SNPs een groot gedeelte van de populatie kunnen bestrijken. Als we elke afzonderlijke mutatie willen gebruiken als target voor de siRNAs, zijn (gezien de grote hoeveelheid aan *VWF* mutaties) veel meer siRNA ontwerpen nodig. In een therapeutisch perspectief zou het niet haalbaar zijn al die siRNAs te testen. Daarom hebben we voor dit proefschrift gebruik gemaakt van vier verschillende SNPs en zijn er siRNAs ontworpen voor beide allelen van deze vier SNPs. Met deze vier SNPs is het mogelijk om 74 procent van de populatie te bereiken. In **hoofdstuk 4** hebben we getest of de siRNAs die we hebben ontworpen, daadwerkelijk effectief zijn. Dit is gedaan in ‘human embryonic kidney’ 293 (HEK293) cellen, cellen die van nature geen *VWF* aanmaken. Door het tegelijkertijd transfecteren van twee *VWF* plasmiden met twee verschillende SNP allelen, en een siRNA die één de twee *VWF* allelen zou moeten remmen, hebben we gekeken of de ontworpen allel specifieke siRNAs functioneel waren. Hierdoor hebben we een set van siRNAs kunnen selecteren die efficiënt en specifiek *VWF* allelen konden remmen. Op het moment dat we de siRNAs aanboden aan cellen die zowel het wild type *VWF* als een mutant (type 2A) *VWF* produceerden, zagen we de productie van het mutante *VWF* verlagen en ook een duidelijke verbetering van het multimerisatiefenotype.

De studies in HEK293 cellen waren heel effectief voor het selecteren van effectieve siRNAs. Echter produceren deze cellen geen *VWF* van nature. Om deze reden wilden we ook in een ander, fysiologisch relevanter, celtype het bewijs leveren dat allel specifieke siRNAs effectief zijn in het verbeteren van een von Willebrand fenotype. ‘Endothelial colony forming cells’ (ECFCs) zijn gekweekte endotheelcellen die uit bloed kunnen worden geïsoleerd en ook daadwerkelijk endotheelspecifieke eigenschappen hebben. Aangezien deze cellen ook uit patiënten kunnen worden geïsoleerd, is het een aantrekkelijk ziektemodel om de allel specifieke siRNAs in uit te testen. In **hoofdstuk 5** optimaliseren we het gebruik van de ECFCs als ziektemodel. Voor de optimalisatie hebben we 16 verschillende ECFC lijnen, die we hebben kunnen isoleren van zes verschillende gezonde proefpersonen, gekarakteriseerd op allerlei *VWF*-gerelateerde eigenschappen. We merkten veel verschillen op tussen de cellen, zowel op

het gebied van de celmorphologie als de productie van VWF door de cellen. Een belangrijke associatie die we vonden was de associatie tussen de celdichtheid en VWF productie, waarbij ECFC lijnen met een hoge celdichtheid (kleinere cellen) meer VWF produceerden dan cellen met een lage celdichtheid (grote cellen). Verder konden cellen met een lage celdichtheid beter tubes (kleine vaatjes) vormen in Matrigel. We hebben ook getracht de oorzaak voor de verschillen tussen de ECFC lijnen te achterhalen door middel van genexpressie studies. Daarbij zagen we dat cellijnen met een lage celdichtheid meer veroudering en mesenchymale eigenschappen hadden. Het is erg belangrijk om de variatie tussen de verschillende ECFC lijnen te erkennen wanneer onderzoek wordt gedaan met ECFCs. Het is daarom aan te raden om alleen ECFC lijnen met dezelfde eigenschappen met elkaar te vergelijken. Bijvoorbeeld bij het karakteriseren van een patiënten ECFC lijn is het belangrijk deze te vergelijken met een controle ECFC lijn met dezelfde cellulaire karakteristieken. Wanneer je de effecten van een bepaalde behandeling, bijvoorbeeld behandeling met siRNA, onderzoekt in een patiënten ECFC lijn, zal je echter de behandelde patiënten ECFCs met onbehandelde patiënten ECFCs vergelijken. Cellen zijn dan hun eigen interne controle en kunnen op die manier zonder aarzeling gebruikt worden.

Voordat de effecten van alle specifieke siRNAs worden onderzocht in patiënten ECFCs is het belangrijk om eerst de effecten te bestuderen die siRNA-gemedieerde verlaging van VWF heeft op de functie van VWF. Zeker aangezien in eerder onderzoek is aangetoond dat het verlagen van de productie van VWF door middel van een siRNA leidt tot kortere, meer rondvormige, Weibel-Palade-lichaampjes. Ook werd in deze eerdere studie een verhoogde secretie van VWF gezien na het verlagen van de VWF productie in endotheelcellen. We hebben deze eerdere bevindingen gereproduceerd in **hoofdstuk 6** van dit proefschrift, maar laten in dit hoofdstuk ook zien dat het remmen van VWF productie door middel van siRNAs resulteert in verhoogde secretie van voornamelijk kleinere VWF multimeren. Deze veranderingen in VWF productie en multimerisatie zijn belangrijk om in het achterhoofd te houden bij het bestuderen van siRNA behandelingen in patiënten ECFCs.

In **hoofdstuk 7** is bekeken of de siRNAs die zijn geselecteerd in de studies in HEK293 cellen (hoofdstuk 4), ook in ECFCs efficiënt en specifiek *VWF* allelen kan remmen. Deze siRNAs bleken inderdaad ook effectief te zijn in ECFCs, wat bestudeerd is op zowel eiwit als RNA niveau in ECFCs verkregen van gezonde controles. Daarnaast hebben we succesvol ECFCs geïsoleerd van een patiënt met de ziekte van von Willebrand type 2A. Deze patiënt had afwijkende VWF multimeren, een verlaagde binding van VWF aan collageen en retentie van VWF in het endoplasmatisch reticulum. Uit genotype data bleek dat deze patiënt heterozygoot is voor één van de SNPs waarvoor siRNAs zijn ontworpen. Behandeling van de patiënt ECFCs met een siRNA gericht tegen de SNP gelegen op hetzelfde allel als de dominant negatieve mutatie, leidde tot een verbetering in de fenotype van de patiënt ECFCs.

De studies in HEK293 cellen en ECFCs resulteerde in veelbelovende resultaten. Echter kunnen een aantal belangrijke aspecten in de fysiologie van de ziekte van von Willebrand niet worden bestudeerd in deze statische celmodellen. Daarom was het laatste doel in dit proefschrift, beschreven in **hoofdstuk 8**, om de effecten van allel specifieke siRNAs te testen in een heterozygoot muismodel voor de ziekte van von Willebrand. Heterozygote von Willebrand muizen met een type 2B fenotype zijn gegenereerd door mutant en wild type VWF tot expressie te brengen in de muizen. Voor deze studie is gebruik gemaakt van een veel bestudeerde type 2B mutatie: VWF p.Val1316Met. Deze mutatie leidt in mensen, maar ook in muizen tot verlaagde plaatjesaantallen, vergrote plaatjes en een verhoging van VWF dat circuleert in een actieve conformatie. Het remmen van het mutante allel, door middel van een siRNA gericht tegen de VWF p.Val1316Met mutatie zelf, leidde tot correctie van het fenotype met een correctie in plaatjesaantallen, normalisatie van de plaatjes grootte en een verlaging van circulerend actief VWF.

Samenvattend leveren studies die beschreven staan in dit proefschrift het bewijs dat allel specifieke remming van VWF door middel van siRNAs effectief is en resulteert in verbeteringen van verschillende fenotypen van de ziekte van von Willebrand. Dit is bestudeerd in HEK293 cellen, in ECFCs en in een muismodel voor de ziekte van von Willebrand. Deze resultaten zijn veelbelovend voor de verdere ontwikkeling van allel specifieke siRNAs als nieuw behandelingsstrategie voor patiënten met de ziekte van von Willebrand.







# Appendix

Dankwoord

Curriculum Vitae

Publication list

PhD portfolio

## Dankwoord

Het moment is aangekomen dat ook ik mijn dankwoord mag schrijven, het enige stukje tekst dat wel door iedereen gelezen gaat worden (no pressure). Het was een enerverend traject, en ik ben enorm dankbaar voor de mogelijkheden die ik heb gekregen.

Jeroen, ik ben echt ontzettend blij dat ik jou als promotor had, en ik denk dat jij voor mij(n) persoonlijkheid) de perfecte begeleider was. Je bent druk, maar je maakte altijd ruim tijd vrij op de momenten dat ik erom vroeg. Daarbij heb je mij de volledige vrijheid gegeven om me te ontwikkelen als wetenschapper.

Bart, buiten praten over de studies hebben we ook vele conversaties gehad over wetenschap in het algemeen en integriteitskwesties. Jouw openheid zou voor iedereen een voorbeeld moeten zijn, ook al blijkt dat die openheid je soms in problemen kan brengen. Voor mij ben je dat voorbeeld in ieder geval geweest.

Richard, bij een groot gedeelte van het werk dat is beschreven in dit boekje heb jij een belangrijke bijdrage geleverd. We hebben nauw samengewerkt en ik heb die samenwerking heel fijn gevonden. Als paranimf wil ik je ook graag bij de laatste stappen van mijn promotietraject betrekken. Bedankt voor de mooie jaren!

Stefanie, jij bent gaan promoveren in Tilburg, ik ben in Leiden gebleven. Het was fijn om met je te praten over het wel en wee van het promoveren, maar ook dingen daarbuiten. Fijn dat je tijdens mijn promotie aan mijn zijde wil staan.

VWFjes: Richard, Yvonne, Suzan, Ester, Stephanie en Maria Teresa. Wat fijn dat ik met jullie de wondere wereld van von Willebrand factor kon delen. Bedankt voor de samenwerking. Ook veel dank aan de studenten Josine, Jasmin en Davy.

Uiteraard wil ik ook de hele afdeling trombose en hemostase en het Eindhovenlab op D2 bedanken. Ik heb het altijd erg naar mijn zin gehad binnen de afdeling en op het lab. Vooral de congressen, inclusief de feestjes en borrels, waren hoogtepunten binnen mijn PhD traject en ik vond het leuk dit met jullie mee te maken.

Als laatste uiteraard de allerbelangrijksten. Papa, mama, Ronald, Mark en Elleke. Bij jullie kon ik terecht in goede, maar ook zeker in minder goede tijden. Fijn dat er altijd een warm thuis is. Liefste oma, je wilde heel graag bij mijn promotie zijn, en ik wilde jou er heel graag bij hebben. Helaas is het net niet gelukt.. Met je warme, onafhankelijke en ondernemende persoonlijkheid ben je altijd een groot voorbeeld voor me geweest.



## Curriculum Vitae

Annika de Jong was born on 23 December 1988 in Spijkenisse, the Netherlands. She completed pre-university education (VWO) in Etten-Leur in 2007 with a focus on Science & Health. In September 2007, Annika moved to Leiden for her bachelor in Life Science & Technology at Leiden University and Delft University of technology. During her bachelor she followed a minor in modern drug discovery and performed an internship at the department of molecular genetics of the Leiden Institute of Chemistry. In this internship she focused on live cell imaging of chromatin modifications under supervision of Claude Backendorf and Mathieu Noteborn. After graduating in 2011, Annika started her master in Life Science & Technology at Leiden University, with the main focus on Research and Development. During her masters, she performed two internships. One at the department of Human Genetics of Leiden University Medical Center, studying the role of epigenetic regulators in the development of the muscular dystrophy FSHD in the research group of Prof. Silvére van der Maarel under supervision of Judit Balog. The second research internship was performed at Prosensa. In this company internship, Annika focused on method development for miRNA detection in Duchenne muscular dystrophy muscle biopsies. She received her master's degree in March 2014. In April 2014, Annika started her PhD studies at the division of thrombosis and hemostasis of the department of Internal Medicine under supervision of Jeroen Eikenboom and Bart van Vlijmen. After her PhD defence, Annika will start a Postdoc in the group of Kathryn Moore at New York University.

## Publication list

**Annika de Jong**, Ester Weijers, Richard Dirven, Suzan de Boer, Jasmin Streur, Jeroen Eikenboom. Variability of von Willebrand factor-related parameters in endothelial colony forming cells. *Journal of Thrombosis and Haemostasis*, 2019, 17(9), 1544-1554

Marco Heestermans, **Annika de Jong**, Sander van Tilburg, Pieter Reitsma, Henri Versteeg, Henri Spronk, Bart van Vlijmen. Use of “C9/11 Mismatch” control small interfering RNA reveals sequence-related off-target effect on coagulation of a small Interfering RNA targeting mouse coagulation factor XII. *Nucleic acid therapeutics*, 2019, 29 (4), 218-223

**Annika de Jong**, Richard Dirven, Josine Oud, Davy Tio, Bart van Vlijmen and Jeroen Eikenboom. Correction of a dominant-negative von Willebrand factor multimerization defect by small interfering RNA-mediated allele-specific inhibition of mutant von Willebrand factor. *Journal of Thrombosis and Haemostasis*, 2018, 16 (7), 1357-1368

**Annika de Jong**, Jeroen Eikenboom. Von Willebrand disease mutation spectrum and associated mutation mechanisms. *Thrombosis research*, 2017, 159, 65-75

**Annika de Jong**, Jeroen Eikenboom. Developments in the diagnostic procedures for von Willebrand disease. *Journal of Thrombosis and Haemostasis*, 2016, 14 (3), 449-460

Judit Balog, Peter Thijssen, Sean Shadle, Kirsten Straasheijm, Patrick van der Vliet, Yvonne Krom, Marlinde van den Boogaard, **Annika de Jong**, Richard Lemmers, Rabi Tawil, Stephen Tapscott, Silvère van der Maarel. Increased DUX4 expression during muscle differentiation correlates with decreased SMCHD1 protein levels at D4Z4. *Epigenetics*, 2015, 10 (12), 1133-1142

## Submitted

**Annika de Jong**, Richard Dirven, Johan Boender, Ferdows Atiq, Seyed Yahya Anvar, Bart van Vlijmen, Frank Leebeek and Jeroen Eikenboom. *Ex vivo* improvement of a von Willebrand disease type 2A phenotype using an allele-specific small interfering RNA

Suzan de Boer, Mackenzie Bowman, Colleen Notley, Aomei Mo, Patricia Lima, **Annika de Jong**, Richard Dirven, Ester Weijers, David Lillicrap, Paula James, Jeroen Eikenboom. Endothelial cell characteristics and von Willebrand factor parameters in healthy endothelial colony forming cells; generating a valid *ex vivo* model for vascular disease

## PhD portfolio

PhD period: April 2014 - November 2018

Promotor: Prof. dr. H.C.J. Eikenboom

Copromotor: Dr. B.J.M. van Vlijmen

<b>Mandatory courses</b>	<b>Year</b>
PhD introductory meeting	2014
Basic course on Regulations and Organisation	2015
Basic methods and reasoning in Biostatistics	2015

<b>Generic/Disciplinary courses</b>	<b>Year</b>
NVTH AIO course - bleeding	2014
NVTH AIO course - venous thrombosis	2015
NVTH AIO course - arterial thrombosis	2016
Communication in Science	2016

<b>Conferences</b>	<b>Location</b>	<b>Type of presentation</b>	<b>Year</b>
NVTH symposium	Koudekerke, the Netherlands		2014
BIC International Conference	Bari, Italy		2014
Rembrandt symposium	Noordwijkerhout, the Netherlands		2014
NVTH symposium	Koudekerke, the Netherlands		2015
Congress of the ISTH	Toronto, Canada	Poster	2015
Oligonucleotide Therapeutics Society meeting	Leiden, the Netherlands	Poster	2015
European Congress on Thrombosis and Haemostasis	The Hague, the Netherlands	Oral	2016
NVTH symposium	Koudekerke, the Netherlands	Oral	2017
Congress of the ISTH	Berlin, Germany	Oral and poster	2017
BIC International Conference	Rome, Italy	Poster	2017
Oligonucleotide Therapeutics Society meeting	Bordeaux, France	Poster	2017
Rembrandt symposium	Noordwijkerhout, the Netherlands	Poster	2017
NVTH symposium	Koudekerke, the Netherlands		2018
Oligonucleotide Therapeutics Society meeting	Seattle, USA	Poster	2018
Dutch Hematology congress	Papendal, the Netherlands	Oral	2019
NVTH symposium	Koudekerke, the Netherlands	Oral	2019
Congress of the ISTH	Melbourne, Australia	Oral (2x)	2019
Rembrandt symposium	Noordwijkerhout, the Netherlands	Poster	2019

Parameters of esteem	Year
Conference participation grant of Leiden University Fund	2015
Award of excellence at the NVTH symposium	2017
Young investigator award of the ISTH congress	2017
Poster award at the Oligonucleotide Therapeutics Society meeting	2017
Travel grant to attend the Oligonucleotide Therapeutics Society meeting	2017
Jan Wouter ten Cate award	2018
Dr. J. Stibbe bokaal NVTH symposium (best oral communication)	2019
Young investigator award of the ISTH congress	2019
Journal of thrombosis and haemostasis editors' award	2019

Tutoring, mentoring, supervising	Year
FOS course: The Pathophysiology of Coagulation	2014
	2016
	2017
	2018
Bachelor student Biomedical Sciences: Davy Tio	2015
Master student Biomedical Sciences: Jasmin Streur	2015/6
Master student Medicine: Josine Oud	2016



(  
1  
(